2002

Targeting Receptor-Histidine Kinase Signaling in Staphylococcus Aureus

Gholson J. Lyon

Targeting Receptor-Histidine Kinase Signaling in *Staphylococcus aureus*

by

Gholson J. Lyon

Submitted in Partial Fulfillment
of the Requirements for the
Degree of Doctor of Philosophy

The Rockefeller University

October, 2002

Acknowledgements

I would like to thank Professor Thomas W. Muir and Adjunct Professor Richard P. Novick for providing research facilities and extraordinary scientific mentorship during the course of this work.

I wish to acknowledge Dr. Jesse Wright for his contributions to the latter half of this work, both on an intellectual and practical level.

I am indebted to all members of the Muir and Novick laboratories for technical assistance and/or advice on various aspects of this project, particularly Ms. Brenda Ayers, Dr. Julio Camarero, Ms. Jane Chao, Dr. Graham Cotton, Ms. Izabela Giriat, Dr. Roseanne Hofmann, Ms. Mande Holford, Dr. Ehab Khalil, Ms. Patricia Mayville, Dr. Alessandra Romanelli, Dr. Hope Ross and Mrs. Michelle Trester-Zedlitz.

I would like to express my appreciation to Dr. Mike Goger, Dr. Jen Ottesen, and Dr. Alex Shekhtman for assistance with NMR spectroscopy.

I wish to thank Dr. Markus Kalkum and Professor Brian Chait for tandem mass spectrometry analyses.

Grateful acknowledgement is made to Professor Arthur Christopoulos for his assistance with pharmacological analyses.

I am appreciative to Dr's Gerard Lina and Yvonne Benito for sharing unpublished data.

Support from the Cornell/Rockefeller/Sloan-Kettering Tri-Institutional MD/PhD program, under the direction of Professor Olaf Andersen, is gratefully acknowedged.

I would like to thank the members of my thesis committee, Professor Tom Sakmar and Professor John McKinney, for their consistent guidance, and Professor Christopher Walsh for serving as my external examiner.

Special thanks are due to my fiancée, Dr. Eun Yang, for her ongoing intellectual and personal support during my medical training and thesis research.

Lastly, I am deeply indebted to my family and particularly my mother, Ms. Gayle Lyon, for her constant encouragement during difficult times.

THE ROCKEFELLER UNIVERSITY
1230 YORK AVENUE • NEW YORK, NEW YORK 10021-6399

Dr. Sidney Strickland
Dean and Vice President for Educational Programs
Office of Graduate Studies
The Rockefeller University

October 18, 2002

Dear Dr. Strickland:

As members of the committee appointed to conduct the final examination of Gholson Lyon, we have read his thesis and have found it to be acceptable (with/without) minor revision in partial fulfillment of the University's requirements for the granting of the doctoral degree. Therefore, we the undersigned, are satisfied that Mr. Lyon has met the requirements for the Ph.D. degree with respect to his written thesis, thesis presentation and examination by this committee.

Dr. Thomas P. Sakmar, Chairman
The Rockefeller University

Dr. John McKinney
The Rockefeller University

Dr. Tom Muir, Advisor
The Rockefeller University

Dr. Christopher Walsh
Harvard Medical School

Dr. Richard Novick, Co-Advisor
NYU School of Medicine

Table of Contents

Academic coursework

Cornell Medical College: Medical school basic-science years, Fall 1997- Spring1999, including Biochemisty, Genetics, Pathology, Anatomy, Immunology, and Neuroscience.

Columbia University, Fall 1999, Advanced Organic Chemistry. Dr's Breslow and Katz.

Rockefeller University, Winter 2000, Microbial Diversity. Dr. McKinney.

Rockefeller University, Spring 2000, Introduction to Protein Structure and Function, Dr's Burley and Kuriyan.

Laboratory rotations

Summer 1997: Dr. Carl Nathan, Weill Medical College

Summer 1998-Spring 1999: Dr. Michael Rosen, Memorial Sloan-Kettering

Summer 1999: Dr. Tom Muir, Rockefeller University

Publications prior to Ph.D. thesis

Undergraduate Research, Dartmouth College:

Hernandez, A.; Park, J. P.; Lyon, G. J.; Mohandas, T. K.; St Germain, D. L. (1998). "Localization of the type 3 iodothyronine deiodinase (DIO3) gene to human chromosome 14q32 and mouse chromosome 12F1." Genomics 53(1): 119-21.

Hernandez, A.; Lyon, G. J.; Schneider, M. J.; St. Germain, D. L. (1999). "Isolation and characterization of the mouse gene for the type 3 iodothyronine deiodinase." Endocrinology 140(1): 124-30.

M.Phil in Genetics Research, University of Cambridge, England:

Gilmour, D. T.; Lyon, G. J.; Carlton, M. B.; Sanes, J. R.; Cunningham, J. M.; Anderson, J. R.; Hogan, B. L.; Evans, M. J.; Colledge, W. H. (1998). "Mice deficient for the secreted glycoprotein SPARC/osteonectin/BM40 develop normally but show severe age-onset cataract formation and disruption of the lens." Embo J 17(7): 1860-70.

Graduate Rotation Research, Weill Medical College:

Fuortes, M.; Melchior, M.; Han, H.; Lyon, G. J.; Nathan, C. (1999). "Role of the tyrosine kinase pyk2 in the integrin-dependent activation of human neutrophils by TNF." J Clin Invest 104(3): 327-35.

Publications related to Ph.D. thesis

Lyon, G.J., Mayville, P., Muir, T. W., and Novick, R. P., Rational design of a global inhibitor of the virulence response in *Staphylococcus aureus*, based in part on localization of the site of inhibition to the receptor-histidine kinase, AgrC. Proc Natl Acad Sci, 2000. **97**(24): p. 13330-5.

Jarraud, S., Lyon, G. J., Figueiredo, A. M., Lina, G., Vandenesch, F., Etienne, J., Muir, T. W., and Novick, R. P., Exfoliatin-producing strains define a fourth agr specificity group in *Staphylococcus aureus*. J Bacteriol, 2000. **182**(22): p. 6517-22.

Lyon, G. J., J. S. Wright, Christopoulos, A., Novick, R. P., and Muir, T. W. (2002). Reversible and specific extracellular antagonism of receptor-histidine kinase signaling. J Biol Chem **277**(8): 6247-53.

Lyon, G.J., J.S. Wright, Muir, T.W., and Novick, R. (2002). Key determinants of receptor activation in the *agr* autoinducing peptides of *Staphylococcus aureus*. Biochemistry, 41 (31): 10095-10104.

Kalkum, M., Lyon, G.J. , and Chait, B.T. (2002) Detection of Secreted Peptides using Hypothesis-driven Multistage Mass Spectrometry. (manuscript submitted).

J.S. Wright, Lyon, G.J., Muir, T.W., and Novick, R. (2002). A Hydrophobic Language Underlies Cross-communication Between Staphylococcal Quorum Sensing AgrC Receptors and Their Peptide Ligands. (manuscript submitted).

Publications unrelated to Ph.D. Thesis work

Miller, J.S., Dudkin, V.Y., Lyon, G.J., Muir, T.W., and Danishefsky, S.J. (2002). Toward Homogeneous, Synthetic N-Linked Glycoproteins. (manuscript submitted).

List of figures

List of Tables

Abbreviations

agr, accessory gene regulator

AIP, *agr* autoinducing or inhibiting peptide

Boc, tertiary butyloxycarbonyl

blaZ, β-lactamase

CAx-y, Group x *agrC* and *agrA* on the Group y *agr*-null background

CFA, complete Freund's adjuvant

CI, confidence interval

DMF, dimethylformamide

DIEA, diisopropylethylamine

DMAP, dimethylaminopyridine

DMSO, dimethyl sulfoxide

EC_{50}, half-maximal effective concentration

ESMS, electrospray mass spectroscopy

Fl, fluorescein

Fmoc, 9-fluorenylmethoxycarbonyl

HBTU, O-benzotriazol-1-yl-N,N,N',N',-tetramethyluronium hexafluorophosphate

HATU; O-(7-Azabenzotriazol-1-yl-N,N,N',N',-tetramethyluronium hexafluorophosphate

HF, hydrogen fluoride

IC_{50} , half-maximal inhibitory concentration

KLH, Keyhole Limpet Hemocyanin

MBP, maltose-binding protein

MEB, para-methylbenzyl

MBHA, methylbenzhydrylamine

m/z, mass/charge ratio in ESMS

NMR, nuclear magnetic resonance

PyBop, benzotriazol-1-yl-oxytripyrrolidinophosphoniumhexafluorophosphate

RHK, receptor-histidine kinase

RP-HPLC, reverse phase high pressure liquid chromatography

SDS-PAGE, sodium dodecyl sulfate polyacrylamide gel electrophoresis

SEM, standard error of the mean

TFA, trifluoroacetic acid

V_{init}, initial velocity

Standard IUPAC single and triple letter amino acid codes are used throughout.

Abstract

Two-component signaling systems involving receptor-histidine kinases (RHKs) are present in all branches of life outside of the animal kingdom. Remarkably, very little is known concerning the extracellular ligands that presumably bind to RHKs to initiate signaling. The two-component *agr* signaling circuit in the bacterial pathogen, *Staphylococcus aureus,* is one system where the ligands are known in chemical detail. These ligands (the AIPs) are short (7-9 aminoacyl residue) peptides containing a thiolactone structure, in which the α-carboxyl group of the C-terminal amino acid is linked to the sulfhydryl group of a cysteine, which is always the fifth amino acid from the C-terminus of the peptide. In the agr system, the AIPs generally activate virulence expression in the producer strain and cross-inhibit virulence expression in *S. aureus* strains expressing other AIPs. In this study, genetic studies on the receptor-histidine kinase, AgrC, have demonstrated that intra-group activation and inter-group inhibition are both mediated by the same group-specific receptors. Pharmacological analysis has shown that the AIPs compete for a common binding site on the receptor, and this site has been partly localized through the use of chimeric receptor analysis. Structure-activity relationship (SAR) studies have identified residues within the AIPs that are critical for receptor binding and activation. These results have facilitated the development of global inhibitors of virulence in *S. aureus*, which, in one case, consists of a truncated version of one of the naturally occurring AIPs. Cell-based *in vitro* assays of this peptide have demonstrated IC_{50}'s in the nanomolar range for inhibition of the transcription of a known global regulator of virulence in *S. aureus*, RNAIII. Virulence inhibition *in vivo* has been seen with native AIPs in a murine subcutaneous abscess model. Ongoing studies are focused on peptidomimetic design to generate stable and pharmacologically relevant lead compounds. These results collectively suggest that the design of molecules that compete with natural agonists for binding at RHK sensor domains could represent a general approach to the inhibition of RHK signaling.

Chapter 1 – Introduction

Receptor-regulated histidine kinase signaling (or two-component signaling) is widespread in nature, and is mainly utilized for cell-cell and cell-environment communication. Receptor-histidine kinases (RHKs) have been extensively characterized in bacteria, and are present in archaea, microbial eukarya, and higher plants, where they have recently been shown (in *Arabidopsis)* to play a role in hormone signaling (Sakakibara et al., 2000). In bacteria, RHKs are involved in sensing the environmental surroundings. Many of these kinases contain two transmembrane helices flanking a periplasmic domain. This domain contains the binding site for the appropriate ligand, such as metal ions (Mg^{2+} in the case of PhoP) (Groisman, 2001; Lesley and Waldburger, 2001). In the vast majority of cases, the ligands or environmental cues that trigger histidine kinase signaling are unknown. Noted exceptions include amino acid ligands, such as aspartate, in the bacterial chemotaxis system (Falke and Hazelbauer, 2001), and more complex peptide ligands, such as thiolactone-containing autoinducing peptides (AIPs), in the *agr* system of *Staphylococcus aureus* (Novick and Muir, 1999). Ligand recognition and signaling by two-transmembrane-helix-containing chemoreceptors has been extensively studied in bacterial chemotaxis systems (Falke and Hazelbauer, 2001; Yu and Koshland, 2001). In contrast, relatively little is known about peptide ligand recognition by polytopic receptor-histidine kinases (RHKs) in *S. aureus* or any other species.

Many RHKs have been shown to exist as preformed dimers in the inner cell membrane of gram-negative bacteria (Stock et al., 2000). In the case of EnvZ, a pair of cytoplasmic α-helices from each monomer forms a four-helix bundle (Tomomori et al.,

1999), and this structure is likely shared among the vast majority of RHKs. In gram-positive bacteria, pheromone-inducible RHKs usually have a polytopic sensor domain, containing five to eight membrane spanning segments. RHKs predicted to possess this polytopic sensor domain include: AgrC from *Staphylococcus aureus* (Lina et al., 1998), ComD from *Streptococcus pneumoniae* (Havarstein et al., 1996), ComP from *Bacillus subtilis* (Tortosa and Dubnau, 1999) and SapK from *Lactobacillus sakei* Lb706 (Axelsson and Holck, 1995). These RHKs respond to secreted signaling peptides, which bind to the sensor domain to initiate the transmembrane signal that activates the intracellular histidine kinase (HK). Activation of the HK domain is known to involve trans autophosphorylation of a conserved histidine residue in the dimerizing four-helix bundle, followed by phosphorelay to a downstream response regulator (Wright et al., 1993; Dutta and Inouye, 2000; Qin et al., 2000).

The ligands of the *agr* system in *Staphylococcus aureus* have been characterized and thereby represent a model system in which to elucidate the mechanistic basis for ligand-mediated RHK activation. As cells grow, an extracellular peptide, known as the AIP, is secreted and accumulates. This AIP is derived from processing of the propeptide, AgrD. Upon reaching a threshold concentration, the AIP triggers activation of the receptor-histidine kinase, AgrC. This kinase activation results in increased transcription of the unique regulator, RNAIII, that ultimately increases secretion of virulence factors and down-regulates various surface proteins (**Fig. 1.1,** and **Table 1.1**) (Novick et al., 1993; Tegmark et al., 1998). This signaling process is an example of density-dependent or "quorum sensing" systems widespread in bacteria (**Table 1.2**) (Fuqua et al., 2001; Schauder and Bassler, 2001; Fuqua and Greenberg, 2002).

Table 1.1 – Virulence Factors in *S. aureus*

Factor	***Pathogenic Activity***	***agr*-regulated**
Systemic toxins		
Enterotoxin A	Food Poisoning, TSS	
Enterotoxin B	Food Poisoning, TSS	+
Enterotoxin C	Food Poisoning, TSS	+
Enterotoxin D	Food Poisoning, TSS	+
Enterotoxin E	Food Poisoning, TSS	
Toxic Shock Toxins		
TSST-1	TSS	+
TSST-O	None (?)	
Exfoliative Toxins		
ETA	Scalded Skin Syndrome	+
ETB	Scalded Skin Syndrome	+
Cytotoxins		
α–hemolysin	Hemolysis, Necrosis	+
β–hemolysin	Hemolysis, Necrosis	+
δ–hemolysin	?	?
γ–hemolysin	Hemolysis, Necrosis	+
Leukocidin	Leukolysis	+
Enzymes		
Proteases	Spread, Nutrition	+
Nucleases	Spread, Nutrition	
Lipases	Spread, Nutrition	+
Hyaluronidase	Spread, Nutrition	-
Esterases	Inactivation of toxic fatty acids	+
Surface Factors		
Protein A	Anti-phagocytosis	+
Coagulase	?	+
Clumping factors	?	?
Fibronectin Binding Protein	Adhesion	+

+, expression of these virulence factors changes in response to activation of *agr* signaling, with decreased expression of surface factors and increased expression of the other listed virulence factors. -, No *agr* effect. ?, undetermined. (Novick and Muir, 1999)

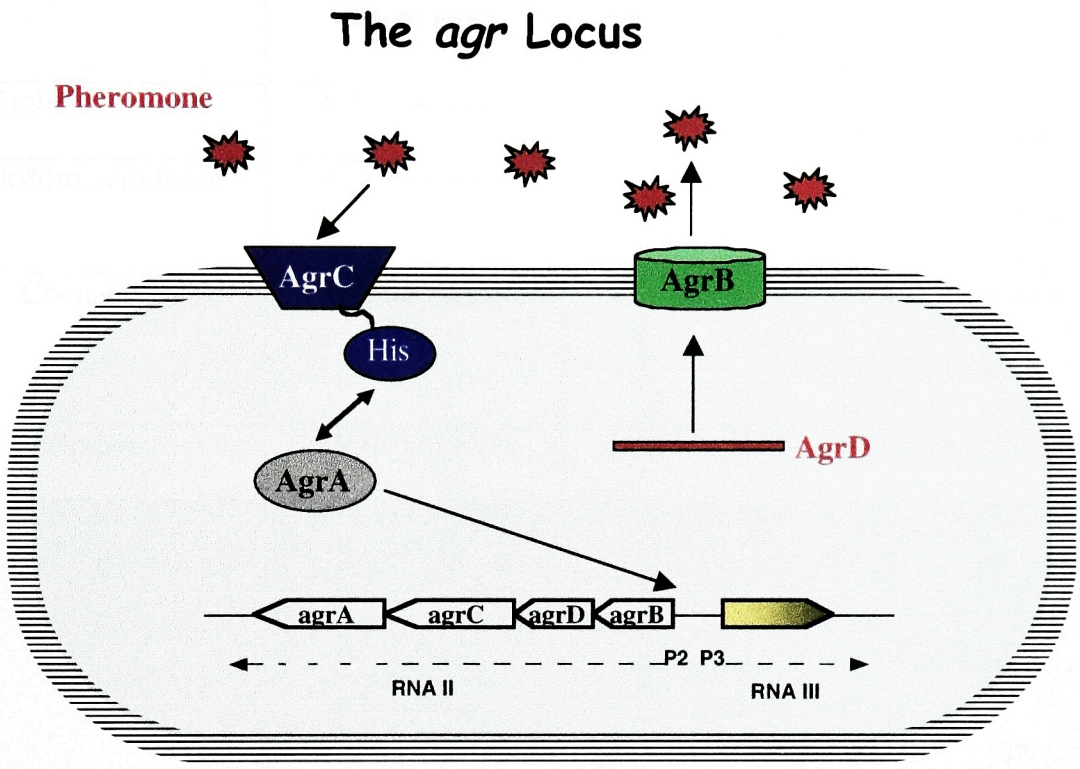

Figure 1.1. The *agr* locus is depicted, showing the various components and their putative actions in the signaling network. This signaling system is a doubly auto-catalytic circuit, as AgrC activation induces transcription of more receptor, along with more of the propeptide inducer, AgrD, processed by AgrB to form the pheromone AIPs. The end-result of the pathway is activation of RNAIII transcription by the response regulator, AgrA, which leads to downstream activation and repression of virulence-associated factors via transcriptional and translational regulation by this unique RNA molecule (Novick et al. 1993).

Table 1.2. Many Bacterial Processes are Controlled by Quorum Sensing

Processes	Bacterial species	Signaling molecules	Reference(s)
Bioluminescence	*Vibrio harveyi*	HSLs, AI-2	(Freeman et al., 2000)
Biofilms/virulence	*P. aeruginosa*	HSLs	(Fuqua and Greenberg, 2002)
Conjugation	*Agrobacterium*	HSLs	(Toyoda-Yamamoto et al., 2000; Vannini et al., 2002)
Virulence	*Vibrio cholerae*	CAI-1, AI-2	(Miller et al., 2002)
Virulence /competence	*S. pneumoniae*	Peptide - CSP	(Morrison, 1997; Lau et al., 2001)
Virulence	*E. faecalis*	Peptide - GBAP	(Nakayama et al., 2001; Qin et al., 2001)
Virulence	*S. aureus*	Peptide - AIP	(Novick and Muir, 1999)
Competence	*B. subtilis*	Peptide - ComX	(Ansaldi et al., 2002)

* Gram-positive bacteria are shaded in grey.

The AIPs were first purified and characterized from bacterial culture supernatants and tested by Northern blotting for their effect on RNAIII expression (Ji et al., 1995). Bacterial supernatants from group I *agr*+ cells, when added to pre-exponential bacterial cultures of similar cells, induced early RNAIII expression, due to activation of RNAIII expression by AIP-I from the added supernatants (**Fig. 1.2**) (Ji et al., 1995). Later studies also utilized Northern blotting of RNAIII expression to demonstrate cross-inhibition (or bacterial interference) of *agr* activation by supernatants derived from different *agr* specificity groups (Ji et al., 1997).

The sequence of the AIPs is highly variable, resulting in at least four specificity groups of strains within *S. aureus* and many more (>25) in other staphylococci (**Fig. 1.3**) (Ji et al., 1997; Otto et al., 1998; Jarraud et al., 2000; Dufour et al., 2002). A group is defined as the collection of strains that produce the same AIP. The *agrB*, *D*, and *C* regions vary in concert to maintain the specificity of AIP processing and function (Ji et al., 1997). This specificity results in four different receptors for the AIPs in *S. aureus*, designated AgrC-I, -II, -III, and –IV, reflecting the group that expresses them. Remarkably, there is extensive cross-communication at the level of ligand-mediated signaling, as most AIPs activate their cognate receptor while inhibiting activation of non-native receptors (Ji et al., 1997). This inhibition is a form of bacterial interference that does not result in growth inhibition but rather in the block of accessory gene functions, presumably resulting in an advantage for the strain producing the most abundant and/or most potent AIP. The native AIPs in *S. aureus* are referred to as AIP-I, -II, -III and –IV, reflecting the group that expresses them.

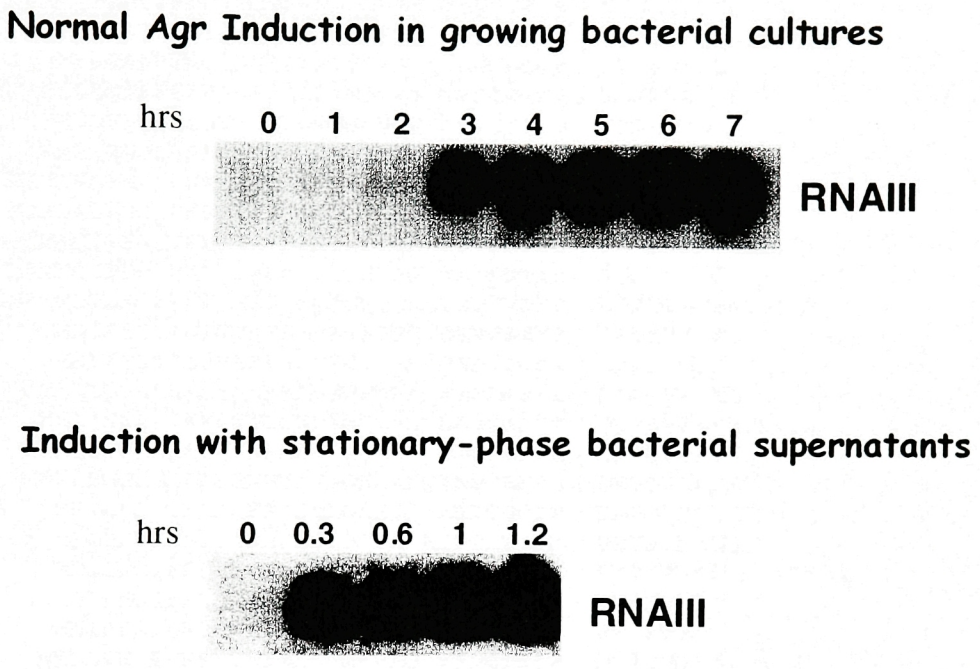

Figure 1.2. Northern blots of RNAIII induction in a Group I, RN6390b, strain. The stationary-phase supernatants were collected as described in Methods and added at $1/10^{th}$ volume to pre-exponential bacterial cultures. Addition of supernatants induces early RNAIII expression. The population doubling timeof *S. aureus* in culture is approximately 30 minutes, and, depending on the initial inoculum size, the time to reach stationary phase of growth can be from 6-12 hours. Control experiments monitoring cell density revealed no difference in cell growth between the strains with and without added supernatants. This experiment was performed by Naomi Balaban.

Figure 1.3. Lineup of Predicted AgrD Propeptide Sequences from Various Staphylococci

```
SaureusI      MNTLFNLFFDFITGILKNIGNIAA YSTCDFIM  DEVEVPKELTQLHE-------
SaurII        MNTLVNMFFDFIIKLAKAIGIVG GVNACSSLF  DEPKVPALLTNLYDK------
SaurIII       MKKLLNKVIELLVDFFNSIGYRAAY INCDFLL  DEAEVPKELTQLHE-------
SaurIV        MNTLLNIFFDFITGVLKNIGNVAS YSTCYFIM  DEVEVPKELTQLHE-------
SlugdI      MNLLSGLFTKGISAIFEFIGNFSAQ  DICNAYF  DEPEVPQELIDLQRK------
SlugdII       MNLLSGLFTKGISVIFEFIGNFSVQ DMCNGYF  DEPEVPQELIDLHRN------
SarlettaeI    MNLLNSFFSFFAKKFFELIGTVAG VNPCGGWF  DEPEVPEELTKYSE-------
SauricI       MMKLVNLLLSSTTSILQMVGNRQK AKTCTVLY  DEPEV-KELTQELEK------
SauricII      MMK-DNLLLSSTTSILQMVGNRSK TKTCTVLY  DEPEV-KELIQELEK------
ScapitisI   MIMNSLFNLIFKFFTVIFEFIGFVAG ANPCQLYY  DEPEVPEELSKLYE-------
ScapII      MIMDALFNLIFKFFTVIFEFIGFVAG ANPCALYY  DEPEVPDELSKLYE-------
ScapraeI      MMQIINLLFKVITAVFEKIGFIAG YSTCSYYF  DEPEVPKELLEIYKK------
ScaprII     MKMMQIFDLLFKVISAVFEKIGFLAG YRTCNTYF  DEPEVPKELFETYQK------
Scarnosus MNFNMDILNGIFKFFAFIFEQIGNIAK YNPCVGYF  DEPEVPSELLDEQK-------
Sconc**       MHIFESIINLFVKFFSVLGAISG GKVCSAYF  DEPEVPKEIKDLYK-------
Sconu***      MNIFESIINLFAKFFAFIGTISS VKPCTGFA  DEPEIPKELTDLYK-------
SepiI         MNLLGGLLLKLFSNFMAVIGSAAK YNPCASYL  DEPQVPEELTKLDE-------
SepiII        MEIIFNLFIKFFTTILEFIGTVAG DSVCASYF  DEPEVPEELTKLYE-------
SepiIII     MNKLLGGLLLKIFSNFMAVIGNASK YNPCSNYL  DEPQVLPEELTKLDE------
SepiIV      MNKLLGGLLLKIFSNFMAVIGNAAK YNPCANYL  DEPQVLPEELTKLDE------
Sgallinarum   MNILDSLLNLATKFFSALGASVG ARPCGGFF  DEPEVPAEITELHK-------
Sintermedius* MRILEVLFNLITNLFQSIGTFA RIPTSTGFF  DEPEIPAELLEEEK-------
SsimulansI    MDLLNGIFKLFAFIFEKIGNLAK YNPCLGFL  DEPTVPKELLEEDK-------
SsimII        MELLNGIFKLFAFIFEKIGNLAK YYPCFGFL  DESEVPQELLDEDK-------
Sxylosus      MNIFESILNLFAKFFSVLGVMAG AKPCGGFF  DEPEVPSEITKLYE-------
Swarnerii   MEFLVNLFFKFFTSIMEFVGFVAG YSPCTNFF  DEPEVPSELTKIYES------
```

* S. intermedius AIP containing a serine in place of the conserved cysteine.

** S. cohnii cohnii

*** S. cohnii urealyticum

• Note the conserved DE (Asp-Glu) processing motif C-terminal to the mature AIP, and the conserved Glycine several residues N-terminal to the mature AIP.

• All AIPs contain hydrophobic amino acids as the two C-terminal residues.

• The length of the AIPs varies from 7-9 residues. Therefore, at the beginning of this study, only AIP-I, AIP-II, and S. epidermidis AIP-II had been fully characterized by mass spectrometry and shown to encode an octapeptide, a nonapeptide, and an octapeptide, respectively (Otto et al. 1998, Mayville et al. 1999). There is also evidence from N-terminal sequencing of a purified *S. lugdenensis* AIP that it is comprised of a heptapeptide (Ji et al. 1997). All other AIPs listed had an undefined N-terminus relative to the conserved DE processing motif at the beginning of this study.

Structure-activity relationship (SAR) studies have been performed on the AIPs (Otto et al., 1998; Mayville et al., 1999; Otto et al., 1999), and have shown that (**Fig. 1.4**): i) the AIPs contain a thiolactone structure that is absolutely required for potent biological activity; ii) the thioester linkage is formed from the condensation of the α-carboxyl group of the peptide with the sulfhydryl group of a conserved cysteine; iii) the conserved cysteine is always the fifth amino acid from the C-terminus; iv) the lactam and lactone analogs of AIP-II are potent *agr* cross-group inhibitors, but lack activity against self, at concentrations up to 5 μM (Mayville et al., 1999); v) the N-terminal four amino acids of the group II AIP, collectively referred to as the "tail region", are necessary for self-activation but not for cross-group inhibition (Mayville et al., 1999); and vi) the sixteen atom-membered ring of the AIPs is also known as the macrocycle.

The structure-activity relationships summarized above were determined by analyzing the effects of chemically synthesized AIPs on *agr* activation. The strategy for the chemical synthesis of the AIPs is shown in **Fig. 1.5**. This strategy uses unprotected peptides in solution or on resin and relies on a chemoselective transthioesterification reaction that proceeds quantitatively and with no epimerization of the C-terminal amino acid (Dawson et al., 1994). All peptides synthesized, tested and reported up to and including the year, 1999, when this study commenced, are listed in **Table 1.3**. Much of the information provided by these AIPs formed the basis for many of the questions addressed in this study. Furthermore, the alanine scanning results of AIP-II are shown in **Fig. 1.6**. These results suggest that residues in the tail region of AIP-II might be critical for receptor activation, while certain residues in the macrocycle might be critical for receptor binding, as these latter alanine analogs have no activity whatsoever.

A)

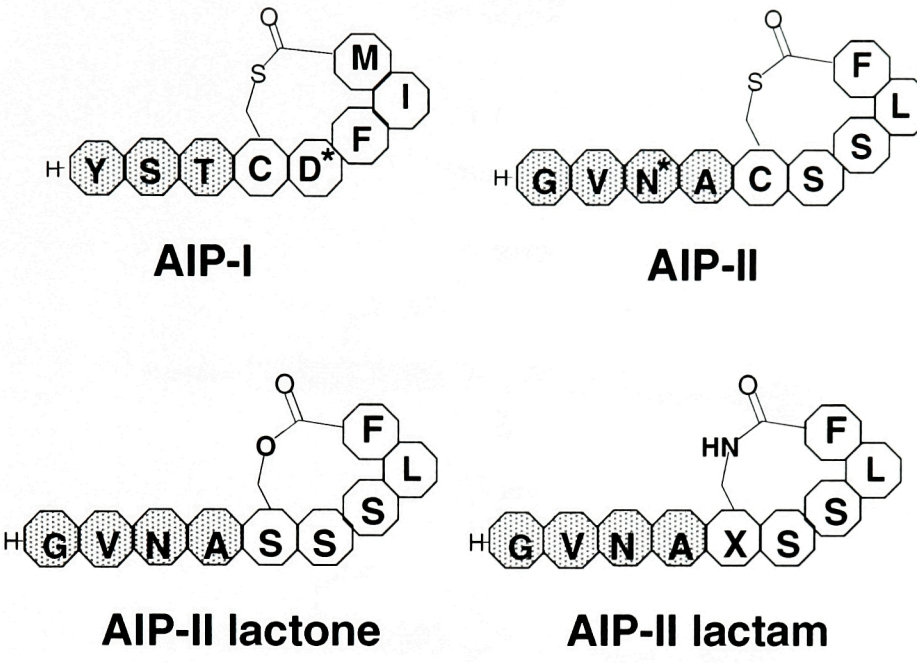

B)

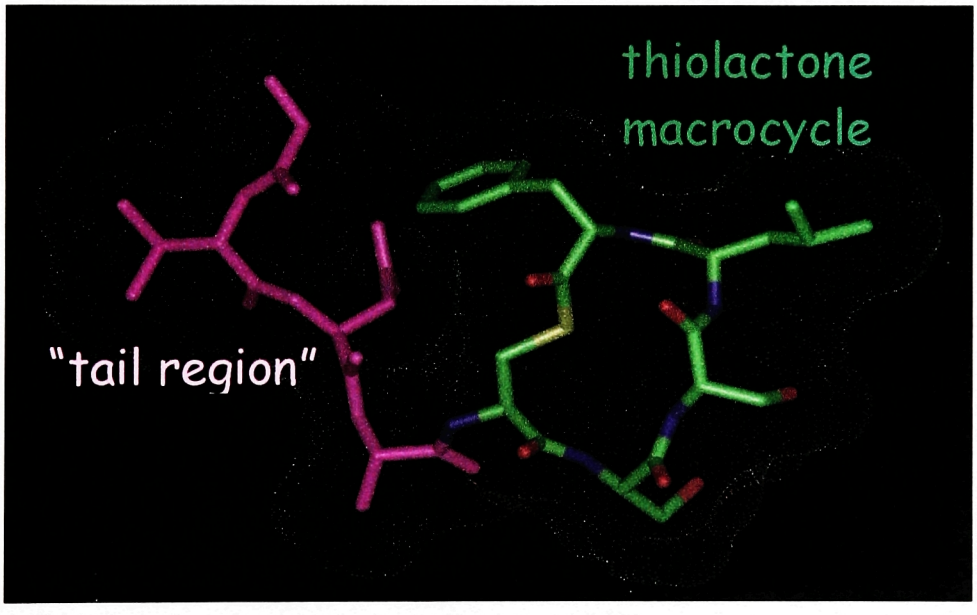

Figure 1.4. AIP structures. A) Chemical structures of AIP-I, AIP-II, AIP-II lactone and AIP-II lactam. **B)** An energy-minimized structural model of AIP-II (using Insight II, MSI). The AIPs consist of a flexible "tail region" and a thiolactone macrocycle.

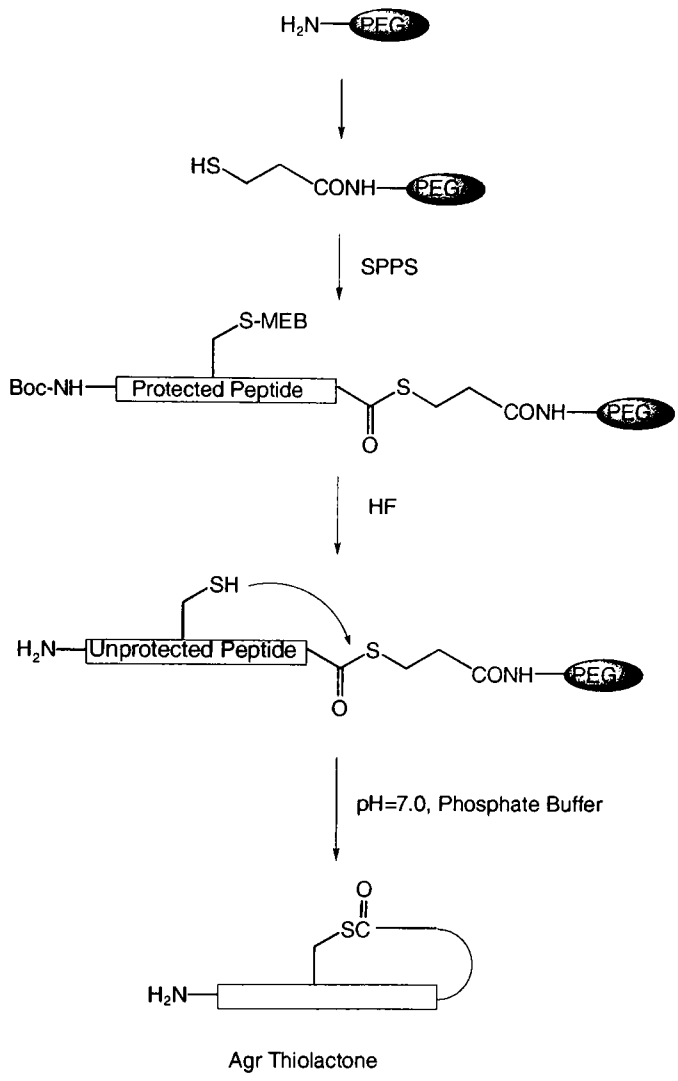

Figure 1.5. Chemical synthesis of AgrD thiolactone-containing autoinducing peptides via a solid-phase intramolecular chemical ligation strategy. Key to this process is the ability to prepare a fully unprotected peptide immobilized on a solid-support through a reactive thiol ester bond. Simply swelling such an unprotected peptide-[thioester]-resin in aqueous buffer results in a chemoselective ligation reaction and concomitant cleavage of the peptide from the support (Mayville et al., 1999).

Table 1.3. AIPs synthesized up to and including the year, 1999.

AIPs	Exocyclic [1]				Endocyclic					mass expected	mass observed
AIP-I		Y	S	T	C [2]	D	F	I	M	961.1	960.9
AIP-II	G	V	N	A	C	S	S	L	F	879.0	878.9
AIP-II lactam	G	V	N	A	X [3]	S	S	L	F	861.9	862.0
AIP-II lactone	G	V	N	A	S [4]	S	S	L	F	863.0	861.9
AIP-II linear free acid	G	V	N	A	C	S	S	L	F	897.0	896.4
AIP-II linear thioester	G	V	N	A	A	S	S	L	F [4]	953.0	952.0
AIP-II G1A	G	V	N	A	C	S	S	L	F	893.0	893.0
AIP-II V2A	G	V	N	A	C	S	S	L	F	850.9	850.0
AIP-II N3A	G	V	N	A	C	S	S	L	F	836.0	835.9
AIP-II S6A	G	V	N	A	C	S	S	L	F	862.9	861.9
AIP-II S7A	G	V	N	A	C	S	S	L	F	862.9	862.0
AIP-II L8A	G	V	N	A	C	S	S	L	F	836.9	836.0
AIP-II F9A	G	V	N	A	C	S	S	L	F	802.9	803.0
AIP-III octapeptide		Y	I	N	C	D	F	L	L	982.2	981.9
S. epidermidis AIP 9-mer	G	D	S	V	C	A	S	Y	F	930.0	Mass not reported [6]
Linear S. epi 9-mer	G	D	S	V	C	A	S	Y	F	948.0	Mass not reported [6]
S. epi. AIP 8-mer		D	S	V	C	A	S	Y	F	873.0	Mass not reported [6]
Linear S. epi 8-mer		D	S	V	C	A	S	Y	F	891.0	Mass not reported [6]
S. epi. AIP 8-mer Lactone		D	S	V	S [4]	A	S	Y	F	857.0	Mass not reported [6]
S. epi. AIP 8-mer Lactam		D	S	V	X [3]	A	S	Y	F	856.0	Mass not reported [6]
S. epi. AIP 7-mer			S	V	C	A	S	Y	F	758.0	Mass not reported [6]
Linear S. epi 7-mer			S	V	C	A	S	Y	F	776.0	Mass not reported [6]

ac: acetylation; bi, biotinylated; fl, fluorescein-conjugated

[1]exocyclic residues are shaded in the table; [2]All of the peptides with a conserved cysteine contain a thiolactone formed via the condensation of the α-carboxyl group of the AIPs with the sulfhydryl group, except for the linear peptides; [3] X=Dapa: diaminopropionic acid; [4] The marked serine contributes its hyrdroxyl group to condense with the α-carboxyl group of the AIP; [5] There is a C-terminal thioester linker on this peptide after HF cleavage; [6] These AIPs were synthesized by another group, that of Otto and Goetz (Otto et al., 1998; Otto et al., 1999), while all other AIPs were synthesized by Mayville et al. 1999.

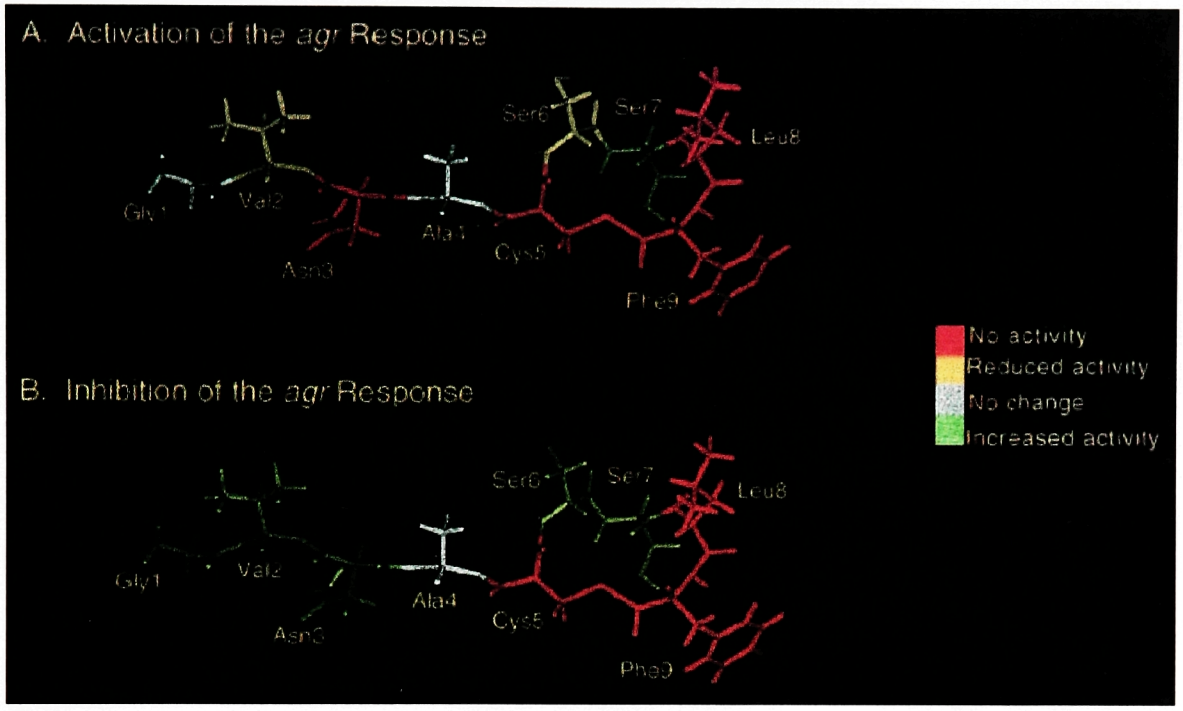

Figure 1.6. Alanine Scanning of AIP-II. Effect of replacing each residue within AIP-II with alanine on activation (**A**) and inhibition (**B**) activity. The results are superimposed on a model of AIP-II created using the program Discover (Biosym/MSI, San Diego, CA). The EC_{50} values (activation, group II cells) were as follows: AIP-II, 3.6 ± 1.1 nM; Ala1, 3.2 ± 2.2 nM; Ala2, 73.7 ± 1.9 nM; Ala3, no activity; Ala6, 33.6 ± 1.5 nM; Ala7, <1 nM; Ala8, no activity up to 10 μM; Ala9, no activity up to 10 μM. The IC_{50} values (inhibition, group I cells) were as follows: AIP-II, 2.9 ± 1.2 nM; Ala1, <1 nM; Ala2, <1 nM; Ala3, <1 nM; Ala6, <<1 nM; Ala7, <1 nM, Ala8, no activity up to 10 μM; Ala9, no activity up to 10 μM. Note, none of the peptides activated the *agr* response in group I *S.aureus* strains. Published results also indicated that none of these peptides were self-inhibitors of group II, although see Results section for clarification of this (Mayville et al, 1999).

It has been suggested that the N-terminal region of AgrC, the sensor domain, contains the binding site for the agonist AIP (Ji et al., 1995; Ji et al., 1997). In contrast with the conserved HK domain, the sensor domain is highly variable, thus suggesting a means for discriminating among AIPs from different groups. Suggestive evidence supporting AIP binding to AgrC was obtained in an AIP pull-down experiment in which cells overexpressing AgrC titrated out AIP-I from biological supernatants (**Figure 1.7**). Paranthetically, this is indirect proof, as it is formally possible that AgrC is or induces an enzyme that destroys the AIP or induces a second protein that binds the activator. Topological mapping via hydropathy analysis and PhoA fusions (Manoil and Beckwith, 1986) suggests that the sensor domain is composed of five or six transmembrane helices, depending on whether the N-terminus of the protein is placed on the inside or outside of the cell (Lina et al., 1998). This same study suggested that the third extracellular loop of AgrC-I is critical for AIP-I induced activation, as an MBP-AgrC fusion protein containing only the third extracellular loop, one transmembrane helix and the HK domain was activated by group I derived supernatants. In this study, attempts have been made to confirm these results using synthetic AIPs. Although these results were not confirmed (see Results), other studies described in this thesis implicate the C-terminal half of the sensor domain of AgrC in AIP-induced receptor activation (see Section 2.5).

The lack of agonist activity of the lactone and lactam analogs of AIP-II (see **Fig. 1.4** for structures) led to the hypothesis that the AIPs might activate AgrC through covalent reaction of the thioester with a nucleophile in AgrC (Mayville et al., 1999). The obvious candidate for such a nucleophile is a cysteine, but there is no such residue in the sensor domain of AgrC-II, although other putative nucleophiles are present. As no ligand-

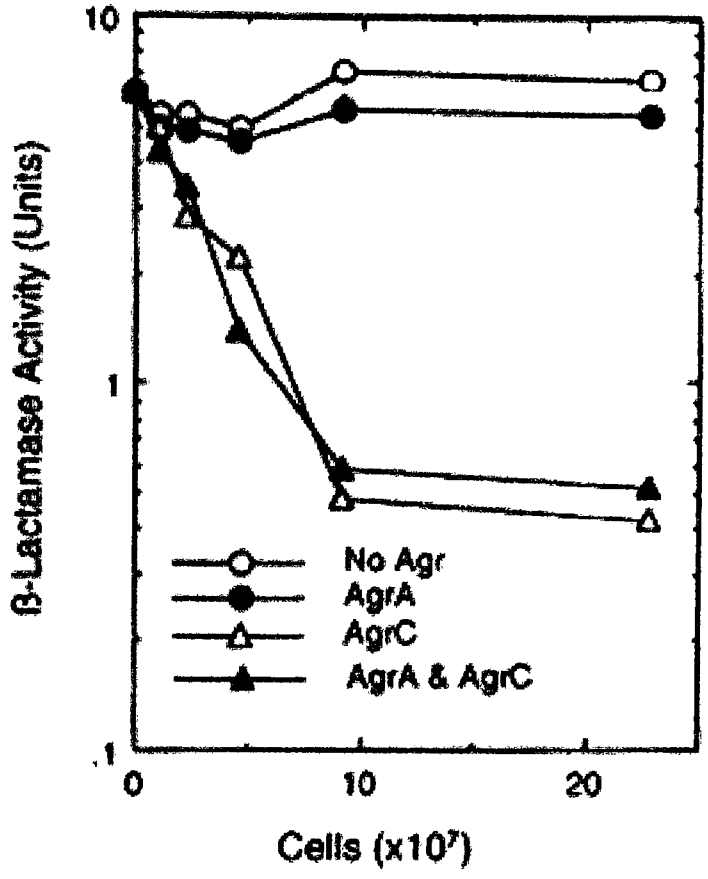

Figure 1.7. AIP Titration by AgrC-overexpressing cells. *Agr* null group I RN6911 strains carrying different *agr* genes cloned under control of the *blaZ* promoter were induced with 5 μg CBAP per mL for two hours, washed with 20 mM Tris-HCl buffer (pH 7.5), incubated for one minute with a standard amount of activator AIP-I from supernatants, and then centrifuged to remove the cells. The resulting supernatants were then assayed for activity (Ji et al., 1995).

receptor signaling cascade has yet been shown to proceed through covalent reaction of the ligand with the receptor, the testing of this hypothesis was of the utmost priority in this work. This analysis has led to the synthesis and characterization of the AIPs from the four known *agr* groups of *S. aureus*, thus yielding significant insight into the mechanism of interaction of the AIPs with the receptors (both as agonists and antagonists).

Agr mutants are greatly attenuated for virulence in several animal models of infection (Abdelnour et al., 1993; Cheung et al., 1994; Booth et al., 1995; Gillaspy et al., 1995; Giraudo et al., 1996; Tegmark et al., 1998). This suggests that blockade of *agr* signaling *in vivo* might have therapeutic utility. Toward this end, the availability of naturally occurring peptide-based *agr* antagonists has opened the door to peptidomimetic and/or small molecule drug discovery efforts. In fact, the *agr* system is the only system described thus far where interfering with quorum sensing can attenuate virulence *in vivo* (Mayville et al., 1999). A subcutaneous abscess mouse model of *S. aureus* infection was used to demonstrate that co-injection of *agr* group I *S. aureus* with the antagonist, AIP-II, led to greatly attenuated abscess formation (**Fig. 1.8**). This co-injection experiment has now been repeated several times with similar results, although preliminary experiments with injection of AIP-II at different sites from the bacterial injection site have not revealed any effect (unpublished observations, Jesse Wright). This outcome could be caused by the base-lability and putative exo- and endopeptidase susceptibility of AIP-II *in vivo*. Therefore, one aspect of this work has included a focus on the development of potent and stable AIP analogs that inhibit *agr* signaling (in all *agr* groups) for future testing in animal models of infection.

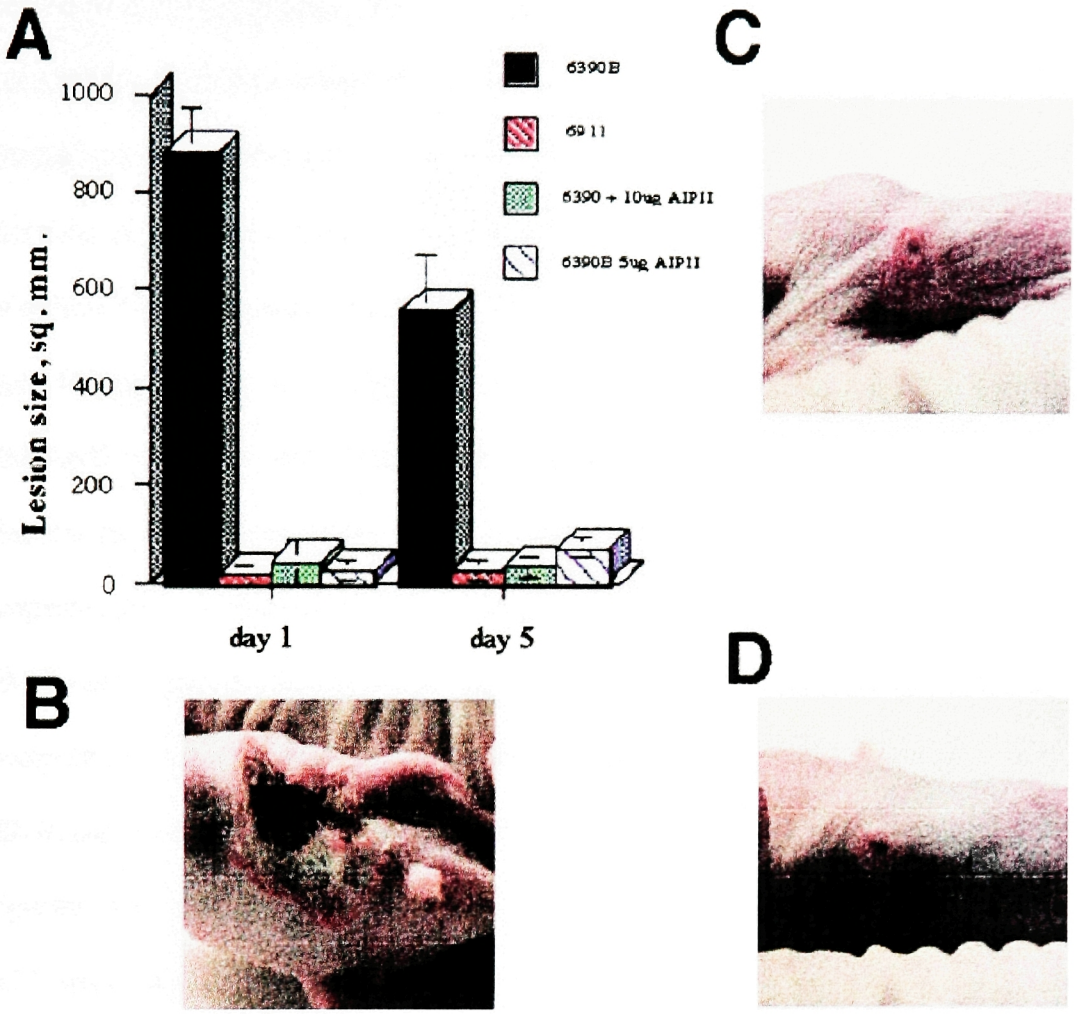

Figure 1.8. Attenuation of staphylococcal skin abscesses by a synthetic thiolactone-containing peptide (Mayville et al., 1999). Mice were injected subcutaneously with 10^8 cfu of either the *agr*+ wildtype group I strain, RN6390B (**B**), or an *agr*-null derivative, RN6911 as the negative control (**C**). For RN6390B, the synthetic AgrDII peptide, at 5 (**D**) or 10 mg per mouse, was included with the injected bacteria in two of the three groups of mice. Photographs were taken on day 5.

Although not studied in this thesis, the mechanism by which the AIPs are processed from the propeptide, AgrD, and subsequently secreted could bear upon the subject of how the AIPs evolved. Therefore, AgrD processing by AgrB is being studied by several groups. AgrB/AgrD swapping experiments have been used to address the mechanism of processing. Strains containing mixed and matched *agrB* and *agrD* genes were cultured and stationary-phase supernatants collected. These supernatants were then assayed for their ability to activate or inhibit AgrC-I (Ji et al., 1997) (see **Fig. 1.9B** for partial AgrD sequences, including the AIP sequences). For the matched AgrB-I/AgrD-I strains, the expected results were obtained: AgrB-I can process AgrD-I to form AIP-I, as the supernatant from this strain activates AgrC-I, and AgrB-II, -III, and *S. lugdunensis* AgrB process AgrD-II, -III and *S. lug.* AgrD to form AIP-II, -III, and *S. lug.* AIP, respectively, which all inhibit AgrC-I activation. For the mixed strains, e.g. AgrB-I with AgrD-II, the result was that AgrB did not process heterologous AgrDs, with notable exceptions. This included AgrB-III processing of AgrD-I to generate an activator of AgrC-I, which was presumably AIP-I, and AgrB-I processing of AgrD-III to generate an inhibitor of AgrC-I, which was presumably AIP-III. The caveat to these results is that the AIPs themselves were not analytically characterized, so it is impossible to know what was formed in the mixed AgrB/AgrD experiments. This is particularly important because the AIPs vary in length, ranging in size from 7-9 amino acids. Thus, it is possible, for example, that AgrB-I could process AgrD-III to form an octapeptide version of AIP-III, even though AIP-III is itself a heptapeptide (see Section 2.4). In fact, this logic was initially used to conclude erroneously that AIP-III might be an octapeptide, as AgrB-I could process AgrD-III to form a group I inhibitory peptide (Ji et al., 1997).

A)

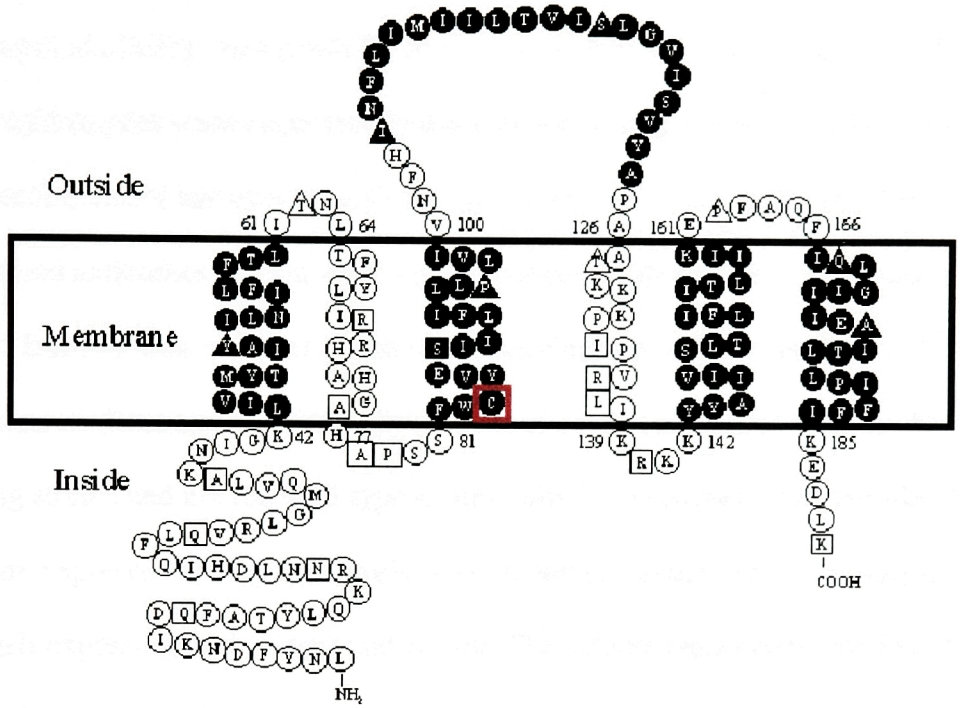

B)

```
          Group 1   --   ...GNIAA YSTCDFIM DEV...
          Group 2   --   ...GIVG GVNACSSLF DEP...
          Group 3   --   ...GYRAAY INCDFLL DEA...
          Group 4   --   ...GNVAS YSTCYFIM DEV...
S. Lugdenensis      --   ...GNFSAQ DICNAYF DEP...
S. epidermidis      --   ...GTVAG DSVCASYF DEP...
S. intermedius      --   ...GTFA RIPTSTGFF DEP...
```

Figure 1.9. AgrD processing by AgrB. A) The putative topology of AgrB-I is shown, with the cysteine residue boxed in red that is speculated to be of importance in AgrD processing. The location of the AgrB-PhoA fusion points are indicated with triangles and rectangles: triangle, high PhoA activities; rectangle, low PhoA activities. This figure has been reproduced from Zhang et al. (2002) *JBC*, 277, 34736. The entire N-terminus of the protein is not shown here, presumably due to space considerations or alternative start site locations. **B)** A portion of the AgrD propeptide sequence from various groups is shown below AgrB for reference. Note that all AIPs contain a conserved cysteine, with the exception of a substituted serine in the AIP of *S. intermedius*. The predicted transmembrane alpha helices by TopPred II, TMHMM, and DAS analyses are indicated by filled shapes.

Recently, two papers have studied AgrB in more detail (Saenz et al., 2000; Zhang et al., 2002). One group overexpressed AgrB and AgrD in *S. epidermidis* and showed that the concentration of AIP produced was equivalent to that produced in wild-type strains, ~20 nM (Saenz et al., 2000). This result led to the suggestion that processing or secretion of the AIPs might require some other rate-limiting factor besides AgrB or AgrD, although no *agr*-independent factor has ever been shown to be required for *agr* signaling. The same group raised antibodies against AgrB and demonstrated that AgrB is localized in the membrane fraction, thus suggesting that it is a membrane protein, consistent with hydropathy analysis (Saenz et al., 2000). These authors could only detect AgrB in the overexpressing strains and not the wild-type strains, which is consistent with the idea that *agr* proteins are expressed at very low levels. The second group utilized a His-tagged version of AgrB expressed in *S. aureus* and *E. coli*. The authors report confirmation of the membrane localization of AgrB in *S. aureus* using an anti-His antibody (Zhang et al., 2002). Secondly, using PhoA fusion analysis, the authors derive a transmembrane topology model of AgrB (**Fig. 1.9A**) that is consistent with some, but not all, of the computer-predicted transmembrane helices. In fact, this new model contains two transmembrane helices that are only twelve amino acids in length, which is not normally long enough to span the membrane The use of PhoA fusion analysis to determine membrane topology relies on the assumption that the C-terminal portion of the membrane protein plays no role in the assembly of the correct topological structure, an assumption that is not always the case and has formed the basis for the development of PhoA "sandwich-fusion" approaches (Ehrmann et al., 1990). Thirdly, the authors detect, upon co-expression of a His-tagged version of the propeptide, AgrD, with AgrB in *S. aureus,* a

His-tagged cleavage product of AgrD that derives either from cleavage at the N- or C-terminus of the AIP; the resolution of SDS-PAGE analysis does not allow distinction between the two possibilities. Finally, the authors speculate that processing of AgrD by AgrB could proceed through an acyl-enzyme intermediate resolved by nucleophilic attack by the thiolate anion of the cysteine side-chain in the AIP. As shown in **Fig. 1.9A**, there is a conserved cysteine in AgrB that could very well play a role in forming a thioester acyl-enzyme intermediate that could be resolved by nucleophilic attack by the cysteine thiolate anion in the AIPs. Future efforts should elucidate the mechanism by which this putative membrane protease/ secreting enzyme produces active AIP.

Objectives of Thesis

Outlined below are the specific aims of the thesis proposal, originally submitted in May, 2000. Significant progress toward each of these aims is reported herein.

Specific aim #1 -- Develop a more efficient assay system for testing synthetic analogs of the AIPs. As the previous assay system was problematic for a number of different reasons, the development of new strains of *S. aureus* containing reporter genes should enable one to assay new compounds more efficiently.

Specific aim #2 -- Design, synthesize and assay analogs of the AIPs to discover which parts of the structure are crucial for activation and which parts for inhibition. Such studies should lead to a more general understanding of how these peptides function, which will lend itself to rational design of potent global inhibitors of *S. aureus* virulence.

Specific aim #3 -- Address by genetic and biochemical means whether activation and inhibition of the *agr* response proceeds directly through the receptor, AgrC. Begin to test experimentally a model that holds that activation and inhibition of virulence involves specific binding of the AIPs (perhaps via covalent acylation) to the cell surface receptor, AgrC.

Specific aim #4 -- Begin to explore genetically and biochemically how activation of AgrC leads to a transcriptional response. Begin to address which parts of AgrC are crucial for its function, including the regions that may interact with the AIPs and the regions that may be involved in receptor dimerization.

Chapter 2 - Results

Section 2.1 -- Assays utilized to study AIP-induced AgrC signaling

Perhaps the most important predictor of success in experimentation is the amount of thought and effort that goes into assay development. There are various methods by which one could assay the effects of various AIPs on *agr* activation in *S. aureus*. Some of these have been developed, tested and refined herein.

Northern blotting to determine *agr*-regulated RNAIII production

Northern blotting was used initially to investigate RNAIII expression in a newly discovered *agr* variant, named group IV, with an AIP of predicted sequence YSTCYFIM (Jarraud et al., 2000), which has now been confirmed through synthetic means (see Section 2.4) and tandem mass spectrometry of biological supernatants (see Section 2.7). As an example of this type of analysis, group III bacterial cells (RN8465) were incubated with or without addition of culture supernatants from a group IV *agr*+ strain, RN4850, and aliquots removed at various timepoints from zero to four hours and analyzed by Northern blotting. As illustrated in **Figure 2.1**, RNAIII expression was up-regulated dramatically in group III cells by four hours, reflecting the normal timing of RNAIII expression in this strain, whereas RNAIII expression was strongly inhibited by the addition of group IV culture supernatants. This inhibition by AIP-IV of *agr* group III activation was later confirmed using a group III reporter strain and synthetic AIP-IV (*vide infra*) (Lyon et al., 2002).

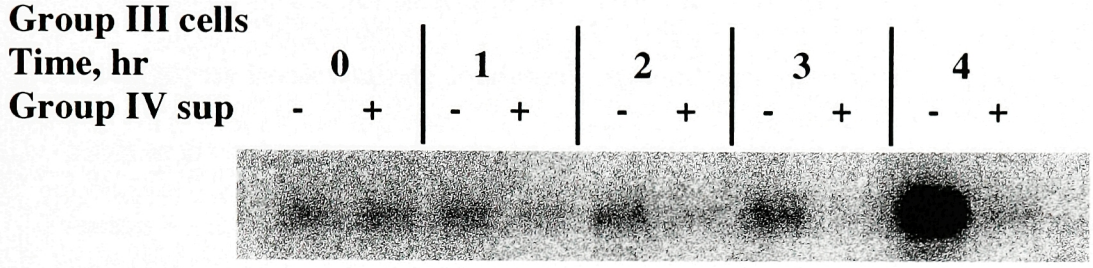

Figure 2.1. Northern blot hybridization analysis of the effects of group IV (RN4850) supernatant on *agr* activation in group III (RN8465) cells . One-tenth volume of post-exponential RN4850 supernatant (+) or broth (-) was added to a mid-exponential phase culture of RN8465 and hourly samples were taken for Northern blot hybridization analysis using an RNAIII-specific probe. The population doubling time is approximately every 30 minutes, and it takes approximately 6-12 hours of growth before *S. aureus* cells enter the stationary phase, depending on the initial inoculum size. For this *agr* group, RNAIII expression is turned on relatively late, after 4 hours of growth. Control experiments monitoring cell density revealed no difference in cell growth between the strains with and without added supernatants.

Analyzing *agr* expression via RP-HPLC analysis of δ-toxin levels

δ–toxin is a ~25 amino acid hemolytic peptide encoded by RNAIII, and the level of this translation product is proportional to the level of RNAIII in the cell (Otto et al., 1998; Mayville et al., 1999; Otto et al., 1999). δ–toxin is an amphiphilic molecule with surfactant-like properties that was discovered to bind under hydrophobic interaction chromatography conditions to a phenyl-derivatized column (Otto and Gotz, 2000). With the relatively harsh washing conditions of water/organic solvents, δ–toxin selectively binds to the column in preference to most other proteins in bacterial supernatants. The reason for this is likely because of the extreme amphiphilic nature and α-helical structure of δ–toxin, although it is unknown how much of this secondary structure is retained under acidic conditions. Very tight binding of such amphiphilic molecules to reversed-phase matrices has been described (Zhou et al., 1990). Therefore, HPLC analysis of δ–toxin binding to a Resource Phe 1-mL column (Amersham Pharmacia Biotech) provides a quantitative readout of RNAIII expression.

This relatively simple assay was utilized in lieu of Northern blotting to monitor RNAIII expression in staphylococcal strains for which reporter strains were not yet available (*vide infra*). For example, construction of a reporter strain for group III was initially problematic for technical reasons, so δ–toxin expression was monitored to analyze the effects of various synthetic AIPs. Two such AIPs are AIP-II and trAIP-II, a truncated version of AIP-II (see Section 2.2). Inhibition of RNAIII expression in early exponential-phase cultures of group I and III *agr*+ cells was monitored by HPLC analysis of δ–toxin production in the presence of increasing concentrations of AIP-II or trAIP-I. Supernatants were collected after nine hours of growth and the amount of δ–toxin

quantitated in each sample. Inhibition of group III *agr* activation by AIP-II and trAIP-II was demonstrated, with IC_{50} values of 17 nM (95% CI, 4-70 nM) and 10 nM (95% CI, 5-20 nM), respectively. A representative curve for inhibition by trAIP-II is shown in **Figure 2.2**. TrAIP-II also inhibited group I *agr* activation, with an IC_{50} of 200 nM (95% CI, 10-3000 nM). These results were later confirmed with group I and III reporter strain. This assay has also been utilized to assess the activity of AIPs in alternative staphylococcal species (*vide infra*).

It is notable that unknown components were detected by ESMS on fractions separated from δ-toxin by optimized RP-HPLC gradient conditions (see Methods), with one mass in particular, 4667.0 Da, repeatedly observed in *S. epidermidis* strains. Unless an optimized HPLC gradient is used to separate these components, it is not possible to quantitate δ-toxin in isolation, although this appears to have been done in the original assay (Otto et al., 1998; Otto et al., 1999). This was only possible because these other components are also *agr*-regulated, as their expression levels decrease in parallel with inhibition of δ-toxin expression (as assessed by the HPLC traces). Furthermore, control experiments with *agr*-null strains, RN6911 for *S. aureus* (Novick et al. 1993) and Tü38 for *S. epidermidis* (Vuong et al., 2000) (kindly provided by M. Otto) demonstrated that these other components as well as δ-toxin are absent from post-exponential phase bacterial supernatants. This confirms that the other components binding and eluting from the Pharmacia Resource PHE column are *agr*-regulated.

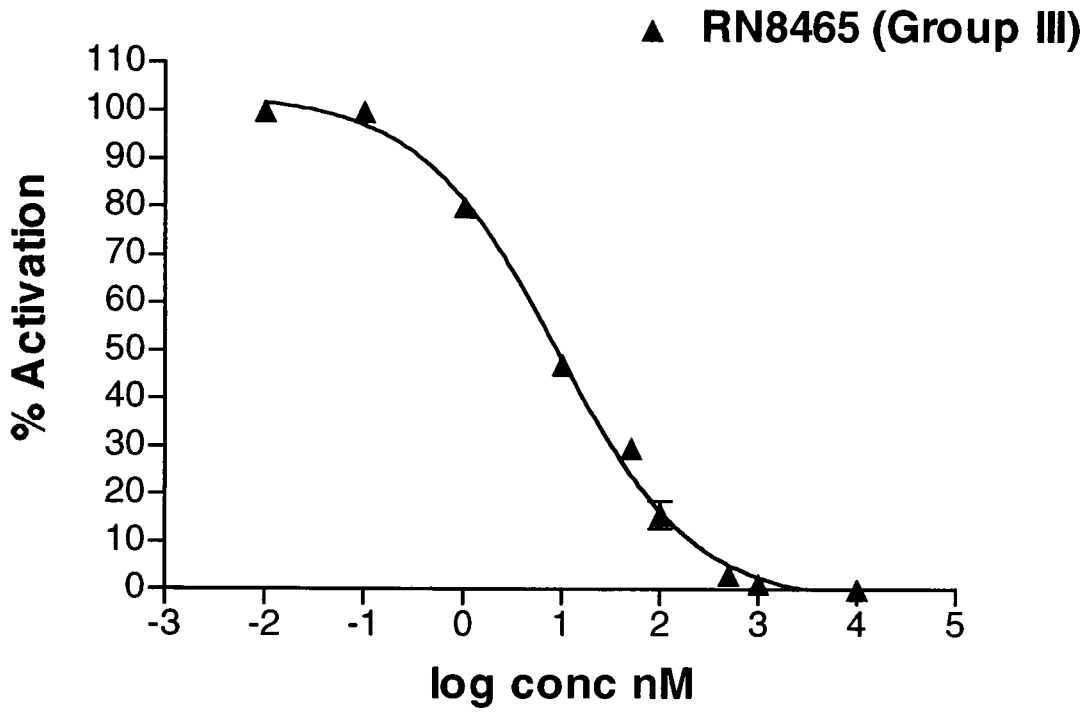

Figure 2.2. δ–toxin Assay with group III cells. The Group III strain, RN8465, was grown in the presence of differing concentrations of trAIP-II for nine hours, after which the supernatants were collected. A representative inhibition curve derived from reversed-phase HPLC analysis of δ–toxin levels in culture supernatants is shown. Quantitation of δ–toxin levels was obtained by integration of peak area from the HPLC trace.

Development of Reporter Strains through reconstitution of *agr* signaling in *agr*-null host backgrounds

Shuttle vectors containing *agrC* and *agrA* under control of the *agr*-P2 promoter, along with a β-lactamase reporter gene driven by the *agr*-P3 promoter, were introduced into *agr*-null strains (see **Fig. 2.3,** and **Table 2.1** for bacterial strains and plasmids). It was reasoned, based upon prior studies (Ji et al., 1997) that these constructs would be sufficient for signaling to occur in *agr*-null backgrounds in response to exogenously added AIP. This was confirmed for the group I and II reporter strains, as shown in **Table 2.2** and by example in **Fig. 2.4**. Two strains were used in these experiments, RN9222 (CA1-I) and RN9372 (CA2-II), containing the cloned *agrCA*/β-lactamase in the corresponding *agr*-null *S. aureus* strain (the reconstituted strains are provided with a descriptor in the format; CAx-y, which indicates Group x *agrC* and *agrA* on the Group y *agr*-null background). In both cases, dose-dependent activation of the *agr*-response was observed upon addition of the cognate synthetic AIP (for example, see **Fig. 2.4**), with EC_{50} values listed in **Table 2.2**. No dose-dependent *agr*-activation was observed in the control strains, RN9033 and RN9416, which contain the vector alone (for example, see **Fig. 2.4A**).

A similar strategy was utilized to construct a reporter strain for group IV, and this strain and the group I and II reporter strains were used to characterize bacterial supernatants from the three groups. As shown in **Fig. 2.5A**, there was no detectable RNAIII activation in cultures of the group IV reporter strain, RN9371, treated with group I, II, or III supernatants (note that ß-lactamase is produced endogenously in group III cells and complicates this assay), whereas there was a strong signal in cultures treated with the

autogenous group IV (RN4850) supernatant. The groups 2 and 3 supernatants inhibited activation by the RN4850 supernatant, as is usually the case with heterologous AIPs (Ji et al., 1997). The Group 1 supernatant, however, did not inhibit group IV *agr* activation by RN4850 supernatant. Conversely, as shown in **Fig. 2.5B**, the group IV (RN4850) supernatant inhibited *agr* activation of group II; however, it activated the group I strain to approximately 30% of the level seen with the group 1 supernatant. These results were later confirmed for groups 1 and 2 with synthetic AIPs (see **Table 2.3**). Lastly, as earlier demonstrated by Northern blotting analysis, group III *agr* activation is inhibited by group IV culture supernatants. Eventually, a group III reporter strain was constructed which provides a reliable readout of *agr* activation by group III supernatants and synthetic AIP-III (see Methods). This strain was utilized to confirm the above findings with group IV supernatants, and to test synthetic AIP-III and other AIPs, including AIP-IV (*vide infra* and **Table 2.3**).

This reporter gene assay method has been extended to the study of various other *agr* groups (*vide infra*) and is different from a previously utilized assay (Ji et al., 1995, Mayville et al., 1999), in enabling an assessment of AIP activity in the absence of skewing effects of endogenous AIP production. In addition, the previous assay utilized cells in which the plasmid was genetically unstable, perhaps due to the presence of two P3 promoters in the cell, one on the chromosome and the other on the plasmid. This resulted in the generation of promoter-negative mutants, as confirmed by DNA sequencing of the recovered plasmids (Novick et al, unpublished data), thus rendering the assay unreliable.

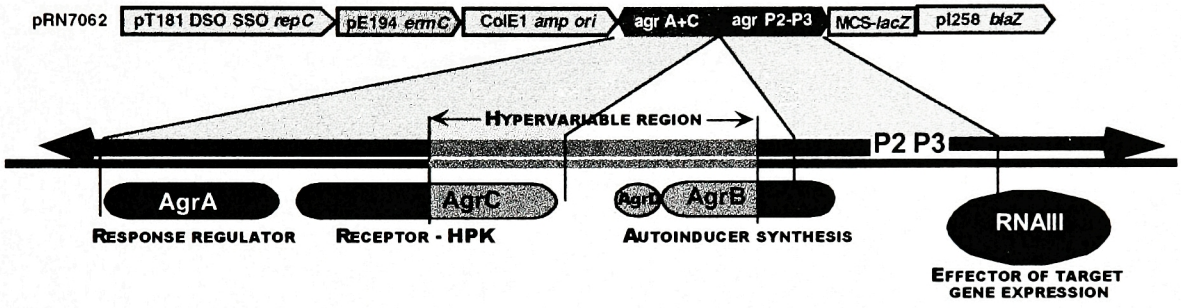

Figure 2.3. Diagram illustrating an example of the type of reporter plasmid developed to monitor P3 promoter activity in response to added AIPs (Jarraud et al. 2000).

A)

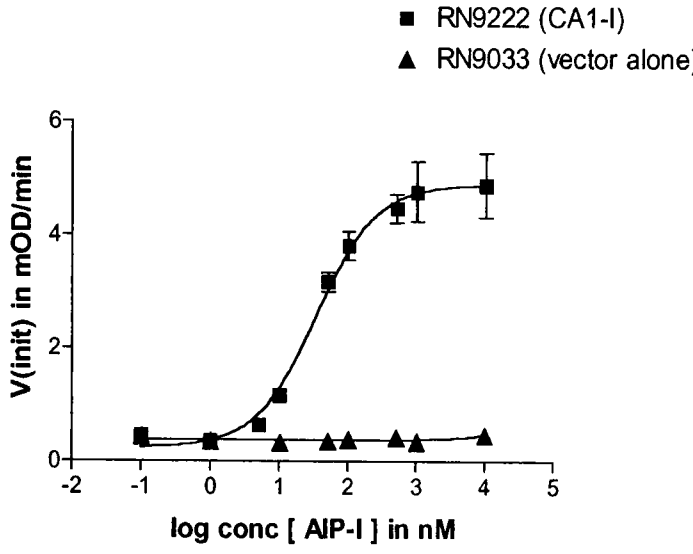

B)

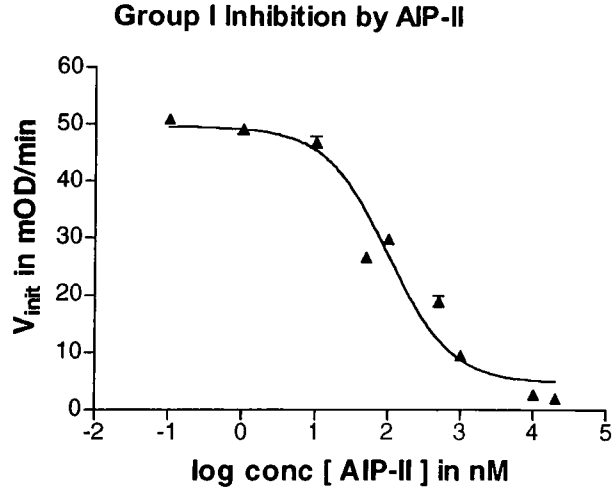

Figure 2.4. Synthetic thiolactone peptides are biologically active in reconstituted strains. Shown are representative data for activation (A) and inhibition (B) of the *agr* response by synthetic AIPs. Degree of activity based upon ß-lactamase activity is shown as a plot of V_{init} (initial velocity) versus peptide concentration. (A) Activation of the *agr* response in RN9222 (CA1-I) by AIP-I. The RN9033 (vector alone) control is shown. (B) Inhibition of the agr response in RN9222 (CA1-I) by Group II AIP in the presence of activating AIP-I at 100 nM.

Table 2.1. Bacterial Strains and plasmids used for cloning and/or monitoring of native *agr* activation

Strains	References	Comments
S. aureus		
RN4220	(Novick, 1991)	mutant of 8325-4 that accepts foreign DNA
RN6390b	(Kornblum et al., 1988)	Group I prototype
RN6734	(Kornblum et al., 1988)	Group I strain, ϕ13 lysogen of 6390b
RN6911	(Novick et al., 1993)	Group I, RN6390b, with *tetM* replacing *agr* (*agr*-null)
RN7206	(Novick et al., 1993)	Group I prototype, RN6734, *with tetM* replacing *agr*
RN6607	(Ji et al., 1997)	Group II prototype
RN9120		Group II with *tetM* replacing *agr* (*agr*-null)
RN8465	(Ji et al., 1997)	Group III prototype
RN4850		Group IV prototype from U. Minn., strain KG, kindly provided by Dr. Patrick Schlievert
RN9121		Group IV with *tetM* replacing *agr* (*agr*-null)
RN9033	(Lyon et al., 2000)	RN6911 with pRN7035
RN9416	(Lyon et al., 2000)	RN6607 with pRN7105
CA1-I (RN9222)	(Lyon et al., 2000)	RN6911 with pRN7062
CA1-I (RN9365)	(Lyon et al., 2000)	RN7206 with pRN7062
CA1-II (RN9366)	(Lyon et al., 2000)	RN9120 with pRN7062
CA2-II (RN9372)	(Lyon et al., 2000)	RN9120 with pRN7105
CA2-I (RN9367)	(Lyon et al., 2000)	RN7206 with pRN7105
CA4-IV (RN9371)	(Lyon et al., 2000)	RN9121 with pRN7107
CA4-I (RN9380)	(Lyon et al., 2000)	RN7206 with pRN7107
Group III reporter (RN9532)	(Lyon et al., 2002)	RN6911 with pRN7131
S. epidermidis RN2375, RN9420, RN9421, RN9422, RN8111, ATCC, Tü3298, Tü38 (agr-null)	(Lyon et al., 2000)	clinical isolates, and ATCC, Tü3298, Tü38 (agr-null) kindly provided by Dr. Michael Otto
S. warnerii, RN3178	(Lyon et al., 2000)	clinical isolate
S. intermedius, RN9423		clinical isolate, kindly provided by Dr. Gerard Lina
E. coli, DH5α		cloning strain
Plasmids		
pRN7035	(Lyon et al., 2000)	Shuttle vector containing only *agr*-P3::*blaZ* fusion
pRN7062	(Lyon et al., 2000)	Shuttle vector containing *agrCA*-I and *agr*-P3::*blaZ*
pRN7105	(Lyon et al., 2000)	Shuttle vector containing *agrCA*-II and *agr*-P3::*blaZ*
pRN7107	(Lyon et al., 2000)	Shuttle vector containing *agCA*-IV and *agr*-P3::*blaZ*
pRN7128	(Lyon et al., 2002)	pRN7107 modified to include an *Afl*II site between the sensor domain and the HK domain of AgrC
pRN7131	(Lyon et al., 2002)	Shuttle vector containing AgrC-III sensor domain fused to the HK domain of AgrC-IV, and AgrA-IV and *agr*-P3::*blaZ*

Table 2.2. ***Agr*** **Activation and Inhibition in different genetic backgrounds**

Activation EC_{50} (nM)				
	RN9222 (CA1-I)	RN9366 (CA1-II)	RN9372 (CA2-II)	RN9367 (CA2-I)
AIP-I	30 ± 10	23 ± 7		
AIP-II			30 ± 10	28 ± 14
Inhibition IC_{50} (nM)*				
AIP-1			26 ± 7	135 ± 52
AIP-II	90 ± 30	78 ± 12		

All results were from ß-lactamase assays. Errors are quoted as ± SEM, which provides a smaller error range than from 95% CI.

- These values were obtained with a constant concentration, 100 nM, of the synthetic autologous (activating) AIP.

  No detectable activity up to a concentration of at least 10 μM.

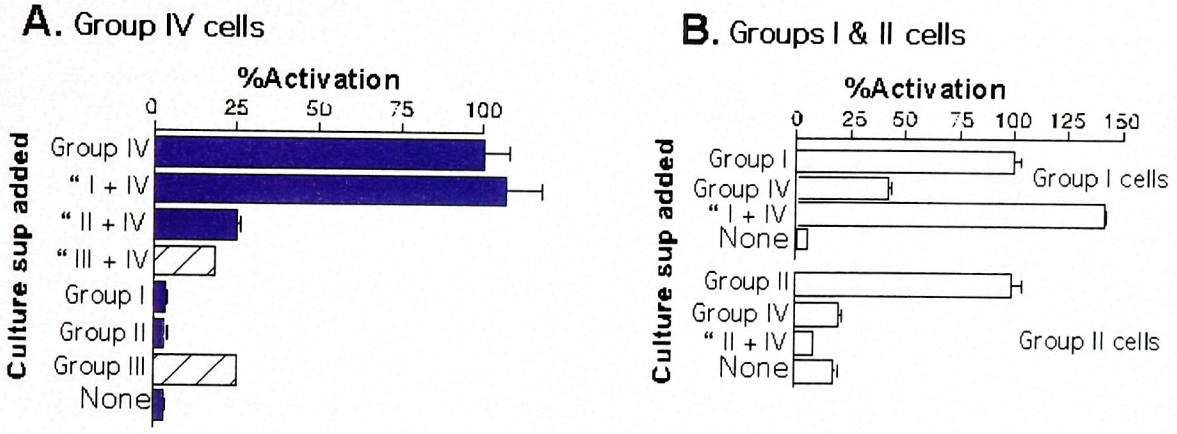

Figure 2.5. ***Agr*** **activation and inhibition by culture supernatants. A & B.** One-tenth volume of postexponential phase culture supernatants or CY broth was added to mid-exponential phase cultures, growth was continued for an additional 1 hr with shaking at 37°C, and samples were then assayed for β-lactamase by the nitrocefin method. Note that β-lactamase activity in samples treated with Group III supernatant (cross-hatched) represents the endogenous β-lactamase activity released from the group III strain into the supernatant and does not represent activation of group IV, as determined in control experiments without the addition of any cells. Furthermore, there is one instance (panel B) where the combination of I and IV supernatants results in greater than 100% activation of group I cells, as compared to the value obtained with Group I supernatant alone. This activation enhancement is thought to result artefactually from pH and/or salt differences brought about by the addition to the cells of $2/10^{th}$ volume of supernatant rather than $1/10^{th}$ volume.

Table 2.3. Agonism and Antagonism by native AIPs and trAIP-II

	Activation (EC_{50})				Inhibition (IC_{50})			
	Group I	Group II	Group III	Group IV	Group I	Group II	Group III	Group IV
AIP-I	30 nM (20-50)			26 μM (23-29 μM)		25 nM (14-45)	3 nM (2-5)	
AIP-II		30 nM (10-90)			40 nM (12-140)		1 nM (0.7-2.6)	86 nM (65-111)
AIP-III			26 nM (22-31)		70 nM (30-150)	6 nM (5-6.5)		150 nM (104-207)
AIP-IV	62 nM (50-75)			13 nM (7-40)		4 nM (3-5)	1 nM (0.5-3)	
trAIP-II					260 nM (95-695)	230 nM (190-270)	4 nM (3-5)	150 nM (90-260)

- No detectable activity up to a concentration of ≥ 10 μM.

All results were from ß-lactamase assays. Inhibition values were obtained using the standard reporter strains for groups I-IV with a constant concentration, 100 nM, of the synthetic autologous (activating) AIP. Errors are quoted as (95% CI). The group III reporter strain includes a chimeric receptor, with the AgrC-III sensor domain attached to the AgrC-IV HK domain (see methods). There is no evidence that this would change in any way the behavior of the AIPs on native AgrC-III, as all data support the notion that the AIPs act only at the level of the sensor domain (see Results).

Section 2.2 -- Rational Design of Global Inhibitors of Virulence in *S. aureus*

The development of anti-infective compounds that target virulence, rather than bacterial growth per se, is a relatively new concept requiring rigorous testing. In the clinical setting, it is unlikely that the *agr* grouping of *S. aureus* clinical isolates will always be known. Therefore, in order to test the efficacy of *agr* inhibitors *in vivo*, it is important to develop compounds that turn off *agr* signaling in all strains of *S. aureus*, independent of their *agr* grouping.

Modification of one residue in AIP-II converts an agonist into an antagonist

It was originally observed that an AIP-II analog with alanine in place of asparagine (N3A) in the tail region was a potent cross-inhibitor but was unable to self-activate and seemed also unable to self-inhibit (Mayville et al., 1999). Using the newly developed reporter gene assay in which no endogenous AIPs are produced (*vide supra*), it has now been discovered that this peptide is, in fact, an antagonist of self-activation, with an IC_{50} value of 180 nM (95% CI, 120-270 nM), as well as an antagonist of group I activation as previously published (Mayville et al., 1999). These data suggest that a key molecular determinant of AIP-II-mediated receptor activation resides in the side-chain of the asparagine residue, and that modification of this residue to alanine still allows for receptor binding but without receptor activation. This is one of the first AIP analogs synthesized that has the property of self-inhibition, thus opening the door to the design of global inhibitors of virulence. The other alanine-modified peptides synthesized previously have been re-tested in the new reporter strains and the published results

(Mayville et al., 1999) confirmed. This includes the lack of self-inhibition (up to 5 μM) by AIP-II analogs in which the remaining amino acids in the tail region and cyclic portion of the peptide were replaced by alanine, and the complete lack of activation or inhibition by AIP-II L8A and F9A, suggesting that these conserved hydrophobic residues in the AIPs may be critical for receptor binding.

Global inhibitors of virulence in *S. aureus*

It was reasoned that a truncated AIP analog containing only the thiolactone ring structure with the conserved hydrophobic residues and lacking the activating tail (and thus the asparagine residue) might be able to bind AgrC but would not have the tail necessary for activation. This analog would therefore be a good inhibitor not only in a cross-group manner but also within the same group. Conversion of a receptor agonist into an antagonist of its autologous group as well as an inhibitor of heterologous groups would result in a global inhibitor of virulence in *S. aureus.*

A truncated group II thiolactone peptide (trAIP-II) was synthesized (see **Figure 2.6A** for structure) and tested for its ability to activate and inhibit the *agr*-response in group I, II, III and IV reporter strains. TrAIP-II had no detectable activation activity for the four groups. Furthermore, the peptide was an inhibitor in the nanomolar range of the *agr*-response in all four groups **(Table 2.3, Figure 2.6B)**. TrAIP-II is therefore a potent inhibitor for all four *agr*-specificity groups of *S. aureus.*

The activity of trAIP-II and AIP-II were also tested in alternative staphylococcal species, using HPLC analysis of δ-toxin production. The results showed weak inhibition (in the μM range) of *S. epidermidis* strain, RN2375, by AIP-II and trAIP-II, and strong

A)

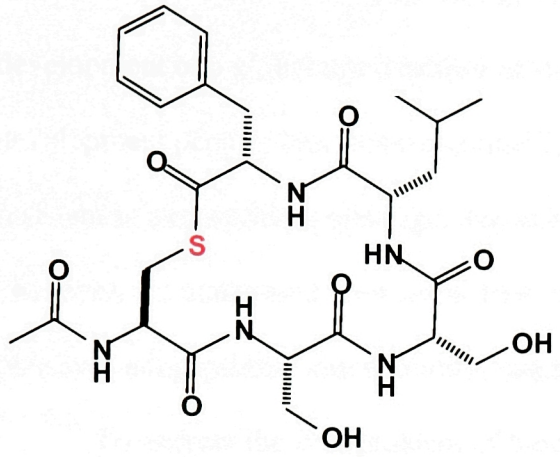

trAIP-II thiolactone
IC50 ~ 200-500 nM

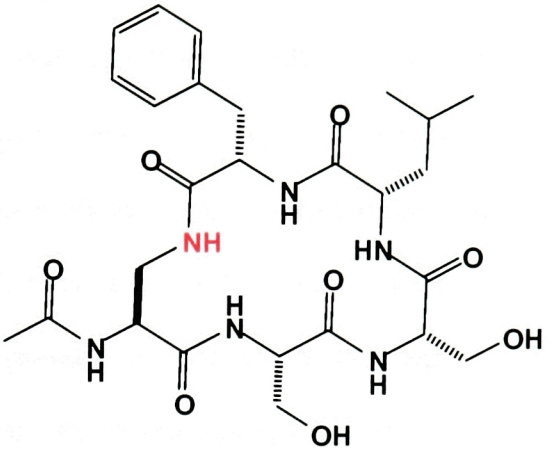

trAIP-II lactam
IC50 ~ 40 µM

B)

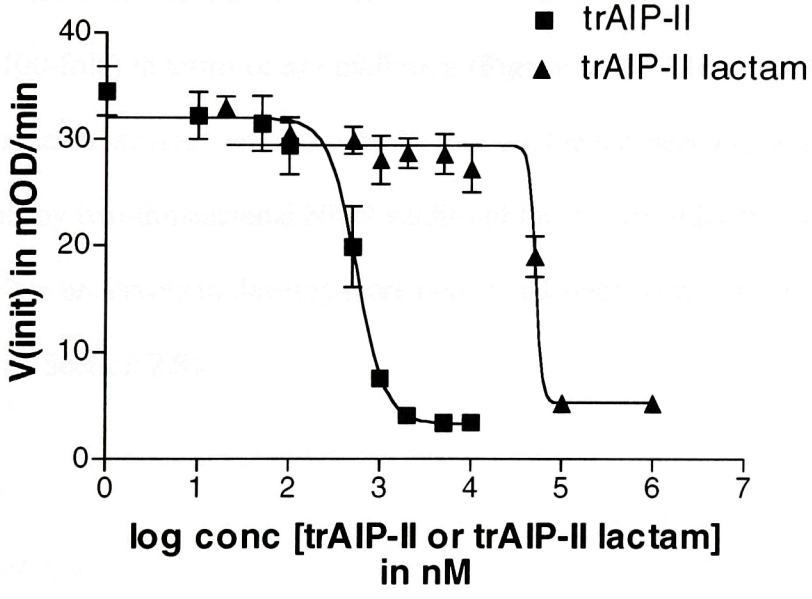

Figure 2.6. Testing of trAIP-II and trAIP-II lactam for inhibition of group II *agr* activation. A) The structures of trAIP-II thiolactone and trAIP-II lactam are shown, illustrating the one atom difference between them, colored in red. B) Both AIPs were tested for inhibition of *agr* activation in group II cells, using the nitrocefin method to quantitate the P3 reporter readout. The degree of activity based upon ß-lactamase activity is shown as a plot of V_{init} (initial velocity) versus peptide concentration.

inhibition of *agr* expression in the *S. warnerii* strain, RN3178, by trAIP-II, with an IC_{50} value of 20 ± 12 nM. Thus, trAIP-II represents a significant advance toward the development of a global *agr* inhibitor of staphylococci (Lyon et al., 2000). From a drug development perspective, this compound is relatively small (579 Da) and should be resistant to exopeptidase cleavage, due to its macrocylization and N-terminal acetylation. However, the compound does suffer from base-lability, due to the thioester linkage, and putative endopeptidase susceptibility, due to the presence of multiple amide bonds.

To address the first problem of base-lability, the lactam analog of trAIP-II (**Figure 2.6A**) was synthesized and assayed. While this lactam analog is completely stable to base-hydrolysis (no decomposition or hydrolysis was observed by HPLC analysis after treatment with 0.5 M NaOH for 30 minutes), the compound is dramatically less potent (~100-fold) in terms of *agr* inhibition (**Figure 2.6B**). The dramatic loss of potency of the lactam analog versus the thiolactone analog has been explained in structural terms by two-dimensional NMR studies of the two peptides in solution (*vide infra*). Efforts are underway to develop more potent and stable peptidomimetic compounds (see Section 2.8).

Section 2.3 -- Agonism/Antagonism occurs through competitive binding at the sensor domain of AgrC

A high priority of this work involved testing the hypothesis that the AIPs, with their highly reactive thioester linkage, react covalently with AgrC. Pharmacological analysis of the AIP-receptor interaction (in collaboration with Dr. Arthur Christopoulos) yielded insights into this hypothesis and the mechanistic basis of the interaction, along with providing suggestive evidence concerning the dimeric status of the receptor.

Reconstitution of cross-strain inhibition in the absence of AgrB

As previously demonstrated (Ji et al., 1997), *S. aureus* culture supernatants inhibit *agr* activation in heterologous strains. A prior study using a reporter gene assay in strains containing the endogenous *agr* locus (Mayville et al. 1999), demonstrated that synthetic AIPs could reproduce these effects. However, the site of action for the inhibition by these peptides was not determined. Although the most likely site seems to be AgrC, the diversity of sequences among inhibitory peptides and their analogs suggests that some mechanism other than competitive blocking of activator binding could be responsible. One possibility would be binding to the putative processing-secretion enzyme, AgrB, causing interference with production or secretion of the activator. Alternatively, the peptides could bind to any range of targets on or within the cells and interfere with the *agr* signaling pathway up- or downstream of AgrC activation.

As was already shown in **Figure 2.4B**, the new group I reporter strain was incubated with AIP-I at 100 nM along with various concentrations of AIP-II. AIP-II inhibits *agr* activation in a dose-dependent fashion, thus demonstrating that inhibition

occurs in the absence of AgrB. Similar experiments were performed with the group II reporter strain and AIP-I, yielding similar results **(Table 2.3).** These results, in two different *agr* specificity groups, confirm that AgrB cannot be the target of inhibition, as the new strains lack AgrB.

The *agrAC* two-component module is necessary and sufficient for group-specific activation and inhibition

It was asked whether AgrC determines the group-specificity of the AIP response. This was addressed by testing the two-component module in *agr*-null host backgrounds derived from different *agr* groups. Transfer of the group-specific signaling phenotype with *agrCA* would argue against any other group-specific determinant. Accordingly, two strains, RN9366 (CA1-II) and RN9367 (CA2-I), were tested for their ability to respond to supernatants from *agr* ± strains, as well as to AIP-I and -II. The identity of the AgrC being expressed on which genetic background is included in the CA nomenclature given to each strain, where CAx-y stands for group x *agrC* and *agrA* on a group y *agr*-null background.

The two strains were compared with the appropriate controls, RN9222 (CA1-I) and RN9372 (CA2-II), which are the normal reporter strains, for activation by post-exponential phase supernatants from a series of *agr* ± strains and by the synthetic AIPs. As illustrated in **Figure 2.7**, only supernatant from the group II *agr* wild-type strain, RN6607, was able to activate β-lactamase expression in RN9372 (CA2-II) and RN9367 (CA2-I). In addition, similar EC_{50} values for activation were obtained for both strains using AIP-II (see **Table 2.2**). Analogous results were obtained using RN9222 (CA1-I)

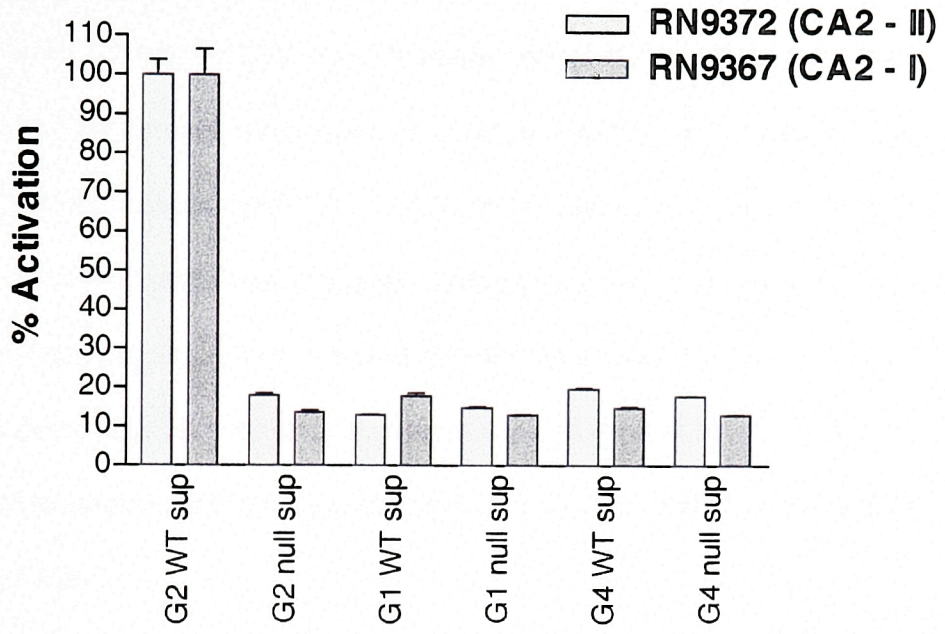

Figure 2.7. Group II *agr* Activation in different genetic backgrounds. A representative example of activation of RN9372 (CA2-II) and RN9367 (CA2-I) by post-exponential supernatants collected from Group 1, 2, and 4 *agr*± cells. Data were collected as ß-lactamase activity (V_{init} in mOD/min) and then normalized to percentage activation.

and RN9366 (CA1-II): these were activated by wild-type group I supernatants (RN6734) and not by Group II supernatant or by *agr*-null supernatants from either group. Moreover, similar EC_{50} values for activation were obtained for both strains using AIP-I (**Table 2.2**). Therefore, the group-specificity of *agr* signaling does not depend upon the host background. Furthermore, the conversion of an *agr*-null group I strain, RN7206, into a group II responsive strain, RN9367 (CA2-I), by the insertion of plasmid-encoded group II *agrC* and *agrA* (and vice versa), suggests strongly that the group-specificity of the *agr* response depends upon the expression of the two-component module containing *agrC* and *agrA*. Since AgrC is a variable transmembrane receptor (Lina et al. 1998) and AgrA is identical at the protein level in all four groups, it is very likely that the agonists act at the level of AgrC.

The next question was whether cross-strain inhibition also proceeds through the AgrC/A two-component cascade. If so, a Group II *agr*-null strain (RN6607) reconstituted with Group I *agrC* and *agrA*, i.e. RN9366 (CA1-II), should be inhibited by Group II agr^+ supernatants or by AIP-II. Alternatively, if inhibition were to involve a group-specific factor outside of the *agr* locus, then inhibition would depend upon the host background in which AgrC and AgrA are expressed. The former scenario was shown to be correct, as very similar IC_{50}'s for inhibition by AIP-II in RN9366 (CA1-II) and RN9222 (CA1-I) were obtained **(Table 2.2).** The same was true for inhibition of RN9372 (CA2-II) and RN9367 (CA2-I) by AIP-I, albeit with a slight difference in the IC_{50}'s **(Table 2.2)**. It is apparent that inhibition by the AIPs is dependent upon which *agrC* and *agrA* genes are expressed and not upon the genetic background in which they are expressed, thereby

indicating that the site of inhibition must lie within Agr C, since AgrA is identical at the protein level in all four groups.

The sensor domain of AgrC determines group-specificity of agonism and antagonism

AgrC consists of a divergent N-terminal sensor domain, and a conserved C-terminal histidine kinase (HK) domain (Ji et al., 1995; Lina et al., 1998), of which the former is predicted to contain the determinant of group specificity. To confirm this prediction, chimeric receptors were constructed (shown in **Fig. 2.8**) in which the sensor domain of AgrC from either group I or II was fused to the HK domain of the group IV receptor (Jarraud et al., 2000). As shown in **Fig. 2.9**, the chimeric receptors were activated or inhibited only by AIP-I or AIP-II (from culture supernatants or chemically synthesized) according to their respective sensor domains, thus confirming the above prediction. The group I chimera was activated not only by group I supernatant but also marginally by group IV supernatant, consistent with previous results (*vide supra*) (Jarraud et al., 2000). Activation and inhibition titration curves of the chimeric receptors with synthetic AIP-I or AIP-II yielded curves similar to those for the wild-type receptors (not shown). As the AIPs appear to activate or inhibit only AgrC, activation or inhibition of each group will henceforth be referred to according to the group-specific sensor domain of the activated or inhibited receptor. For example, group II activation will be referred to as AgrC-II activation, and inhibition of group I activation will be referred to as AgrC-I inhibition, thus reflecting the mechanistic basis for these processes.

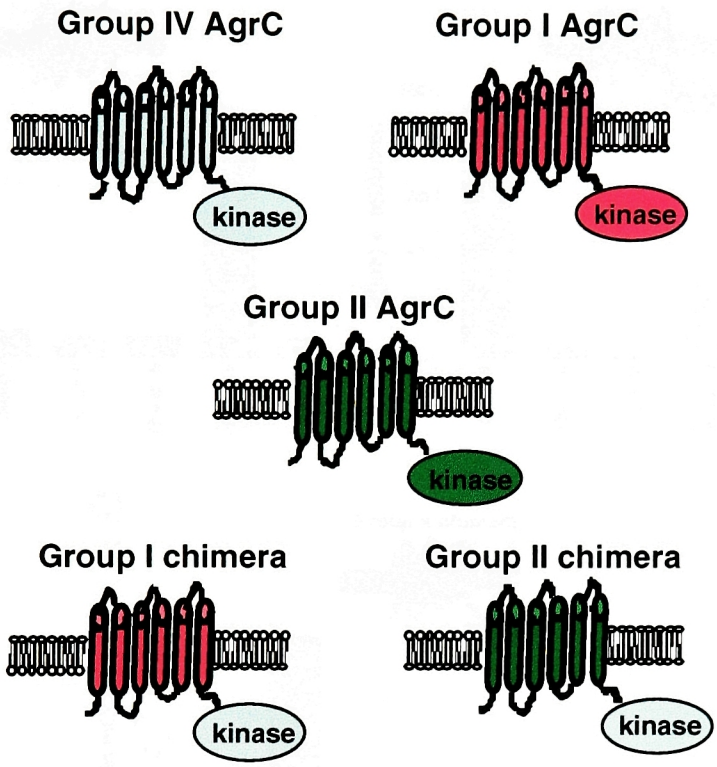

Figure 2.8. Schematic representation of the sensor-domain-swapped AgrC RHKs. The Group I and Group II chimeras have the polytopic sensor domains from the Group I and Group II receptors, respectively, fused to the Group IV receptor HK domain.

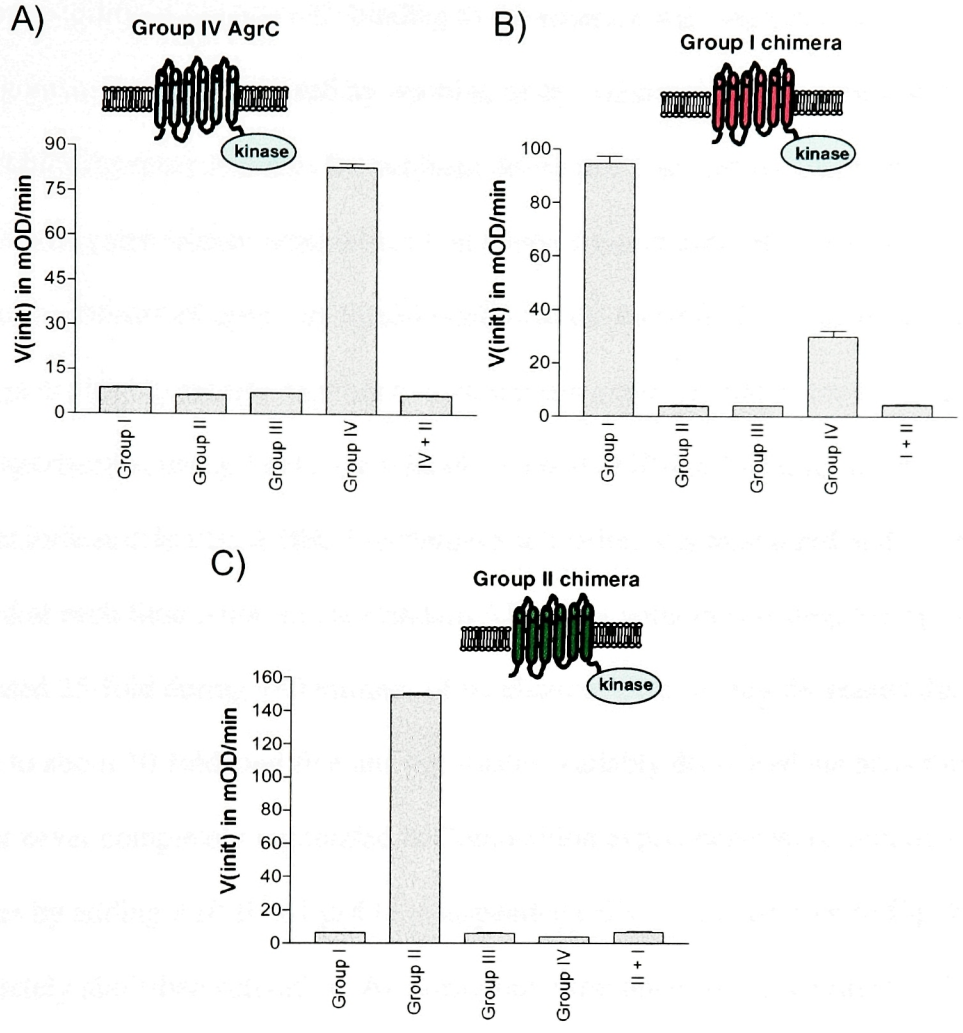

Figure 2.9. Sensor Domain-swapping results. A) Testing of the Group IV receptor with bacterial supernatants from the four *agr* groups, collected as previously described (Lyon et al., 2000). Cross-group inhibition was confirmed by co-incubating cells with AIP-II at 1 μM. **B)** Testing of the Group I chimera with bacterial supernatants from the four *agr* groups. Cross-group inhibition was demonstrated as in (A). **C)** Testing of the Group II chimera with bacterial supernatants from the four *agr* groups. Cross-group inhibition was demonstrated by co-incubating cells with AIP-I at 1 μM. Data were collected as ß-lactamase activity (V_{init} in mOD/min) and are shown ± standard error of the mean (SEM). Unless otherwise visible, error bars are contained within the confines of the border of the bar.

Activation by the native AIP is reversible

Reversibility of agonist AIP binding to the receptor was analyzed by determining whether agonism could be reversed by washing or by competition from added antagonist. As a direct binding assay has thus far not been developed (*vide infra*), functional assays of ligand binding and release were utilized, in which downstream reporter gene activation was used as a read-out of upstream ligand binding at the receptor (Lyon et al., 2000). Such assays are highly sensitive owing to downstream amplification of the binding event. In these experiments, group I cells were incubated with AIP-I at 1 μM, followed by washing as indicated in **Fig. 2.10A.** ß-lactamase activation was monitored and the data normalized at each time point. In the standard AIP assay without washing, the *agr* system was activated 25-fold during 180 minutes of incubation. Two washes decreased the activation to about 10-fold, and five and ten washes variably decreased the activation further but never completely eliminated it. Competition experiments were conducted after two washes by adding AIP-II at 1 μM to resuspended cells. As can be seen in **Fig. 2.10A**, this completely abolished activation. An analogous experiment was performed with group II cells, where it was shown that 40-fold activation was reduced to 15-fold by two washes, and was eliminated by addition of AIP-I at 1 μM. Similar results were obtained when the truncated AIP-II (trAIP-II) was used as the antagonist of group II activation. In this case, 70-fold activation was reduced to 15-fold with two washes and abrogated completely by addition of trAIP-II **(Fig. 2.10B).**

A low level of ß-lactamase activity was consistently observed in all experiments in the absence of added AIP. To test for the possibility that this might be *agr*-dependent, the basal transcription level of the ß-lactamase reporter gene was monitored in the

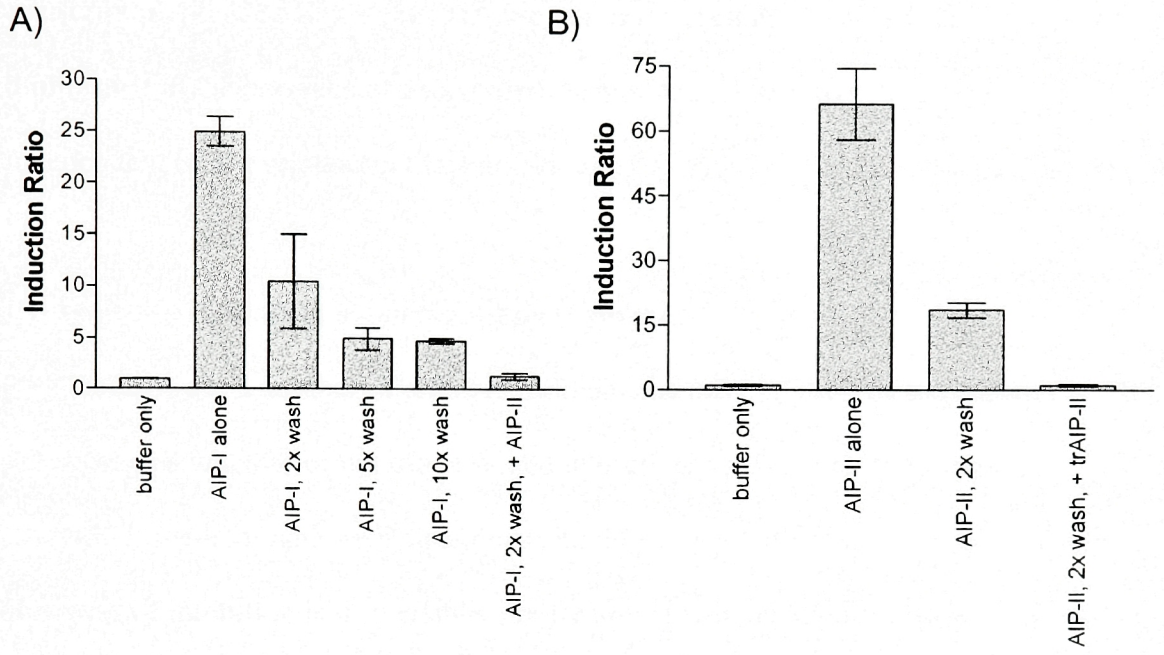

Figure 2.10. Functional binding and competition studies. **A)** Group I cells were activated with buffer or AIP-I at a concentration of 1 μM, followed by washes as indicated. For one set of cells, AIP-II was added after two washes at 1 μM. Data were collected as ß-lactamase activity (V_{init} in mOD/min) and then normalized to an induction ratio (induced/basal). The data points from the final time point of activation (at 210 minutes) were combined from four separate experiments, and are shown ± SEM. **B)** Similar to (A), except that Group II cells were used with AIP-II as the agonist and trAIP-II as the antagonist.

presence or absence of antagonists. Group II cells were incubated for one hour in the absence of agonist, followed by the addition of buffer, AIP-I or trAIP-II (both at 1 μM) and monitoring of ß-lactamase activity and cell density over the next three hours. Basal transcription proceeded at a constant rate per unit of cell mass, and this activity was not diminished in the presence of antagonists, demonstrating that this basal level is independent of *agr* regulation (data not shown).

Cross-group inhibition of *agr* signaling is reversible

There are a number of possible mechanisms for inhibition by the antagonist AIPs depending on whether or not the observed inhibition is reversible. If inhibition is reversible, pre-treatment with antagonist should have no effect on subsequent activation. However, if inhibition is irreversible, pre-treatment with antagonist followed by washout should prevent subsequent activation. This was tested by pre-incubation of group I cells with AIP-II, followed by washing and then challenge with AIP-I. Pre-treatment with the antagonist versus buffer (followed by washing and then addition of agonist) did not affect subsequent activation, as the induction ratios for pre-treatment with buffer versus pre-treatment with antagonist were 14.8 ± 2.7 and 13.9 ± 2.9, respectively (**Fig. 2.11A**). Thus, inhibition is reversible. Varying the time of pre-incubation from 5 minutes up to one hour (or, in the case of activation, from 30 minutes to one hour) gave results similar to those observed in the above experiment.

The kinetics of inhibition were analyzed by titration of AIP-II in the presence of AIP-I. In these experiments, the agonist was added to group I cells five minutes before, simultaneously, or five minutes after the antagonist, followed by a one hour incubation

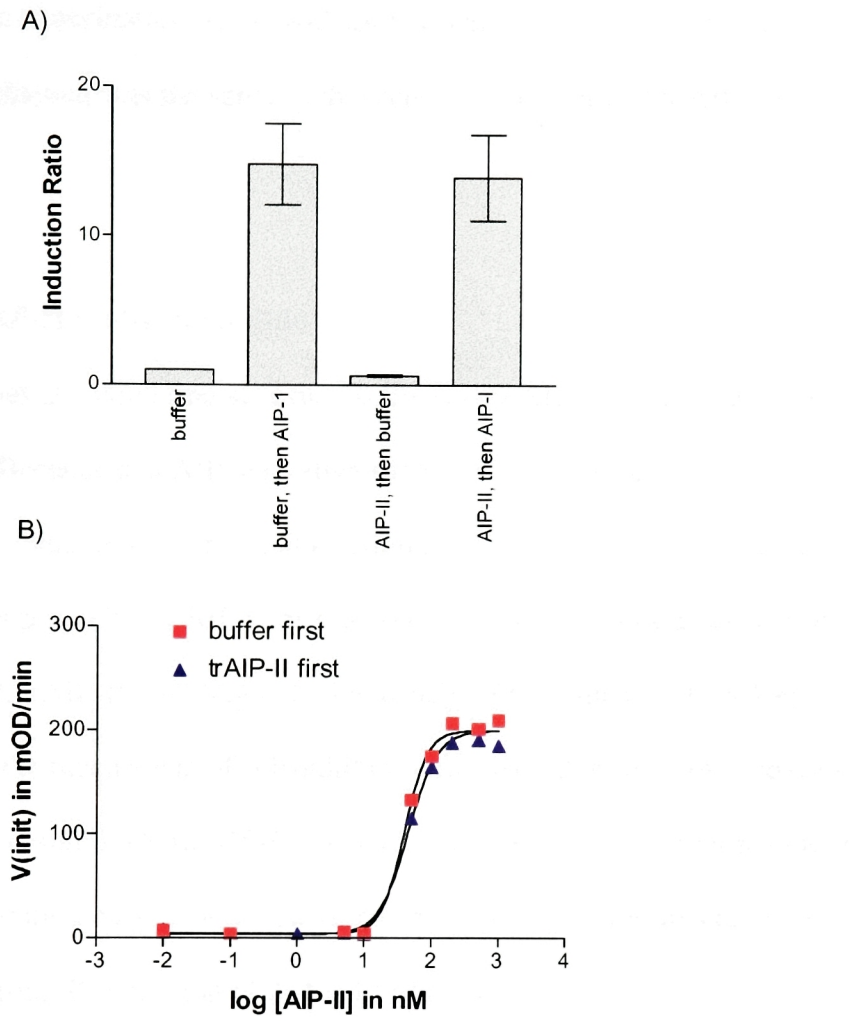

Figure 2.11. Pre-incubation and washing studies. A) AIP-II pre-incubation, followed by washing and subsequent activation of Group I cells with a fixed concentration of AIP-I. Data were collected as ß-lactamase activity (V_{init} in mOD/min) and normalized to an induction ratio (induced/basal). Data are shown ± SEM, and are derived from several timepoints (150, 180 and 210 minutes) combined after normalization. **B)** TrAIP-II preincubation, followed by washing and subsequent activation with AIP-II of group II cells. Data were collected as ß-lactamase activity (V_{init} in mOD/min). Data are shown ± SEM, and, unless visualized, error bars are within the confines of the symbol.

period. Under the conditions used in this experiment, the three curves were indistinguishable within experimental error, with an IC_{50} value of 281 ± 19 nM, and the maximal stimulation achieved was the same as that seen with activation by AIP-I alone (**Fig. 2.12A**).

Self-inhibition by trAIP-II is also reversible

Since trAIP-II has the same ring structure as the native AIP, it is likely to bind to the same receptor site. Because this AIP derivative shows self-inhibition, it was investigated whether its antagonism is reversible, similarly to that of the cross-inhibitory AIPs. Activation of group II cells by AIP-II over a 60 minute incubation was unaffected by prior incubation with trAIP-II, yielding indistinguishable EC_{50} values of 45 ± 5 nM (**Fig. 2.11B**). To probe the mechanism of self-inhibition further, inhibition concentration-response curves were measured where AIP-II was added before, during or after the global inhibitor. The three inhibition curves were indistinguishable within experimental error, with an IC_{50} value for group II inhibition of 244 ± 12 nM (**Fig. 2.12B**).

Pharmacological analysis of concentration-response curves

Agonist concentration-response curves were generated with increasing concentrations of antagonist. Shown in **Figure 2.13A** is an example of this type of experiment, in which AIP-I was used to activate AgrC-I in the presence of [AIP-II] at 0, 10, 100, and 1000 nM. In this example and in other experiments of this type, the agonist curves shifted in a parallel, dextral fashion with increasing concentrations of the antagonist, with no significant effect of the antagonist on the maximum response to the

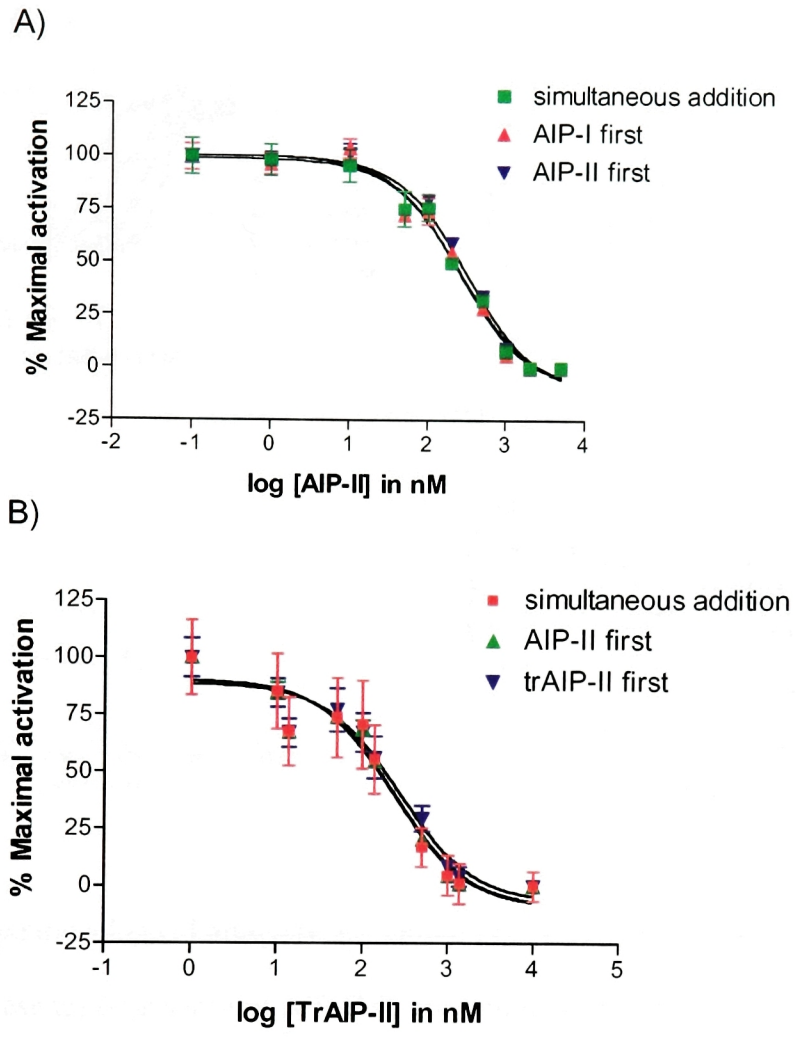

Figure 2.12. Order of addition studies. A) Group I cells were either pre-treated for five minutes with AIP-II at various concentrations, followed by addition of AIP-I at a fixed concentration of 100 nM, or both peptides were added simultaneously. In a third instance, AIP-I was added at a fixed concentration five minutes before titration of AIP-II. **B)** Similar to (A), except that Group II cells were used, with AIP-II as the agonist and trAIP-II as the antagonist. Data were collected as ß-lactamase activity (V_{init} in mOD/min) and then normalized to percentage maximal activation. Data are shown ± SEM.

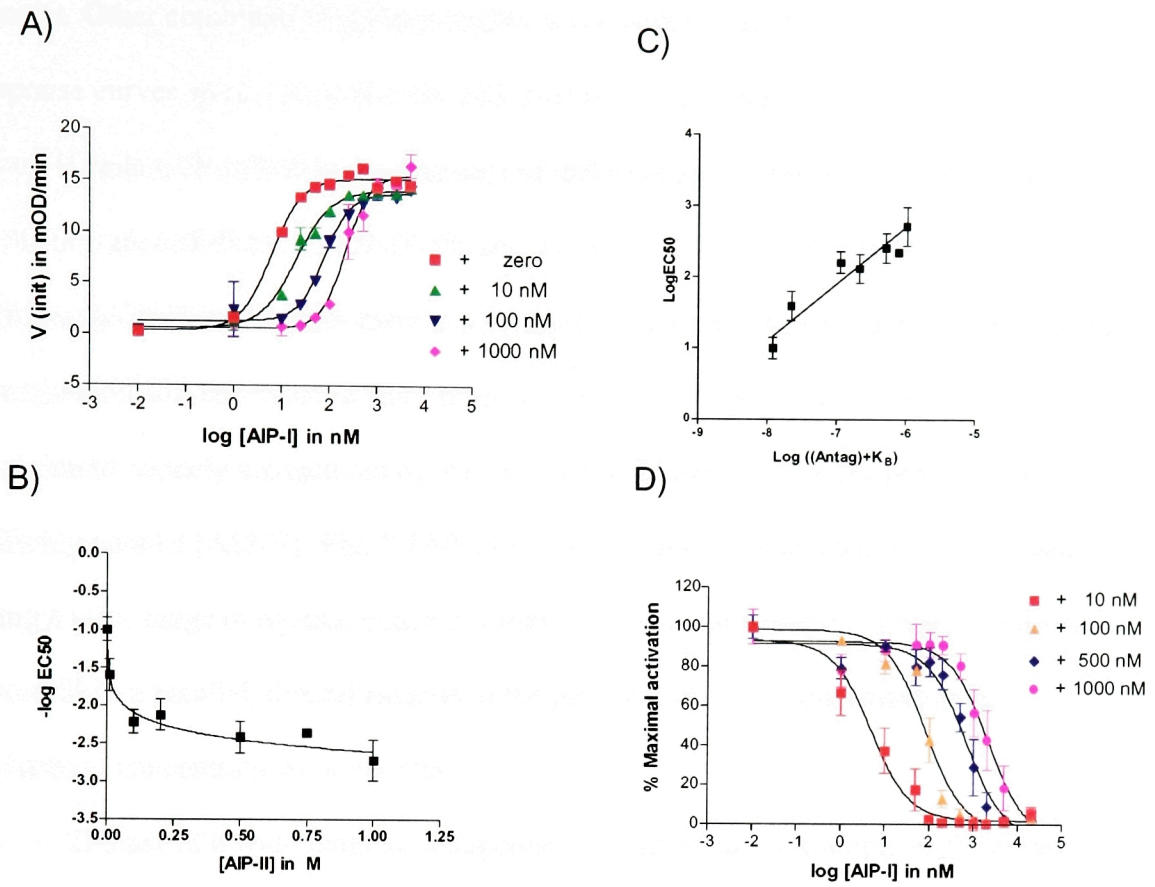

Figure 2.13. Pharmacological analysis. A) Group I cells were treated with varying [AIP-I] in the presence or absence of AIP-II at concentrations indicated as + zero, 10, 100, or 1000 nM. Data were collected as ß-lactamase activity (V_{init} in mOD/min). Data are shown ± SEM. **B)** Non-linear regression analysis (equation 2 in Methods), showing the relationship between antagonist concentration and the shift of the agonist concentration-response curve location parameter (pEC_{50}). Shown on the plot is the nonlinear curve-fit to the data compiled from four separate experiments. **C)** Clark plot, displaying the data from (B) in linear fashion. **D)** Group II cells were treated with varying [AIP-I] in the presence or absence of AIP-II at concentrations indicated as + 10, 100, 500, or 1000 nM.

agonist. Other combinations giving qualitatively similar translocations of concentration response curves were: group II cells with AIP-II in the presence of differing [AIP-I], group II cells with AIP-II in the presence of differing [trAIP-II], group I cells with AIP-I in the presence of differing [trAIP-II], and group I cells with AIP-I in the presence of differing [AIP-II lactam]. As there is a reciprocal relationship between the AIPs in terms of activation and inhibition of their respective groups, we also performed the reciprocal experiment, namely antagonism by AIP-I of AgrC-II activation in the presence of differing agonist [AIP-II]. **Fig. 2.13D** shows representative data from two experiments using a wide range of agonist concentrations. The data show that the inhibition curves also shift in a parallel, dextral fashion in the presence of increasing (maximally-activating) concentrations of agonist.

The use of a wide range of antagonist concentrations in multiple experiments allows for the assessment and quantification of the data according to a model of simple competitive antagonism (equation below and repeated as equation 2 in Methods), using nonlinear regression analysis (Lew and Angus, 1995; Christopoulos et al., 2001).

$$pEC_{50} = -\log([B]^{s} + 10^{-pK}) - \log c$$

where pEC_{50} is the negative logarithm of the EC_{50}, [B] is the antagonist concentration, pK and log c are fitting constants, and *s* is equivalent to the Schild slope factor.

This method provides greater precision than the standard and older linear regression method of Arunlakshana and Schild (Arunlakshana, 1959), for the following two reasons, first, the control curve pEC_{50} values (i.e., absence of antagonist) are included in the analysis, increasing the degrees of freedom; second, the data weighting is more even because the control pEC_{50} values are treated equally to all other pEC_{50} values; in

contrast, the Schild method relies heavily on the determination of the "concentration-ratio", which could be overly and incorrectly biased by a poorly defined control agonist curve. Importantly, an advantage of all analyses based on the method of Schild and its variants is that the determination of the Schild slope parameter (*s* in the above equation) tests the conformity of the data to a competitive model while the pK parameter allows for the quantification of antagonist potency when the slope is equal to one.

Concentration response curves of Group I cells with AIP-I in the presence of differing [AIP-II] were analyzed. **Fig. 2.13B** shows the relationship between antagonist concentration and the shift of the agonist concentration-response curve location parameter (pEC_{50}) with data combined from four experiments. Also shown on the plot is the nonlinear curve-fit to the data. The equation with the variable Schild slope parameter generated the better fitting curve, as judged by the extra sum of squares test, with a P value of 0.016. The slope value obtained in this case was 0.55 ± 0.14, which is significantly less than the value of unity seen with simple competitive inhibition. The results from the nonlinear regression analysis can be displayed in linear fashion in the form of a Clark plot **(Fig. 2.13C)** (Stone and Angus, 1978; Lew and Angus, 1995). Because the data did not conform to simple, competitive antagonism, pK_B could not be estimated. However, an estimate of antagonist potency, pA_2, could be obtained (see Methods), and this value was 8.90.

The Schild slopes, p values and pA_2 values obtained from various analogs tested on AgrC-I or -II are summarized in **Table 2.4**. It is notable that in all cases tested, the Schild slope values are considerably less than the value of unity normally seen with simple competitive antagonism. Thus, the application of a competitive model of agonist-

Table 2.4. Schild slopes, pA_2 values, and EC_{50} values

Group I inhibition[a]				
AIPs	**slope**	**P value**	**pA_2**[c]	**IC_{50}**[d]
AIP-II	0.55 ± 0.14	0.016	8.90	40 nM (12-140)
AIP-II Lactam	0.71 ± 0.09	0.012	7.60	155 nM (75-315)
trAIP-II	0.62 ± 0.05	0.130	6.50	260 nM (95-695)
Group II inhibition[b]				
AIPs	**slope**	**P value**	**pA_2**[c]	**IC_{50}**[d]
AIP-I	0.45 ± 0.09	0.004	9.70	25 nM (14-45)
trAIP-II	0.55 ± 0.09	0.005	7.50	230 nM (190-270)

[a, b] All experiments were performed at least in duplicate, yielding concentration-response curves in the presence of at least five different antagonist concentrations. Curves were generated with either the Schild slope held constant at unity or with the slope allowed to vary, and the better-fitting model was determined by an extra-sum-of-squares test using PRISM. In this test, a P value < 0.05 indicates a slope value significantly less than one. In the case of trAIP-II group I inhibition, the p value was trending toward <0.05.

[c] The pA_2 is an estimate of antagonist potency, irrespective of underlying mechanism, determined via the relationship, $pA_2 = pK/s$ (Christopoulos et al., 1999).

[d] The IC_{50} values from bioassays are shown, with their 95% CI in parentheses, for comparison to the pA_2 values, thus revealing a trend between biological activity of the inhibitors and their empirical binding estimates.

antagonist interactions to the data reveals significant deviations from the predictions of simple competition. As a consequence, estimates of antagonist dissociation constants (pK_B values) cannot be obtained, but empirical estimates of antagonist potency, pA_2, are still possible and at least provide a semi-quantitative basis for comparing antagonist activities. The pA_2 values are consistent in their trend with the IC_{50} values for inhibition by various analogs (**Table 2.4**), albeit with the relatively wide 95% confidence intervals for the IC_{50} values (reflecting the inherent sources of error in this assay- see Methods) and the errors associated with the Schild slope determinations. This provides suggestive evidence that the differences in IC_{50} values between these analogs results from decreased binding to the receptor, rather than from post-binding effects on receptor activation.

On the basis of sequence similarities to other bacterial RHKs that are known to be dimeric (Stock et al., 2000) along with structural homology modeling (*vide infra*), it is very likely that AgrC is also dimeric with two agonist binding sites. Therefore, it is possible that the competitive interactions of agonist and antagonist at the receptor might involve cooperativity between the binding sites (see **Figure 2.14** for a model of this process). For example, an allosteric change induced upon binding of antagonist to one sensor domain in a dimer could inhibit binding of antagonist to the second, in addition to directly competing with the agonist at the first domain. Such negative cooperativity between antagonist molecules would make the antagonists appear less potent at higher concentrations, thus yielding a Schild slope substantially less than 1.0. A similar type of cooperativity has been observed in the chemotactic aspartate receptor (Koshland, 1996), which lends indirect support to this hypothesis.

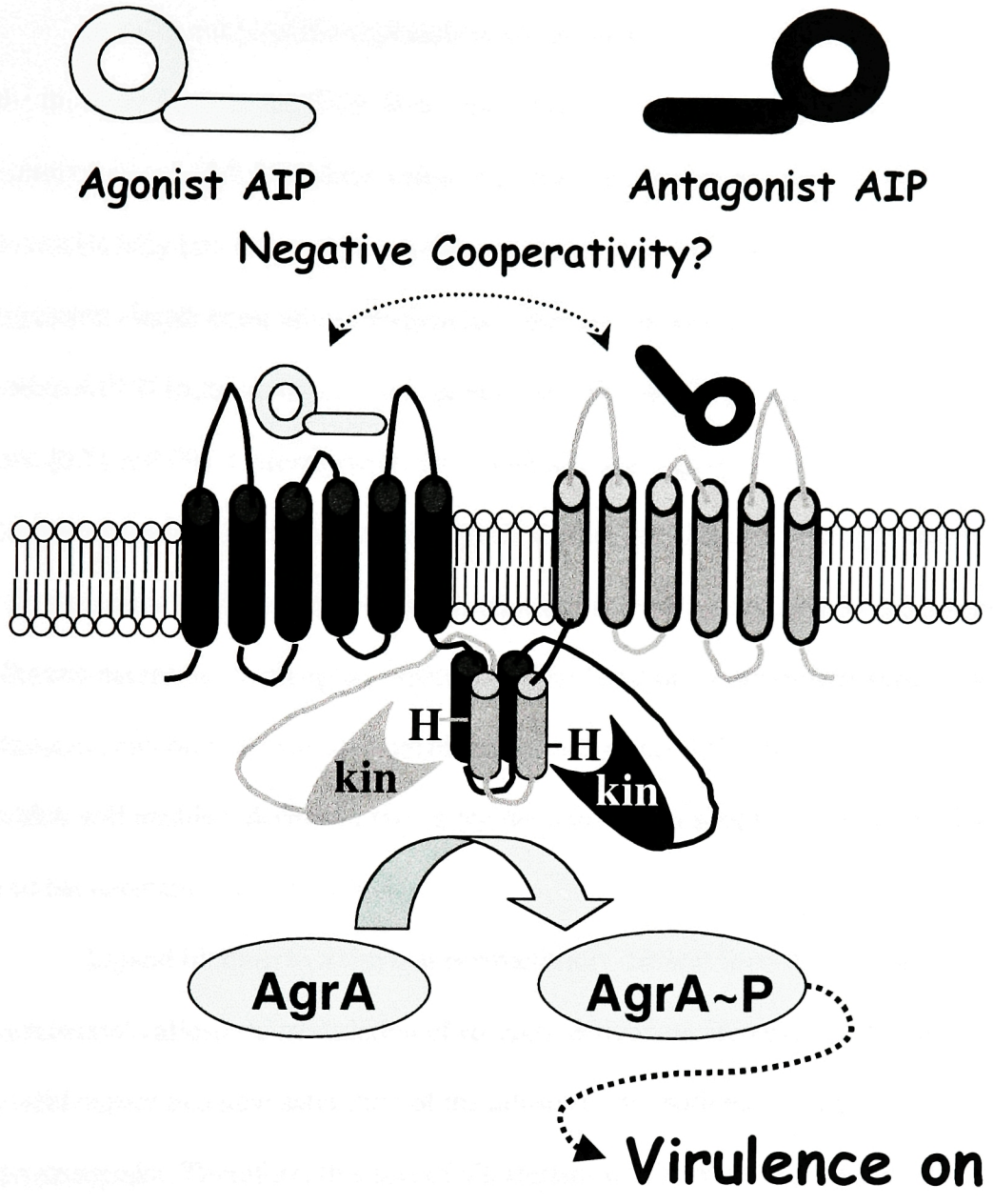

Figure 2.14. A putative model of AgrC, indicating the dimeric nature or the receptor, mediated via a cytoplasmic 4-helical bundle and possibly via interaction between the sensor domains, which themselves each have six transmembrane helices. The pharmacological data suggest possible allosteric negative cooperativy between the binding sites in a receptor dimer.

A different possible explanation for the observed Schild slopes is the lability of the thioester bond in the AIPs. It is well-documented that drug-removal mechanisms are a common cause of Schild slope values less than one (Kenakin, 1997). If the slope values are artificially low due to AIP breakdown, the agonist-antagonist interaction could represent simple competitive antagonism after all. However, experiments utilizing the stable AIP-II lactam analog as antagonist still yielded a slope value significantly less than one (0.71 ± 0.09). Unfortunately, all available potent agonists contain a labile thioester bond by necessity, thus making it difficult to rule out definitively drug-removal and/or other possible explanations. Further studies in this area are focused on confirming the dimeric nature of the receptor, especially at the level of the transmembrane sensor domains, and on the continued development of a direct AIP binding assay (*vide infra*), which will enable a definitive test of the deviation from simple competitive antagonism and the determination of its basis.

Ligand binding to a site that is structurally distinct from the primary site can lead to reversible allosteric modulation of receptor activation. However, in this instance, one would expect eventual saturation of the allosteric site with increasing concentrations of the antagonist. Therefore, this sort of allosterism would result in a rightward shift of the curves similar to competitive antagonism, but, unlike the latter, a maximal shift would be obtained when the allosteric site becomes saturated (Kenakin, 1997). The concentration-response curves in this study were generated in the presence of increasing antagonist concentrations that spanned a 1000-fold range. In no instance was a maximal, limiting, shift demonstrated, a finding which is inconsistent with a mechanism of allosteric modulation from a separate site on the receptor.

The lactam analog of AIP-II is an agonist at high concentrations

A central question of this research revolved around whether the AIPs bind covalently to AgrC, given their highly reactive thioester linkage. The above pharmacology data suggest that a stable covalent linkage does not form between AIP and receptor, although the data do not necessarily rule out a transient covalent linkage. A previous study speculated that a stable or transient covalent linkage might occur, as supported by the inactivity of a lactam analog tested up to a concentration of 10 μM (Mayville et al., 1999). As the pharmacology data are inconsistent with stable covalency, the lactam analog was re-tested at higher concentrations. As shown in **Figure 2.15A**, starting at around 10 μM, activation increases linearly with increasing concentrations of AIP-II lactam. The lactam analog was also tested for its ability to cross-inhibit group I and IV cells and to self-inhibit group II cells. Potent cross-inhibition was observed, with an IC_{50} value of 140 ± 70 nM for Group I and 48 ± 22 nM for Group IV, consistent with previous results (Mayville et al., 1999). Significant self-inhibition was not detected at any concentration tested up to 20 μM. These results suggest that the lactam analog binds to its own receptor extremely weakly, although it binds heterologous receptors quite strongly. This suggests that activation of AgrC requires very specific AIP-receptor interactions, while cross-inhibiton does not. This will be addressed further in the Discussion.

The activation seen with the lactam analog was unusual in that the Hill slope of activation was shallower as compared to AIP-II and a maximal activation level, i.e. a plateau, was not observed up to the solubility limit of the peptide. Thus, it was uncertain

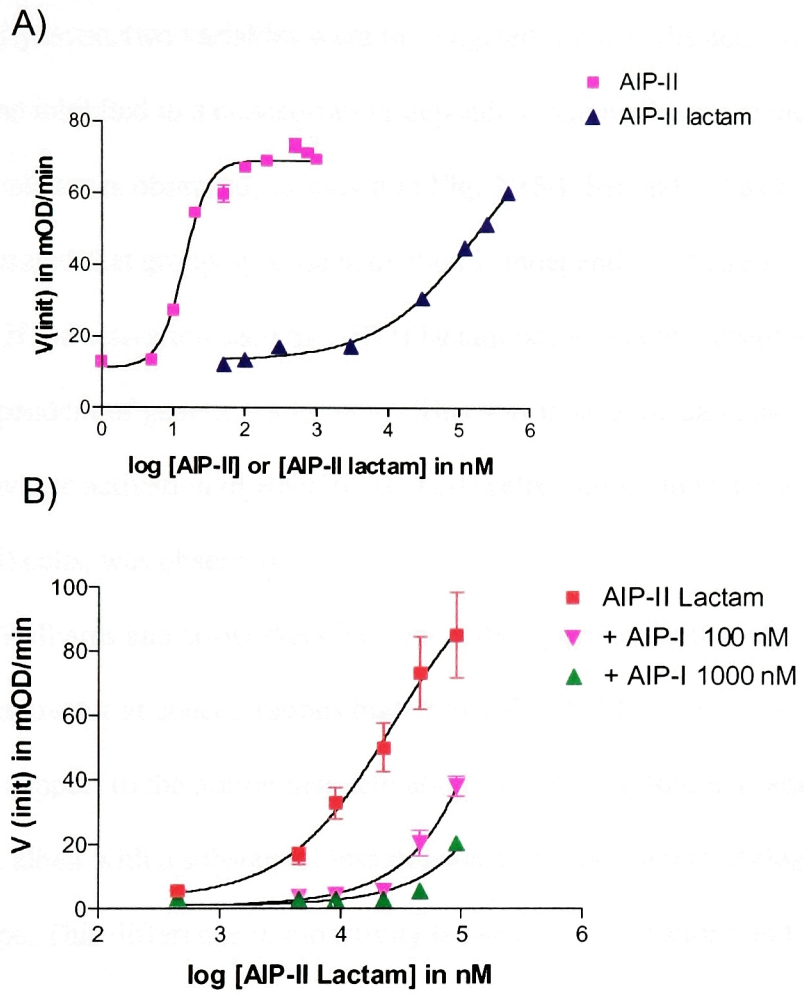

Figure 2.15. AIP-II lactam studies A) Group II cells, RN9372 (CA2-II), were incubated with varying [AIP-II lactam]. The AIP-II concentration-response curve is shown for comparison. **B)** Cells expressing Group II *agrC-A* in an *agr*-null group I background, RN9367 (CA2-I), were incubated with the AIP-II lactam analog at various concentrations in the absence or presence of AIP-I at 0, 100, or 1000 nM. Data were collected as ß-lactamase activity (V_{init} in mOD/min) and are shown ± SEM.

whether the activation by the lactam analog was truly specific to the receptor or a result of non-specific effects of the peptide at such high concentrations. In order to address this specificity issue, two variables were investigated. First, if the activation were specific, it should be inhibited in a concentration-dependent manner by the antagonist, AIP-I. This is exactly what was observed, as shown in **Fig. 2.15B**. Second, it has been previously demonstrated that group-specific activation is independent of strain background (see above). If the activation seen by AIP-II lactam occurs via the receptor, then it should also be independent of genetic background. This was indeed the case, as is shown in **Figure 2.15B**, where activation of RN9367 (CA2-I) cells, similar to that seen with RN9372 (CA2-II) cells, was observed.

Williams and co-workers have recently reported that the AIP-I lactam analog is also an activator at concentrations higher than 5 μM (McDowell et al., 2001), thus lending support to the notion that activation by the AIPs does not require the thioester linkage, albeit with a substantial loss in potency for the lactam analogs and a shallower Hill slope. This difference in bioactivity between the thiolactone and lactam analogs is partially explained by dramatic differences in their structures in solution, as characterized by 2D NMR (*vide infra*).

Attempts to Detect AIP-I Binding to AgrC-I

As an initial foray into the detection of an AIP-receptor complex, a previously published pull-down experiment ((Ji et al., 1995) and see Introduction) was re-visited. A cell line, RN8559, overexpressing AgrC from a ß-lactam inducible promoter (via BlaR signaling) was utilized to investigate AIP binding (**Figure 2.16A&B**). As in the previous

study, different amounts of induced cells were added to a fixed concentration of AIP for five minutes, followed by spin-down of the cells and recovery of the supernatant. This supernatant was then assayed on a reporter strain, in this case, the group I RN9222 strain, for any remaining AIP activity. In this experiment, the AIP was synthetic, rather than purified from bacterial supernatants, as in the published study (Ji et al., 1995). In confirmation of previous results, increasing amounts of cells titrated out AIP-I, as assessed by remaining biological activity (**Figure 2.16C**). In contrast, attempting to use the group I reporter strain, RN9222, or *agr*-null cells, RN6911, did not result in any titration of AIP-I, indicating that overexpression of AgrC is critical for significant and detectable AIP-I depletion. An alternative explanation is that treatment of the cell line, RN8559, with methicillin results in physiological changes to the cell wall that cause increased uptake or non-specific binding of AIP-I to the cells. According to the previous study (Ji et al., 1995), the same cell line expressing AgrA alone and also treated with methicillin did not titrate AIP-I, thus indicating that methicillin treatment is not the cause of increased AIP-I binding. This control was not repeated in the present study, although it probably should be repeated in future experiments involving this cell line.

AIP-I was labeled with fluorescein to undertake fluorescence studies of AIP binding to AgrC+ cells, RN8559 and RN9222 (**Figure 2.17A** and *vide infra* for biological activity data). However, endogenous and variable auto-fluorescence, with a maxima near to the fluorescein emission wavelength, of *S. aureus* cells complicated the interpretation of the resulting data, as assessed by fluorescence spectroscopy and microscopy (not shown). SDS-PAGE analysis, followed by in-gel fluorescence detection, of whole cell lysates from bacterial cultures pre-treated with fluorescein-AIP-I or buffer

A) ***S. aureus*** **cells overexpressing AgrC**

Plasmid: pBla---AgrC

Chromosome: pBla---ß-lactamase

Addition of methicillin induces ß-lactamase production via transcriptional induction of the pBla promoter.

B)

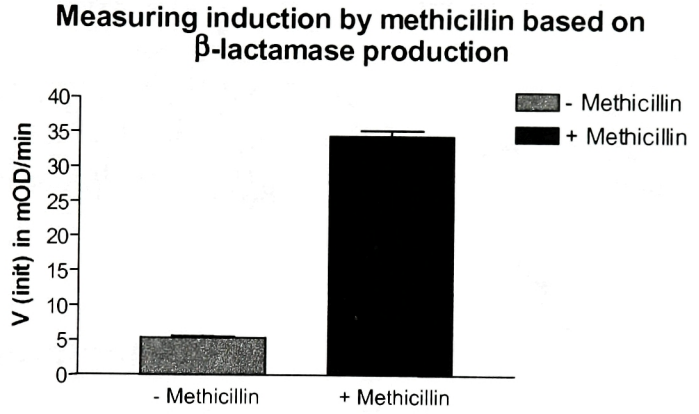

C)

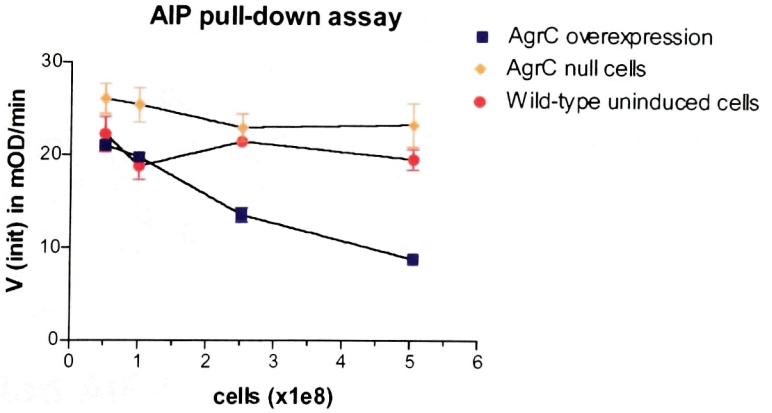

Figure 2.16. AgrC over-expression. A) A cell line overexpressing AgrC from a plasmid in response to a ß-lactam compound was investigated for use in a direct binding assay. **B)** After methicillin induction, the production of ß-lactamase from the chromosomal pBla promoter was monitored as an indirect readout of plasmid pBla activity, leading to AgrC over-expression. **C)** AgrC-I overexpressing cells (RN8559), *agr*-null cells (RN6911) and uninduced AgrC-I expressing cells (RN9222) were titrated with a fixed amount of AIP-I, followed by spin-down and bioassay of supernatants. Control experiments quantitating the bioactivity of the same amount of AIP-I in the absence of cells showed little to no depletion of AIP-I by the addition of the *agr*-null cells.

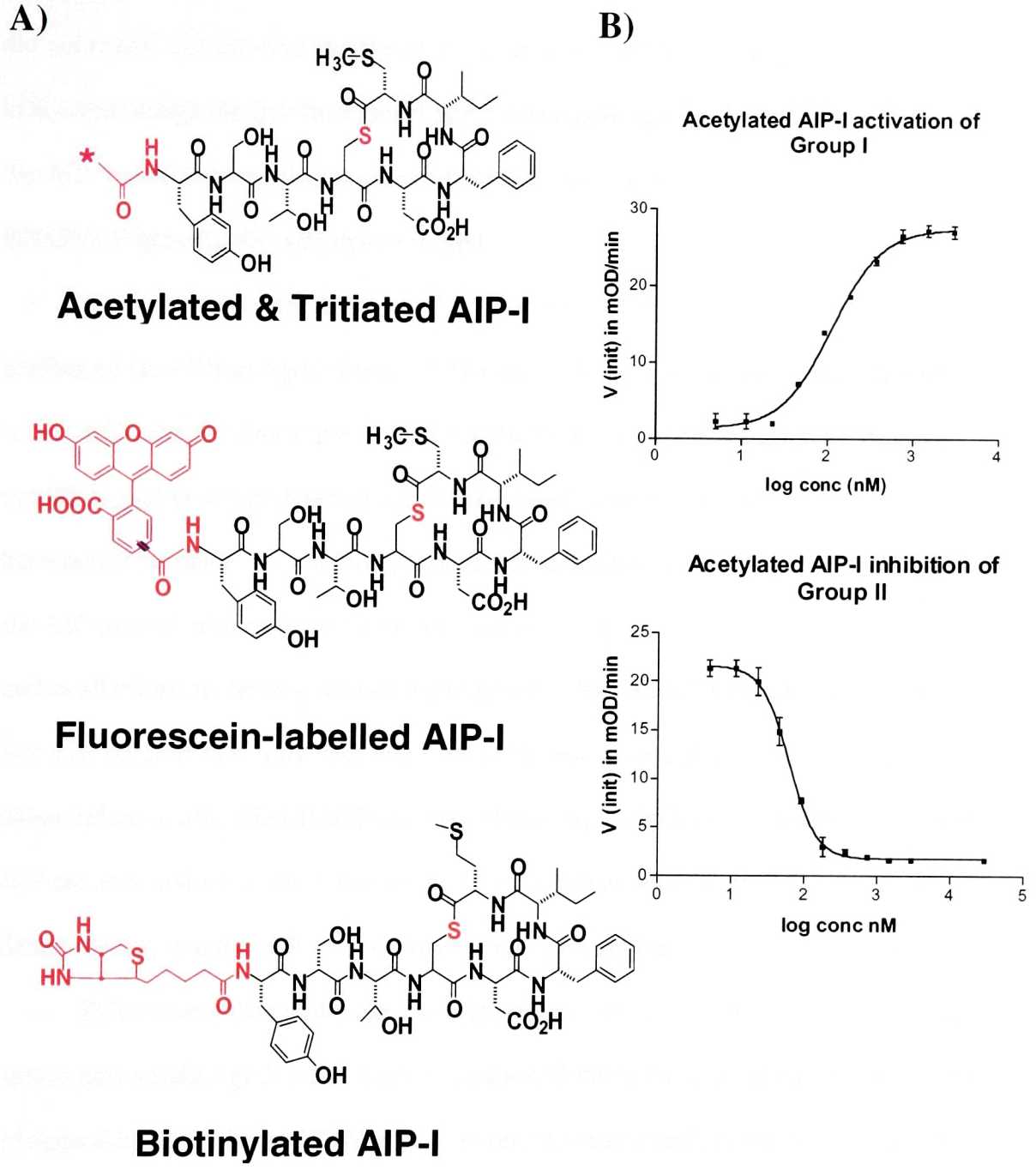

Figure 2.17. AIPs for Direct Binding Assays. A) The structures of various N-terminally modified AIPs are shown. An asterisk * indicates the site of tritium [^{3}H] incorporation in acetylated AIP-I. **B)** Dose-response curves show activation of group I and inhibition of group II by acetylated AIP-I. Similar analyses were performed with the tritiated and/or otherwise N-terminally modified analogs, yielding similar results, albeit with slightly different EC_{50} and IC_{50} values.

did not reveal a fluorescent protein of the approximate molecular weight of AgrC, ~50 kDa, even though the free fluorescent AIP-I was readily detected and *agr*-activation of the AIP-treated cultures (in the case of RN9222) or ß-lactamase induction (in the case of RN8559, **Figure 2.16B**) was demonstrated.

Furthermore, biotinylated AIP-I was utilized in efforts to demonstrate covalent binding of the AIPs to AgrC (**Figure 2.17A** and *vide infra* for bioassay data). In cell lysates of bacterial cultures pre-treated with biotinylated-AIP-I or buffer, no AgrC-specific signal was ever detected via Western blotting with streptavidin-conjugated horseradish peroxidase, even though parallel experiments demonstrated *agr*-activation in the AIP-treated cultures (data not shown). As the receptor, AgrC, was not epitope-tagged and as all efforts to develop an anti-AgrC antibody have thus far failed (*vide infra*), it is formally possible that AgrC was degraded or otherwise absent from the cell lysates, either before or after SDS-PAGE analysis. However, the lack of detection of a covalent AIP-receptor adduct by the above methods is consistent with the pharmacology results demonstrating that the AIP-receptor interaction is reversible.

Efforts were then undertaken to prepare radioactively labeled AIPs for binding assays with whole AgrC+ cells. Radioiodination of the tyrosine amino acid in AIP-I was attempted (by B. Ayers and T. Muir); however, this was abandoned due to extremely facile hydrolysis of the thioester linkage in the AIPs during the labeling procedure (data not shown). Acetylation in solution of the N-terminus of AIP-I with tritiated acetic anhydride, followed by hydrophobic column chromatography, produced a pure, tritiated AIP-I, which was shown to activate *agr* in group I cells (**Figure 2.17A&B** and not

shown). However, whole cell binding assays, utilizing filter binding or cell pelleting methods, yielded mixed results, mainly due to a high level of non-specific binding of AIP-I in parallel with low specific activity of the radioligand and unknown receptor expression levels. For example, in some experiments, binding of tritiated AIP-I to cells overexpressing AgrC appeared to be greater than in uninduced or *agr*-null cells (**Figure 2.18A&B**). This difference was reproducible with uninduced versus induced RN8559 cells. However, the difference between induced RN8559 cells and *agr*-null RN6911 cells was not reproducible and, in fact, indicated more binding to RN6911 cells on one occasion, despite considerable efforts to equalize cell densities between the different populations. Furthermore, attempts at competition with cold non-radioactive AIP-I or –II actually increased the amount of tritiated AIP-I bound to the cells (**Figure 2.18B**), a result inconsistent with receptor-specific binding of tritiated AIP-I. In binding experiments comparing *agr*+ RN9222 cells with *agr*-null RN6911 cells, no difference in binding of tritiated AIP-I was ever detected, a result consistent with the pull-down experiments (*vide supra*). Successful development of a direct radioactive binding assay may hinge upon the use of radioligands with much higher specific activities; overexpression of an epitope-tagged receptor using a metal ion-inducible promoter such as cadmium, instead of a cell wall disrupting drug like methicillin (which could indirectly lead to an increase in non-specific binding); and/or enrichment of receptor levels through the use of bacterial cell membrane preparations or liposomal reconstitution.

A)

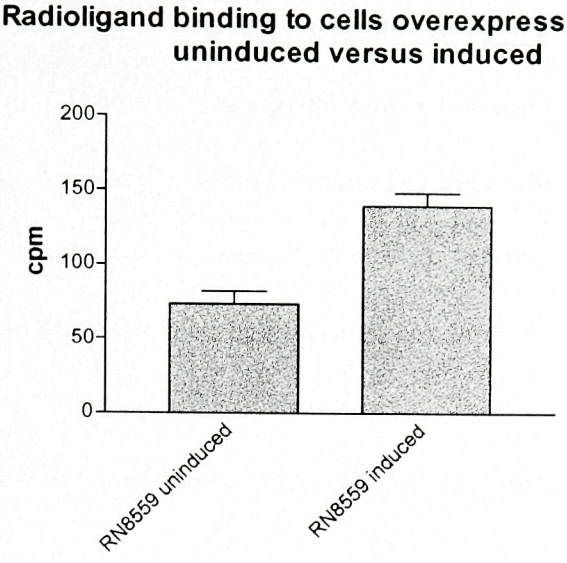

B)

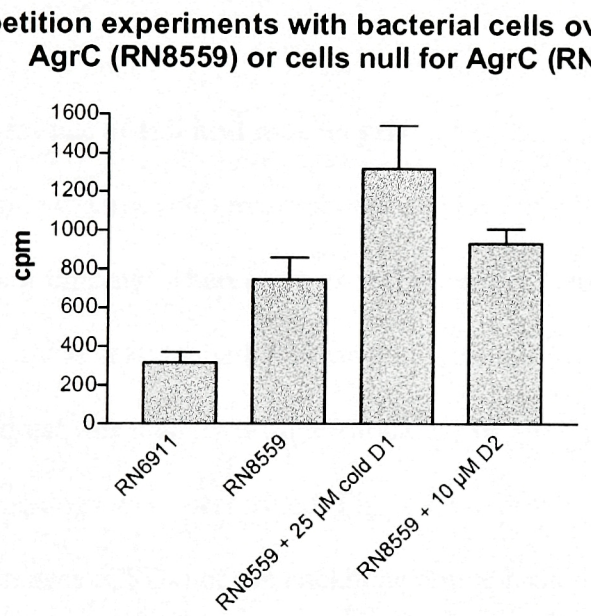

Figure 2.18. Whole cell binding assays. A) RN8559 cells (± methicillin induction and corrected for cell density differences) were incubated with tritiated AIP-I at 1 µM for 20 minutes, followed by spin-down, washing, and radioactive counting of the pellet. **B)** Binding of tritiated AIP-I to induced RN8559 cells was higher than binding to *agr*-null cells, RN6911. The same binding experiments with RN8559 cells were conducted with a ten-minute competition with a large excess of non-radioactive (cold) AIP-I (DI) or AIP-II (D2). These results are counter-intuitive, as one should expect to observe decreased binding of radioactive AIP-I in the presence of cold AIP-I (see Results).

Section 2.4 -- Key Determinants of Receptor Activation in the AIPs

AIP-induced receptor activation proceeds through specific, reversible and extracellularly-mediated AIP binding to the sensor domain of AgrC, followed by receptor activation. A central question therefore revolves around which components (or determinants) in the AIPs are important for receptor binding and/or activation. Toward this end, a chemical approach was taken to analyze the AIPs, complemented by a genetic approach to analyze the receptor (this section and section 2.5). This powerful combination of chemistry and genetics has yielded new insights into AIP-induced receptor activation.

Structural independence of tail and macrocycle

Endocyclic (within macrocycle) hydrophobic residues in AIP-II appear to be important for receptor binding, whereas an exocylic residue (asparagine) is important for receptor activation. It was asked whether these two regions of the peptide are structurally independent. To address this idea, two-dimensional NMR studies of AIP-II, trAIP-II and alanine-substituted analogs were performed. **Fig. 2.19A** shows a comparison of the chemical shift differences (CSDs) of the backbone amide protons of AIP-II alanine analogs (determined in 90% H_2O/10% D_2O, pH 4.0) relative to the native AIP-II. Substitution with alanine at any position slightly affects the CSDs surrounding the site of modification, without affecting other regions of the peptide backbone. The trend exhibited for the amide protons also holds true for the alpha and beta protons (see **Appendix 1** for all NMR chemical shift assignments), thus suggesting that the side-chains in the tail of AIP-II do not influence the backbone and sidechain structure of

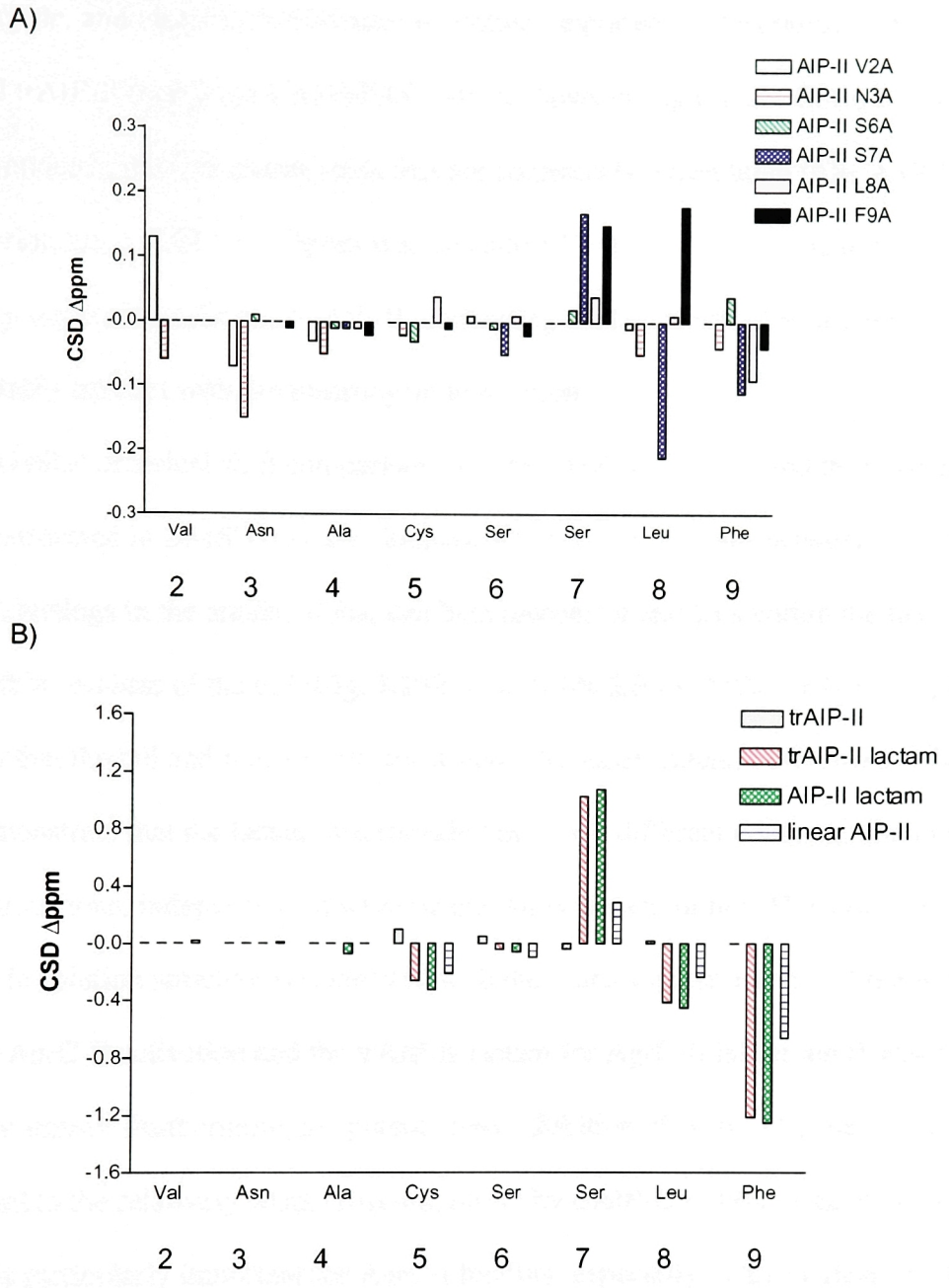

Figure 2.19. Chemical shift comparisons of AIP analogs. A) The backbone amide ^{1}H chemical shifts of AIP-II alanine analogs are depicted as chemical shift differences (CSDs) relative to native AIP-II normalized to zero (performed in 90% H_2O/10% D_2O, pH 4.0 at 298 K) **B)** The backbone amide ^{1}H chemical shifts of trAIP-II thiolactone, AIP-II lactam, trAIP-II lactam and the linear free acid version of AIP-II are depicted as chemical shift differences (CSDs) relative to native AIP-II normalized to zero (performed in DMSO-d_6 at 298 K).

the macrocycle, and vice-versa. This idea is further supported by the comparison between AIP-II and trAIP-II (performed in DMSO), which shows no significant CSDs between the two peptides in the five amino acids that are common between them **(Fig. 2.19B).** In these experiments, a CSD > 0.1 Δppm was considered significant. These results collectively suggest that the tail of AIP-II, containing the key asparagine at position 3, does not stably interact with the macrocycle in solution.

A similar chemical shift comparison between AIP-II, trAIP-II and their lactam analogs (performed in DMSO) reveals dramatic CSDs (>>0.1 Δppm) between the thiolactone and lactam analogs in the amide, alpha, and beta protons of residues within the macrocycle but not within residues of the tail (**Fig. 2.19B**, and **Table 2.5** for AIPs synthesized), further suggesting that the tail and macrocycle are structurally independent. Furthermore, these results demonstrate that the lactam macrocycle has a very different conformation in solution than the thiolactone, independent of whether the tail is present or not. This dramatic difference in solution structure is correlated with the much weaker activity of the AIP-II lactam for AgrC-II activation and the trAIP-II lactam for AgrC-II inhibition (Lyon et al., 2002) (*vide supra*). Furthermore, the potent cross-inhibition of AgrC-I by the AIP-II lactam, as compared to the relatively weak cross-inhibition by trAIP-II lactam, suggests that the tail of AIP-II is particularly important for AgrC-I binding, especially in the context of a lactam analog. This is supported by the decrease in potency of the thiolactone trAIP-II in comparison to AIP-II for cross-group inhibition (see **Table 2.6** for IC_{50} values).

Table 2.5. AIPs and derived analogs

AIPs	exocyclic[1]				endocyclic					mass expected	mass observed
AIP-I		Y	S	T	C [2]	D	F	I	M	961.1	960.9
AIP-I D5N		Y	S	T	C	N	F	I	M	960.1	959.9
AIP-IV		Y	S	T	C	Y	F	I	M	1009.2	1008.9
AIP-IV Y5F		Y	S	T	C	F	F	I	M	993.2	992.9
AIP-I D5A		Y	S	T	C	A	F	I	M	917.1	916.9
AIP-I M8I		Y	S	T	C	D	F	I	I	943.1	942.9
Acetyl-AIP-I	ac	Y	S	T	C	D	F	I	M	1003.2	1003.0
Biotinylated-AIP-I	bi	Y	S	T	C	D	F	I	M	1187.4	1186.9
Fluorescein-AIP-I	fl	Y	S	T	C	D	F	I	M	1319.4	1318.8
AIP-I linear free acid		Y	S	T	C	D	F	I	M	979.1	978.9
trAIP-I				ac	C	D	F	I	M	651.8	652.0
trAIP-IV				ac	C	Y	F	I	M	699.9	700.0
trAIP-I D2A				ac	C	A	F	I	M	607.8	607.0
AIP-II	G	V	N	A	C	S	S	L	F	879.0	878.9
trAIP-II				ac	C	S	S	L	F	578.7	579.0
AIP-II lactam	G	V	N	A	X [3]	S	S	L	F	861.9	862.0
AIP-II linear free acid	G	V	N	A	C	S	S	L	F	897.0	896.4
AIP-II/I	G	V	N	A	C	D	F	I	M	951.1	951.0
AIP-I/II		Y	S	T	C	S	S	L	F	889.0	889.0
AIP-III			I	N	C	D	F	L	L	819.0	818.9
AIP-III octapeptide		Y	I	N	C	D	F	L	L	982.2	981.9
AIP-III nonapeptide	A	Y	I	N	C	D	F	L	L	1053.2	1052.9

ac: acetylation; bi, biotinylated; fl, fluorescein-conjugated

[1]exocyclic residues are shaded in the table; [2]All of the peptides with a conserved cysteine contain a thiolactone formed via the condensation of the α-carboxyl group of the AIPs with the sulfhydryl group, except for AIP-I and -II linear free acid, which have a C-terminal carboxylic acid and a free thiol group; [3]X=Dapa: diaminopropionic acid

Table 2.6. AIP activity on the four *agr* groups of *S. aureus*

	Activation (EC_{50})				Inhibition (IC_{50})			
AIPs	AgrC-I	AgrC-II	AgrC-III	AgrC-IV	AgrC-I	AgrC-II	AgrC-III	AgrC-IV
AIP-I	30 nM (20-50)	-	-	26 μM (23-29 μM)		25 nM (14-45)	3 nM (2-5)	
AIP-I D5N	90 nM (60-130)	-	360 nM (280-450)	-		32 nM (20-50)		20 nM (15-30)
AIP-IV	62 nM (50-75)	-	-	13 nM (7-40)		4 nM (3-5)	1 nM (0.5-3)	
AIP-IV Y5F	10 nM (1.5-30)	-	-	14 nM (7-24)		2 nM (1.5-3)	0.2 nM (0.05-0.3)	
AIP-I D5A	-	-	-	-	5 nM (3-7)	8 nM (4-17)	0.3 nM (0.2-0.4)	3 nM (2-5)
AIP-I M8I	30 nM (20-45)	-	-	730 nM (640-820)		13 nM (8-20)	8 nM (7-9)	
AcAIP-I	98 nM (56-173)	-	-	-		60 nM (50-70)	12 nM (8-18)	
Linear AIP-I	-	-	-	-		540 nM (500-590)	190 nM (150-240)	
trAIP-I	5.8 μM (3-10 μM)	-	-	-	4.5 μM (3.5-6 μM)	47 nM (40-55)	240 nM (40-1200)	
trAIP-IV	-	-	-	-	930 nM (570-1521)	8 nM (6-10)	10 nM (5-22)	4.1 μM (3-5.5 μM)
trAIP-I D2A	-	-	-	-	5 nM (3-7)	5 nM (3-8)	0.1 nM (0.03-0.2)	5 nM (4-6)
AIP-II	-	30 nM (10-90)	-	-	40 nM (12-140)		1 nM (0.7-2.6)	86 nM (65-111)
trAIP-II	-	-	-	-	260 nM (95-695)	230 nM (190-270)	4 nM (3-5)	150 nM (90-260)
Linear AIP-II	-	-	-	-				
AIP-II/I	-	-	-	-	510 nM (360-810)	70 nM (33-147)	350 nM (290-420)	9.9 μM (6-16 μM)
AIP-I/II	-	-	-	-	10 nM (6-15)	230 nM (140-370)	0.3 nM (0.2-0.4)	12 nM (9-15)
AIP-III	-	-	26 nM (22-31)	-	70 nM (30-150)	6 nM (5-6.5)		150 nM (104-207)

The dash ( ) indicates no activity at any concentration tested up to at least 10 μM. It is worth noting that AIPs that are full agonists cannot simultaneously be antagonists.

Furthermore, chemical shift assignments (in DMSO) of the linear free acid version of AIP-II (see **Table 2.5** sequence) reveals dramatic CSDs in comparison to AIP-II, thus highlighting the necessity for the presence and appropriate structure of the AIP-II macrocyle for potent agonist activity (**Fig. 2.19B**). Similarly large structural differences were observed between the linear free acid version of AIP-I and native AIP-I (see **Appendix 1** for chemical shift assignments and **Table 2.5** for peptide sequences).

Structural independence was also examined between the macrocycle and tail of AIP-I and AIP-IV. Two-dimensional NMR was performed on full-length AIP-I and –IV and compared to their truncated analogs, trAIP-I and trAIP-IV (see **Table 2.5** and **Appendix 1**). The CSDs in the amide, alpha and beta protons were never any greater than 0.3 Δppm and were in most instances less than 0.1 Δppm. This outcome is similar to the case of AIP-II and trAIP-II, supporting the inference of structural independence. Furthermore, acetylation of the N-terminus of AIP-I (**Table 2.5**) only results in local CSDs within the tail, as compared to AIP-I, without causing significant CSDs in the macrocycle.

Probing the Importance of the Macrocycle for Biological Activity

The linear free acid version of AIP-II was previously reported to be biologically inactive on AgrC-I, -II, and –III, utilizing the prior bioassay (Mayville et al., 1999). In this previous report, the sample of linear AIP-II was obtained by hydrolysis of a small quantity of AIP-II thiolactone, followed by RP-HPLC purification. As this procedure did not yield enough material for 2D-NMR characterization, the peptide was re-synthesized using standard Fmoc methods and characterized by NMR (*vide supra*). Furthemore, linear AIP-II was re-tested on AgrC-I, -II, and –III, and tested for the first time on AgrC-

IV. In no case was *agr* activation or inhibition observed, up to a final concentration of 55 μM, thus confirming and extending the prior results with the new reporter strains. Thus, in the case of AIP-II, the macrocycle is critically important for biological activity.

It was initially assumed that this result would extend to all of the AIPs examined. Upon synthesis and testing of linear AIP-I (**Table 2.5, 2.6**) it was found that this molecule does not fully activate or inhibit AgrC-I and –IV up to a concentration of 69 μM. However, it does inhibit AgrC-II and –III activation, with IC_{50} values in the sub-micromolar range (**Table 2.6**). These results indicate that linear AIP-I can bind to AgrC-II and –III, most likely through the two C-terminal hydrophobic side-chains. However, the IC_{50} values for inhibition of AgrC-II and –III by linear AIP-I are at least 20-fold higher than those values observed for AIP-I thiolactone inhibition. It is very likely that macrocylization in AIP-I serves the purpose of rigidifying the peptide backbone and orienting the side-chains, thus increasing binding affinity to the receptor, perhaps through a decrease in entropic costs incurred upon binding. It is also possible that, in an *in vivo* infection, the concentration of hydrolyzed linear AIP-I does not reach concentrations high enough to cross-inhibit other groups, as the reported concentration of AIPs in culture supernatants is around 30 nM (Saenz et al., 2000). However, further testing is required to verify the lack of activity of hydrolyzed linear AIP-I in wild-type strains during the course of natural infections. In summary, the macrocycle of AIP-I and –II appears to play an important (if not critical) role in the biologically relevant activity of the AIPs.

Role of the N and C termini, using AIP-I

To probe the steric and electrostatic requirements of the N-terminus of AIP-I in terms of receptor binding, a series of N-terminally modified analogs were synthesized. N-acetylated AIP-I activates AgrC-I and inhibits AgrC-II and –III with values comparable to those obtained with native AIP-I (**Table 2.6**- unless otherwise listed, all activation and inhibition results are presented in the table, including 95% confidence intervals). N-acetylated AIP-I does not activate or inhibit AgrC-IV at any concentration tested, which is consistent with the fact that AIP-I only weakly cross-activates AgrC-IV (**Table 2.6**). Relatively bulky fluorescein or biotin groups were attached to the free amino terminus of AIP-I. These additions did not have any major effect on AIP-I function, as both fluorescein-conjugated AIP-I and biotinylated AIP-I could activate AgrC-I and inhibit AgrC-II at concentrations comparable to AIP-I in the nanomolar range, with an EC_{50} value for AgrC-I activation by fluorescein-conjugated AIP-I of 40 nM (22-74 nM, 95% CI). Thus, the function of AIP-I is not dramatically affected by acetylation or the addition of bulky groups on the N-terminus, suggesting that the ligand binding pocket can either accommodate these bulky groups or, more likely, that the N-terminus is solvent exposed.

In other studies, it was tested whether the C-terminal hydrophobic amino acid, methionine, in AIP-I could be replaced by another hydrophobic amino acid without affecting function. Therefore, AIP-I with isoleucine replacing methionine at position 8 was synthesized. AIP-I M8I activates AgrC-I as well as native AIP-I (**Table 2.6**), and similarly inhibits AgrC-II and –III, as compared to native AIP-I. AIP-I M8I activates AgrC–IV more effectively than does AIP-I (730 nM vs. 26 μM), suggesting that this substitution permits improved binding and/or ligand-induced receptor activation by this

analog. Lastly, substitution of methionine with leucine in *agrD* by genetic methods results in a bacterial strain that autoinduces in a manner similar to wild-type cells (Ji, G. and R.P.N, unpublished observations). These data collectively indicate that the thioether linkage in methionine is not required for agonist activity, which is inconsistent with a recent proposal from McDowell et al. that this linkage is critical (McDowell et al., 2001).

Effect of tail length, using AIP-III

The chemical structures of various AIPs have been previously ascertained either by preparation of synthetic peptides with demonstrated activity or by peptide sequencing of AIPs purified from culture supernatants by RP-HPLC. The AIPs thus far examined by these methods include: a heptapeptide from *S. lugdunensis* (Ji et al., 1997), octapeptides from group I *S. aureus* (Ji et al., 1997), group IV *S. aureus* (see below), *S. epidermidis* (Otto et al., 1999), and a nonapeptide from group II *S. aureus* (Ji et al., 1997). The former method of synthetic peptide preparation was chosen to verify the sequence of AIP-III. Based on sequence similarities to AIP-I and the ability of AgrB from group I or III to process the group I or III AgrD propeptide *in vivo*, it was initially assumed that AIP-III would be an octapeptide (Ji et al., 1997). Accordingly, the octapeptide thiolactone was synthesized and shown to have cross-inhibitory activity toward group I cells. However, *agr* activation of AgrC-III could not be demonstrated with this peptide (Mayville et al., 1999). Indeed, the thiolactone octapeptide turns out to be an antagonist of AgrC-III activation by group III *agr*+ supernatant, with an IC_{50} of 360 nM (300-430 nM, 95% CI) **(Fig. 2.20A).** Therefore, the octapeptide is clearly not the native AIP-III. The group III thiolactone hepta- and nonapeptides were synthesized according to the group III *agrD*

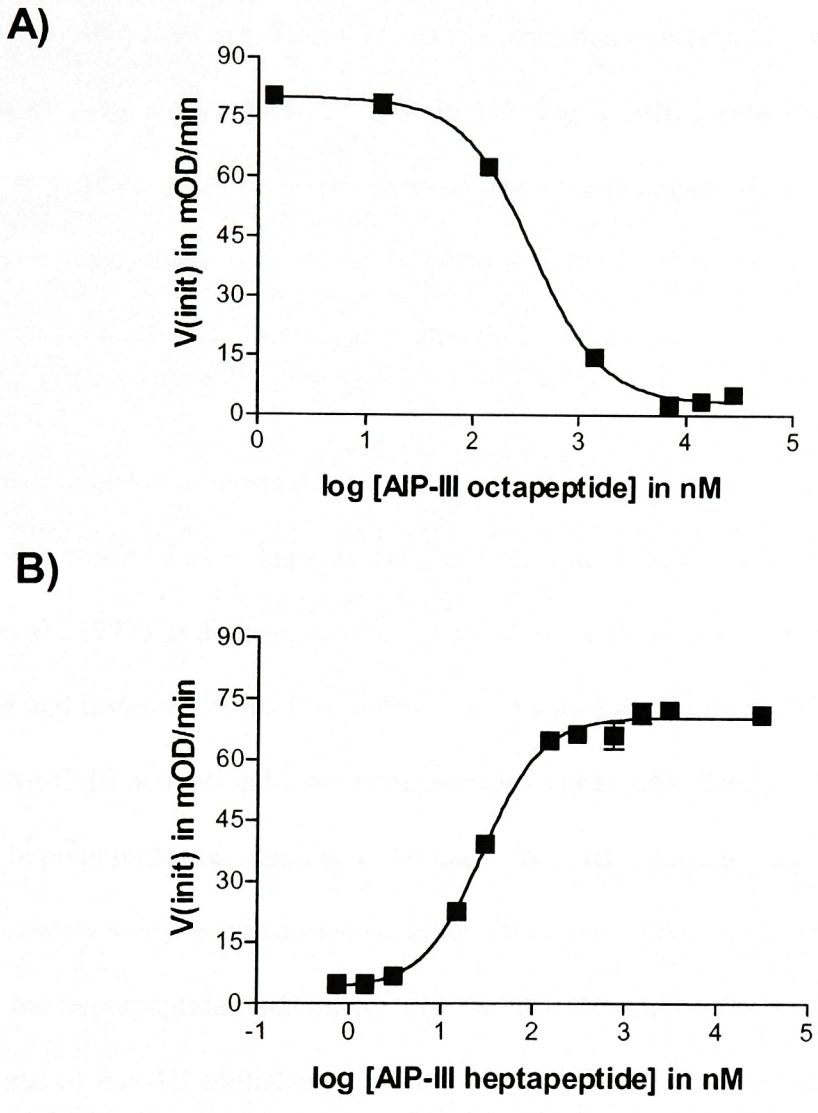

Figure 2.20. AIP-III studies. A) Group III cells were incubated with a constant amount of group III culture supernatant with varying [AIP-III octapeptide]. **B)** Group III cells were incubated with varying [AIP-III heptapeptide]. Data were collected as ß-lactamase activity (V_{init} in mOD/min) and are shown at each concentration ± SEM. Unless otherwise visible, error bars are contained within the confines of the symbol.

amino acid sequence. The nonapeptide does not activate AgrC-III up to a concentration of 2.6 μM and instead inhibits AgrC-III activation by group III *agr*+ supernatant, with an IC_{50} of 790 nM (480-1310 nM, 95% CI). On the other hand, the thiolactone heptapeptide is an activator of AgrC-III, with an EC_{50} of 26 nM **(Fig. 2.20B, Table 2.6)**. Furthermore, no additive or inhibitory effects were observed when the heptapeptide was added with group III *agr*+ supernatant to the group III cells, with the synthetic peptide at various concentrations up to 60 μM. This suggests that the heptapeptide is likely to be the native AIP-III.

Further analysis supports this hypothesis, as the heptapeptide mimics what has been seen with group III *agr*+ supernatants, as well as with supernatants from other groups (Ji et al., 1997). It does not activate AgrC-I, II, or IV at any concentration tested up to 30 μM and instead inhibits their activation **(Table 2.6)**. Furthermore, AIP-I, -II, and -IV inhibit AgrC-III activation by the heptapeptide **(Table 2.6)**. The fact that the thiolactone heptapeptide corresponds to the native AIP-III is further supported by tandem mass spectrometry analysis performed on group III culture supernatants indicating the presence of the heptapeptide (*vide infra*). The fact that the addition of amino acids onto the N-terminus of AIP-III abolishes activation of AgrC-III, but that the addition of functional groups onto the N-terminus of AIP-I has little effect on its activity, indicates that the N-terminus plays different functional roles in the AIPs thus far examined. This is indicated in **Figure 2.21**, where the N-terminus of AIP-III is marked with an asterisk to denote its importance for *agr* activation.

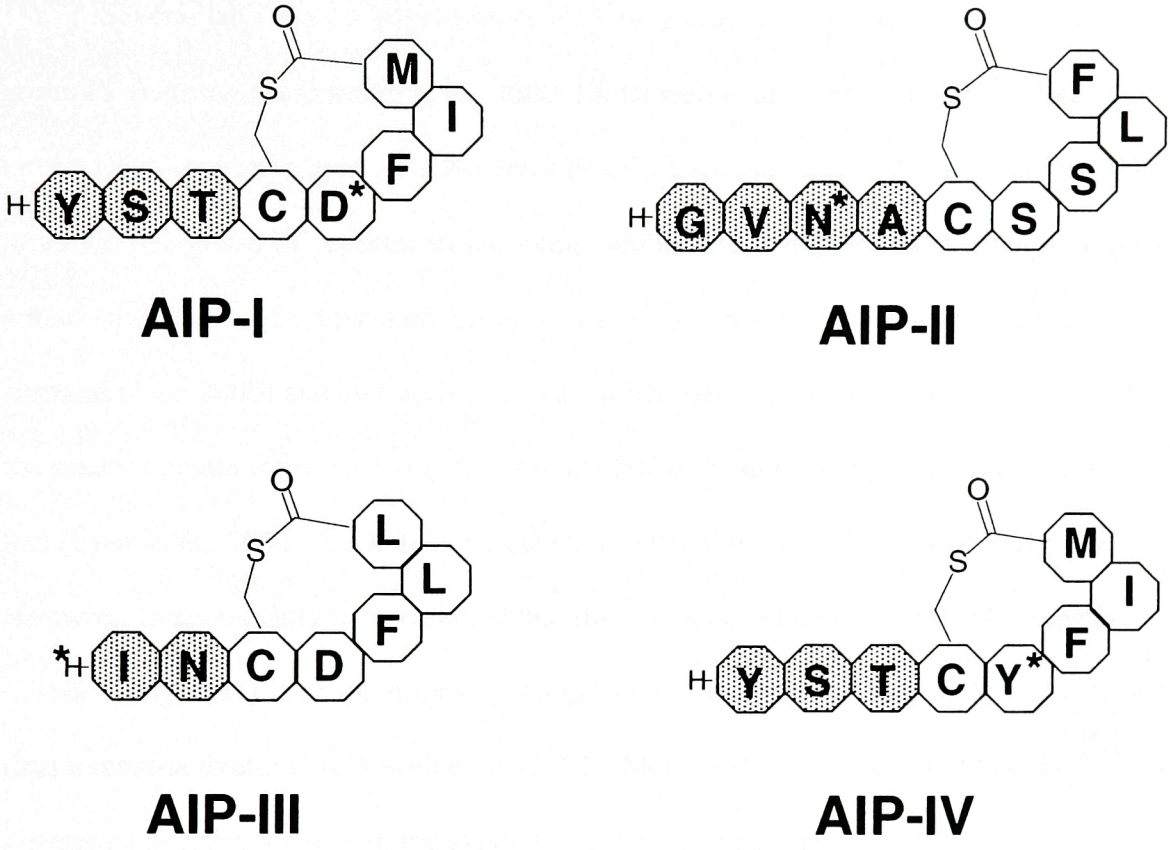

Figure 2.21. Structure and key determinants of the AIPs. Standard single letter codes for amino acids are indicated. The sulfur atom of the cysteine and the carbonyl contributed from the C-terminal amino acid are shown in a thioester linkage, which closes the macrocycle. Exocyclic (tail) residues are represented in shaded grey circles, whereas endocyclic residues are represented in clear circles. Residues that are critical for receptor activation are marked with an asterisk (*). The N-terminus of AIP-III is marked with an asterisk (*), to reflect the fact that additional amino acids on the N-terminus abolish receptor activation.

Activity of AIP-IV

Several laboratories have identified a new group of *S. aureus* strains, designated group IV (*vide supra*) (Jarraud et al., 2000; McDowell et al., 2001; Otto et al., 2001). Group IV *agr*+ supernatant activates RNAIII expression in group IV strains and the P3 promoter in a group IV reporter strain, while inhibiting *agr* expression in group II and III strains (*vide supra*). Furthermore, group IV *agr*+ supernatant activates group I cells (Jarraud et al., 2000) and also activates to a similar extent a chimeric receptor, in which the sensor domain from AgrC-I is fused to the HK domain from AgrC-IV (*vide supra*) and (Lyon et al., 2002). Such data indicate that AIP-IV is a cross-activator of AgrC-I. However, it has recently been reported that the synthetic octapeptide AIP-IV (sequence shown in **Fig. 2.21)** is an inhibitor of group I *agr* expression, with an IC_{50} of 7 μM, rather than a cross-activator (McDowell et al., 2001). McDowell *et al.* suggested that the difference in activity between the synthetic AIP-IV and bacterial supernatants could be accounted for by the presence in the supernatant of other components capable of influencing *agr* expression. As there is no other known extracellular signal that has been reproducibly confirmed to activate the *agr* system (Novick, 2000), it would be important to confirm the existence of such a factor, if it does exist. Accordingly, the octapeptide thiolactone AIP-IV was synthesized and assayed in the absence of group IV culture supernatant.

Synthetic AIP-IV is an activator of AgrC-IV and -I, with EC_{50} values in the nanomolar range (**Table 2.6**). Synthetic AIP-IV is, as expected, an antagonist of AgrC-II and -III activation. Conversely, both AIP-II and AIP-III inhibit AgrC-IV activation by AIP-IV (**Table 2.6**). The above results mimic the activity previously seen with group IV

agr+ supernatant (Jarraud et al., 2000; Lyon et al., 2002), providing strong evidence that the octapeptide thiolactone corresponds to the native AIP-IV. This is also consistent with tandem mass spectrometry analysis performed on group IV culture supernatants, which has indicated the presence of the octapeptide (*vide infra*). Since the activity of the synthetic AIP-IV mimics that of culture supernatants, this strongly suggests that there is no additional factor in group IV culture supernatants activating group I cells, and confirms that AIP-IV can cross activate AgrC-I. It is noteworthy that McDowell *et al.* did not report whether their synthetic AIP-IV activates group IV cells (McDowell et al., 2001). Furthermore, none of their peptides were characterized by two-dimensional NMR, thus making it impossible to verify that their peptides are identical to the ones reported herein. This is particularly important, as it is well-known that the synthetic methodology utilized by McDowell *et al.* to prepare their AIPs can promote C-terminal epimerization (Goodman and McGahren, 1967, Nakayama et al., 2001) (*vide infra* concerning synthesis of lactone AIPs).

Probing the critical side-chain differences between AIP-I & -IV

AIP-I and AIP-IV differ by only one amino acid: an endocyclic aspartate versus tyrosine in AIP-I and -IV, respectively (**Figure 2.21**). As shown above, the amino acid at this position profoundly affects the properties of the peptide, as AIP-I strongly activates AgrC-I but only weakly activates AgrC-IV, whereas AIP-IV strongly activates both. This contrasts with AIP-II, where substitution of this position by alanine (AIP-II S6A) did not result in any major change in bioactivity (Mayville et al., 1999). This prompted structure-activity relationship studies of this critical residue in AIP-I and –IV to determine what

role it plays in ligand-receptor binding and/or activation (**Fig. 2.22, Table 2.6**). Initially, this residue was replaced with alanine. This peptide, abbreviated AIP-I D5A, does not activate AgrC-I or -IV at any concentration tested (up to 10 μM), and instead potently inhibits activation of both receptors (**Table 2.6**). The inhibition of AgrC-I by this analog is consistent with the results on group I cells obtained by McDowell *et al.* using the same analog (McDowell et al., 2001). AIP-I D5A is also as potent as AIP-I and -IV in inhibiting AgrC-II and -III (**Table 2.6**), thus resulting in universal inhibition of all four *agr* groups. Thus, replacing the relatively bulky side-chain at this position with an alanine methyl group has little to no effect on receptor binding but switches the peptide from an agonist into an antagonist.

To probe the role of this position further, more subtle modifications were introduced. Substitution of the AIP-IV tyrosine with phenylalanine (Y5F) had no effect, as the peptide was similar to native AIP-IV in its activation/inhibition activities (**Table 2.6**), suggesting that the polar hydroxyl in tyrosine at position 5 is not required for bioactivity. In the case of AIP-I, the aspartate side chain is expected to be deprotonated at physiological pH, thus generating a negative charge at this position. In order to test whether a negative charge is required, we introduced an asparagine residue at this position. AIP-I D5N activates AgrC-I with an EC_{50} value only slightly higher than that of AIP-I (**Table 2.6**), thus demonstrating that the negative charge of the aspartate side-chain is not essential for AgrC-I activation. In contrast to AIP-I, AIP-I D5N does not activate AgrC-IV at any concentration up to 50 μM and instead inhibits AgrC-IV and AgrC-II activation (**Table 2.6**). Remarkably, AIP-I D5N does not inhibit AgrC-III activation by AIP-III, but rather activates group III cells, with an EC_{50} of 360 nM (**Table 2.6**). This

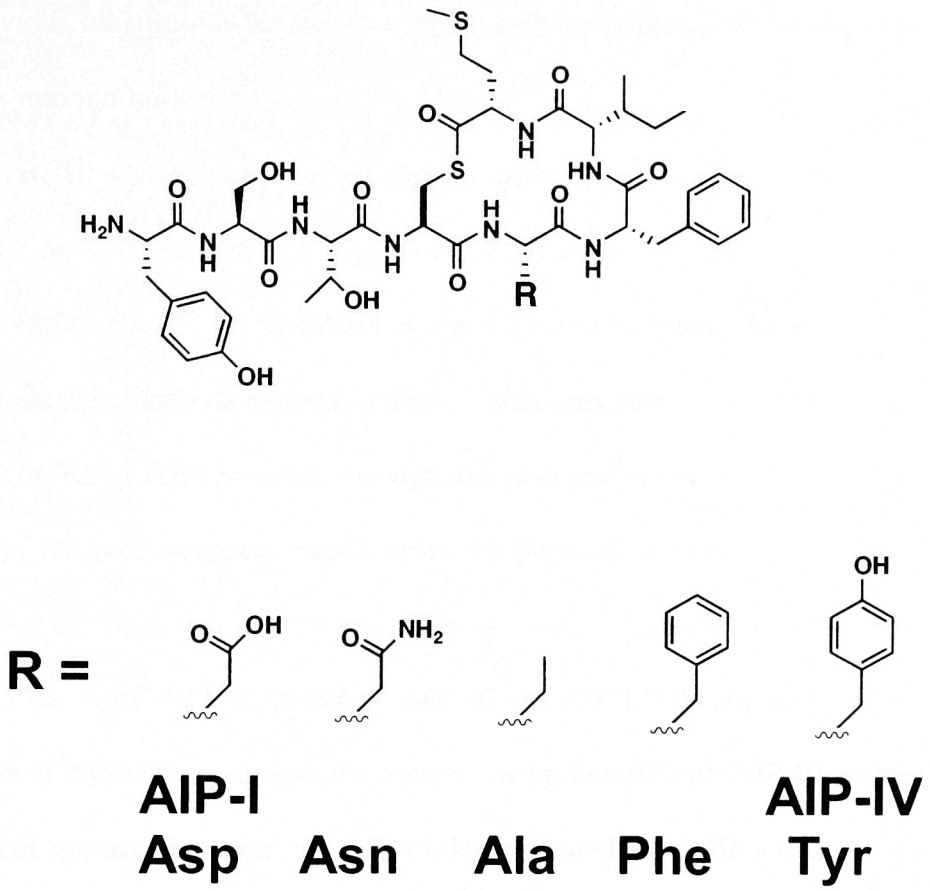

Figure 2.22. Structure-activity relationship studies on AIP-I and –IV. The chemical structure of the invariant portion of AIP-I and –IV is depicted, with an "R" group representing the site of modification. Various chemical groups were introduced at this position to probe different aspects of AIP-I and –IV function.

example is the only case to date of conversion of an inhibitory AIP into an activator. All other previous substitutions have either inactivated the peptides or converted them from activators into inhibitors.

AgrC-III activation by AIP-I D5N was investigated further. As the functional readout for AgrC-III activation is comprised of the sensor domain of AgrC-III fused to the HK domain of AgrC-IV, upstream of AgrA-IV and including the P3-*blaZ* reporter gene cassette (see Methods and *vide supra*), it was important to confirm that the activation by AIP-I D5N proceeds through this chimeric receptor. Therefore, in analogy with earlier receptor-swapping experiments, the plasmid containing the chimeric AgrC-III and other elements was moved onto different genetic backgrounds. As shown in **Figure 2.23A**, AgrC-III is activated by AIP-III and AIP-I D5N regardless of receptor expression in different group-specific genetic backgrounds, with AIP-III acting as the more potent agonist. However, the AIP-I D5N-mediated AgrC-III activation is highly resistant to inhibition by the known inhibitors of AIP-III mediated AgrC-III activation, e.g. AIP-I and AIP-II **(Figure 2.23B).** Furthermore, the self-inhibitor, AIP-III octapeptide, is also a very weak inhibitor of AgrC-III activation by AIP-I D5N, and it furthermore appears that inhibition by all 3 AIPs occurs at approximately the same high concentrations, which could represent non-specific inhibition. This profile is clearly distinct from that observed with competitive inhibition of AIP-III mediated AgrC-III activation, suggesting that activation of AgrC-III by AIP-I D5N could be occurring through a non-competitive mechanism. This activation most likely occurs through the sensor domain of AgrC-III, as it occurs regardless of the genetic background in which AgrC-III is expressed and all AIPs thus far tested have acted through extracellular

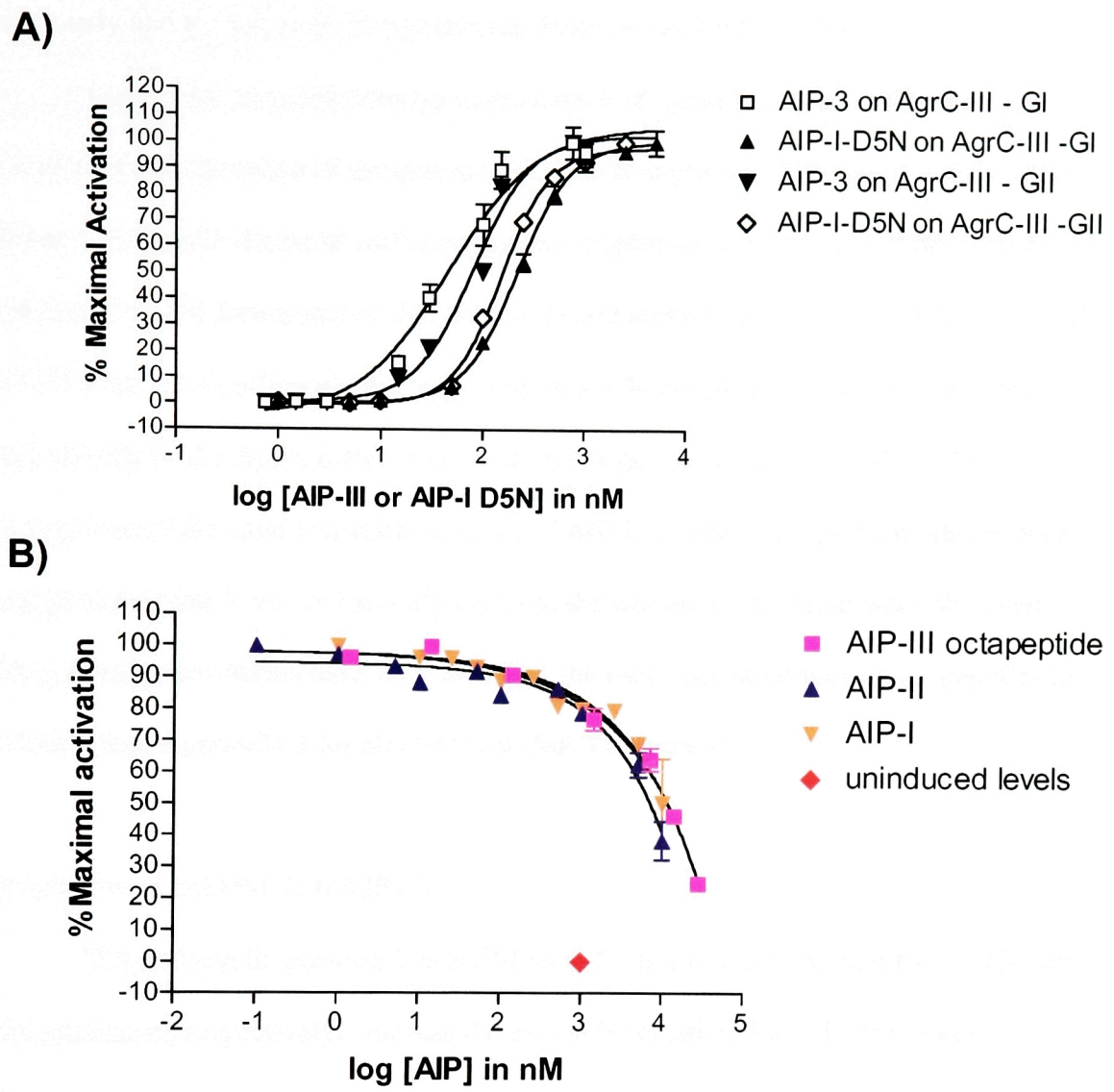

Figure 2.23. Testing AIP-I D5N activation of group III cells. A) The activation by AIP-III or AIP-I D5N of AgrC-III is shown, with AgrC-III expressed on two different agr-null genetic backgrounds (*agr* GI and GII). **B)** The marginal inhibition of AIP-I D5N-induced AgrC-III activation by three analogs, i.e. AIP-III octapeptide, AIP-II, and AIP-I. In contrast, all of these analogs are potent nanomolar range inhibitors of AIP-III-induced AgrC-III activation.

binding to the sensor domain of AgrC. However, further studies are needed to prove this rigorously and to elucidate the mechanistic basis of activation by this analog.

Lastly, it was tested whether modification of the side-chains of AIP-I and AIP-IV could affect the structure of the macrocycle, which might alter biological activity. Two-dimensional NMR chemical shift assignments confirmed the presence of the correct substitutions and demonstrated that the amide and alpha protons of AIP-IV Y5F and AIP-I D5N were not significantly different from those determined for AIP-IV and AIP-I, respectively (< 0.1 Δppm differences at all positions). In the case of AIP-I D5A, comparison of the chemical shifts to those of AIP-I revealed no significant differences, except at position 5, where local effects from the alanine substitution were observed. Thus, these substitutions have little effect on the backbone structures of the peptides in solution (see **Appendix I** for all chemical shift assignments).

Properties of trAIP-I & trAIP-IV

The endocyclic position 5 in AIP-I and –IV is a key determinant for AgrC-I and –IV activation, respectively, whereas the exocyclic position 3 in AIP-II is a key determinant for AgrC-II activation (Lyon et al., 2002). Removal of the tail of AIP-II and thus removal of position 3 converted AIP-II into an antagonist (Lyon et al., 2000). Therefore, removal of the tail in AIP-I might produce a peptide retaining activating activity. Accordingly, an AIP-I derivative (trAIP-I) was synthesized, in which the tail was replaced by an acetyl group **(Table 2.5 and 2.6)**. This expectation seems to have been realized, at least in part, as this peptide by itself activates AgrC-I very weakly at high concentrations but also inhibits AgrC-I activation by AIP-I, with EC_{50} and IC_{50}

values that are not significantly different from one another (**Table 2.6**). This concentration-dependent inhibition by trAIP-I reduces AgrC-I activation by AIP-I to the maximal activation observed with trAIP-I alone (**Fig. 2.24A**). A ligand with decreased efficacy of activation is defined as a partial agonist (Pliska, 1999), and it is the first time that such a ligand has been characterized in a bacterial signaling system (to the knowledge of this author).

TrAIP-I neither activates nor inhibits AgrC-IV at any concentration up to 44 μM, indicating that it most likely does not bind AgrC-IV. Therefore, the very weak activity of full-length AIP-I on group IV cells is abolished completely by removal of the tail. The fact that trAIP-I is a partial agonist only at very high concentrations for AgrC-I and no longer activates AgrC-IV at the highest concentration tested suggests that the tail contributes to receptor binding and/or activation in both instances, but that the macrocycle itself can partially activate AgrC-I. TrAIP-I inhibits AgrC-II with similar potency to AIP-I (**Table 2.6**) and more weakly inhibits AgrC-III as compared to AIP-I (240 vs. 3 nM). Therefore, removal of the tail has little effect on cross-inhibition of AgrC-II but does affect the potency of AgrC-III inhibition.

A truncated version of AIP-1 D5A was also tested to determine whether the loss of activity by the substitution also resulted in a loss of partial agonism. This peptide, abbreviated trAIP-I D2A, has no detectable AgrC activation activity and is a strong inhibitor of activation of all four AgrC's (**Table 2.6, and Fig. 2.24B** for group IV inhibition). This result underscores the key role of the amino acid at position 5 in AIP-I for AgrC-I activation.

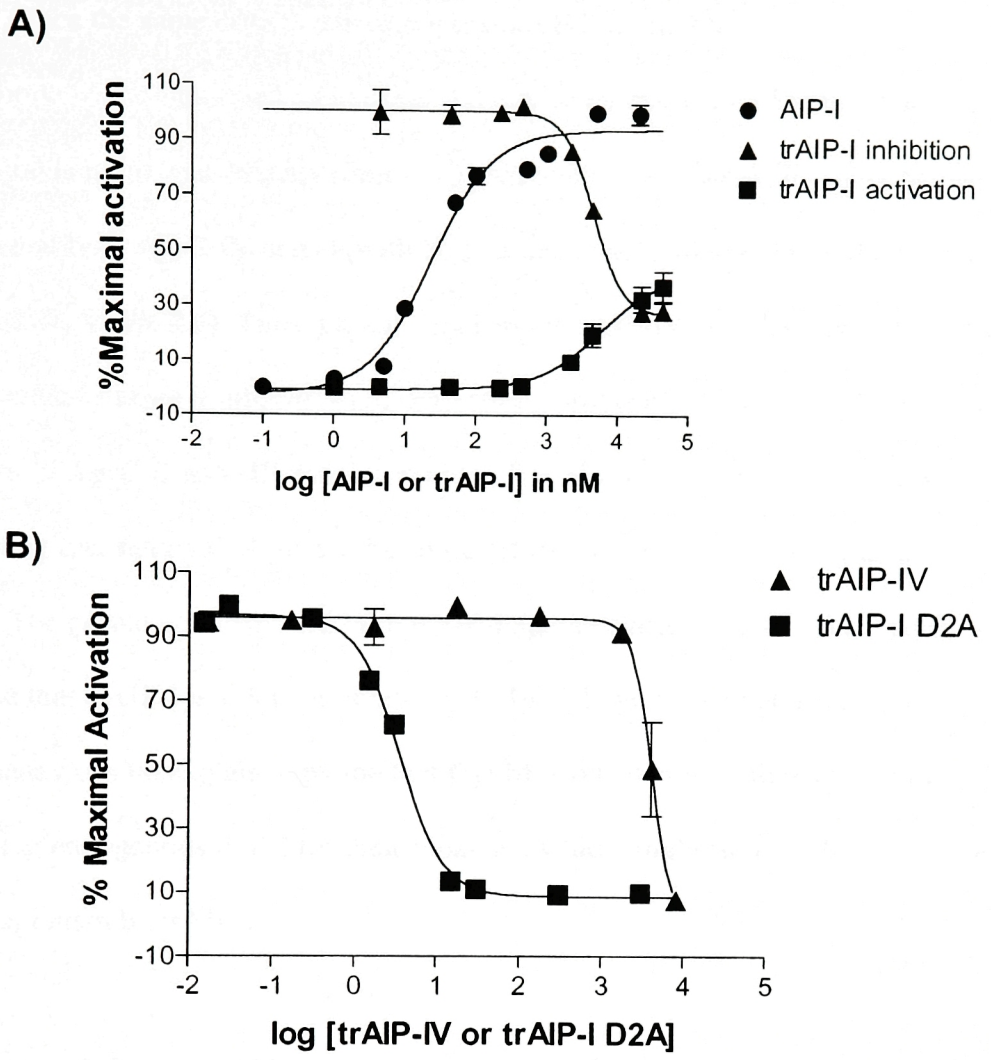

Figure 2.24. trAIP studies. **A)** Group I cells were incubated with varying [trAIP-I] alone or varying [trAIP-I] and a fixed concentration of AIP-I at 100 nM. The AIP-I concentration-response curve is shown for comparison. **B)** Group IV cells were co-incubated with varying [trAIP-IV] and a fixed concentration of AIP-IV at 100 nM or [trAIP-I D2A] and a fixed concentration of AIP-IV at 100 nM. Data were collected as ß-lactamase activity (V_{init} in mOD/min), normalized to %Maximal Activation and are shown at each concentration ± SEM. Unless otherwise visible, error bars are contained within the confines of the symbol.

Since the same critical activating residue occurs in AIP-IV, a truncated version of this peptide was synthesized and tested. Activation by trAIP-IV (**Table 2.5 and 2.6**) was undetectable up to its solubility limit (~10 μM) and it was a weak, though complete, inhibitor of both AgrC-IV and -I, with IC_{50} values of 4.1 μM and 930 nM, respectively **(Fig. 2.24B, Table 2.6)**. Thus, partial agonism by trAIP-IV could not be detected and seems unlikely since it inhibits AgrC activation completely. Lastly, trAIP-IV is an inhibitor of AgrC-II and -III activation in the low nanomolar range **(Table 2.6)**, suggesting that removal of the tail has little effect on cross-inhibition by trAIP-IV.

The partial agonism seen with trAIP-I again contrasts with a recent study, which reported that trAIP-I is solely an inhibitor of AgrC-I (McDowell et al., 2001). This discrepancy can be explained by the fact that McDowell *et al.* utilized a cell line producing endogenous AIP-I for their bioassay, which might impede the observation of partial agonism by trAIP-I.

Properties of chimeric AIPs

In an attempt to analyze further the remarkable differences between AIP-II and –I/-IV with respect to critical residues, chimeric peptides were prepared in which the tail of AIP-II was attached to the macrocycle of AIP-I and vice-versa. If the macrocyle from AIP-I binds to AgrC-II in a similar orientation to that of AIP-II, then one might expect that this chimeric peptide, designated AIP-II/I **(Table 2.5)** might be able to activate AgrC-II. However, a different orientation of binding would most likely result in inhibition of AgrC-II activation. This idea was tested, which yielded the latter result, as AIP-II/I, inhibits AgrC-II activation **(Table 2.6)**. Furthermore, AIP-II/I also contains the

key endocyclic residue for AgrC-I activation, aspartate, within its macrocyle, and the macrocyle alone (trAIP-I) is a partial agonist for AgrC- I. However, AIP-II/I does not activate AgrC-I at concentrations up to 20 μM, and instead fully inhibits AgrC-I activation **(Table 2.6)**. Therefore, addition of the tail from AIP-II to the macrocycle of AIP-I increases its inhibitory potency relative to trAIP-I and eliminates partial agonism by this analog. Finally, AIP-II/I inhibited AgrC-III and –IV activation, with IC_{50} values of 350 nM and 9.9 μM, respectively, which compares to IC_{50} values of 240 nM and > 44 μM for inhibition of AgrC-III and –IV by trAIP-I. This outcome suggests that addition of the AIP-II tail to the AIP-I macrocycle increases its affinity for binding to AgrC-IV while having no effect on binding to AgrC-III.

The reciprocal chimera, AIP-I/II, in which the tail from AIP-I was fused to the macrocyle of AIP-II **(Table 2.5)**, inhibits AgrC-I, -II, -III, and -IV activation **(Table 2.6)**. Comparing these IC_{50} values to those for trAIP-II **(Table 2.6)** suggests that the addition of the tail of AIP-I to the AIP-II macrocycle increases affinity for AgrC-I, -III, and –IV relative to trAIP-II without increasing the affinity for AgrC-II. The lack of activation by this analog was expected, as it possesses neither of the residues from AIP-I or –II critical for activation.

Lastly, chemical shift mapping was utilized to determine whether the structure of the swapped macrocycles and tails in the chimeric AIPs changed as a result of fusing two different group-specific segments together. Two-dimensional NMR chemical shift assignments demonstrated that the amide and alpha protons of the macrocycles of AIP-I/II and AIP-II/I were not significantly different from those determined for AIP-II and AIP-I, respectively (**Figure 2.25**). In addition, the amide and alpha protons of the tails of

AIP-I/II and AIP-II/I were not significantly different from those determined for AIP-I and AIP-II, respectively (**Figure 2.25** and see **Appendix 1** for chemical shift assignments). This further supports the inference of structural independence of tail and macrocycle, and suggests that the tails and macrocycles of the chimeric AIPs can assume similar structures to the segment of the native AIPs from which they are derived.

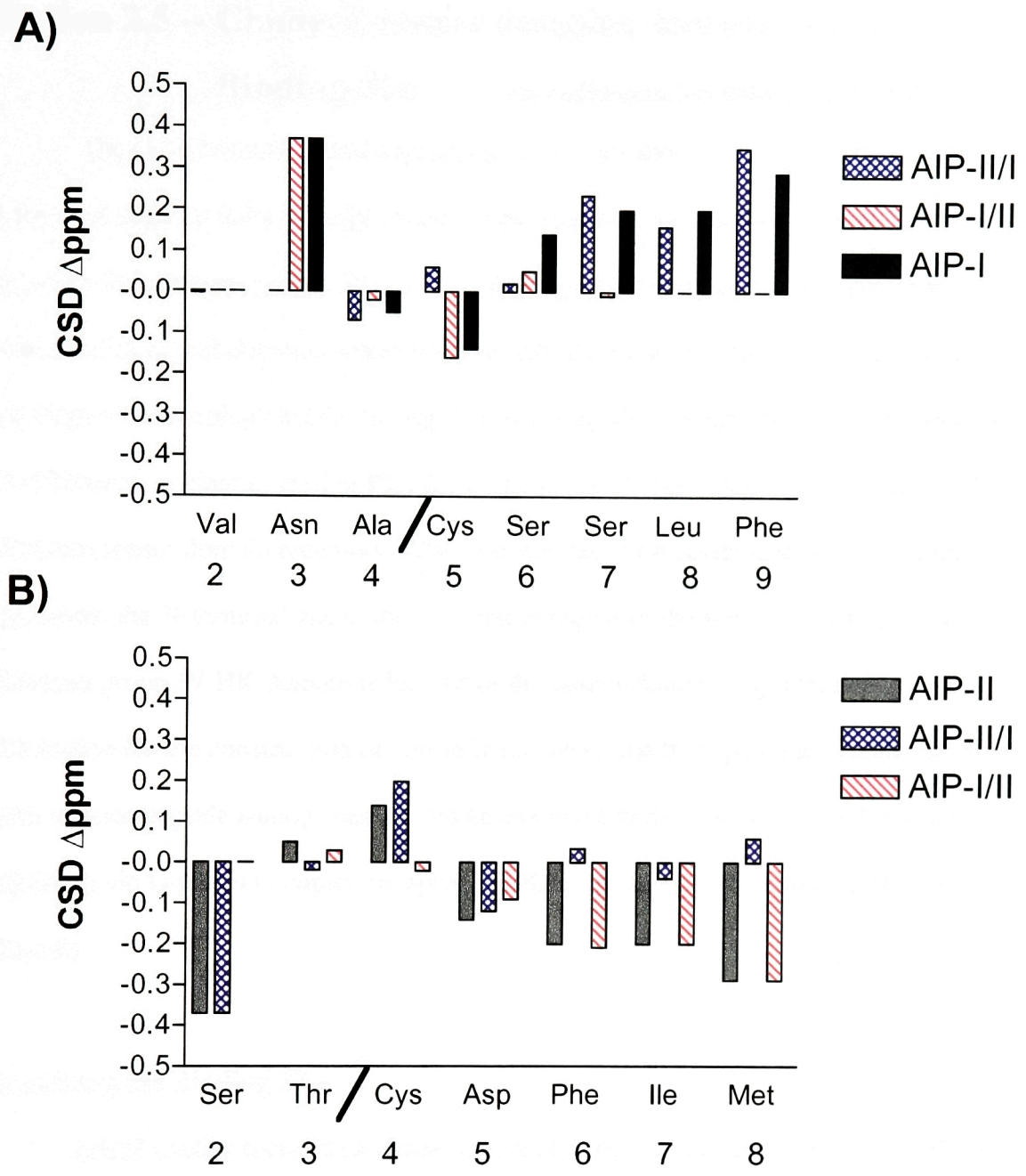

Figure 2.25. Chemical shift comparisons of chimeric AIPs with native AIPs. A) The backbone amide ^{1}H chemical shifts of the chimeric AIPs are depicted as chemical shift differences (CSDs) relative to native AIP-II normalized to zero (performed in DMSO-d_6 at 298 K). The N-terminal amineof AIP-I does not have an amide chemical shift, so AIP-I and AIP-I/II are assigned a value of zero at position 2. **B)** The backbone amide ^{1}H chemical shifts of the chimeric AIPs are depicted as chemical shift differences (CSDs) relative to native AIP-I normalized to zero (performed in DMSO-d_6 at 298 K).

Section 2.5 -- Chimeric sensor domains localize the AIP-Binding Site (in collaboration with Jesse Wright)

The close homology and asymmetric cross-reactivity between AgrC-1 and AgrC-4 for their cognate AIPs initially prompted an examination of sensor domain chimeras between these two receptors. This is to be distinguished from previous experiments in which entire sensor domains were swapped onto the same HK domain. A suggested topology and homology model for AgrC, illustrating the breakpoint for construction of the chimeras, is diagrammed in **Fig. 2.26**. The group IV HK domain is common to all chimeric sensor domain receptors. Chimeras are therefore designated as N::C, where N represents the N-terminal and C the C-terminal region of the sensor domain (and the common group IV HK domain is left out of the nomenclature). Paranthetically, one inspiration for the construction of chimeric receptors and their pharmacological analysis with various peptide analogs came from an extensive body of literature on hormonal signaling via G-protein coupled receptors (GPCRs) ((Unson, 2002) and references therein).

Localizing the Binding Site

Initial studies focused on chimeric sensor domains between AgrC-I and –IV, as these receptors share 87% identity. The AgrC-IV::I chimera was activated upon addition of either AIP-I or AIP-IV (Table 2.7, Fig. 2.27A,B). However, AIP-I was a more potent activator than AIP-IV on the AgrC-IV::I chimera (Table 2.7). The AgrC-I::IV chimera responded in an analogous but reverse fashion (Table 2.7). Again, both AIP-I and

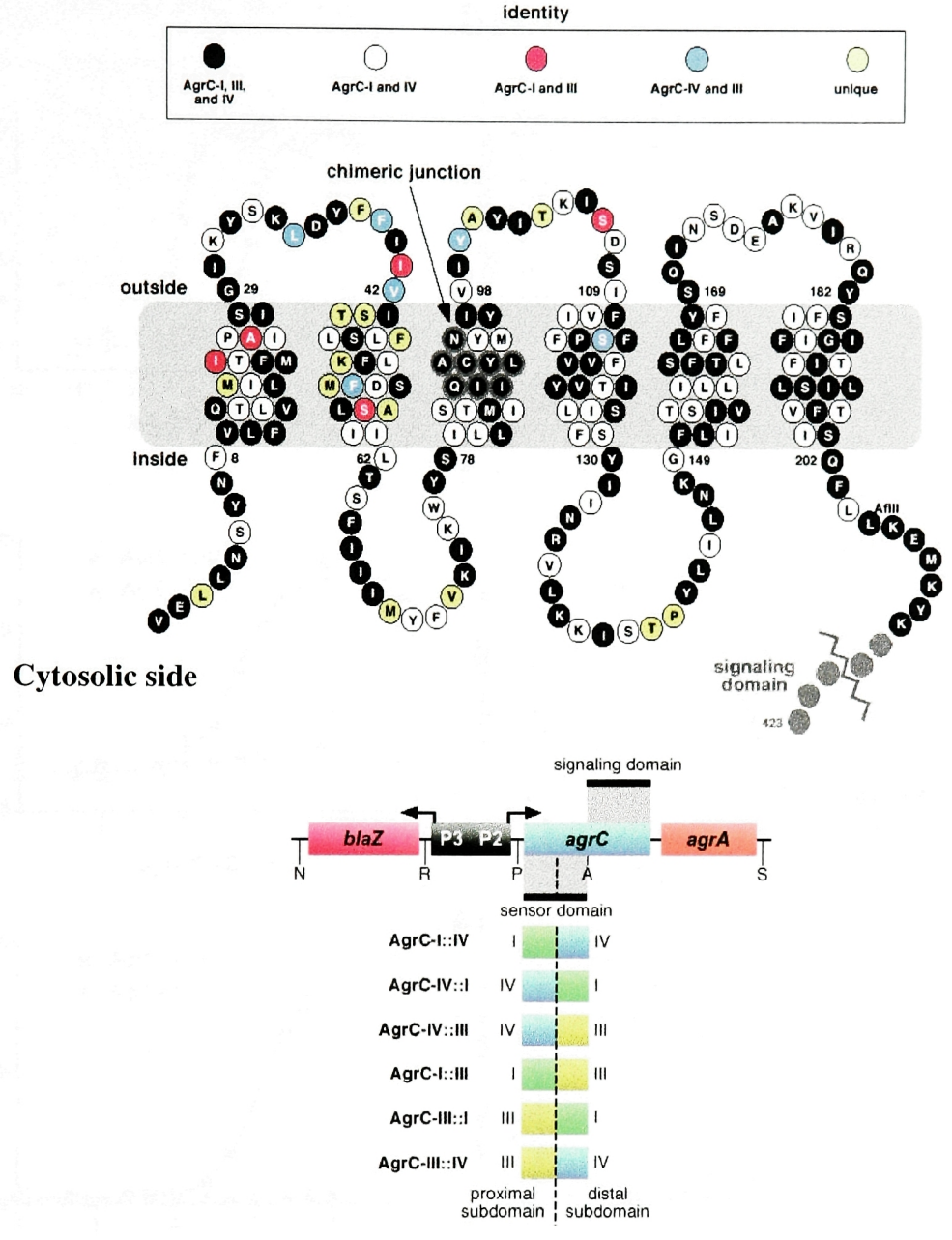

Figure 2.26. Topology and Homology model of AgrC. A) The putative topology of AgrC is shown, with six transmembrane helices as predicted by bioinformatics and sequence alignment of multiple AgrCs. The highly conserved breakpoint (or chimeric junction) for the construction of chimeric sensor domains is shown with an arrow. The conservation of amino acids between AgrC-I, -III and –IV is depicted with various shaded colors, and the residues unique between all three receptors are marked as such. **B)** Cloning strategy. At top is a diagram of the *agrCA* reporter construct using *blaZ* transcriptionally fused to the P3 promoter. The six subdomain chimeras for which results are reported are illustrated below. In each case, the recombinant *agrC* gene was cloned to the reporter construct replacing the receptor domain-encoding region of the native gene. Chimeras involving AgrC-II were also constructed but were essentially inactive and are not presented.

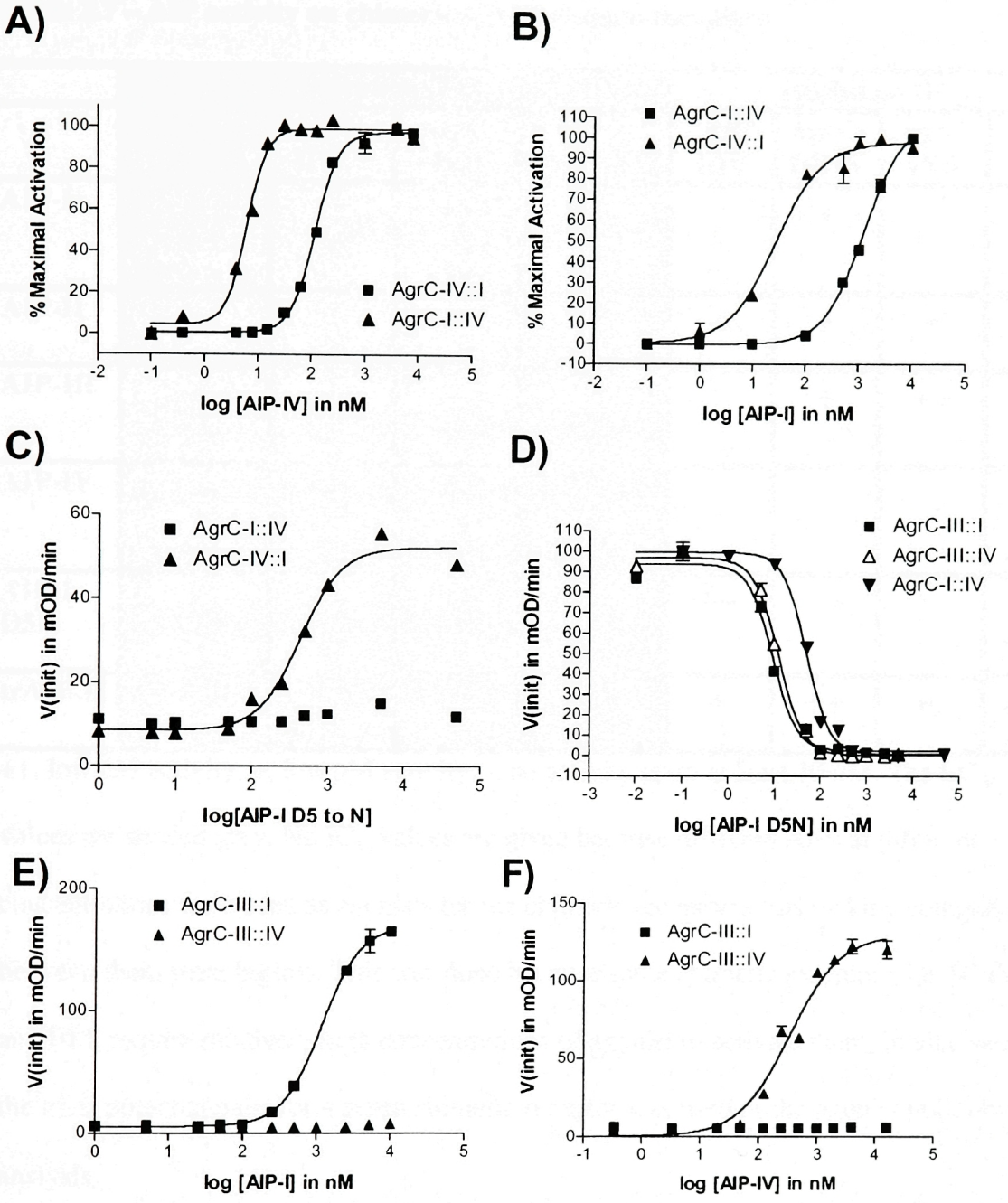

Figure 2.27. Activity of various AIPs on the chimeric sensor domain receptors.

Shown are representative data for activation (A, B, C, E, F) and inhibition (D) of the *agr* response in various chimeric sensor domain receptors by synthetic AIPs. Degree of activity based upon ß-lactamase activity is shown as a plot of V_{init} (initial velocity) or %Maximal Activation versus peptide concentration.

Table 2.7 – AIP activity on chimeric sensor domain receptors

	Activation (EC_{50})				Inhibition (IC_{50})			
	AgrC-I:IV	**AgrC-III:IV**	**AgrC-IV:I**	**AgrC-III:I**	**AgrC-I:IV**	**AgrC-III:IV**	**AgrC-IV:I**	**AgrC-III:I**
AIP-I	+ 1220 nM (1050-1410)	-	++ 30 nM (15-45)	+ 1700 nM (1500-1900)	-	+	-	-
AIP-II	-	-	-	-	+	+	+	+
AIP-III	-	-	-	-	-	+	++	++
AIP-IV	++ 6 nM (5-7)	+ 340 nM (290-410)	+ 120 nM (110-125)	-	-	-	-	++
AIP-I D5N	-	-	++ 440 nM (350-530)	-	++	++	-	++
trAIP-II	-	-	-	-	+	++	+	++

++, low nM activity, +, low μM activity, -, no activity up to at least 10 μM. The EC_{50} values are shaded grey. No IC_{50} values are given because different AIPs at different concentrations were used as agonists for the chimeric receptors, thus making comparisons between them meaningless. This was done because some chimeric receptors, i.e. III:IV and III:I, require relatively high concentrations of agonist to activate them. In all cases, the most potent agonist for a given chimeric receptor was used as the agonist in inhibition analysis.

AIP-IV activated AgrC-I::IV, but AIP-IV was more potent than AIP-I (AIP-I in the μM range and AIP-IV in the nM range). Thus, the potency for activation for both AIP-I & IV appeared to be associated with the C-terminal region of the sensor domain. Additionally, the activation of AgrC-I::IV by AIP-I represents a gain of receptivity by the chimera in comparison to the native AgrC-IV. The AgrC-I sequence at the N-terminus is most likely responsible for this effect. Interestingly, most of the sequence divergence between AgrC-I and AgrC-IV lies in this N-terminal region, which leads to the conclusion that AIP-I must be interacting with both subdomains of AgrC-I::IV. Moreover, both AgrC-IV::I and AgrC-I::IV were inhibited by the heterologous AIPs II & III, as well as by trAIP-II, a global inhibitor (Lyon et al. 2000), suggesting that these chimeric receptors retain the functional characteristics and overall specificities of native AgrCs I & IV (**Table 2.7).**

To investigate further the location of the AIP binding site for AgrC-I and AgrC-IV receptors, chimeras were constructed in which the N-terminal sensor subdomain was replaced with that of the less closely related AgrC-III receptor (AgrC-I and AgrC-IV share approximately 54% identity with AgrC-III in the receptor domain). The AgrC-III::I chimera was activated only in response to AIP-I, and the AgrC-III::IV chimera responded positively only to AIP-IV (**Table 2.7, Fig. 2.27E,F**). These responses were inhibited by AIP-II, and neither chimera was activated by AIP-III (**Table 2.7**). Activation of AgrC-III::I and AgrC-III::IV required rather high concentrations of AIP-I and AIP-IV respectively (in the low μM range), as compared to AgrC-I, -IV and the -I::IV and -IV::I chimeras (activation in the nM range). Moreover, neither AgrC-III::I and AgrC-III::IV showed cross-activation with the opposite AIP, i.e. AIP-IV and –I, respectively (**Table 2.7, Fig. 2.27E, F**). In fact, AIP-IV inhibited activation of the III::I chimera by AIP-I, and

AIP-I inhibited activation of the III::IV chimera by AIP-IV (**Table 2.7**). In other words, the potency of activation by AIP-IV and AIP-I of AgrC-I::IV and AgrC-IV::I, respectively, was greatly decreased by replacement of the N-terminal moiety with the corresponding region of AgrC-III, perhaps due to the loss or gain of binding contacts with the N-terminal subdomain. Furthermore, the AgrC-III N-terminal subdomain either directly or indirectly influences the binding orientation of AIP-I and AIP-IV on AgrC-I::IV and AgrC-IV::I, respectively. This different binding orientation converts them into inhibitors of receptor activation. These results confirm that the specific contacts necessary for AIP-I & IV activation reside in the C-terminal half of the receptor sensor domain, but suggest that the N-terminal sensor subdomain has an important functional role.

Orientation of AIP binding to the receptor.

Since activation by AIPs I & IV is associated with sequences in the C-terminal subdomain of the receptor, it is clear that this region plays the prominent role in imparting potency for AIP I and IV activity. Moreover, the only difference between AIP-I and AIP-IV is at position 5, located within the AIP ring. This variable position is responsible for i) asymmetric activation of AgrC-I & IV, ii) differential activation of the AgrC-IV::I and -I::IV chimeras by the two AIPs, and iii) specificity of activation of the AgrC-III::I and -III::IV chimeras. This suggests that the AIP moiety responsible for interaction with the C-terminus of the receptor is the ring (or macrocycle) rather than the linear tail.

Further support for this concept was provided by an assessment of the activity of the AIP-I D5N analog. This analog activates AgrC-I but is a potent inhibitor of AgrC-IV, rather than a weak activator, suggesting that the side chain at position 5 is crucial for determining cross-activation specificity for AgrC-IV (see above Results). When assessed against the chimeric receptors, AgrC-I::IV and AgrC-IV::I, the activity of AIP-I D5N was identical to its activities with native AgrC-I and AgrC-IV: AIP-I D5N activated AgrC-IV::I and inhibited AgrC-I::IV (**Fig. 2.27C, D**), again focusing attention on the macrocycle:C-terminal sensor subdomain interaction as the determinant of AIP-receptor specificity for AIPs I & IV. However, the N-terminal subdomain plays an important accessory role in this activation, as neither of the chimeric receptors, AgrC-III::I and AgrC-III::IV, is activated by AIP-I D5N, but, rather, their activation by AIP-I and AIP-IV, respectively, is inhibited by AIP-I D5N. Therefore, AIP-I D5N binds to these receptors but must fail to make specific contacts necessary for activation, and this failure can be attributed to the N-terminal sensor subdomain of AgrC-III. Failure to make these contacts could also be responsible for the relatively high concentrations of AIP-I and AIP-IV required for activation of the AgrC-III::I and AgrC-III::IV chimeras, respectively.

The above results imply that both AIP-I D5N and AIPs I & IV can provide activating contacts with the AgrC-IV::I chimera and the native AgrC-IV since the AgrC-IV N-terminal sensor subdomain is more closely related to that of AgrC-I than is the N-terminal sensor subdomain of AgrC-III. With the native AIPs I & IV, weakened contacts with the AgrC-III::I and AgrC-III::IV chimeras can be compensated by high concentrations of agonist; these weakened contacts are presumably not present upon binding of AIP-I D5N, no matter how high the concentration. Instead, AIP-I D5N binds

strongly to the AgrC-I:IV, AgrC-III::I and AgrC-III::IV chimeras, but does so with a binding orientation that does not provide activation contacts but rather competitively antagonizes activation by known agonists. In any case, it seems that one or more of the contacts necessary for activation of AgrC-IV::I & I::IV by AIPs I & IV must be missing in the AgrC-III::I & III::IV chimeras. This is supported by the complete lack of agonist activity of the AIP-I D5A alanine analog (not shown), which has been previously shown to be a universal inhibitor of *agr* activation (Lyon et al. 2002). These observations lend further support to the idea that the N-terminus of the receptor has an important role in AIP binding for activation.

A comparison of AIPs I & IV with III suggests that it is the tail moieties that are responsible for the discrimination between these AIPs by the N-terminal sensor subdomain of AgrC-III. The AIP-III tail is conspicuously different from that of AIPs I & IV, containing only two residues, both of which differ from those of AIP I/IV. It has been previously established that the AIP tail plays a significant role in receptor activation, as addition of a single amino acid to the AIP-III tail converts this peptide into an AgrC-III inhibitor (see Section 2.4) The effect of the AgrC-III N-terminal sequences and the different length and amino acid requirements of the AIP-III tail for activation could indicate that it is the tail sequences of AIPs I, IV, and D5N that fail to make effective contacts with the N-terminal subdomain of the AgrC-III::I and III:IV chimeras. With the native peptides, the macrocycle contacts with the cognate C-terminal subdomains plus higher AIP concentrations are presumably sufficient to activate the III::I or III::IV chimeric receptors in the absence of the putative tail contacts (activation of AgrC-III::I with AIP-I and AgrC-III::IV with AIP-IV); however, these contacts must not be

sufficient when macrocycle contacts with the C-terminus of the receptor domain are suboptimal or when these contacts change the binding orientation of the AIP so as to break possible activating contacts, as with AIP-I D5N (Lyon et al. 2002).

The foregoing argument is clearly an oversimplification since it does not begin to account for the inhibitory behavior of various AIPs and the general properties of several other chimeras. In particular, as shown in **Table 2.7**, AIP-III is a strong inhibitor of AgrC-III::I and AgrC-IV::I, a poor inhibitor of AgrC-III::IV and has no detectable activity on AgrC-I::IV up to a concentration tested of at least 10 μM. AIP-I D5N is a potent inhibitor of AgrC I::IV, III::IV and, as noted, III::I. Additionally, D5A is a universal inhibitor of AgrC activation, and an AIP-I analog without the tail (truncated AIP-I) inhibits AgrC-I and AgrC-III but not AgrC-IV.

During the course of this study, other chimeras, I::III, IV::III, II::III, III::II, I::II and II::I, were constructed using the same break junction. No activity could be detected with the last three of this set of six; it is not known whether these are expressed and inserted into the membrane. The other three were functional, but mostly in strikingly unpredictable ways. The II::III chimera was activated by AIP-II and AIP-IV at very high concentrations, but not by AIP-III or –I (not shown). Even more striking was the behavior of the I::III and IV::III chimeras. As shown in Table 2.8, both of these chimeras were strongly activated by most of the AIPs tested. This included not only AIP-III, but also AIPs I, II, and IV, which are strong inhibitors of AgrC-III (Mayville et al. 1999), AIP-I D5A and truncated AIP-II (trAIP-II), which are strong inhibitors of all four AgrCs (Mayville et al. 1999, Lyon et al., 2000), and even linear AIPs I and II, which have never

Table 2.8 – AIP promiscuous activation of two chimeric sensor domain receptors

	Activation (EC_{50})		Inhibition (IC_{50})	
	AgrC-I:III	AgrC-IV:III	AgrC-I:III	AgrC-IV:III
AIP-I	+	++	-	-
AIP-II	+ 3.1 μM	++ 640 nM	-	-
AIP-III	++ 48 nM	++ 4nM	-	-
AIP-IV	++	++	-	-
AIP-I D5N	++	++	-	-
AIP-I D5A	++	++	-	-
TrAIP-II	++ 160 nM	++ 50 nM	-	-
AIP-II F9A	-	-	ND	ND
Linear AIP-I	+ 3.1 μM	+ 6.7 μM	-	-
Linear AIP-II	-	+	ND	ND

++, low nM activity, +, low μM activity, , no activity up to at least 10 μM, ND, not determined. EC_{50} values are listed in those instances where they were determined with reasonable accuracy.

been shown before to activate *agr*. The important implication from these results is that the mismatch between the sensor subdomains alters the structure of the receptor in such a manner as to poise it for activation by any ligand that can bind - that is, that activation can occur without any of the putative group-specific contacts that are presumed to be responsible for activation of the native receptors.

This observation prompted an examination of the AIP sequences. Overall, the AIPs show a gradient of increasing hydrophobicity from their N- to C-termini, ending generally with bulky hydrophobic amino acids (**Fig. 2.28**). With the exception of the central cysteine, no other position in the AIPs is so strongly conserved. This analysis, coupled with the behavior of the I::III and IV::III chimeras, suggests an activation mechanism in which the AIP binds to a hydrophobic pocket in the receptor, involving one or both of the C-terminal hydrophobic residues, and then makes other site-specific contacts that result in activation. According to this concept, the structural distortion of the I::III and IV::III sensor domain chimeras bypasses the need for these other specific contacts; all that is required for activation is binding. And if the two C-terminal hydrophobic residues are required for binding, then replacing one or the other or both with a neutral residue such as alanine is predicted to eliminate binding and thus to eliminate activation of the I::III and IV::III chimeras. This prediction was confirmed as shown in **Table 2.8**: the F9A variant of AIP-II, which had previously been shown to lack activity with the four native AgrCs (Mayville et al, 1999) is totally inactive towards these two chimeric receptors.

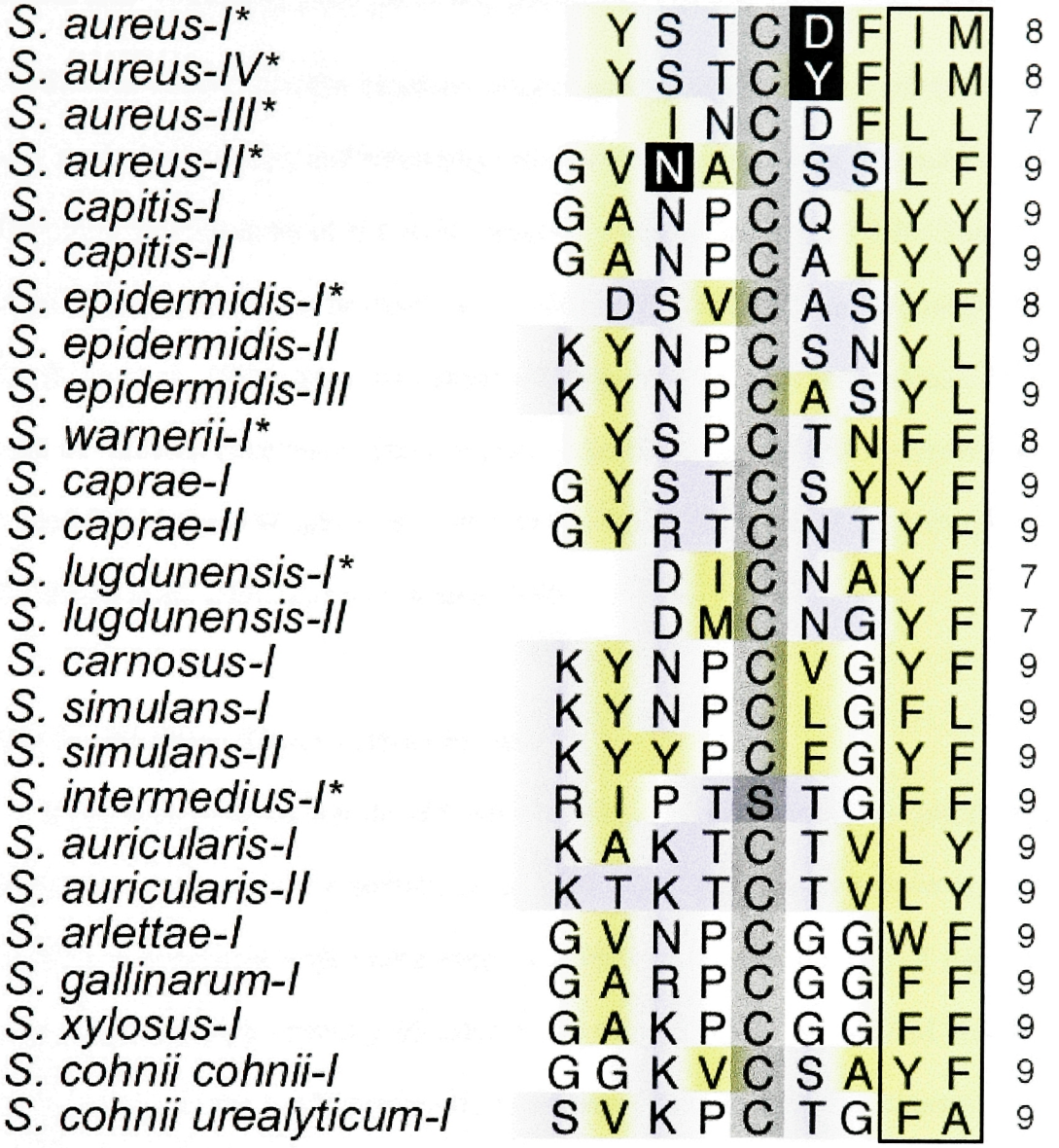

Figure 2.28. AIP Alignment from the known *agrD* sequences. The conserved cysteine (other than the *S. intermedius* serine-to be discussed later) is shaded and the conserved C-terminal hydrophobic amino acids are boxed. Hydrophobic amino acids are shaded in yellow, while hydrophilic amino acids are shaded in blue. The asterisks indicate those AIPs whose biologically active structures have been determined, with the exception of *S. lugdunenesis*-II, which is assumed to be a heptapeptide thiolactone, based on its strong homology to *S. lugdunenesis*-I.

Section 2.6 -- AgrC is a prototypical receptor-histidine kinase

Studies concerning the histidine kinase activity of AgrC were initiated with the primary goal of confirming and extending prior results concerning an AIP-inducible MBP-AgrC protein lacking most of the AgrC sensor domain (Lina et al., 1998). These studies included *in vitro* and *in vivo* analyses of the HK activity of AgrC, and, although the prior results (Lina et al., 1998) were not confirmed, important insights were gained and future avenues of research developed. These studies were in part inspired by extensive work on other histidine kinases (Wright et al., 1993; Fisher et al., 1995; Qin et al., 2000; Zhu et al., 2000; Marina et al., 2001; Zhu and Inouye, 2002).

Testing for Histidine Kinase activity *in vitro*

It has been reported that the HK domain of AgrC constitutively autophosphorylates *in vitro*, when assayed in the context of an MBP-AgrC HK fusion protein (Lina et al., 1998). This is consistent with bioinformatics studies of the HK domain of AgrC, which have revealed with high certainty (E-value 4e-50 using SMART and PFAM search tools) strong homology to the HATPase motif, commonly found in histidine kinases of known structure such as EnvZ (Tanaka et al., 1998) and PhoQ (Marina et al., 2001). Furthermore, transmembrane histidine kinases function as preformed dimers (Dutta et al., 1999). Once again, AgrC seems to fit this picture, as computer analysis has revealed that the linker spanning from the sensor domain to the kinase domain of AgrC has high helical propensity and the potential to form a coiled coil, followed by a helix-turn-helix motif (**Figure 2.29**). This is consistent with structural studies on the *E. coli* osmosensor EnvZ, which has a four-

AgrC-I Protein Sequence: two putative helices underlined

1-VELLNSYNFVLFVLTQMILMFTIPAIISGIKYSKLDYFFIIVISTLSLFLFKMFDS
ASLIILTSFIIIMYFVKIKWYSILLIMTSQIILYCANYMYIVIYAYITKISDSIFVIF
PSFFVVYVTISILFSYIINRVLKKISTPYLILNKGFLIVISTILLLTFSLFFFYSQIN
SDEAKVIRQYSFIFIGITIFLSILTFVISQFLLKEMKYKRNQEEIETYYEYTLKIE
AINNEMRKFRHDYVNILTTLSEYIREDDMPG**LRDYFNKNIVPMKDNLQMNAIKLNGI**E
NLKVREIKGLITAKILRAQEMNIPISIEIPDEVSSINLNMIDLSRSIGIILDNAIEAS
TEIDDPIIRVAFIESENSVTFIVMNKCADDIPRIHELFQESFSTKGEGRGLGLSTLKE
IADNADNVLLDTIIENGFFYSKS-425

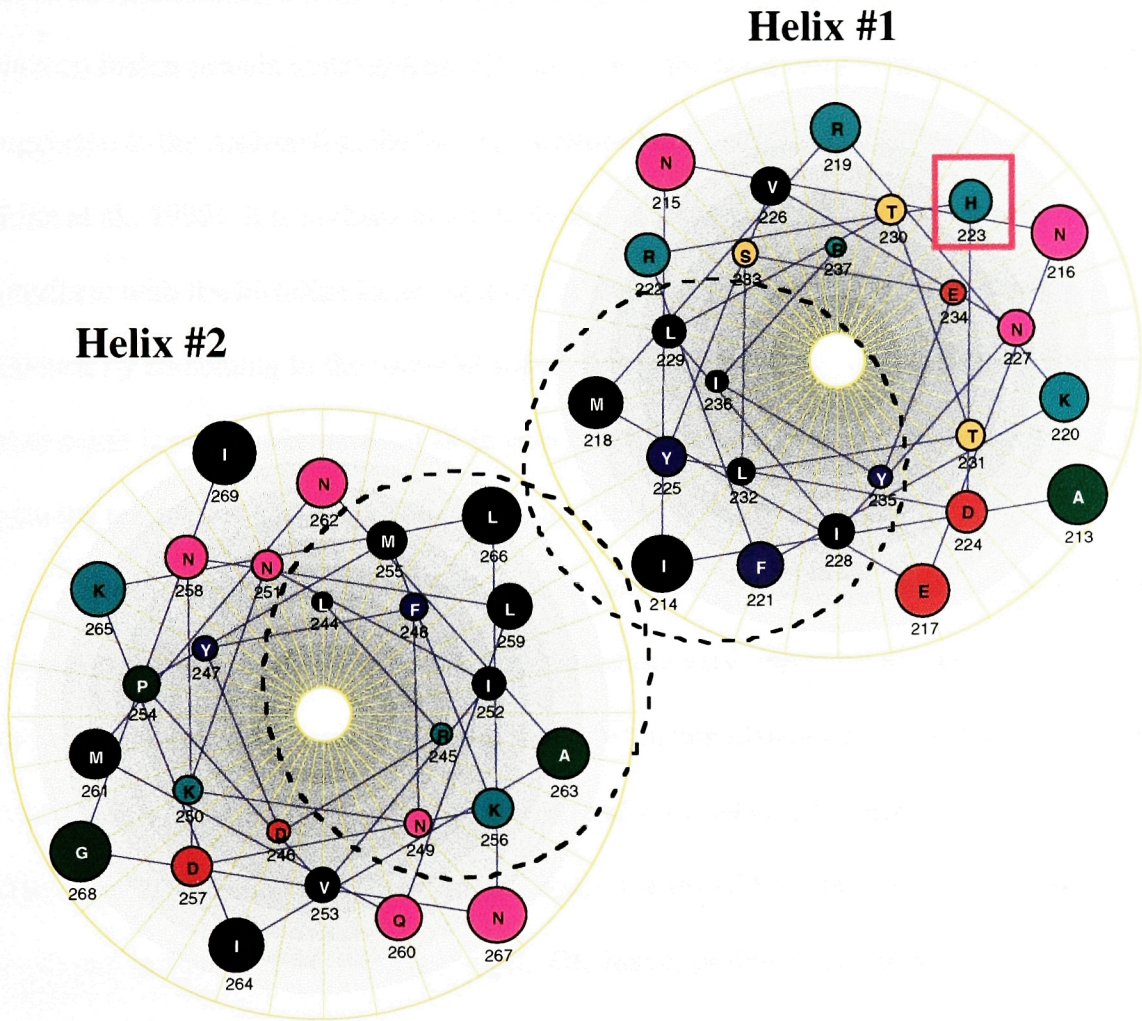

Figure 2.29. Helical wheel analysis, performed on the linker region of AgrC using the program, Protean, in the DNASTAR package. The critical and conserved histidine residue that is predicted to be phosphorylated is boxed and/or colored in red. A dotted circle surrounds the hydrophobic residues in the two helices that are predicted to pack together to form the four-helix bundle in a dimeric receptor.

helix bundle dimerization motif formed from within the linker region (Tomomori et al., 1999).

The above-mentioned study on AgrC (Lina et al., 1998) reported that fusion of the last extracellular loop and transmembrane helix of the AgrC sensor domain to the HK domain in an MBP fusion protein caused the kinase to only be active in the presence of bacterial supernatants containing the activating AIP-I. This experiment was conducted *in vitro* on fusion protein isolated from *E. coli* cells in the absence of detergents. This result suggested to the authors that the last extracellular loop contains the AIP binding site (Lina et al., 1998). It is perhaps more likely that the last extracellular loop somehow interferes with the histidine kinase activity of the receptor, and that this interference is relieved by something in the bacterial supernatant or perhaps by AIP binding. This *in vitro* result is very different from an *in vivo* situation where the transmembrane domain(s) span the membrane and is not solubilized by fusion to MBP.

As the results with chimeric sensor domains suggest that the entire sensor domain is important for AIP binding (*vide supra*), it became very important to reproduce the above *in vitro* results. Toward this end, the MBP-fusion plasmid constructs were obtained from Gerard Lina and the proteins expressed and purified (see Methods). Initially, the MBP-AgrC HK fusion protein (**Figure 2.30A**) was tested for constitutive kinase activity. As shown in **Figure 2.31**, the MBP-AgrC HK fusion protein constitutively autophosphorylates *in vitro* upon addition of ATPγ^{32}P, reaching saturation by 30-60 minutes of incubation. These results confirm that the soluble HK domain of AgrC is a kinase on its own without any portion of the sensor domain attached (Lina et al., 1998).

A)

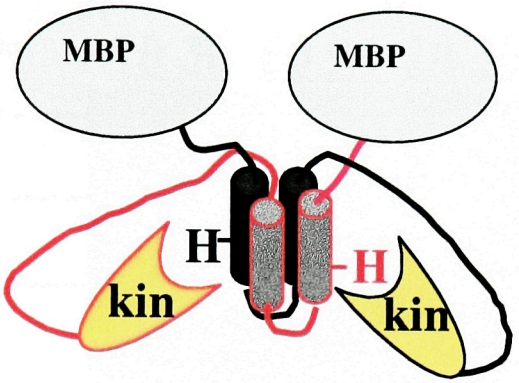

B)

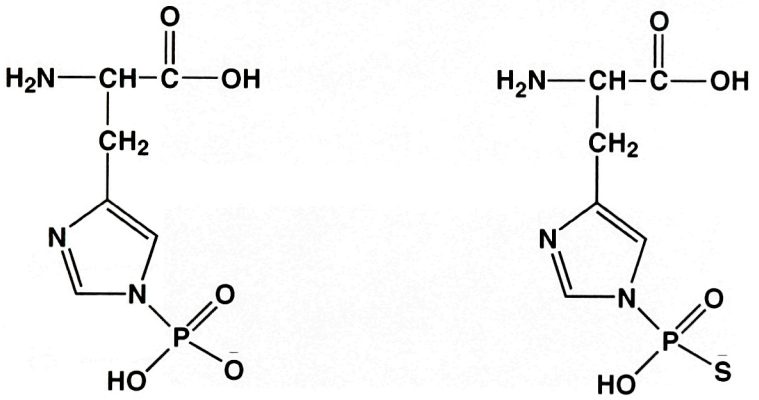

3-phosphohistidine **3-thiophosphohistidine**

Figure 2.30. Studies on the kinase domain of AgrC. A) A schematic diagram of the MBP-AgrC HK fusion protein, depicting the trans-autophosphorylating nature of histidine kinase domains. B) The chemical structures of 3-phosphohistidine and 3-thio phosphohistidine are shown. Histidine kinases autophosphorylate in the presence of ATP, yielding phosphohistidine derivatives.

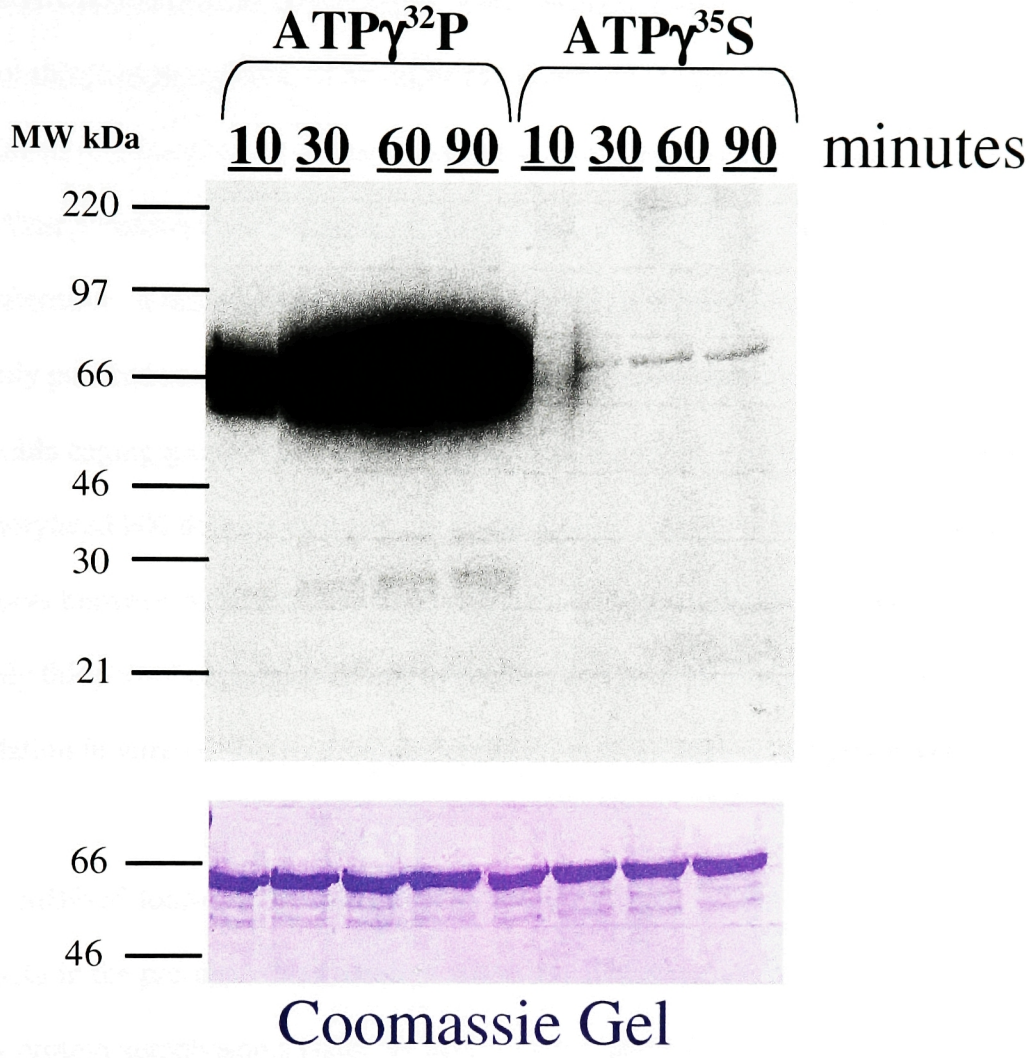

Figure 2.31. AgrC is a kinase. The MBP-AgrC HK fusion protein was phosphorylated *in vitro* in the presence of ATPγ^{32}P or ATPγ^{35}S of approximately similar specific activities. Different time-points were taken (10, 30, 60, and 90 minutes) and quenched with SDS-PAGE buffer. Parallel SDS-PAGE gels were run, one for radioactive imaging and the other for Coomassie Staining to verify equal protein loading.

As a control, ATPγ^{35}S, a pseudo-substrate competitive inhibitor, was tested in the MBP-AgrC HK fusion protein kinase assay. Some labeling was observed (**Figure 2.31**), indicative of thiophosphorylation of histidine in the protein (**Figure 2.30B**). Recently, it has been shown that thiophosphorylated histidine is much more stable to acidic conditions than phophorylated histidine, in the context of HK proteins (Lasker et al., 1999). Furthermore, it has also been recently shown that thiophosphorylated proteins can be selectively purified using a disulfide-capture resin and then modified with photocleavable caging groups (Zou et al., 2002). Thus, the ability to obtain a pure, stably thiophosphorylated HK domain of AgrC opens the door to a range of studies, including binding assays between AgrC and AgrA, potential thiophosphate transfer to AgrA to form a stably thiophosphorylated response regulator, and photoactivation of HK phosphorylation *in vitro* or *in vivo* through deprotection of a caged thiophosphorylated histidine.

The MBP-3rd loop-TM helix-AgrC HK protein (**Figure 2.32A**) was tested for kinase activity in the presence or absence of AIP-I at 1 μM. In contrast to published results, this protein autophosphorylates by itself *in vitro*, and this activity is unaffected by the addition of synthetic AIP-I (**Figure 2.32B**). The activity of equimolar amounts of the MBP-AgrC HK and the MBP-3rd loop-TM helix-AgrC HK proteins was not directly compared, so it is not possible to state that they have equal activity. However, it is certain that synthetic AIP-I had no effect on the activity of the MBP-3rd loop-TM helix-AgrC HK protein, thus casting doubt on the previous claim that the third extracellular loop is sufficient for AIP-I binding and HK activation (Lina et al., 1998). It is more likely that the reported increased activity upon supernatant addition resulted from changes in pH or

A)

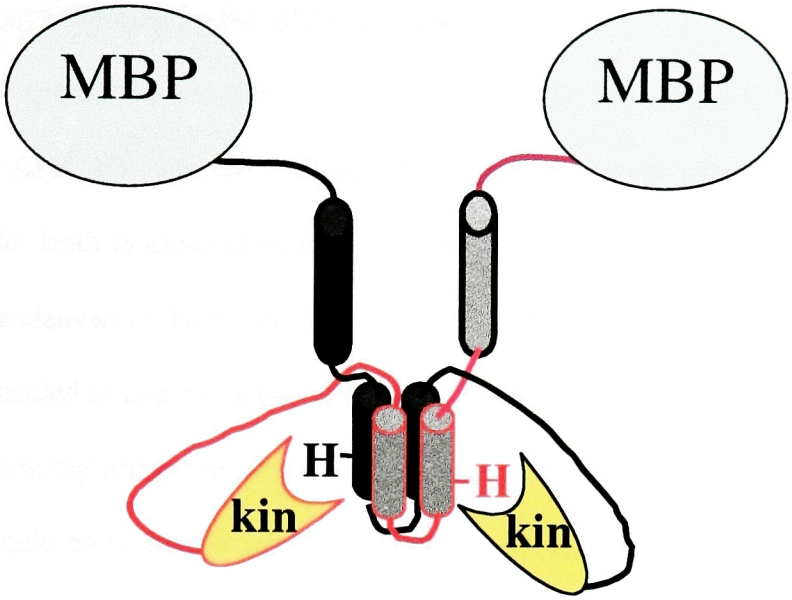

B)

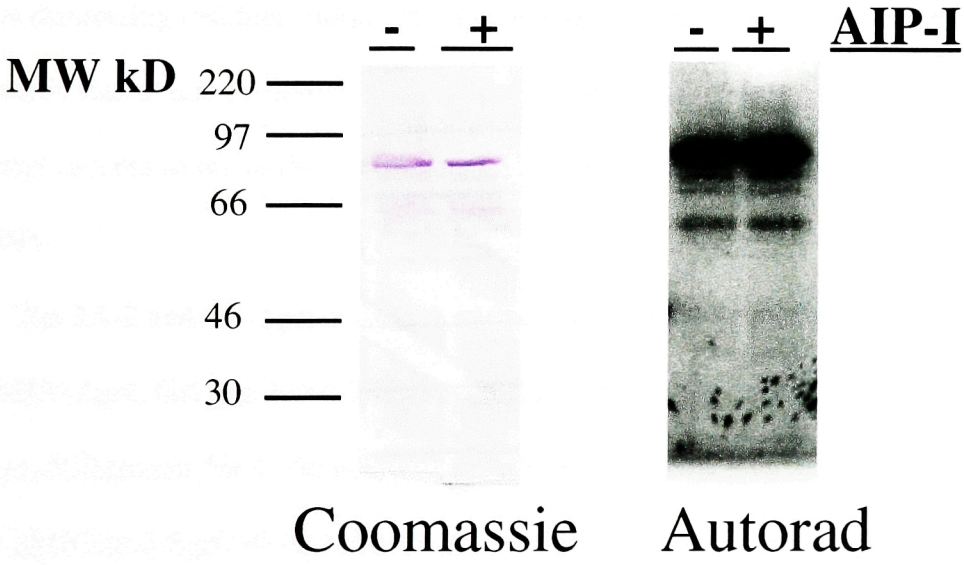

Figure 2.32. Kinase assay on MBP-3rd loop-TM helix-AgrC HK protein. A) Schematic diagram of MBP-3rd loop-TM helix-AgrC HK protein. **B)** Autophosphorylation of MBP-3rd loop-TM helix-AgrC HK protein in the presence or absence (±) of AIP-I at 1 μM.

osmolarity that affected kinase activity independently of AIP addition. These findings are also more consistent with the observation that the entire sensor domain of AgrC is necessary for potent activation by the AIPs (*vide supra*).

Extensive experimentation with Factor Xa cleavage of the MBP-AgrC HK, MBP-3rd loop-TM helix-AgrC HK, and the 3A-2 and 4A-2 proteins (see below and Methods) yielded poor results, both in terms of percent cleaved and percent recovered. The percent of the MBP fusion cleaved by Factor Xa never exceeded 50%, and the HK domain of AgrC on its own tended to aggregate and disappear during gel filtration, RP-HPLC, or ion-exchange chromatography (not shown). In the end, it was decided that efforts to purify the HK domain on its own would be abandoned. For the future, it might be worthwhile to demonstrate that the MBP-AgrC HK fusion protein is dimeric, either by gel filtration or analytical ultracentrifugation, followed by site-directed mutagenesis of putative dimerizing residues. Initial attempts to express His-tagged versions of the AgrC HK domain failed, due to cloning difficulties (see Methods). His-tagging has been used with great success to prove the dimeric nature of other RHKs, including EnvZ (Hidaka et al., 1997)

The 3A-2 and 4A-2 proteins (see Methods) are MBP-AgrC fusion proteins similar to the MBP-AgrC HK and MBP-3rd loop-TM helix-AgrC HK proteins, respectively, with two main differences. First, the number and composition of amino acids at the junction between MBP and AgrC differ between the proteins (Methods); and, second, both proteins lack a signal sequence in MBP, thus directing their expression to the cytoplasm rather than the periplasm (see Methods). Surprisingly, the 3A-2 and 4A-2 proteins were completely devoid of kinase activity. It is well known that the linker domain connecting

the sensor domain of RHK's to the HK domain is crucially important for proper function, including the proper topological arrangement of the HK domain in relation to the histidine-containing 4-helix bundle (Park and Inouye, 1997, Singh, 1998 #745), and it is also well known that bacterial chaperones in the periplasm can assist in proper protein folding (Gilbert, 1994; Rizzitello et al., 2001). As experiments with osmotic shock with the MBP-AgrC HK protein did not release significant amounts of protein, even though a large amount of protein was subsequently recovered after cell lysis, it seems likely that the vast majority of the functional protein was en route to the periplasm or simply expressed in the cytosol. Furthermore, there is very little (if anything) known concerning folding of histidine kinases in the periplasm of *E. coli* (B. Wanner, personal communication). Therefore, it appears more likely that modification of the linker region between MBP and the HK domain abolishes kinase activity, although further experiments are necessary to differentiate between the "linker" hypothesis and the "improper folding" hypothesis. In any case, as neither protein was active as a kinase, further experiments using them were abandoned, other than as reagents to test anti-AgrC antibodies in Western blotting (*vide infra*).

Expressing the AgrC HK domain *in vivo*

As it has been shown that MBP-AgrC HK protein is an active kinase *in vitro*, it was thought that expression of this protein *in vivo* would result in *agr* activation independent of AIP addition. Toward this end, the shuttle vector, pRN7035, previously used to make the group I, II and IV reporter strains, was utilized to express truncated version of AgrC along with full-length AgrA. A ribosome-binding site was incorporated

directly upstream of the start codon to ensure proper translation of these N-terminally truncated proteins. Unfortunately, the cloning of the AgrC HK domain into the *S. aureus* vector occurred prior to the knowledge that linker length and composition might be of critical importance to AgrC HK activity. Therefore, the construct lacks 3 amino acids (SQF) from AgrC that were present in the MBP-AgrC HK protein, i.e. MLLKEMKYK...cont... versus MBP-SQFLLKEMKYK...cont... (see Methods).

Upon testing three independent clones (6A, B, C) of the AgrC HK domain in *S. aureus*, no detectable uninduced or AIP-inducible *agr* activation was detected (**Figure 2.33A**), leading to the conclusion that this protein was not a consitutive kinase *in vivo*. Other constructs with N-terminal portions of AgrC appended onto the kinase (TM3TMHK and 3TMHK - see Methods) were also inactive *in vivo* (**Figure 2.33A**). However, the inclusion of transmembrane helices in these segments made it uncertain about the correct incorporation of AgrC into the membrane and/or possible aggregation of AgrC, and attempts to detect their expression with an anti-AgrC antibody on Western blots failed due to the fact that the antibody itself did not recognize AgrC (*vide infra*).

As one final means of confirming expression from these construct *in vivo*, the plasmids were introduced into the *agr*+ strain, RN6734, and checked for a possible dominant-negative effect on native *agr* signaling. In fact, the strains containing 3 independent clones of the AgrC HK construct produced significantly less *agr* activation, as assessed by transcription from the P3-blaZ promoter on the plasmid and also by transcription of RNAIII from the chromosome and subsequent translation of δ-toxin (**Figure 2.33B&C**). The 3TMHK construct exerted a similar effect (in two independent clones), whereas the TM3TMHK construct did not (in two independent clones) (data not

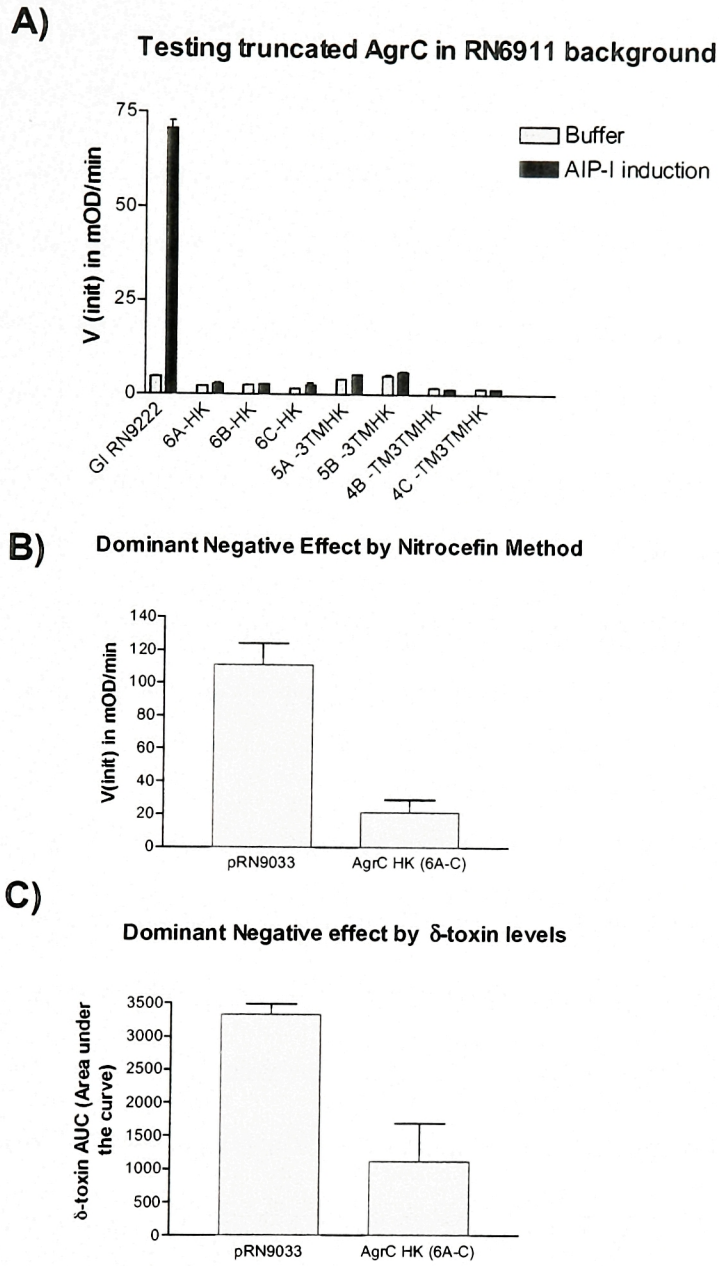

Figure 2.33. Expressing truncated version of AgrC *in vivo*. **A)** Independent clones from the 3 truncated versions of AgrC (see Results and Methods) were tested for *agr* activation by the β-lactamase assay, with or without AIP-I at 1 μM. The group I reporter strain, RN9222, is the positive control. **B)** The AgrC HK domain was checked for a dominant negative effect in the *agr*+ strain, RN6734, by the β-lactamase assay. Each clone exhibited this effect, so the data were combined to generate the SEM error bars associated with possible plasmid copy number differences. **C)** A similar result was obtained with the δ-toxin assay.

shown). Therefore, the HK and 3TMHK proteins are being expressed *in vivo*, but, instead of being constitutively active as kinases, they are exerting a dominant negative effect. The dominant-negative effect could result from several different possibilities (see (Wright et al., 2000; Wright and Kadner, 2001) for a discussion and analysis of such effects). The one most favored at this time is the possibility that the HK domain of AgrC dimerizes with the transmembrane native AgrC via four-helix bundle formation, thus disrupting signaling through a normally dimeric transmembrane receptor. However, it is also possible that the HK domain of AgrC on its own has phosphatase activity instead of kinase activity *in vivo*, as has been suggested from *in vitro* work in other HK signaling systems (Wright et al., 2000; Zhu et al., 2000).

Attempts to Develop an Anti-AgrC Antibody

During the course of this work, attempts were made to develop an anti-AgrC antibody, as this reagent would obviate the need for epitope-tagging of AgrC and would provide a readout for AgrC expression levels. Toward this end, a peptide from the 3rd extracellular loop of AgrC-I was synthesized, conjugated to Keyhole Limpet Hemocyanin (KLH), and injected into rabbits for polyclonal antibody development (assisted by Brenda Ayers). The amino acid sequence of this peptide was: C-Ahx-INSDEAKVIRQY, where a cysteine amino acid was added, N-terminal to an aminohexanoic acid (Ahx) spacer, for KLH conjugation (see Methods). Sera from two rabbits recognized the peptide epitope, containing the aminohexanoic acid (Ahx) spacer, on dot blots, and the same peptide (minus KLH) was used for affinity purification, resulting in substantial concentration of reactive antibodies (Methods).

However, extensive experimentation with Western blotting of whole cell lysates and/or membrane preparations from various *agr*± strains, including strains lacking protein A (known to bind strongly to the Fc region of IgGs, used for primary and secondary detection), never revealed a reactive band of the approximate molecular weight of intact AgrC (~50 kDa) (not shown). In addition, this antibody did not react with the purified MBP-3rd loop-TM helix-AgrC HK protein, containing most of the epitope sequence (SDEAKVIRQY), nor did it react with MBP fusion proteins constructed to contain the entire epitope (INSDEAKVIRQY) (see Methods). In the end, it was concluded that inclusion of the aminohexanoic acid spacer in the injected peptide biased the immune system to produce antibodies against this unnatural amino acid. In the future, the peptide, CINSDEAKVIRQY, should be synthesized and used to affinity-purify any reactive antibodies from the original rabbit serum. If anti-AgrC antibodies cannot be obtained in this fashion, then rabbits will need to be immunized with the peptide without Ahx, or else with a recombinantly expressed fragment of AgrC. It would be far superior to use chickens as the antibody producer, as it is known that, unlike mammalian IgG, neither the Fc region nor the Fab region of chicken IgY (IgG) reacts with protein A (Langone et al., 1983). However, unless the primary antibody is directly conjugated to alkaline phosphatase, this does not circumvent the problem that the Fc region of the anti-chicken secondary antibody (conjugated to alkaline phosphatase and presumably raised in rabbit or mouse) would also still bind to protein A. To get around this problem, the use of chicken anti-protein A antibodies is a viable option for blocking all protein A binding sites (Hoffman et al., 1996). Even with this, it is noteworthy that other secondary IgG binding proteins have recently been characterized in *S. aureus* (Zhang et al., 1998; Zhang

et al., 1999; Zhang et al., 2000). Even in *agr*-null, protein A-null strains, proteins of ~50 kDa in MW were observed to react with the anti-rabbit secondary antibody, so one must exercise caution in this molecular weight range when attempting to attribute a Western blot band to the primary antibody.

Regarding immunization with a recombinantly expressed fragment of AgrC, it is important to note that the MBP-AgrC HK protein discussed above has been used to generate an anti-AgrC antibody, which was reported to recognize an autophosphorylated AgrC, thus confirming AIP-induced AgrC autophosphorylation *in vitro* and *in vivo* (Lina et al., 1998). However, it is noteworthy that these authors did not check for whether their anti-AgrC antibody recognized the AgrC HK domain after removal of the highly antigenic MBP by Factor Xa cleavage. Therefore, this antibody (kindly provided by Gerard Lina) was checked for AgrC HK binding after Factor Xa cleavage of the MBP-AgrC HK protein (**Fig. 2.34**). Although the cleaved HK domain was relatively unstable after removal of MBP (thus making it hard to visualize on Commassie staining, **Fig. 2.34A**), radioactive kinase assays demonstrated its presence in the cleavage mixture (**Fig. 2.34B**). However, the antibody did not recognize the HK domain of AgrC, and instead only recognized MBP, thus leading one to question its validity as an anti-AgrC antibody (**Fig. 2.34C**). In the future, antibodies raised against MBP-fusion proteins should either be affinity-purified with some version of AgrC and/or immuno-depleted of MBP-recognizing antibodies. Unfortunately, these results raise uncertainty concerning the published data on autophosphorylation of AgrC *in vivo* in response to culture supernatants (Lina et al., 1998), as it is possible that the "reactive bands" resulted from IgG-binding proteins in *S. aureus* (*vide supra*). It is most likely the case that the observed

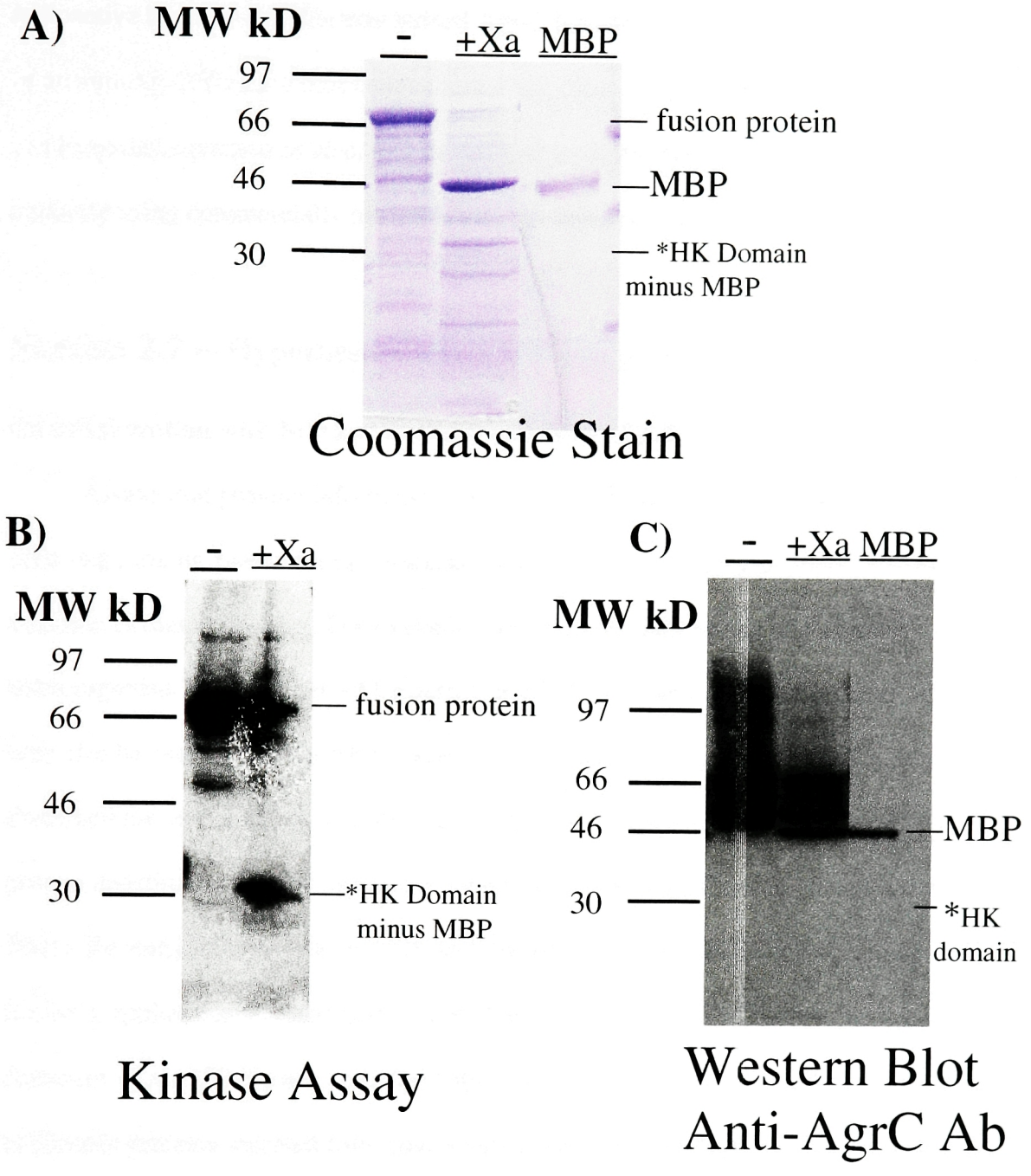

Figure 2.34. Testing of G. Lina Anti-AgrC Antibody. **A)** The MBP-3rd loop-TM helix-AgrC HK protein was proteolyzed with Factor Xa to remove MBP, as demonstrated by Coomassie staining. The HK domain of AgrC is unstable on its own and is thus only faintly visible on the Coomassie gel. **B)** However, a radioactive kinase assay demonstrates the presence of the HK domain after Factor Xa cleavage. **C)** Under these conditions, the anti-AgrC antibody appears to bind MBP but does not bind the HK domain.

radioactive band at ~50 kDa was indeed AgrC, but the proof of this provided in the form of an anti-AgrC Western blot is uncertain at this time. Perhaps, an epitope-tagged AgrC can be (over)expressed *in vivo,* and its AIP-induced phosphorylation can be proven with certainty using commercially available anti-epitope antibodies.

Section 2.7 -- Hypothesis-driven MS^n analysis of Staphylococcal AIPs.

(in collaboration with Markus Kalkum and Brian Chait)

Assays that provide information on specific peptides that are secreted by living cells (e.g., toxins, pheromones, virulence factors, quorum sensing peptides) can be valuable as diagnostic aids. For example, the presence and identity of a specific microorganism may be inferred by detection of characteristic secreted peptides, which may also be used to distinguish between subtypes of a given strain. Several authors have described the use of MS to identify microorganisms based on fingerprint masses of protein constituents as well as secreted peptides and proteins (Fenselau and Demirev, 2001). Recently, electrospray ionization-Fourier transform tandem MS of intact proteins has been applied for the characterization of biomarkers from *Bacillus cereus* T spores (Demirev et al., 2001) and a combined approach of single-stage and tandem MS was used to identify proteins secreted from adipocytes (Kratchmarova et al., 2002). Because these methods rely on the initial detection by single-stage MS of intact peptide ions from a highly complex milieu, it may be difficult to detect trace amounts of the secreted peptides. In addition to limitations imposed by dynamic range and signal suppression effects, low-level signals of interest tend to disappear into the "chemical noise" (Barnett et al., 2002; Krutchinsky and Chait, 2002). Here, a method, developed by M. Kalkum and

B. Chait and applied herein to a biological problem, is presented for the rapid, unambiguous detection of trace amounts of peptides secreted from microorganisms, utilizing multi-stage MS (MS^2 and MS^3) analysis of crude supernatant mixtures with a novel MALDI-quadrupole ion trap mass spectrometer (Krutchinsky et al., 2001). In this procedure, secreted peptide ions that are hypothesized to be present in the supernatant, but that are not sufficiently abundant to be observed in the regular single-stage mass spectra, are subjected to multi-stage MS. Highly specific fragmentation signatures enable unambiguous identification of the peptides of interest and differentiation of the signals from the background.

This method, termed *hypothesis-driven multistage mass spectrometry* (HMS-MS), is based on the ability of MALDI-ion trap mass spectrometry to separate specified peptide ions from a complex and noisy mixture and to convert these selected peptide ions into a few informative fragment species with low noise background. Resonant excitation within the ion trap provides an efficient method to cleave peptide bonds at preferred positions, leading to relatively simple fragmentation signatures with high signal-to-noise ratios. Key to the success of the approach is the very small fraction of the total sample that is consumed to obtain each multi-stage mass spectrum. Consequently, one can test a large number of different hypotheses on a given sample before it is depleted. In contrast to HPLC-coupled-MS, this method has no significant time limits on obtaining this information.

This method was used for the rapid detection and structural characterization of the autoinducing peptides (AIPs) of *Staphylococcus aureus*. Concentration or desalting steps were useful for the analysis of staphylococcal AIPs from bacterial culture supernatants. A

fast (~1 min) and simple purification procedure performed with small culture volumes (0.01–1 ml) was adequate. Despite this, it was not generally possible to decide on the presence or absence of AIPs based on single stage MS spectra (**Fig. 2.35**, top left hand panels of I, II, II and IV). Indeed, it was necessary to perform both double-stage (MS/MS) and triple-stage (MS^3) experiments on synthetic AIPs to assess the most intense fragment-ions that should be expected when analyzing the naturally occurring AIPs from supernatants. For example, the fragmentation of synthetic AIP-I ions yields an intense y_6 ion peak at m/z 711.5 and less intense y_5 and y_7 ion peaks at m/z 610.6 and 798.5, respectively (**Fig. 2.35, I**). However, only the intense y_6 ion can be distinguished from the background noise in the MS/MS spectrum of natural group-I AIP supernatants. Indeed, due to residual background in the MS/MS spectrum, it proved necessary to perform a triple-stage MS experiment (MS^3) to test whether the peak at m/z 711.5 from the MS/MS experiment can be attributed with high confidence to AIP-I. The MS^3 experiment with the supernatant sample of AIP-I revealed essentially the same fragmentation pattern as that obtained with the corresponding synthetic peptide. In general, MS/MS fragmentation of groups I, III, and IV AIPs lead to fragment ions that retain the cyclic component of the intact peptides. Since two cleavages are necessary to obtain observable fragments from a ring, such fragment ions were first detected in the MS^3 experiments (**Fig. 2.35**).

A deviation from this scheme was observed for AIP-II. This peptide was predominantly desorbed as the singly natriated ion ($M+Na^+$) rather than the more commonly observed protonated form ($M+H^+$) (**Fig. 2.35, II, synthetic**), even though the sample is prepared at low pH. Loss of phenylalanine in the MS/MS experiment indicates dissociation of the ring (**Fig. 2.35, II**, ion peak at m/z 754.5), which was not observed

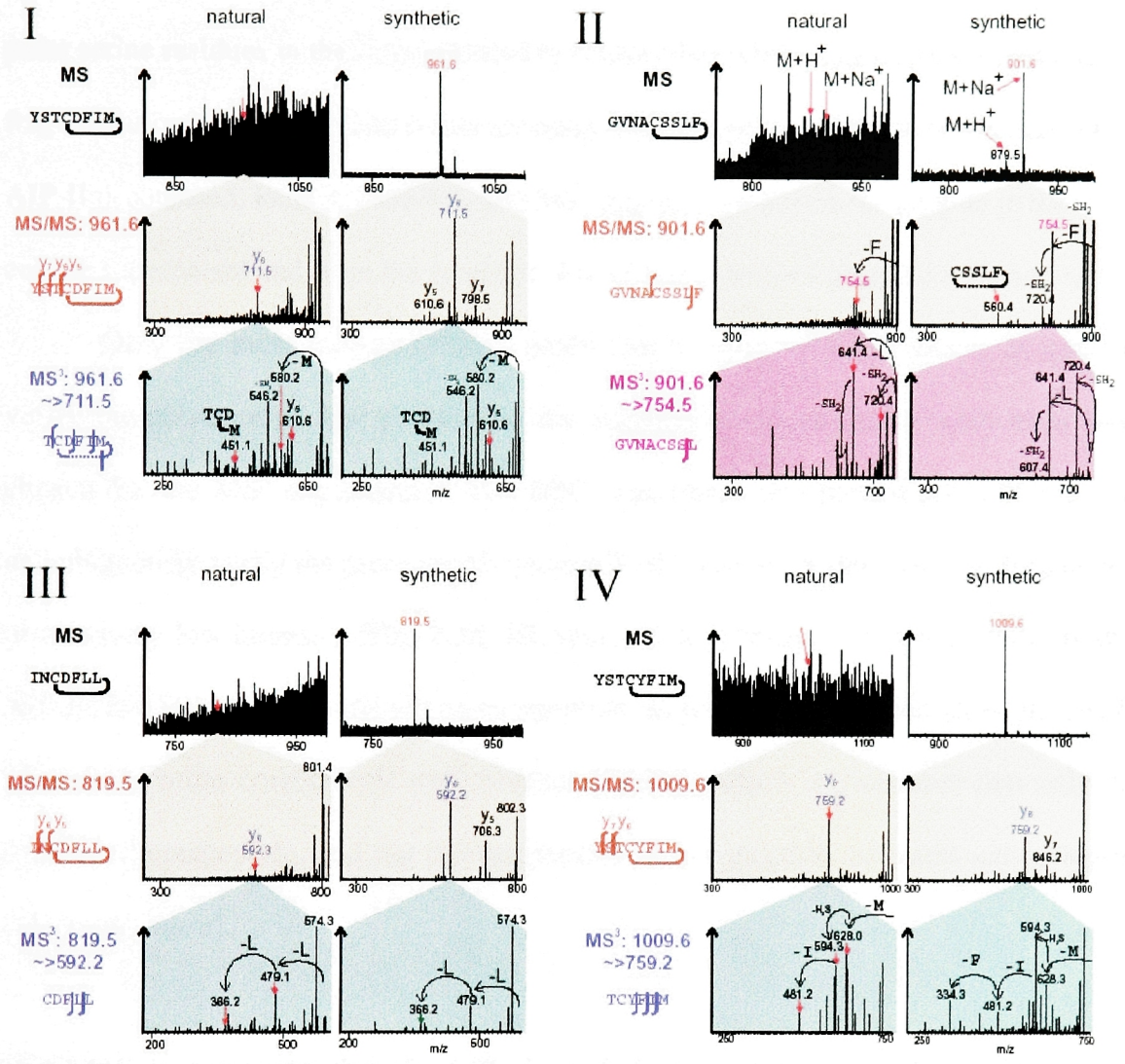

Figure 2.35. *Hypothesis-driven MS^n* analysis of groups I to IV autoinducing peptides (AIPs) from *S. aureus* culture supernatants (natural) and comparison with MS^n spectra of synthetic AIPs. Only the most abundant fragmentation pathways of these lariat-like peptides are indicated using the sequences on the left for each MS stage. Note that MS/MS and MS^3 experiments for AIP-II were performed on the more abundant natriated ions (M+Na$^+$), all other spectra are those of protonated ions and their fragments. The tip of the beige background underlying the MS/MS spectra points to the parent ion. MS^3 spectra are marked in blue for parental-y ions and in purple when derived from parental b-ions. This experiment was performed by Markus Kalkum.

when fragmenting the protonated synthetic peptide (data not shown). In this case, the polar serine residues in the ring appeared to chelate the sodium cation, thus altering the fragmentation behavior. When it was assumed that the hypothetical parent ion mass of AIP-II is natriated, identical MS/MS and MS^3 fragment ions from the peptide in the culture supernatant and from the synthetic AIP-II were obtained (**Fig. 2.35, II**, natural).

Only the most intense MS/MS peaks can be used with confidence in order to verify the presence of AIP peptides in the supernatants; hence, only their m/zs were chosen for the MS^3 experiments. The MS^3 experiment was particularly necessary to unambiguously verify the presence of native AIP-III because its diagnostic y_6 fragment is of relatively low intensity (**Fig. 2.35, III**, natural). In addition, the spectra indicate that AIP-III is a heptapeptide and not an octapeptide, as previously assumed (Ji et al., 1997). This observation corresponds well to other findings, which demonstrate that only the synthetic heptapeptide, and not the octapeptide or nonapeptide, activates *agr* group-III cells (*vide supra*).

HMS-MS demonstrates that the AIP of *Staphylococcus intermedius* is a Lactone

Five-fold concentrated, desalted culture supernatant of *Staphylococcus intermedius* gave a clearly discernable signal at m/z 1007.8 in the single-stage MS mode (**Fig. 2.36**). It would be possible to assign this signal to the AIP of *S. intermedius* if one assumes that the AIP is a nonapeptide and that cyclization is accomplished via a lactone bond rather than as a thiolactone (because the *S. intermedius* AIP contains a serine instead of a conserved cysteine residue at the corresponding position in all other AIPs examined). In order to test this hypothesis, multistage MS experiments were performed

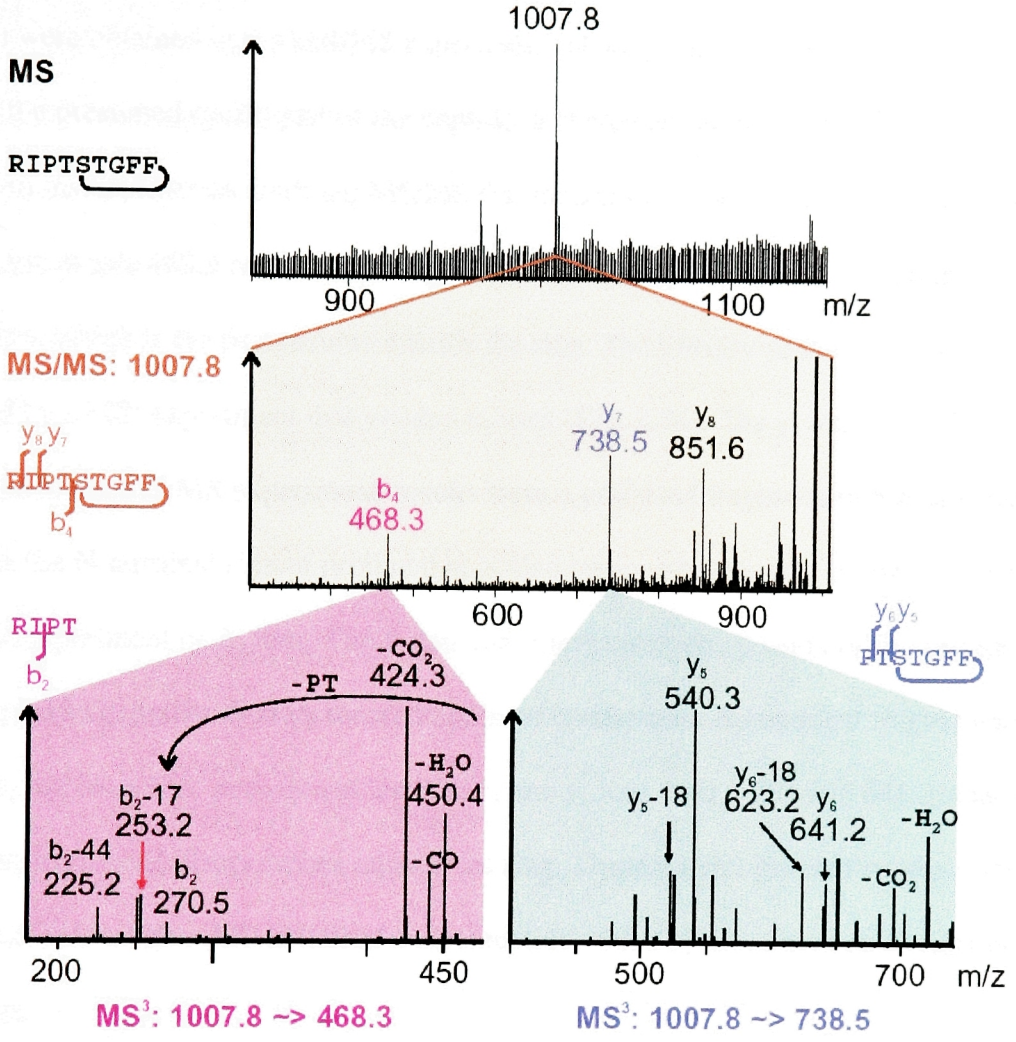

Figure 2.36. MALDI-ion trap MS^n characterization of the *S. intermedius* AIP from culture supernatants. Third stage fragmentation spectra are marked in blue for parental-y ions and in purple when derived from parental b-ions. The AIP is a nonapeptide whose circular portion comprises a lactone. This experiment was performed by Markus Kalkum.

on the ions at m/z 1007.8 and on fragments thereof (**Fig. 2.36**). Three fragments (y_8, y_7 and b_4) were obtained in the MS/MS experiment. None of these fragmentations occurs within the presumed cyclic part of the peptide, a characteristic that corresponds to observations made when studying MS/MS fragmentation of protonated *S. aureus* AIPs. The b_4 ion at m/z 468.3 results from fragmentation of the peptide bond C-terminal to the threonine, which is the first residue outside the ring. The identity of the b_4 ion was verified by a MS^3 experiment that yielded b_2 ions (**Fig. 2.36**). The y_7 ion at m/z 738.5, observed in the MS/MS experiment, results from a preferred fragmentation of the peptide bond on the N-terminal side of proline that is also responsible for generating b_2 ions in the MS^3 experiment on b_4 ions. The y_7 ion comprises the cyclic portion of the peptide, making it 18 Da lighter then its theoretical linear counterpart. Subsequent fragmentation of the y_7 ion in an MS^3 experiment leads to y_5 and y_6 ions (m/z 540.3 and 641.2) that also originate from bond dissociations outside the ring. These spectra provide strong evidence that the *S. intermedius* AIP is indeed a nonapeptide with a cyclized portion comprised of a lactone.

Hypothetical masses that form the basis for any HMS-MS experiment have to be assessed carefully as the example of the natriated AIP-II ions demonstrates. Although no synthetic form of the *S. intermedius* AIP was available for analysis, the MS^2 and MS^3 experiments of the natural AIP (**Fig. 2.36**) unambiguously characterize it as a nonapeptide lactone, which is the first such peptide characterized in *agr* signaling. This finding has important implications for understanding the detailed interaction of AIPs with their receptor (*vide infra*). The use of lactone peptides for quorum-sensing was also

recently shown in the gram-positive bacterium, *Enterococcus faecalis* (Nakayama et al., 2001).

Lactone AIPs – Implications for AIP-receptor interaction

The detection and characterization of a lactone AIP from *S. intermedius* has important implications for *agr* signaling, as an ester linkage is far less reactive than a thioester linkage to nucleophilic attack by a residue in AgrC. Therefore, signaling by this AIP would most likely proceed through a non-covalent interaction, thus making it unlikely that AIP-induced AgrC signaling occurs through any sort of covalent interaction in the entire *agr* system. However, one must first demonstrate that this AIP indeed activates its corresponding AgrC. Northern blot analysis in the laboratory of G. Lina has revealed up-regulation of RNAIII expression in pre-exponential cultures of RN9423 treated with stationary phase supernatants from the same strain (**Figure 2.37**-kindly provided by G. Lina), thus indicating that the lactone AIP most likely activates AgrC from this strain. The complete DNA sequence for the *agr* operon in this *S. intermedius* strain, RN9423, including the sequence of RNAIII, has been obtained. These data reveal that RNAIII includes what appears to be a viable δ-toxin sequence of: MAGDIISTIVDFIKLIAETVKKFTK. However, all efforts to detect δ-toxin production by RP-HPLC analysis of post-exponential or stationary phase bacterial cultures from this strain have failed (data not shown). Yet, blood plate analysis reveals a large clearing zone surrounding the streaked strain, consistent with the production of a very active hemolytic component (although it is unknown if this component is *agr*-regulated). Genomic DNA

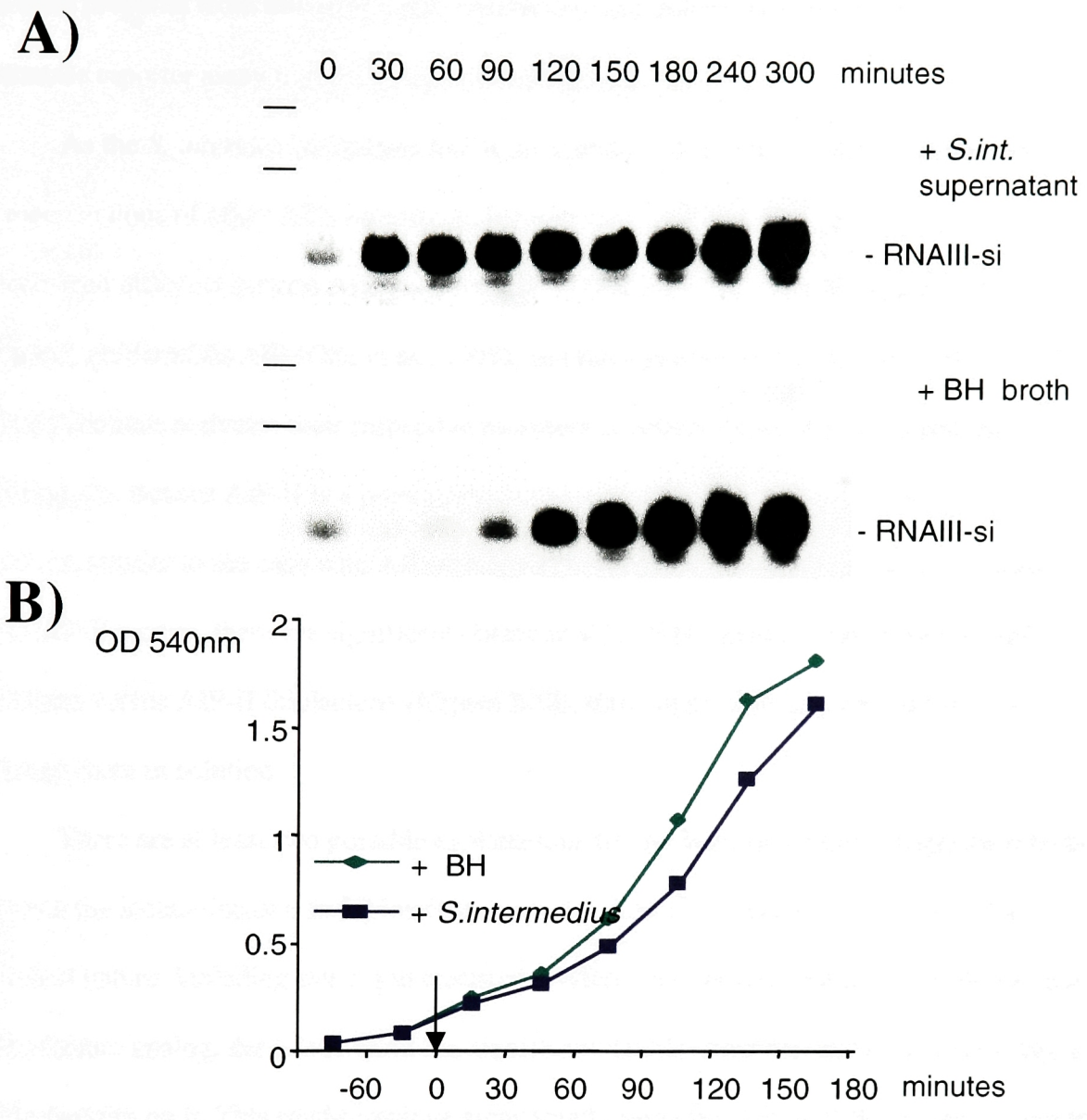

Figure 2.37. *S. intermedius* (RN9423) supernatant activates *agr* in *S. intermedius* (RN9423) cells . A) Northern blot analysis. One-tenth volume of post-exponential RN9423 supernatant (+ *S. intermedius*) or broth (+BH) was added to an early-exponential phase culture of RN9423 and samples were taken every 30 minutes for Northern blot hybridization analysis using an RNAIII-specific probe. RNAIII expression increased earlier in the culture induced by *S. intermedius* AIP lactone. **B)** Cell density was monitored over the course of the experiment, indicating that addition of *S. intermedius* supernatant had only a mild effect on growth of the cells. This experiment was performed by Yvonne Benito and Gerard Lina.

has been prepared from this strain, and experiments are underway to develop a β-lactamase reporter assay to monitor *agr* activation more easily.

As the *S. intermedius* lactone AIP is an activator of *agr*, it was asked whether the lactone versions of other AIPs activate their respective receptors. Two groups have synthesized different lactone AIPs, one for AIP-II (Mayville et al., 1999) and the other for the *S. epidermidis* AIP (Otto et al., 1999), and have published that neither of these lactone versions activates their respective receptors at concentrations up to ~5 μM. In addition, the lactone AIP-II is a potent cross-inhibitor of group I, but is not a self-inhibitor, similar to the case with AIP-II lactam (Mayville et al., 1999). As was also seen with AIP-II lactam, there are significant chemical shift differences (CSDs) between AIP-II lactone versus AIP-II thiolactone (**Figure 2.38**), thus suggesting structural difference between them in solution.

There are at least two possible explanations for the large difference in agonist activity between the lactam/lactone and thiolactone peptides. The first reason could be one of a chemical nature, including steric and electronic differences between the peptides. In the case of the lactam analog, the amide bond has significant double-bond character, thus imposing a rigid planarity on it. This might impinge significantly upon the ability of the ligand to bind to and activate the receptor, as the energetic cost for adopting an active conformation could be too high. In the case of the lactone analog, there are subtle electronic and stereochemical differences between sulfur and oxygen in the context of a thiolactone versus a lactone linkage, which could collectively account for the difference in activity between them. Some of these differences are: 1) Sulfur is a nonpolar atom relative to oxygen and more polarizable; 2) sulfur has a larger radius than oxygen, 2.0 A vs 1.72 A; and 3) the bond angle around a sulfur atom

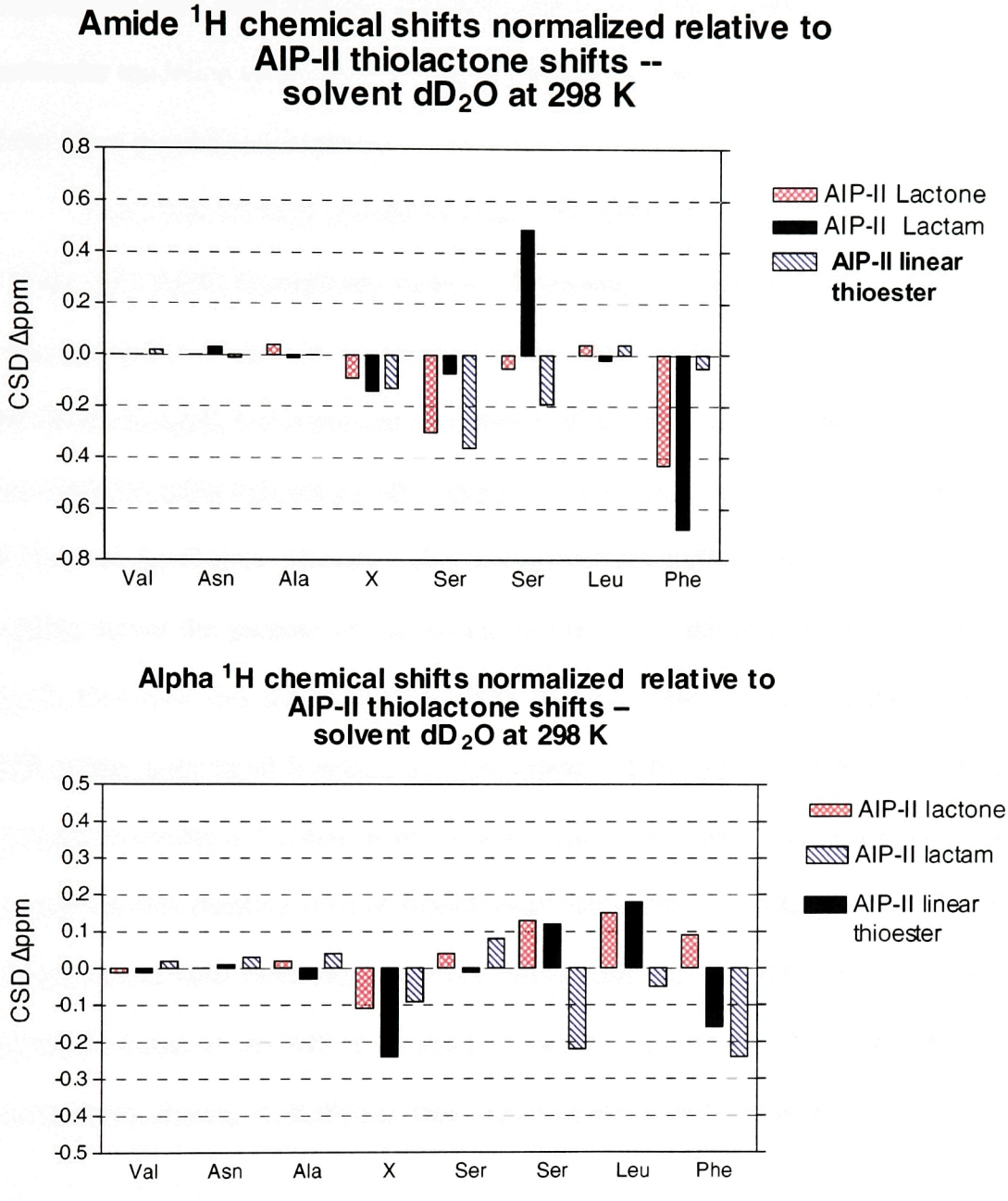

Figure 2.38. Chemical Shift Difference (CSD) Mapping of the Lactone AIP-II relative to AIP-II thiolactone, AIP-II lactam, and AIP-II linear thioester. Two-dimensional NMR assignmetns of each peptide in dD_20 at 298 K allowed for comparison between them, revealing significant amide and alpha ^1H differences between the lactone AIP-II and the thiolactone AIP-II, comparable in magnitude to the difference seen with AIP-II lactam or AIP-II linear thioester.

is generally more acute than around an oxygen atom. X-ray crystallography, NMR and molecular modeling studies of the AIPs and analogs derived thereof should delineate such differences in a detailed manner.

The second formal possibility is that the AIPs could be forming a transient covalent linkage with AgrC, through any number of potential nucleophiles, such as the side-chains of serine, aspartate, glutamate, tyrosine, cysteine (although this last amino acid is not present in the Group II AgrC, but is present in a conserved position in the Group I, III, and IV AgrC's) and histidine (although not possible in this case because histidine is not found in the sensor domain of AgrC from Groups I-IV). Such a model would predict that transient covalent binding serves the purpose of increasing the affinity of the ligand for the binding pocket in AgrC. However, this mechanism would be feasible only if release of the covalently bound AIP occurs with rapid kinetics, as slow release of the AIP or of trAIP-II should lead to pseudoirreversible activation or inhibition, respectively, which has not been observed (*vide supra*). As this putative release would most likely involve hydrolysis of the AIP-receptor adduct, rather than re-formation of the thiolactone peptide, HMS-MS was used to detect linearized forms of any AIP in groups I-IV culture supernatants. No such peptides were ever detected (not shown, M. Kalkum), thus rendering this possibility more unlikely.

Section 2.8 -- Peptidomimetic Design to develop more stable and potent universal *agr* inhibitors

There are several methods available to develop more stable and potent agr inhibitors, based on the lead compound, trAIP-II thiolactone, which has been shown to be a global inhibitor of *agr* activation (*vide supra*). Alternatively, high throughput screening

of small molecule libraries can lead to compounds radically different from trAIP-II, but with enhanced stability and/or potency. Both of these approaches are currently being applied in the laboratory.

Toward the first goal of converting trAIP-II thiolactone to a peptidomimetic, efforts have been initiated along the lines illustrated in **Figure 2.39**. The methods illustrated are by no means comprehensive, and there is a large body of literature relating to the art of peptidomimetic design (al-Obeidi et al., 1998; Steer et al., 2002).

As already discussed, trAIP-II lactam was synthesized and tested, and although it is a much more stable compound, it has a dramatic (~100-fold) loss in potency (*vide supra*). This loss in potency has been explained by structural differences between the lactam and thiolactone AIPs in solution. Paranthetically, it is noteworthy that the synthesis of trAIP-II lactam included macrocyclic ring closure mediated via intramolecular aminolysis of a linear thioester precursor, which resulted in one stereochemically correct product (see Methods). It is worth noting here that a recent paper detailing the synthesis of quorum-sensing lactone peptides via the different method of macrolactonization of protected peptide active esters in DMF reported racemization of the C-terminal amino acid during the procedure, as evidenced by chiral amino-acid analysis (Nakayama et al., 2001). Mechanistic studies of oxazolone-mediated racemization of peptide active esters are well-documented (Goodman and McGahren, 1967), and it is very likely that such a process can occur with synthetic strategies using cyclization of protected peptides in solution, as was done by other groups to sythesize the AIPs (Otto et al., 1998; Otto et al., 1999; McDowell et al., 2001) and by this group for the

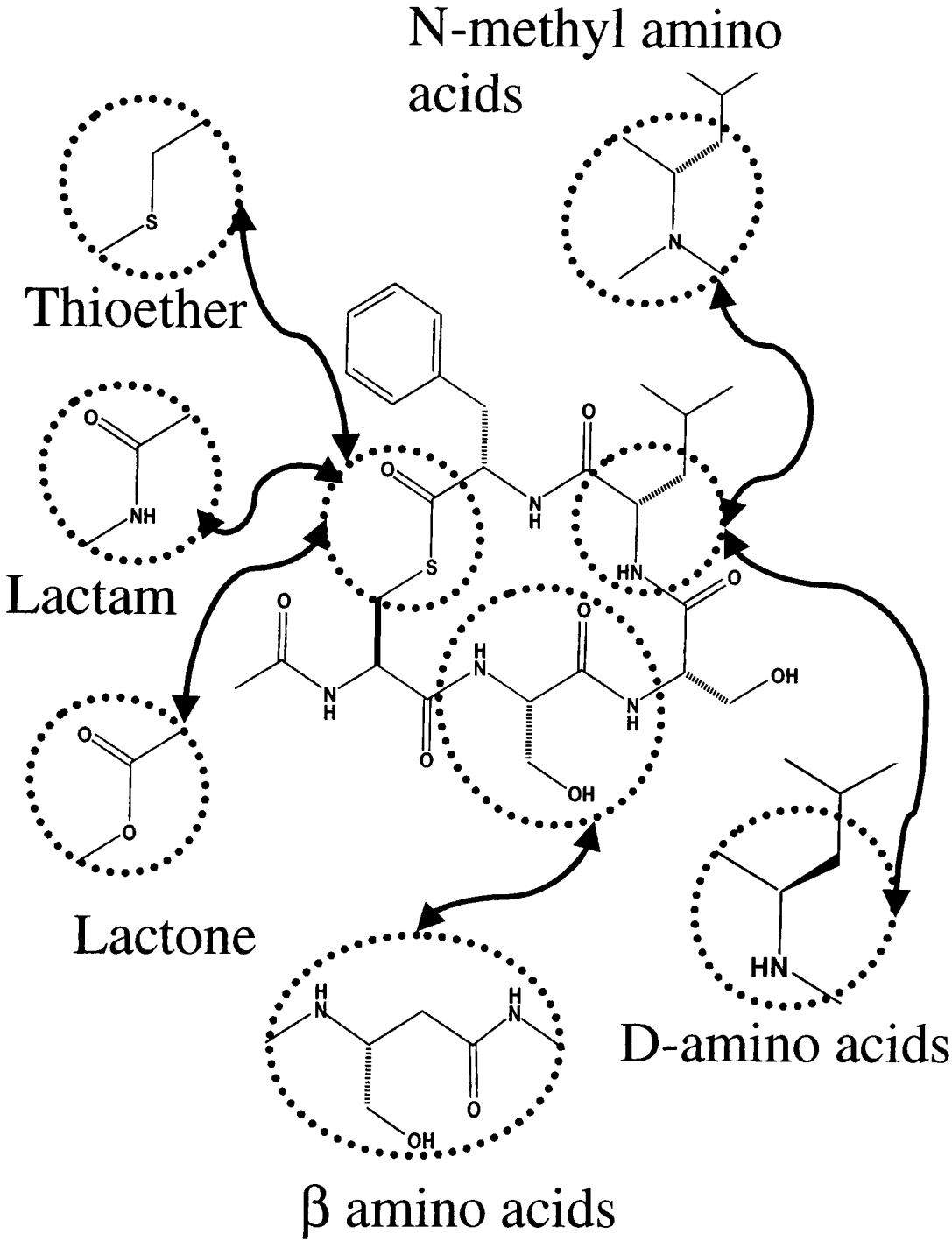

Figure 2.39. TrAIP-II Peptidomimetic Design. A diagram illustrates some of the many possible approaches to developing a proteolytically and pH-stable global inhibitor of virulence. Such approaches focus on stabilization of the base-labile thioester linkage, followed by efforts to minimize proteolytic cleavage of amide bonds by endopeptidases. Varying key side-chains and the peptide backbone of the AIPs, including the construction of smaller and larger macrocycles, promises to yield much insight into the sequence and structural requirements for AIP-induced AgrC activation or inhibition.

lactam and lactone AIP-II (Mayville et al., 1999). In the future, any AIP made by this latter method should be fully characterized to establish with certainty the stereochemical integrity of every stereogenic center. This could include the use of chiral amino acid analysis or other methods (Hayashi and Sasagawa, 1993; Vandenabeele-Trambouze et al., 2000).

To allow more flexibility in the thioester-replacing linkage without sacrificing stability considerations, a thioether AIP was envisioned. A synthetic strategy was devised, which commenced with conversion of protected linear trAIP-II thioester to a primary alcohol in solution with $NaBH_4$-mediated reduction in the presence of thiols. The inclusion of thiols ensured deprotection of the cysteine residue, which was protected with a thiosulfonate protecting group, while leaving the serine protecting groups (O-Benzyl) intact. The key step of the synthesis was to include a thiol-mediated Mitsunobu condensation with the C-terminal primary alcohol to form the thioether linkage. This was inspired by recent work demonstrating alkyl thioether synthesis via imidazole mediated Mitsunobu condensation (Falck, 1999).

After considerable optimization, the pure primary alcohol was obtained from the linear thioester starting material in an overall yield of 24% (not shown). However, extensive experimentation with Mitsunobu chemistry never resulted in thiol-mediated macrocyclization, as evidenced by RP-HPLC and MS. Although disappointing, this was not entirely unexpected, as the one paper concerning this key Mitsunobu step only formed highly favored 5- and 6-membered rings, using small molecules and not peptides (Falck, 1999). Two recent papers concerning the synthesis of cyclic lanthionine enkephalin analogues (Rew, 2002) and cyclic melanocortin receptor agonists

(Bondebjerg et al., 2002) suggest alternative schemes for the synthesis of trAIP-II thioether, which are actively being explored.

An alternative molecule to the trAIP-II thioether is the trAIP-II lactone (**Figure 2.39**). This molecule contains an ester linkage, which is much more stable than the corresponding thioester, and which has the advantage of flexibility that a lactam linkage does not possess. However, the results with full-length AIP-II lactone, including the dramatic CSDs observed in comparison to AIP-II thiolactone, raise doubts concerning the potency of self-inhibition by trAIP-II lactone, although it is important to assay a lactone molecule that has been fully characterized chemically with regard to stereochemistry. Therefore, efforts were undertaken to synthesize trAIP-II lactone (see Methods). The reaction resulted in formation of two products of identical mass, with the major product (presumably the unracemized L-version) eluting earlier on RP-HPLC as the more hydrophilic species. Unfortunately, the mass of these products did not correspond to that of trAIP-II lactone, but rather to that of a side-product brought about by reaction of trace pyrrolidine amines in the PYBOP with the activated ester in the linear trAIP-II starting material. Nonetheless, these results lend support to the possibility of racemization during cyclization of protected peptides in DMF with ester-activating reagents, such as PYBOP or HBTU, and catalytic DMAP.

Ongoing work in the laboratory, in collaboration with a graduate student, Jane Chao, is focused on the synthesis of AIPs incorporating ß-amino acids, N-methyl amino acids, and D-amino acids. In fact, one group has already begun D-amino acid scanning in the AIPs, although quantitative EC_{50} and IC_{50} values were not reported (McDowell et al., 2001). Preliminary results thus far have shown that the macrocyclization kinetics of the

AIPs in solution are dramatically slowed by peptide backbone modification, thus supporting the notion of structurally-assisted macrocyclization and thereby accounting for the extremely rapid and quantitative ring-closure of the AIPs in solution (on average, >95% complete in < 2 hours). This stands in dramatic contrast to the extremely slow and low-yielding macrocyclization of protected thiolactone AIPs in solution (McDowell et al., 2001).

Recently, Rockefeller University has established a high-throughput screening facility for the identification and analysis of small molecule agonists and antagonists. The *agr* project was used initially as a pilot project in the center. The normal 96-well assay format was converted to a 384-well format, and ~7000 compounds were screened for agonist activity and ~2000 for antagonist activity. This pilot project demonstrated that a 384-well format was suitable and efficient for high-throughput analysis in the *agr* system, and further demonstrated that the best signal-to-noise ratio was obtained when the bacteria were grown at 37°C, rather than at the somewhat more convenient room temperature. Several molecules were identified that appear to have agonist or antagonist activity, and efforts are currently underway to confirm these "hits". In the future, ~20,000 compounds will be screened for agonist and antagonist activity using the optimized assay format. This will hopefully lead to stable and potent *agr*-active compounds that can then be assessed for activity in mouse models of infection.

Chapter 3 - Discussion

General Significance of the *agr* System

Two-component systems are the major means by which bacteria sense environmental stimuli. In most cases, the activating ligands for the receptors are unknown (Hoch, 2000). The *agr* system is one of a few cases where the ligands have been chemically characterized, as thiolactone peptides (AIPs), and the system is unique in that AIPs from heterologous strains are naturally occurring inhibitors of *agr* signaling. Herein, the mechanism by which naturally-occurring AIP sequence variants activate and inhibit *agr* has been investigated. Although the *agr* locus is conserved throughout the staphylococci, the *agr* autoinducing peptides and their cognate receptors have radically diverged, generating at least four autoinduction specificity groups in *S. aureus*. In general, AIPs activate *agr* expression in strains belonging to the same *agr* group as the producer strain, and inhibit *agr* expression in organisms belonging to any other group. It is very possible that this divergence causes intergroup interference, leading to environmental isolation, and is at least partially responsible for speciation within the staphylococci. Similar divergence within the structurally similar *comAP* locus, required for competence in bacilli, is also thought to be responsible for speciation in these organisms (Tortosa and Dubnau, 1999).

The AIPs Activate and Inhibit *agr* Signaling through AgrC

It was previously hypothesized that activation and inhibition by native AIPs might involve different mechanisms - either different modes of interaction with the AIP receptor, AgrC, or interaction with cellular components other than AgrC - *e. g.*, AgrB

(Mayville et al., 1999). This latter possibility was clearly ruled out by means of plasmid constructs containing a ß-lactamase reporter driven by the (conserved) *agr* P3 promoter and including the P2 driven *agrA+C* modules from different specificity groups. Placement of these plasmids in *agr*-null derivatives of the *agr* specificity group corresponding either to that of the cloned module or to that of other groups, enabled the direct *in vivo* analysis of AIP-specific activation/inhibition in the absence of AgrB or of any endogenous AIP. Since these tests demonstrated the predicted cross-group inhibition, it is clear that AgrB is not the site of inhibition. Since these tests also demonstrated that cross-group inhibition occurs independently of host background, and with similar dose responses, it is also clear that the only determinant of *agr* group specificity is the AgrA+C module. Although AgrA and C were not tested independently, AgrA is identical between the *S. aureus agr* specificity groups, whereas the sensor domain of AgrC is highly variable; thus there is little doubt that AgrC is the key determinant. This was confirmed through sensor domain swapping, in which it was shown that activation and inhibition follow with the sensor domain of the respective AIP receptors. Although there are certainly other cellular factors involved in *agr* signaling, the results indicate that none of these determines group-specificity.

AIP-Receptor Interaction is Reversible and Competitive

A primary focus of this work has been on the reversibility (or irreversibility) of the *agr* AIP-receptor interaction. The theoretical basis for this focus was the possibility that the AIPs, with their highly reactive thiolactone bond, unique for signaling peptides, might act by acylating their receptor, leading to irreversible activation. This was initially

supported by experiments in which it was not possible to eliminate AIP-induced signaling completely by extensive washing. However, a definitive test for reversibility was enabled by the natural antagonism among variant AIPs produced by strains belonging to different *agr* specificity groups. In these experiments, AIP-I and –II and their synthetic analogs were tested versus reporter strains belonging to either group. Using several different experimental protocols, it was shown clearly that AIP-receptor binding/activation is completely reversed by the addition of an antagonist AIP. Thus the residual activity remaining after extensive washing was eliminated by treatment of the cells with an antagonist, and only the relative concentrations of agonist and antagonist but not the order of their addition determined the outcome of an experiment. Furthermore, an extracellular site of action for the AIPs is supported by the sensor domain swapping results as well as by the washout data. Although these data and the activation seen with the lactam analog rule out a stable covalent linkage between the AIPs and the receptor, a transient covalent linkage formed between the AIP and receptor cannot be completely ruled out.

Pharmacological experiments were performed in which agonist concentration-response curves were measured in the presence of increasing concentrations of antagonist AIP. In all cases examined, the agonist and antagonist curves shifted in a parallel, dextral fashion with no depression of the agonist maximal response. Qualitatively, these observations are consistent with a simple competitive interaction in which the agonist and antagonist AIPs compete for the same binding site on the receptor, AgrC. The data sets were also analyzed using the non-linear regression method of Lew and Angus (Lew and Angus, 1995). The calculated Schild slopes were all considerably less than unity.

Surprisingly, this does not conform to a simple 1:1 competitive interaction, which predicts a Schild slope of one. It should be noted, however, that because the assays in the current study quantified downstream transcriptional effects, mechanistic interpretations of the Schild slope factors and pA_2 values remain speculative until future (direct binding) experiments can determine such values more directly. This caveat aside, the results do raise the possibility that the receptor-ligand interaction occurs through some more subtle mechanism. In this regard, it is worth noting that bacterial RHKs are generally thought to be dimeric (Stock et al., 2000), raising at least the possibility of cooperativity between two AIP binding sites. Although this is an intriguing idea, additional experiments along the lines of a direct binding assay will be required to test this hypothesis.

The Thioester linkage is Not Required for *agr* Activation

The lactam analogs of AIP-I (McDowell et al., 2001) and AIP-II can activate their cognate receptors, but only at very high concentrations. The finding that this activation is competitively blocked by a native heterologous AIP suggests that the lactam analog binds its cognate receptor on the same site as the native thiolactone but only very weakly. Furthermore, this suggests that the highly reactive thiolactone linkage is not absolutely required for activation of the receptor, although this linkage does confer much increased affinity to the AIP. The difference in affinity between the lactam and thiolactone AIPs is explained by their different conformations in solution, as determined by two-dimensional NMR analysis, which further demonstrated that the trAIP-II lactam and trAIP-II thiolactone have very similar conformations to their corresponding full-length analogs (see Results). It is very likely that the lactam analogs of the AIPs (full-length and

truncated) have a conformation in solution that is very different from the receptor-bound conformation of the signaling AIP. There are two possible reasons to explain why it might be thermodynamically more costly for the AIP lactams to assume a receptor-bound conformation. First, the lactam analogs have a hydrogen bond donor in the form of an amide proton that does not exist in the thiolactone peptides, which could result in a different hydrogen bonding network. Second, the activation energy barrier for rotation around an amide linkage is much higher than for rotation around a thioester linkage. Therefore, a thermodynamic penalty is incurred when the lactam analogs bind to AgrC, thus decreasing affinity.

Cross-inhibition by the AIP-II lactam analog is similar in potency to cross-inhibition by the native AIP-II, suggesting that the lactam binds the heterologous receptor with similar affinity as the native peptide. Thus, the cross-inhibitory action of the AIPs involves an interaction with the heterologous receptor that is different from binding to the cognate receptor. This cross-inhibitory binding is also very permissive with respect to the AIP amino acid sequence, since many variant AIPs so far tested are strong antagonists though their sequences are highly divergent (Ji et al., 1997; Otto et al., 1998; Jarraud et al., 2000). However, the C-terminal hydrophobic amino acids in the AIPs appear to be critical for receptor binding and subsequent inhibition (discussed further below).

Key Determinants of Receptor Binding and Activation in the AIPs

Extensive structure-activity relationship (SAR) studies have been performed on the AIPs (Otto et al., 1998; Mayville et al., 1999; Otto et al., 1999; Lyon et al., 2000;

McDowell et al., 2001; Otto et al., 2001; Lyon et al., 2002; Lyon et al., 2002), and have shown:

i) The length of the AIPs varies from 7-9 amino acids in length, with an invariant cysteine located five amino acids from the C-terminus, which is fixed based on the absolute conservation of a presumed AgrD processing motif (DE) directly following it in over 30 different AgrDs (Dufour et al., 2002).

ii) The AIPs contain a thiolactone that is formed from the condensation of the α-carboxyl group of the peptide with the sulfhydryl group of the conserved cysteine

iii) The macrocycle is required for agonist activity (residues contained within the macrocycle are referred to as endocyclic, whereas residues N-terminal to the conserved cysteine and therefore outside of the macrocycle are referred to as the "tail" or exocyclic.

iv) The nature of the linkage forming the macrocycle, comprised of a thioester bond, is critical for certain aspects of biological activity, as the lactam analogs of AIP-I and AIP-II are potent cross-group inhibitors but activate receptors within their group only at very high concentrations (McDowell et al., 2001; Lyon et al., 2002).

v) In the case of AIP-II, the tail is necessary for AgrC-II activation but not for AgrC-I inhibition (Mayville et al., 1999) and substitution of asparagine for alanine at position 3 in the tail of AIP-II converts an agonist into an antagonist of AgrC-II activation (Lyon et al., 2002).

vi) The C-terminal three and two residues in AIP-I and –II, respectively, are hydrophobic, and substitution of these residues by alanine decreases activation and cross-inhibition dramatically, thus leading to the conclusion that these residues are critical for AIP binding to AgrC (Mayville et al., 1999; McDowell et al., 2001).

vii) Subsitution of the endocyclic aspartate by alanine at position 5 in AIP-I converts it from an agonist into an antagonist of AgrC-I activation (McDowell et al., 2001).

In addition, characterization of the AIPs from the four known *S. aureus agr* groups with respect to their activating and inhibiting activities has been completed. Several analogs of the AIPs demonstrate further that certain residues in the AIPs are critical for receptor activation. These key residues are not all located at corresponding positions, being endocyclic in some peptides and exocyclic in at least one (AIP-II). Furthermore, the interaction of these key residues with the receptor is critically dependent on the composition of the rest of the peptide. Moreover, the presence and composition of the tail exerts profound effects on the function of the AIP, even though it has little to no impact on the structure of the macrocycle, as determined by two-dimensional ^{1}H NMR.

While AIP agonist activity is very sensitive to amino acid side chain and structural changes, cross-inhibition by the AIPs seems to be more tolerant of sequence and structural diversity, as the AIP-II lactam and several alanine-substituted analogs have potent antagonist activity (Mayville et al., 1999; McDowell et al., 2001). This observation has led to the suggestion that cross-inhibition by the AIPs involves a binding interaction that is different from that of agonist AIP binding, although the inhibition is

competitive (Lyon et al., 2002) (illustrated schematically in **Fig. 3.1**). This hypothesis is supported by experiments performed with chimeric AIPs, in which it was shown that a peptide possessing both of the residues in AIP-I and -II critical for agonist activity did not activate and instead universally inhibited AgrC activation (**Table 2.6**). Therefore, in the chimeric AIPs, these critical residues are not presented in the proper orientation within the ligand binding pocket of the receptor (**Fig. 3.1**). This result provides a sharper focus on the general phenomenon of cross-inhibition by native AIPs, which usually differ from the group-specific AIP agonists at many positions. This means that particular residues in the tail and macrocycle must match in order for the AIP to bind in the correct orientation to activate the corresponding receptor; otherwise, competitive inhibition results.

The apparent difference in the roles of the ring and tail moieties of AIP-II could be interpreted to mean that the ring structure is responsible for recognition of and binding to the putative ligand pocket of the receptor, and that the tail region is responsible for initiating the signaling process. It was reasoned that removal of the tail region might render a ligand which should be unable to activate AgrC signaling but should be a strong inhibitor of its cognate AgrC as well as of the heterologous AgrCs. This was confirmed using a truncated AIP-II (trAIP-II) lacking the tail but retaining the thiolactone structure. This peptide inhibited not only AgrC-II, but also AgrC-I, III, and IV (which, based upon the current understanding of *agr* grouping, represents global *agr* inhibition in *S. aureus*). Furthermore, trAIP-II weakly inhibited δ-toxin production in the *S. epidermidis* strain, RN2375, and strongly inhibited δ-toxin production in the *S. warnerii* strain, RN3178. These results suggest that trAIP-II may serve as a model for a global inhibitor of staphylococcal *agr* activation, which may be of therapeutic relevance. Furthermore, the

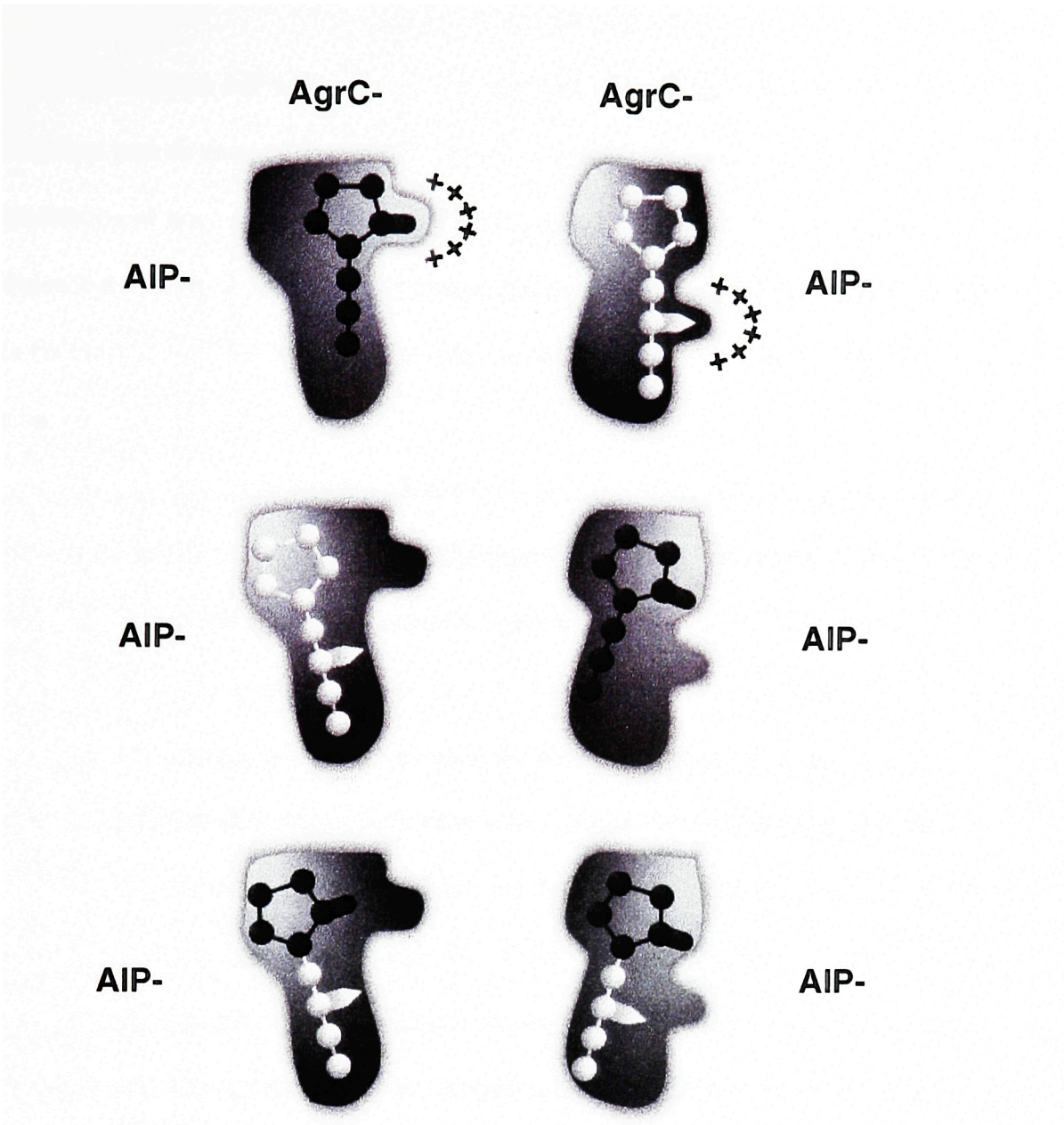

Figure 3.1. Model of receptor binding modes - AIP-I, AIP-II, and the chimeric peptide, AIP-II/I, are depicted schematically as bound to the ligand binding pocket of AgrC-I and –II. The key endocyclic residue (D5) of AIP-I and the key exocyclic residue (N3) of AIP-II insert into hypothetical grooves of AgrC-I and -II, respectively, triggering receptor activation, as illustrated by +++++. Cross-inhibition most likely involves different orientations of binding to the heterologous receptor, as depicted by the tilt of the ligands in the binding pockets of AgrC-I and –II. The chimeric peptide, AIP-II/I, does not activate and instead inhibits AgrC-I and –II because it also binds in a different orientation, thus preventing the key residues from activating their respective receptor. This is a highly schematic model for the sole purpose of illustrating different modes of binding, and there is currently no information available concerning the ligand binding pocket within the sensor domain of AgrC.

observation that an AIP agonist of the *agr* response (i.e. the intra-group AIP) can be converted into an antagonist of that response by removing the tail (i.e. trAIP-II) or by substitution of asparagine for alanine in AIP-II N3A, provides further, compelling evidence that AgrC is the molecular locus of activation and inhibition. Ongoing studies are focused on the design and/or discovery of peptidomimetic or small molecule agonists or antagonists of *agr* signaling.

Two-dimensional NMR studies did not reveal any significant chemical shift differences in the backbone protons of the truncated analogs versus their respective full-length AIPs, suggesting that the backbone structure of each macrocycle is not dramatically altered upon removal of the tail. However, the large difference in bioactivity between these analogs, with EC_{50} values in the nanomolar range for agonists and substantially higher IC_{50} values for truncated antagonists (**Table 2.6**), suggests that removal of the tail usually, but not always, results in decreased affinity of the ligands for the receptors. In the case of AIP-I and –IV, affinity can be regained through modification of the ligand, since trAIP-I D2A inhibits receptor activation in the nanomolar range. Another way in which affinity can be restored is by adding the tail from a different AIP. As the heterologous tail does not materially affect the structure of the macrocycle, it is likely to exert its effect through increased interactions with the receptor. For example, the chimeric peptide, AIP-I/II, inhibits AgrC-I, -III and –IV activation with IC_{50} values that are substantially lower than those seen with trAIP-II. In addition, AIP-II/I inhibits AgrC-I at nanomolar concentrations, in contrast to the inhibition in the micromolar range by trAIP-I (**Table 2.6**). This is not the whole story, however, since trAIP-I and -IV are only marginally less potent as inhibitors of AgrC-II than are the corresponding native AIPs.

Structure-activity studies of the endocyclic residue at position 5 in AIP-I and –IV revealed several significant features of the peptide-receptor interaction. Substitution of asparagine for aspartate in AIP-I converted a weak activator of AgrC-IV to a potent inhibitor, suggesting that the negative charge of the aspartate residue in AIP-I cannot be readily accommodated in the binding pocket of AgrC-IV. In contrast, the electrically neutral asparagine binds with relative ease in the AIP-IV binding pocket, though this does not result in AgrC-IV activation. The mechanistic basis for weak activation by AIP-I and inhibition by AIP-I D5N will only be fully understood once the ligand binding pocket in AgrC-IV has been characterized.

Activation of AgrC-I by AIP-I, AIP-IV, AIP-I D5N, AIP-IV Y5F and inhibition by AIP-I D5A suggests that a single side-chain methyl group at position 5 (i.e. AIP-I D5A) is insufficient for AgrC-I activation, but that bulkier groups will do, with the exception that positively charged side-chains have not been tested. Furthermore, the partial agonism of AgrC-I by trAIP-I but not by trAIP-I D2A suggests that the key aspartate residue confers activating properties on the macrocycle in the absence of the tail. Lastly, in the course of testing the various analogs, it was found that AIP-I D5N activates *agr* signaling in group III cells. This activation is surprising, as native AIP-I and AIP-III are cross-inhibitors of AgrC-III and –I, respectively, and both AIP-I and AIP-III share a common endocyclic aspartate residue that has been shown to be critical for AgrC-I activation by AIP-I. Initial studies of this activation of AgrC-III by AIP-I D5N have indicated that it might be proceeding through a non-competitive mechanism at the level of AgrC. Future studies should attempt to localize this non-competitive activation to the sensor domain of AgrC-III, as it is possible that activation by this analog might be

occurring through some other mechanism other than binding to the AIP-III binding pocket of AgrC-III.

The native AIP-III is a heptapeptide, as determined by synthetic means and by HMS-MS. The addition of extra residues on the N-terminus of AIP-III switches it from an agonist into an antagonist, and the addition of an N-terminal glycine to the *S. epidermidis* AIP inactivates the peptide (Otto et al., 1999). In contrast, N-acetylation or the addition of relatively bulky groups (such as fluorescein or biotin) to the N-terminus of AIP-I does not affect its activity. These contrasting results suggest that the effect of N-terminal modification varies for different AIPs. Furthermore, the contrasting lengths of the AIPs (7, 8, or 9-mers), along with the complete lack of detection by HMS-MS of any other shorter or longer forms in bacterial superatants of the respective *agr* groups, suggests that the processing enzyme, AgrB, specifies the length of the corresponding AIPs relative to the conserved C-terminal (DE) motif in the AgrD propeptide. The mechanistic basis by which this is achieved remains a complete mystery.

An enduring question is why evolution has favored the use of a thioester linkage in the AIPs, which has not been described in any other receptor-ligand based signaling system. If the thioester linkage is not involved in acylation of the receptor, then other theories must be invoked to explain its presence. One possibility is that enzymatic formation of these peptides by the protein, AgrB, utilizes the relatively reactive thiolate anion of the cysteine side chain for cleavage of the pro-peptide sequence. Alternatively, it is possible that the transient nature of a thioester linkage at physiological pH could provide a means for the signal to be abolished in a relatively short time period. This might be advantageous for the bacteria in allowing them to modulate their own virulence

by continual synthesis of the AIP in settings where virulence genes need to remain on and to stop synthesis in settings where virulence genes need to be switched off rapidly.

Localization of Binding Determinants in AgrC for the AIPs

The identification of a peptide ligand recognition site in AgrC and the ligand orientation has been established through the construction and assessment of chimeric sensor domain receptors. Obviously, the architecture of the ligand-receptor complex can be confirmed only by structural analysis of an AgrC receptor-AIP co-crystal. Nevertheless, significant progress has been made through the study of receptor sensor domain chimeras and their interactions with native and variant peptide ligands. The *agr* system is especially amenable to this type of analysis because the respective protein homologues are closely related and have the same function. The site of segment exchange was chosen with a view toward localizing the determinant of receptor specificity for the two most closely related *agr* loci in *S. aureus*, those of specificity groups I and IV. Because the site was within a set of 8 amino acid residues that are absolutely conserved between AgrC-I and IV, it was considered unlikely that the exchange would disrupt the putative recognition site.

Two important features of the Agr quorum sensing system have been identified which emphasize the relative location and probable orientation of the AIP on the AgrC receptor: i) The potency for binding and activation resides in the C-terminal half of the AgrC sensor domain. This is supported by the observation that activation follows with the C-terminal region of the sensor domain. Hence, AgrC-I:IV and AgrC-III:IV are preferentially activated by AIP-IV, and AgrC-IV:I and AgrC-III:I are preferentially

activated by AIP-I. ii) The AIP ring makes contacts necessary for activation with the C-terminal region of the AgrC sensor domain. Activation follows the presentation of a critical activating residue in the AIP-I ring. This is demonstrated by the action of the AIP-I D5N analog, which can activate AgrC-IV:I but is now inhibitory towards AgrC-I:IV. It is also noteworthy that the C-terminal region of the sensor domain, which confers potency for activation, is also the region boundary closest to the intracellular signaling domain. Thus, conformational changes, induced by AIP binding to the C-terminus of the receptor domain, may be communicated directly to activate HK autophosphorylation and the signaling cascade in a manner functionally similar to two-transmembrane sensor-HKs.

Perhaps most remarkably, there was a dramatic broadening of AIP recognition specificity seen with the I::III and IV::III chimeras. This does not mean simply that the N-terminal contribution to AIP recognition was responsible, since if that were the case, the broadening would have included only AIPs I and IV. Since it included AIPs, such as AIP-II, that are strong inhibitors of all three of the native AgrCs, the broadening of specificity must reflect a profound change in the structure of the receptor, a re-organization of the binding pocket enabling it to accommodate and be activated by a wide variety of ligands, without simply eliminating the need for a ligand. That is, the overall structure of the receptor must determine in a large measure the outcome of any AIP-receptor interaction. Incidentally, the I::II and II::I chimeras are non-functional, as is the III::II (data not shown - it has not been confirmed that these molecules are expressed and emplaced correctly in the membrane). It would seem that exchanging intradomain segments between AgrC-I/IV and III is probably as far afield as one may go and still have

a functional receptor. Whereas the results with AIPs I & IV and their interactions with the AgrC-I/IV sensor domain chimeras support the hypothesis that site-specific ligand-receptor recognition underlies the activation mechanism, this hypothesis is fundamentally inadequate to explain the very broad range of results presented with the other functional chimeras.

On the basis of the strong hydrophobicity of all 27 staphylococcal AIPs of known sequence, it is suggested that the AgrC receptor domain forms a hydrophobic pocket into which various AIPs and their analogs can be inserted. AIP interactions with the receptor would then occur in two stages: the first would be entry into this pocket, driven energetically by the potential for hydrophobic interactions between ligand and receptor. The second would be sequence-specific, presumably hydrophilic, interactions with correctly positioned residues in the receptor, thus triggering activation through a series of receptor isomerization steps. It will be recalled that the ultimate and penultimate residues in 26 of the 27 known AIPs are bulky hydrophobic amino acids (Dufour et al., 2002) and that replacement of either of these, in AIP-II, with alanine abolished all activity of the peptide (both activation and cross-inhibition), up to the maximum concentration tested of 10 μM (Mayville et al. 1999) and in AIP-I virtually eliminated activity (McDowell et al., 2001). This predicts that peptides with these alanine replacements would enter the pocket very poorly, if at all; *i.e.*, would not bind the receptor. According to this model, entry into the pocket would require hydrophobic interactions involving these two residues and activation would require additional specific contacts. The greatly broadened activation specificity of the I-III and IV-III chimeras could mean that the chimeric receptors are structured in such a way as to be poised for activation by almost anything that can occupy

their putative hydrophobic pocket, obviating the need for any specific hydrophilic contact. This is supported by the lack of activation by AIP-II F9A, which lacks a key hydrophobic contact, on these chimeras. Furthermore, the failure of AIP-I to activate the I::III chimera could mean that the negatively charged aspartate residue at position 5 interferes with the formation of an intimate hydrophobic complex. Consistent with this is activation of the chimeras by the D5N and D5A analogs, which are electrically neutral at this position.

Inhibition has been viewed as the result of occupation of the ligand binding pocket by the inhibitor; according to the present view, inhibition would result when a peptide is able bind in the putative pocket but is unable to make specific activating contacts with the receptor. This is consistent with the very wide range of inhibitory peptides, all of which contain C-terminal hydrophobic amino acids. However, the conformation in solution of these hydrophobic amino acids can be quite important, as the linear AIP-II cannot activate or inhibit any receptor, while the AIP-II lactam is a potent cross-inhibitor (but a very weak self-activator). On the other hand, the linear AIP-I peptide can inhibit AgrC-II and –III but cannot activate or inhibit AgrC-I or –IV, while the AIP-I lactam is a weak self-activator and it was not tested for cross-inhibiton (McDowell et al., 2001). These results collectively suggest that the content and conformation of the AIPs plays a critical role in the process of inhibition.

Several transmembrane signal receptors for which peptides serve as activating ligands have been described in Gram-positive bacteria. Unlike their counterparts in Gram-negative bacteria, which do not have peptide ligands and usually have one or two transmembrane helices, each of these has 4-6 transmembrane helices. Data presented in

this study suggest that in the staphylococcal *agr* system the entire complex polytopic receptor domain may be involved in the receptor-ligand interaction, which seems to be based largely on hydrophobic interactions followed by other specific activation contacts.

Conclusions

Staphylococcus aureus is an important nosocomial pathogen that has developed resistance to most antibiotics and has lately become the focus of novel therapeutic initiatives. The possibility of identifying agents that block the expression of virulence factors represents one such initiative. In previous studies, it has been shown that this initiative is valid in principle, as interference with *agr* expression *in vivo* can attenuate an experimental *S. aureus* infection (Mayville et al., 1999). Furthermore, global inhibitors of the *agr* response have been developed, which provide initial leads for drug optimization. The data described herein have demonstrated that the mechanism of interference proceeds through reversible and specific extracellular antagonism of signaling through the sensor domain of the RHK, AgrC. It has been recently demonstrated that the well-characterized peptide-based competence induction system in *Streptococcus pneumoniae* is required for virulence in a mouse model of infection (Lau et al., 2001) and that a lactone-containing peptide in *Enterococcus faecalis* activates expression of virulence factors (Nakayama et al., 2001; Qin et al., 2001). By analogy, these systems and many other RHK-based systems in bacteria, plants and other species will be amenable to this type of antagonism. Therefore, the design of molecules that compete (reversibly or irreversibly) with naturally occurring agonists for binding at RHK sensor domains could represent a generally applicable approach to the inhibition of RHK signaling.

Chapter 4 – Materials and Methods

General Methods

All amino acid derivatives and resins were purchased from Novabiochem (San Diego, CA) and Peninsula Laboratories (Belmont, CA). All other chemical reagents were purchased from Aldrich Chemical Co. Restriction enzymes were purchased from New England Biolabs (Beverly, MA) unless otherwise specified. Dimethyl-d_6 sulfoxide was purchased from Isotec Inc. (Miamisburg, OH), and nitrocefin was purchased from Becton-Dickinson (Franklin Lakes, NJ). Analytical gradient reversed-phase HPLC was performed on a Hewlett-Packard 1100 series instrument with diode array detection. Analytical HPLC was performed on a Vydac C18 column (5 micron, 4.6 x 150 mm) at a flow rate of 1 mL/min. Preparative HPLC was routinely performed on a Waters DeltaPrep 4000 system fitted with a Waters 486 tunable absorbance detector using a Vydac C18 column (15-20 micron, 50 x 250 mm) at a flow rate of 30 mL/min. All runs used linear gradients of 0.1% aqueous TFA (solvent A) *vs.* 90% acetonitrile plus 0.1% TFA (solvent B). Mass spectrometric analysis was routinely applied to all synthetic peptides and components of reaction mixtures. ESMS was performed on a Sciex API-100 single quadrupole electrospray mass spectrometer.

Bacterial strains and growth conditions

Staphylococcal strains are derivatives of NTCC8325, and *Esherichichia coli* strains JM109 or DH5α were used for cloning. RN6734 is our standard laboratory strain and is *agr* group I. RN7206 is a derivative of RN6734 in which the *agr* locus has been

replaced by *tetM* [Novick et al. 1993). RN4220 is a heavily mutagenized derivative of *S.aureus* that readily accepts foreign DNA (Novick et al. 1991). *S. aureus* cells were grown in CYGP broth (Novick, 1991) with shaking at 37°C. Overnight cultures on GL plates (Novick, 1991) were routinely used as inocula. Cell growth was monitored with a Klett-Summerson colorimeter with a green (540 nm) filter (Klett, Long Island City, NY). Antibiotics used were erythromycin (10 μg/ml) and tetracycline (5 μg/ml). Biotyping of staphylococci was performed at the Tisch Clinical Microbiology Lab, which confirmed the species classification of the non-*aureus* strains.

Construction of strains and plasmids

A shuttle vector, pRN7035, was used which carries a P3:*blaZ* reporter, an *ori* from pT181 (for replication in *S.aureus*), the *ermC* gene from pE194 (for selection in *S.aureus*), and an ampicillin/ColE1 *ori* fragment from pUC19 (for replication and selection in *E.coli*). This plasmid was constructed by cloning a polymerase chain reaction (PCR) product containing the 180 nucleotide *agr* P2P3 region into the pUC polylinker site of plasmid, pRN7034. Plasmids pRN7062, pRN7105, and pRN7107 were constructed by cloning PCR fragments, containing *agrC*, *agrA*, and downstream termination signals amplified from the genomic DNA of various prototypical *agr* groups, into the PstI or PstI/SphI sites of the pUC polylinker of pRN7035. The following PAGE-purified primers (Integrated DNA Technologies, Inc.) were used in the PCR reactions: for group I pRN7062, forward primer, 5'-CCAACTGCAGGAAGTACCAAAAGAATTAACACAA (PstI site underlined), reverse primer, 5'-TTATACTGCAGACGTTTGCCAACATTACAAGAGG (PstI site

underlined), for group II pRN7105, forward primer, 5'-TTTGAACTGCAGAAAGTACCCGCTGAATTAACG (PstI site underlined), reverse primer, 5'-GGTGAAGCATGCAGTTTGCCAACATTACAAGAGGTTGAACAAGCATTTTAA, (SphI site underlined), for group IV pRN7107, forward primer, 5' TCTTAACTGCAGAAGTTGAAATACCTAAAGAATTAA CTCAATTACACG (PstI site underlined), reverse primer, 5'-GGTGAAGCATGCAGTTTGCCAACATTACA AGAGGTTGAACAAGCATTTTAA, (SphI site underlined). Plasmid DNA from the corresponding *E. coli* DH5α derivative was introduced into the restriction-defective *S. aureus* strain, RN4220, by the protoplast method (Novick et al. 1991). Plasmids were then moved onto various genetic backgrounds by phage transduction to develop new strains, such as RN9222 (CA1-I), RN9372 (CA2-II), and RN9371 (CA4-IV), which are referred to as group I, II or IV or AgrC-I, -II or –IV, respectively (Novick, 1991). Note, RN9365 (CA1-I) is an additional strain with Group I *agrC* and *agrA* in a different group I agr-null background, RN7206. This strain was tested and the results for RN9222 (CA1-1) were reproduced in this strain.

Group I, II, and III chimeric receptor construction

Chimeric receptors were assembled by Jesse Wright by fusing the N-terminal sensor domain of the Group I and Group II *agrC* coding sequence to the Group IV *agrC* HK - *agrA* coding region in the reporter construct pRN7107. The Quik Change Mutagenesis kit (Stratagene) was used to introduce an *Afl* II restriction site at the probable junction between the (N-terminal) sensor and (C-terminal) HK domains in *agrC*

(JSW1 and JSW2) creating pRN7128. The Group I and Group II sensor domains were amplified from pRN7062 and pRN7105 with Pwo polymerase (Roche) using a common upstream primer (JSW5) and downstream primers complementary to either Group I (JSW2) or Group II (JSW7) incorporating the new *Afl* II site. The PCR products were digested with *Pst* I and *Afl* II and ligated into pRN7128 digested with the same enzymes to create the chimeric reporters pRN7107-2-GI and pRN7107-2-G2 (referred to in the text as Group I chimera and Group II chimera). Plasmid inserts were identified by restriction analysis and DNA sequencing. Primer sequences -- complementary primers:

JSW1 5' – CAATTTCTC**CTTAAG**GAGATGAAATA – 3'

JSW2 5' – TATTTCATCTC**CTTAAG**GAGAAATTG – 3'

upstream primer: JSW5 -- 5' - GCACATGGTGCACATGCACCT - 3'

downstream primers: JSW2 (for Group I),

JSW7-- 5' – TATTTCATCTC**CTTAAG**GGTGAAAAG – 3' (for Group II)

The group III sensor domain was amplified from chromosomal DNA isolated from group III strain RN8465 with *Pwo* polymerase (Roche) using the 5' oligonucleotide JSW9 5'-GGCGC**CTGCAG**GAAGTACCAAAAGAATTAACTC (*Pst*I site in bold) and 3' oligonucleotide JSW8 5'- TATTTCATTTC**CTTAAG**AGTAAATTG (*Afl*II site in bold). The PCR product was digested with *Pst*I and *Afl*II and ligated into pRN7128 with the same enzymes to create the reporter pRN7131. The introduced sequence was confirmed by DNA sequencing. Plasmid DNA from the corresponding *E. coli* DH5α derivative was introduced into the restriction-defective *S. aureus* strain, RN4220, by the protoplast method (Novick, 1991). Plasmids were then moved into the Group I *agr*-null cell line, RN6911, by phage transduction (Novick, 1991).

The new group III reporter strain, RN9532, uses ß-lactamase production from a P3-*blaZ* fusion to monitor group III activation and lacks any endogenous AIP-III. Group III cells are induced for ß-lactamase activity by culture supernatants of group III strains but not of group I, II or IV strains, and synthetic AIP-I, -II and -IV do not activate this cell line at concentrations up to 10 μM. Group III culture supernatants were filtered through a 10 kDa-cutoff Centricon filter to remove ß-lactamase, which is endogenously produced by all group III strains in our collection, as tested by the nitrocefin method.

Construction of chimeric sensor domain receptors

Plasmid pRN7128 served as the vector for expression of the receptor chimeras in RN7206. Plasmid pRN7128 has a unique *Afl*II restriction site at the boundary between the receptor and the HK motifs in *agrC*. Two-step PCR (Higuchi et al., 1988) with appropriate primers and receptor templates was used to construct the chimeric fusions (performed by Jesse Wright). The PCR fragments were then ligated back into pRN7128 using an upstream *Pst*I site and the *Afl*II site. Sequences of the chimeras were confirmed by dye terminator DNA sequencing chemistry (Skirball DNA Sequencing Core Facility). pRN7128 derivatives were electroporated into *S.aureus* RN4220 and moved into an *agr*-null strain, RN7206, by phage transduction to eliminate the effects of endogenous AIPs on function. The AgrC RHKs are referred to in the text as AgrC-N (N corresponding to the Agr group) and the chimeras as AgrC-N:C (designating AgrC group N at the amino-terminal end of the sensor domain and AgrC group C at the C-terminal end of the sensor domain).

Preparation of AIP-containing supernatants

S. aureus strains were grown in CYGP broth with shaking at 37°C for 9 hr starting with an inoculum of ~$3x10^7$ cells/ml in 10 mL of broth. Cells were removed by centrifugation at 4°C, and the supernatant was filtered (0.22-μm filter, Gelman). The filtrate was stored at -80°C and used as a source of AIP. The group-specific activity of each supernatant was the same as that of the corresponding synthetic peptide.

Synthesis of the Thiolactone AIPs and Analogs, including trAIP-II lactam

In the initial published studies (Mayville et al., 1999), thiolactone peptides were synthesized manually on preloaded t-butoxycarbonyl–amino acyl-3-mercapto propionamide –polyethyleneglycol-poly-(N,N-dimethylacrylamide) (Boc–AA–[COS]–PEGA) supports (Camarero et al., 1998) according to the in situ neutralization O-benzotriazol-1-yl-N,N,N',N',-tetramethyluronium hexafluorophosphate (HBTU) activation protocol for Boc solid-phase peptide synthesis (Schnölzer et al., 1992). After chain assembly, peptides were treated with HF for 1 hr at 0°C to give the corresponding fully unprotected peptide–[COS]–PEGA resins, which were then washed with cold ether and then CH3CN/ H2O containing 0.1% TFA. The alkyl–thioester linkage between the peptide and the resin is completely stable to anhydrous HF (Camarero et al., 1998). Unprotected peptides then were simultaneously chemoselectively cyclized (via attack by the sulfhydryl group from the cysteine) and cleaved from the support by swelling the beads in a mixture of 0.1 M sodium phosphate buffer (pH 7.0) and acetonitrile (80:20). After a 12-hr reaction, the beads were removed by filtration and washed with 0.1% TFA in water, and the peptides were purified from the filtrate by

reverse-phase HPLC. In each case, the yield of the final cyclization/cleavage reaction was between 60% and 90%, as determined by HPLC analysis of the crude reaction mixtures and integration of the peaks. Key to this process is the ability to prepare a fully unprotected peptide immobilized on a solid support through a reactive thioester bond. Simply swelling such an unprotected peptide-[thioester]-resin in aqueous buffer results in a chemoselective ligation reaction and concomitant cleavage of the peptide from the support. This final step is made possible because of the excellent swelling properties of the PEGA support in water (Mendal, 1992). However, the very sticky nature of PEGA resin does incur handling losses.

A significant improvement to the above procedure involves the use of preloaded t-butoxycarbonyl-amino acyl-3-mercapto-propionamide-4-methylbenzhydrylamine-copoly(styrene-1% DVB) (Boc-AA-[COS]-MBHA) support instead of the previously used Boc-AA-[COS]-PEGA support. The 3-thiopropionic acid linker on MBHA resin is labile to HF-cleavage conditions, thereby releasing linear thioester peptides upon global deprotection. Following removal of HF, crude peptide products were precipitated using cold ether, washed thoroughly with ether, and then dissolved in 50% CH_3CN/50% water/0.1% TFA. After lyophilization, linear thioester peptides were dissolved again in CH_3CN and water with 0.1% TFA, and cyclized in solution by the addition of at least 1x volume of 0.1-0.2 M phosphate buffer at pH 7. The advantage of this solution-based approach over on-bead cyclization is that the kinetics of cyclization can be more easily monitored. In the majority of cases, >90% conversion of linear thioester to cyclic product was achieved in three hours or less. After cyclization, all peptides were purified by preparative RP-HPLC and characterized by analytical RP-HPLC, ESMS, amino acid

analysis, chemical reactivity to neutral hydroxylamine or sodium hydroxide, and ^{1}H NMR, which collectively demonstrated that all peptides were of the correct composition and >95% pure. In addition to AIP thiolactone peptides, the synthesis of trAIP-II lactam was carried out with this methodology (aided by Ehab Khalil), with the exception that diaminopropionic acid (DAPA) was incorporated in place of cysteine in the following peptide: Acetyl-DAPA-Ser-Ser-Leu-Phe. The amino group from DAPA (rather than the usual sulfhydryl group from Cys) chemoselectively reacted with the activated carboxyl α-thioester to form the lactam analog. This strategy was possible due to the fact that the N-terminal amine of the AIP was acetylated.

Synthesis of Linear free acid peptides

In some instances, standard linear free acid peptides, e.g. linear AIP-I and AIP-II, were prepared on a 0.1 millimole scale by automated continuous flow solid-phase synthesis on a PE Biosystems Pioneer Peptide Synthesizer (kindly provided by the Danishefsky laboratory) using standard 9-fluorenylmethoxycarbonyl (Fmoc) chemistry. Fmoc-AAs (≥ 4 eq.) were weighed into labeled, letter coded, 13 x 100 mm test tubes; HATU (≤ 4 eq.) was then added to each test tube. After placing the test tubes in the appropriate racks, the appropriately preloaded NovaSyn TGA resin (~0.20 mequiv/g, ~500 mg) (NovaBiochem) was weighed into a synthesis column and washed in with methanol. DMF was washed through the column on the synthesizer at a flow rate of 30 mL/min while the resin was compressed and released by successive tightening and loosening of the column to remove bubbles and swell the resin. When no air bubbles remained (about 1 minute, with gentle tapping when the resin was not compressed), the

column was tightened to accommodate only the volume of the swollen resin and the flow of DMF was stopped. Fmoc removal (deblock) was accomplished using a 1:1:48 (v:v:v) mixture of DBU : piperidine : DMF for 5 minutes at a flow rate of 6 mL/min directly to waste and was monitored by integrating over time the UV absorbance of cleaved Fmoc chromophore. Each coupling step involved the reagents in a single test tube and excess DIEA in DMF for 30 - 60 minutes at a recycling flow rate of 30 mL/min. Multiple successive washes of DMF and methanol were used to prepare the growing resin-bound peptide for successive steps. The final deblocked peptide was washed out of the synthesis column with methanol into a manual peptide synthesis vessel and dried in vacuo.

Linear peptides prepared by Fmoc synthesis on NovaSyn TGA resin were cleaved in a manual peptide synthesis vessel for two hours under an argon atmosphere with 7 mL of a cocktail prepared directly before usage consisting of approximately 95 % TFA, 2.5 % triisopropylsilane, 2.5 % water (all by volume), and then filtered with washing (to collect all peptide and to remove the resin) into a 250 mL round-bottom flask by simply opening the stopcock. This solution was then rotavapped to remove most of the TFA, and peptide precipitated by addition of dry diethyl ether. The cold ether slurry was allowed to warm to room temperature over 10 minutes, at which time it was transferred to a conical tube and placed in a centrifuge and spun at 3.5×10^3 revolutions per minute (krpm) for 5 minutes. The precipitate was washed three times with ether. Each time the supernatant was decanted and the conical tube closed and vortexed for < 1 minute, until the solid clump loosened. Ether at room temperature was then added (20 mL), the tube capped and the suspension vortexed for a short time and placed back in the centrifuge for

5 minutes. After decanting the final wash, the conical cap was closed halfway and the peptide placed under vacuum and dried on the lyophilizer. The linear fully-deprotected free acid peptides synthesized using this procedure were dissolved in 50% CH_3CN/50% water/0.1% TFA and purified by HPLC.

Synthesis of the Lactone and Lactam AIP-II Analogs.

The protected peptides Z-Gly-Val-Asn-Ala-Ser(t-Butyl)-Ser(Benzyl)-Ser(Benzyl)-Leu-Phe and Z-Gly-Val-Asn-Ala-DAPA(Boc)-Ser(Benzyl)-Ser(Benzyl)-Leu-Phe, corresponding to the AIP-II sequence with a Cys-5-Ser modification [lactone] and a Cys-5-diaminopropionic acid (DAPA) modification [lactam] respectively, were synthesized manually on a Wang-resin by using a fluorenylmethoxycarbonyl (FMOC) N-α-protection strategy with HBTU activation protocols. After chain assembly, the peptides were cleaved from the support and the Ser-5 or DAPA-5 side chain deprotected by treatment with a TFA-anisole-water mixture (90:5:5) for 4 hr.The partially protected peptide–α carboxylates then were dissolved in DMF (0.5 mg/ml) and treated with benzotriazol-1-yl-oxytripyrrolidinophosphoniumhexafluorophosphate (PyBop; Nova Biochem) (5 eq) and DIEA, and in the case of the lactone precursor, a catalytic amount of dimethylaminopyridine. The cyclization reactions were monitored with HPLC, which indicated 2 hr to be sufficient for complete reaction. The remaining protecting groups were then removed by treatment with HF and the desired peptides purified by reverse-phase HPLC and characterized by MS and 2D ^{1}H NMR spectroscopy.

As an alternative approach to the synthesis of the AIP-II and trAIP-II lactone peptides, NovaSyn TGT resin (NovaBiochem) was utilized (*vide supra*). The advantage

of TGT resin is that mild cleavage with 0.5% TFA in DCM yields protected peptide acid fragments without any loss of 95% TFA-sensitive side-chain protecting groups, thus allowing the use of TFA, instead of HF, for the analysis of trial macrolactonization attempts. The protected peptides Boc-Gly-Val-Asn(Trityl)-Ala-Ser(Trityl)-Ser(t-Butyl)-Ser(t-Butyl)-Leu-Phe and acety-Ser(Trityl)-Ser(t-Butyl)-Ser(t-Butyl)-Leu-Phe, corresponding respectively to the AIP-II and trAIP-II sequences with a Cys-5-Ser modification, were synthesized on preloaded Phe-NovaSyn TGT resin (~500 mg resin/peptide) as described for the synthesis of linear peptides by automated Fmoc synthesis (*vide supra*). Peptides prepared by Fmoc synthesis on NovaSyn TGT resin were cleaved for one hour with 7 mL of a cocktail prepared directly before usage consisting of approximately 1 % TFA / 5% triisopropylsilane in DCM. These cleavage conditions cleave the peptide off the resin and selectively remove the trityl protecting group from Ser5, while leaving the Asn3 trityl and other protecting groups intact. After one hour, the cleavage mixture was filtered into a 250 mL round-bottom flask, rotavapped to near-dryness, and precipitated by addition of dry diethyl ether. The cold ether slurry was allowed to warm to room temperature over 10 minutes, at which time it was transferred to a conical tube and placed in a centrifuge and spun at 3.5 x 10^3 revolutions per minute (krpm) for 5 minutes. The precipitate was washed three times with ether. Each time the supernatant was decanted and the conical tube closed and vortexed for < 1 minute, until the solid clump loosened. Ether at room temperature was then added (20 mL), the tube reclosed and the suspension vortexed for a short time and placed back in the centrifuge for 5 minutes. After decanting the final wash, the conical tube was closed halfway and the peptide placed under vacuum and dried on the lyophilizer. Macrolactonization efforts

were as described above, with the exception that the use of HATU was also attempted in place of PyBop, in the presence of DIEA and DMAP in DMF.

Peptide Stock Solution Preparation

The concentrations of peptide stock solutions for bioassays (*vide infra*) were calculated based on amino acid analysis, with the peptides dissolved in 45% CH_3CN/55% water/ 0.1% TFA. This amino acid analysis is associated with a ±10% error, as determined by multiple hydrolyses and HPLC analyses of single samples. Amino acid analysis and UV measurements of the same sample agreed closely (±20%) when UV readings were measured at 280 nm for those peptides containing at least one tyrosine residue (extinction coefficient for tyrosine = 1100 $mol^{-1} cm^{-1}$). However, a major discrepancy between amino acid analysis and UV measurements occurred for those peptides for which the absorbance at 254 nm for phenylalanine was utilized (extinction coefficient for phenylalanine = 200 $mol^{-1} cm^{-1}$). In these cases, the UV-determined concentration was always substantially higher (~5-6 fold) than that determined by amino acid analysis. This discrepancy is explained by the fact that thioesters are known to absorb at 240 nm, thus yielding a characteristic shoulder to the right of the amide bond absorbance profile on the UV spectrum. This thioester absorbance results in an artificially high reading at 254 nm. As such, the concentrations of all peptides were adjusted to that determined by amino acid analysis, and new extinction coefficients were calculated for each peptide based on the amino acid analysis. For example, the extinction coefficient for AIP-II at 254 nm is 1230 $mol^{-1} cm^{-1}$, which is substantially higher than that of phenylalanine (200 $mol^{-1} cm^{-1}$). In contrast, the extinction coefficient for AIP-II lactam,

which lacks a thioester linkage, is 350 mol^{-1} cm^{-1}. Alternatively, the extinction coefficient for AIP-I at 280 nm is 1290 mol^{-1} cm^{-1}, which is similar to that of tyrosine (1100 mol^{-1} cm^{-1}), due to the lack of thioester absorbance at 280 nm. The calculated coefficients were utilized in subsequent experiments when UV measurements were made on the same batch of RP-HPLC purified and re-lyophilized peptides. However, this was rarely done as the first aliquoting of AIP was usually more than sufficient for bioassays and analytical characterization.

After UV measurements were performed on a peptide (dissolved in 45% CH_3CN/55% water/ 0.1%) and samples set aside for amino acid analysis and NMR, small aliquots (usually 100 μL) were lyophilized in eppendorf tubes. Peptide stocks were made by dissolving the lyophilized peptides in 25% propylene glycol, 0.05 M phosphate pH 5.7 at a known concentration (based initially on UV absorbance and corrected later if necessary by the amino acid analysis results) and serially diluting them into the same buffer for assays with cells. In some instances, e.g. trAIP-IV and trAIP-I/IV D/Y2A, the AIPs were insoluble in this solvent system due to their extreme hydrophobicity. In these cases, DMSO was used initially to solubilize the peptides, which were then serially diluted into 25% propylene glycol, 0.05 M phosphate pH 5.7, paying careful attention to avoid peptide precipitation.

NMR Spectroscopy for characterization and comparison of the AIPs

Two-dimensional ^1H NMR analysis yielded complete assignments for all published synthetic peptides, and all chemical shift data are listed in **Appendix 1**. All NMR spectra were recorded on a Bruker AMX-400 spectrometer and processed using the

XWINNMR software package (Bruker). The measurements were performed at 298 K using 0.5-2.0 mM solutions of the peptides in 90% H_2O/10% D_20, pH 4.0 or DMSO-d_6, and all chemical shifts are referenced to the solvent signal [either TMS at 0 ppm (^1H) or the solvent signal of DMSO- d_6 at 2.50 ppm (^1H)]. Assignment of resonances was achieved by 2D-NMR techniques (TOCSY (Bax, 1984) and ROESY (Kessler, 1987)). Mixing times were 77 ms for TOCSY spectra and 200 ms for ROESY spectra. The chemical shifts of the amide, alpha and beta protons were compared between the different peptides in the same solvent system and were normalized to the shifts of the most closely related native AIP.

RP-HPLC analysis of δ-toxin levels

A modification of the assay originally described by Otto and co-workers (Otto and Gotz, 2000) was used to quantify δ-toxin in supernatants from various strains. Early exponential-phase cultures were treated with increasing concentrations of synthetic peptides and then allowed to grow for nine hours. Supernatants, obtained by centrifugation, were analyzed by reversed-phase HPLC on a Hewlett-Packard 1100 series instrument with diode array detection. Typically, 400 μL aliquots of supernatant were injected onto a 1 mL Pharmacia Resource PHE column, which was eluted at 1 mL/min as follows: isocratic at 35% buffer B in buffer A for 3 minutes, which allowed the majority of the UV-absorbing material to wash through the column, followed by a linear gradient of 35-50% B in A over 20 minutes, where A = 0.1% TFA in water and B = 0.1% TFA in 90% acetonitrile/10% water. This optimized gradient achieved excellent separation of δ-toxin from other components (>95% pure by HPLC and MS), which permitted direct

quantitation by peak integration. δ-toxin is usually N-formylated, and the additional 28 daltons of the N-formyl group was included in the calculated mass. We observed this mass by ESMS on HPLC-purified fractions of δ-toxin: *S. aureus* group I and III, observed mass for both groups = 3007.1 ± 2.2 Da, predicted (average) mass = 3006.5 Da (all S. aureus *agr* groups encode identical δ-toxin); *S. epidermidis* strains, observed mass = 2848.7 ± 1.5 Da, predicted (average) mass = 2848.4 Da, and *S. warnerii* strains, observed mass = 2900.1 ± 0.8 Da, predicted (average) mass = 2899.4 Da. In summary, δ-toxin was detected in the following biotyped strains in the R.P.N. strain collection (NYU): *S. epidermidis*, RN9420, RN9421, RN9422, RN8111, ATCC, and Tü3298 (kindly provided by M. Otto), *S. aureus*, RN6734 and RN8465, and *S. warnerii*, RN3178. δ-toxin was not detected in *S. intermedius*, RN9423 (*vide infra*).

Whole cell lysates and Northern blotting for RNAIII expression

Bacteria were collected at the indicated time points, and whole-cell lysates were prepared as described (Kornblum et al., 1988). Cultures were centrifuged, fixed in acetone-ethanol (1:1), and washed in N-tris(hydroxymethyl)methyl-2-aminoethanesulfonic acid (TES)-sucrose buffer. Equalized cell samples were incubated on ice for 30 min with lysostaphin (150 mg/ml) in TES-sucrose buffer (20% [wt/vol] sucrose, 20 mM Tris [pH 7.6], 10 mM EDTA, 50 mM NaCl) and shaken for 1 h with proteinase K (50 mg/ml; Sigma) and 2% SDS at 4°C. For Northern blotting (Vandenesch et al., 1991), the same amount of cell lysate was electrophoresed through a 0.66 M formaldehyde–1% agarose gel in MOPS (morpholinepropanesulfonic acid) buffer (Maniatis, 1982). Nucleic acids were transferred to a nitrocellulose membrane

(Amersham) with a VacuGene apparatus (Pharmacia) in 20x SSC (3 M NaCl, 0.3 M sodium citrate [pH 7]) and fixed under UV light. The membrane was preincubated for 2 h at 52°C in 2x Denhardt's solution (0.02% bovine serum albumin, 0.02% Ficoll, 0.02% polyvinylpyrrolidone, 0.05 M EDTA [pH 8], 0.2% SDS, 5x SSC, with sonicated and heat-denatured salmon sperm DNA [100 mg/ml]) and 10% (wt/vol) dextran (Sigma) and then hybridized overnight with a ^{32}P-labeled DNA probe in hybridization solution. ^{32}P-labeled RNAIII probes were prepared by PCR using oligonucleotide primers corresponding to nt 1259-1280 and nt 1558-1571 of RNAIII, and pRN6735 DNA as template. In labeling reactions, dATP concentration was reduced to 2 μM and the reaction mixture contained 50 μCi of [α-^{32}P]dATP (Amersham; 1 Ci = 37 GBq). The blot was exposed to a storage phosphor screen (Molecular Dynamics).

Agr activation and inhibition reporter-gene assays

Assays were performed with bacterial cultures in early exponential phase (~2x10^8 cells/ml) and used a ß-lactamase reporter gene readout. For activation assays, 80 μL of cells (9x10^8 cells/mL) were treated in duplicate with AIPs at varying concentrations and incubated with shaking at 37°C for 60 or 90 minutes in a THERMOmax microplate reader (Molecular Devices) with monitoring of cell density at OD_{650}, followed by determination of *agr* activation by the ß-lactamase/nitrocefin assay (Ji et al., 1995). For inhibition assays, 80 μL of cells (9x10^8 cells /mL) were treated in duplicate with AIP analogs in the presence of the group-specific wild-type AIP agonist at a concentration of 100 nM, followed by the ß-lactamase assay. An agonist concentration of 100 nM is a saturating but not over-saturating dose of activator, which generates maximal activation

against which to test various concentrations of inhibiting heterologous AIPs. The time of incubation usually did not exceed 90 minutes, but in some cell preparations, an additional 30-60 minutes was required to achieve at least a 5-10 fold induction over basal activity in response to the AIPs.

Functional binding and competition experiments

RN9222 (CA1-I) cells or RN9372 (CA2-II) cells (both at $9x10^8$ cells/mL) were treated for one hour with AIP-I or -II at 1 μM. Aliquots (1 mL) of the cells were pelleted and resuspended in 1 ml of CYGP broth. This washing procedure was repeated up to 10 times. After the washes, cells were resuspended in CYGP broth with or without AIP-I or -II at a concentration of 1 μM. In one set of experiments, trAIP-II was added at 1.0 or 3.3 μM. Timepoints were then taken every 30 minutes for 3 hours to monitor the kinetics of ß-lactamase induction. Washing exerted only a minimal effect on subsequent growth, and the data were normalized to cell density to account for any small differences. Control experiments in which activated cells were either untreated or re-activated with their group-specific AIPs after washing showed that washing had a minimal effect on subsequent activation. All experiments were performed at least twice, and the single corresponding timepoints from all experiments were combined for error analysis.

Effects of antagonist AIP preincubation and washing on subsequent activation

In the case of cross-group inhibition, 3 mL of RN9222 (CA1-I) cells ($9x10^8$ cells/mL) were pre-incubated for one hour (or five minutes) with either AIP-II at 1 μM or 25% propylene glycol, 0.05 M phosphate (pH 5.7) buffer. Time-point zero was then

taken with 50 µL of cells added to 75 µL of CYGP supplemented with sodium azide at 5 mM, and the samples were placed on ice. Cultures were then divided into 500 µL aliquots, pelleted, washed with 1 mL of CYGP broth, pelleted again and then resuspended in 495 µL of CYGP broth with addition of either buffer alone or AIP-I at a final concentration of 1 µM, bringing the total volume to 500 µL. Cells were then incubated with shaking at 37° C and samples taken every 30 minutes as described above. The ß-lactamase assay was performed at the conclusion of 210 minutes, and the data were normalized by calculating the induction ratio (induced/basal) at each timepoint. Data are quoted ± SEM, and are derived from several timepoints (150, 180 and 210 minutes) combined after normalization.

In the case of self-inhibition, 1 mL of RN9372 (CA2-II) cells were pre-incubated with or without trAIP-II at 1 µM for 30 minutes at 37°C. The cells were pelleted, washed, pelleted again and resuspended in 1 mL of CYGP broth. The cells were then treated for 60 minutes with AIP-II at varying concentrations and *agr* activation was evaluated by the nitrocefin assay. The data were used to plot concentration-response curves, from which EC_{50} values were derived. These values are quoted ± SEM.

Order of Addition experiments

RN9222 (CA1-I) cells (80 mL at $9x10^8$ cells/mL) were treated in duplicate with varying [AIP-II]. AIP-I was added at 100 nM, either five minutes before, simultaneously, or five minutes after addition of the antagonist. The cells were incubated at 37° C in a 96-well plate with shaking during these five minute periods. The cells were then incubated for 60 minutes at 37° C. *Agr* activation was evaluated by the ß-lactamase assay as above.

A similar series of experiments was performed on RN9372 (CA2-II) cells using AIP-II vs. trAIP-II. Data were collected as ß-lactamase activity (V_{init} in mOD/min) and then normalized to % maximal activation. Data are quoted ± SEM.

Agonist-Antagonist Interactions: Concentration-Response Curves

For the activation experiments, 80 µL of cells ($9x10^8$ cells/mL) were treated in duplicate with AIP agonist at varying concentrations in the absence or presence of the antagonist at fixed concentrations up to 1000 nM. For inhibition experiments, 80 µL of cells (9x10e8 cells/mL) were treated in duplicate with the antagonist in the presence of a fixed concentration of the agonist at concentrations up to 1000 nM. In both instances, incubation was for one hour at 37° C, and *agr* activation was evaluated by the ß-lactamase assay.

Data Analysis

The data from the ß-lactamase assay are plotted as initial ß-lactamase reaction velocity versus log peptide concentration. In some instances, the data are normalized to % maximal activation for comparison of curves between assays. Individual agonist or antagonist concentration-response curves, in the absence and/or presence of antagonist, were fitted via nonlinear regression to the following four-parameter Hill equation, using PRISM 3.0 (GraphPad Software, San Diego, CA, USA):

$$E = Basal + \frac{E_{max} - Basal}{1 + 10^{(LogEC_{50} - Log[A])\, n_H}} \qquad (1)$$

where E denotes effect, [A] the agonist concentration, n_H the midpoint slope, EC_{50} the midpoint location parameter, and E_{max} and Basal the upper and lower asymptotes, respectively. For inhibition curves, the midpoint location parameter from equation (1) was the IC_{50}, rather than the EC_{50}. All EC_{50} and IC_{50} values are listed in tabular format with a 95% confidence interval (CI), which represents the error associated with the measurements using each peptide stock solution. EC_{50} is not a binding constant, but rather a composite of equilibria for both binding and receptor activation. An advantage of EC_{50} is that it represents a *functional* assay, so that a response, either activating or inhibiting, indicates that mutant receptors are structurally intact. When Vmax is fully attained, one assumes that receptor activation by the AIP proceeds normally. Under this assumption therefore, variations in EC_{50} should represent differential agonist-binding ability. This was confirmed in part through determination of antagonist potency (pA_2) values (see next paragraph and Results).

In those experiments generating concentration response curves in the presence of varying antagonist concentrations, antagonist potency was determined by taking the agonist EC_{50} values obtained in the absence and presence of antagonist and fitting them to the following equation (Lew and Angus, 1995; Christopoulos et al., 2001) using nonlinear regression:

$$pEC_{50} = -\log([B]^s + 10^{-pK}) - \log c \qquad (2)$$

where pEC_{50} is the negative logarithm of the EC_{50}, [B] is the antagonist concentration, pK and log c are fitting constants, and *s* is equivalent to the Schild slope factor. Curves were generated with either the Schild slope held constant at unity or with the slope allowed to

vary, and the better-fitting model was determined by an extra-sum-of-squares test using PRISM. In this test, a p value < 0.05 indicates a slope value significantly less than one.

Pull-down experiments with RN8559, RN9222, and RN6911

Various preparations of cells (RN8559, induced with methicillin, RN9222, and RN6911) were concentrated in PBS to different cell concentrations, starting with an initial concentration of 3000 klett units (kU). 14 µL of a 3000 kU culture in PBS is equal to $5.04x10e^7$ cells; concentration was therefore required to increase the number of cells added while maintaining the same volume. 14 µL of cells from the various stocks were added to 112 uL of PBS followed by 14 µL of a 1 µM AIP-I solution to a final concentration of 100 nM AIP-I. The tubes were vortexed and left sitting for 5 minutes followed by spin-down and assaying of 10 µL supernatant aliquots (in duplicate) with 90 µL of RN 9222 cells (kU60) for one hour in the Thermomax plate reader, followed by the nitrocefin assay of 50 uL aliquots from each well.

Using Fluorescein-conjugated AIP-I to detect a covalent AIP-AgrC adduct

Agr+ (RN6734) and *agr*-null (RN6911) cells (klett unit=800, $\sim 6x10^{10}$ cells) were incubated for five minutes with fluorescein-conjugated AIP-I at a final concentration of 3 µM. Protoplasts were prepared to remove the cell wall (Novick, 1991), and the cells lysed by the addition of lysostaphin and SDS buffer. Lysates were run on SDS-PAGE gels, followed by in-gel fluorescence imaging. As a control, the Fl-AIP-I peptide by itself was strongly fluorescent in these gels. To increase the sensitivity of detection, SDS-PAGE gels were also transferred to nitrocellulose filters and subjected to Western blotting with

an anti-Fluorescein antibody (Molecular Probes, Inc.). In no instance was a fluorescent or chemiluminescent band detected corresponding to fluorescent AgrC. In another experiment, the use of a fluorometer was investigated for whole cell binding assays. However, it was found that *S. aureus* cells are auto-fluorescent with a maxima near to the emission wavelength of fluorescein, thus rendering the use of this molecular probe difficult. This was further confirmed using fluorescence microscopy (aided by M. Goulian).

Using Biotinylated-AIP-I as a molecular probe for AIP-AgrC interactions

4.5 mL of *S. aureus* cells (RN9222 and RN9033) at 65 kU were incubated for one hour with biotinylated-AIP-I, AIP-I, or buffer, with the peptides at a final concentration of 500 nM. At the end of the hour, *agr* activation was confirmed by the nitrocefin method in RN9222 cells treated with biotinylated-AIP-I or AIP-I, but not in any of the controls (using 2x30 μL aliquots). 1 mL aliquots of the cells were taken in duplicate, spun-down, and the pellet washed once with 1 mL of Tris-buffered Saline, pH 7.8 (50 mM Tris, 0.85% NaCl). The cells were resuspended in 500 μL of CY broth + 100 μL of a 1:100 dilution of Streptavidin-conjugated Horseradish Peroxidase (Amersham), to which 100 μL of para-nitrophenyl phosphate (PNPP) (Sigma) was added. 100 μL aliquots were transferred in duplicate to a 96-well plate, and the cells monitored kinetically with shaking in a Thermomax plate reader, reading at 405 nm and 650 nm. PNPP cleavage by Streptavidin-conjugated Horseradish Peroxidase results in an increasing signal at 405 nm, while cell growth is monitored at 650 nm. Control experiments demonstrated that a $1:10^4$ dilution of Streptavidin-conjugated Horseradish Peroxidase still resulted in active

cleavage of PNPP, while a $1:10^5$ dilution was slightly detectable. However, in this instance and in other similar experiments, there was no increased cleavage of PNPP in *agr*+ (RN9222) cells that had been treated with biotinylated-AIP-I, in comparison to the controls.

Similarly treated samples were lysed and run on SDS-PAGE gels, for Western blot detection with Streptavidin-conjugated Horseradish Peroxidase. These efforts met with limited success, due in large part to the many already biotinylated proteins in metabolic pathways of *S. aureus*. However, even given the high background seen on Western blots using Streptavidin-conjugated Horseradish Peroxidase as the "secondary antibody" for ECL detection, no band corresponding to AgrC was seen in lanes containing *agr*+ cell lysates (RN9222). It is noteworthy that dot blots with biotinylated-AIP-I on its own only gave a faint signal after incubation with Streptavidin-conjugated Horseradish Peroxidase, followed by ECL detection. This could be because the peptide did not bind well to the nitrocellulose filter (0.2 micron pore size), due to its small size. However, it is formally possible that streptavidin did not bind well to the biotin, in the context of their conjugation with Horseradish Peroxidase and AIP-I, respectively.

Acetylation and Purification of AIP-I in solution

To label the N-terminus of AIP-I in solution, the radioisotope, tritium ^3H, was chosen, using acetylation with acetic anhydride [^3H] as the method of choice. The isotope ^3H has the added advantage of a relatively long half-life, 12 years, making the preparation of radioactive AIPs independent of decay considerations. However, if necessary, the

Bolton-Hunter reagent (containing ^{125}I) can be used for N-terminal acylation, if considerably higher specific activities are required.

Initially, acetylated AIP-I was prepared via standard peptide synthesis methods and was confirmed to have similar activity to that of AIP-I (see Results). Therefore, a range of conditions were initially tested for acetylation of AIP-I in solution (using cold acetic anhydride), as radioactive acetylation during solid-phase peptide synthesis would contaminate all subsequent equipment. Conditions tested included: 10 eq. Ac_2O:1 eq. AIP-I with 1% or 10% v/v DIEA, 1 eq. Ac_2O:1 eq. AIP-I with 1% or 10% v/v DIEA, 10 eq. Ac_2O:1 eq. AIP-I with 10% v/v 0.2 M phosphate buffer, pH7.0, with each reaction analyzed at 10 or 30 minutes, where 1 eq. of AIP-I was 7.5 μg dissolved in 90 μL DMF and the total volume of the reaction was 106 μL. All conditions and time-points were quenched with 100 μL 50%TFA/50%H_20 on ice, and aliquots were injected onto analytical RP-HPLC to determine acetylation yields. The best reaction conditions were 10 eq. Ac_20:1 eq. AIP-I with 10% v/v 0.2 M phosphate buffer, pH 7.0, for 10 or 30 minutes, which gave nearly quantitiative yields, with minor side-reactions. The contents of this reaction were: 90 μL AIP-I (7.5 μg) in DMF, 10 μL 0.2 M phosphate buffer, pH7.0, and 6 μL of a 1:1000 dilution of Ac_2O in DMF.

As the lab did not have access to a radioactive HPLC, the use of disposable C18 SepPak columns was investigated for purification. 2 1-mL columns were connected in series, and the remaining reaction (minus that used for analytical HPLC) diluted to 1 mL with Buffer A (0.1% aqueous TFA). This was loaded onto the column at a manual flow-rate of ~1 mL/5 minutes. The column was washed with 1 mL of Buffer A at the same flow-rate, followed by 10 mL of Buffer A over a 5 minute period. AIP-I was then eluted

with Buffer B (90% acetonitrile plus 0.1% TFA) with 7 mL at a rate of 1 mL/min, with collection of 1 mL fractions. The bed volume of the column is 2 mL, so 5 elution fractions were collected. The fractions were individually analyzed and then combined, and the recovery from the column deduced from the area under the curve on analytical HPLC traces of the product, adjusted for volume differences before and after SepPak purification. This purification procedure on 7.5 μg of AIP-I was repeated twice, with recovered yields of 42% and 35%, respectively, with the vast majority of the material found in the third elution fraction.

Given the quantitative conversion of AIP-I to acetylated-AIP-I with these reaction conditions, the relatively low recoveries resulted most likely from loss of AIP-I on the SepPak column given the low amount of material added (7.5 μg). To investigate this, the reaction was performed on ten times more material, 75 μg, of AIP-I, dissolved in 900 μL DMF, with 100 μL 0.2 M phosphate buffer, pH7.0, and 60 μL of a 1:1000 dilution of Ac_2O in DMF. The reaction was quenched after 10 minutes with 1 mL of 50%TFA/50%H_20, and analytical RP-HPLC demonstrated quantitative yield with this 10x scale-up. The reaction was diluted to 10 mL with Buffer A, and the purification conditions on the SepPak column were slightly changed. This included: Loading at 10 mL/10 min, followed by an additional 10 mL/10 min Buffer A, then 2x with 10 mL/5 min Buffer A, 10 mL/5 min 20% Buffer B, followed by elution with 70% Buffer B at 5 mL/5 min, with collection of 1 mL fractions. Once again, RP-HPLC analysis demonstrated that the vast majority of the material eluted in fraction #3, indicating that the peptide dissociates readily from the column after the dead volume has been eliminated. The overall yield for the reaction (including purification) was 90%, which was deemed

acceptable for radioactive labeling experiments. Most importantly, 1D-NMR analysis of fraction #3, lyophilized and redissolved in dDMSO, revealed the complete absence of acetic anhydride, which was of crucial importance for future whole cell binding experiments.

Radioactive Labeling of AIP-I in Solution

Acetic anhydride [^{3}H] was ordered from ICN and had a specific activity of 64 mCi/mmol, and a concentration of 677 μCi/μl. The reaction was set up with the same 10:1 ratio of Ac_2O:AIP-I. This included 100 μg AIP-I in 1200 μL DMF, 140 μL 0.2 M phosphate buffer, pH7.0, and 80 μL 1:1000 dilution of Ac_2O [^{3}H] in DMF. The reaction proceeded for 30 minutes, as previous analysis had demonstrated that the difference between 10 and 30 minutes was minimal in terms of yield. The reaction was divided into two eppendorf tubes with 600 μL in each tube, and quenched with 100 μL 50%TFA/50%H_20. Normally, a slight whitish precipitate forms during the labeling procedure, which had always been ascribed to salt precipitation. Upon addition of 50%TFA/50%H_20, this precipitate previously disappeared in non-radioactive labeling efforts. On this occasion, the precipitate became worse, and it is possible that addition of more 50%TFA/50%H_20 might have made it better, as the previous large-scale attempt used a 1:1 addition instead of a 1:6 addition. However, this was not attempted due to concern about further precipitation, and the pH was already ~1. Therefore, the precipitate was removed by centrifugation. The precipitate resisted attempts to solubilize it with 20% B, so it is unlikely that it was entirely salt. The supernatant was diluted to 10 mL with Buffer A. The loading, washing, and elution followed the same procedure as the large-

scale non-radioactive attempt (*vide supra*), with the exception that the elution was at 10 mL/10 min, resulting in the collection of more fractions.

After elution, 100 μL aliquots of each elution fraction, along with aliquots from the initial reaction, flow-through and washes of the column, were added to 4 mL ReadySafe Scintillation fluid in 7 mL Scintillation vials and counted in a ß-counter. The total radioactive counts per minute (adjusted for volume differences) in the diluted 10 mL starting reaction prior to SepPak purification and the various fractions counted after SepPak purification are shown in Table 4.1. It is apparent that all radioactivity was accounted for, and radioactive AIP-I appears in elution fraction #3, as evidenced by the spike in radioactive counts.

Table 4.1. Monitoring Radioactive Recovery

Material Counted	Counts per Minutes (cpm)
Diluted reaction mixture pre-SepPak	2.21×10^7 cpm
Flow-through	1.67×10^7 cpm
Washes	3.18×10^6 cpm
Elution Fraction #1	8.93×10^4 cpm
Elution Fraction #3	2.17×10^6 cpm
Elution Fraction #4	3.78×10^5 cpm
Elution Fraction #5	6780

Based on the radioactive counts, elution fractions #3 and 4 were combined to a total volume of ~2.5 mL, with a total cpm of 2.54×10^6 cpm. It is interesting to note that this is roughly consistent with the 10:1 ratio of acetic anyhydride to AIP-1, as the total amount of radioactive acetic anyhydride in the reaction was 2.21×10^7 cpm. However,

only one acetyl group from the symmetrically labeled acetic anhydride should have transferred to AIP-I, so the ratio should have been closer to 20:1. A calculation of the number of cpm's expected in the reaction mixture, based on the volume added, specific activity (64 mCi/mmol) and concentration (677 μCi/μl) of acetic anhydride predicts that 8.04 $x10^7$ cpm should have been present. It is most likely the case that the problematic precipitation and subsequent centrifugation removed radioactivity from the reaction mixture in the pellet.

In preparation for bioassays, the acetonitrile was removed from the sample by blowing N_2 gas over the top of the vial. This was highly inefficient, as it took ~two hours to decrease the volume to ~1 mL, and such a procedure carries some risk of oxidation of any methionine residues in the peptide (even with blowing N_2 gas). In the future, it is recommended that samples be rotavapped to remove acetonitrile. The 1 mL aliquot was then buffered with 1 mL of 0.05 M phosphate buffer, pH5.7, giving a final volume of 2 mL of presumably tritiated and acetylated AIP-I (*Ac-AIP-I).

To more accurately determine the specific activity and hence concentration of *Ac-AIP-I, 4 μL aliquots of the 2 mL solution were counted in duplicate. The average cpm from this counting was 486 ± 31 cpm/1 μL solution, leading to a total count in 2 mL of $9.72x10^5$ cpm, which is a result more consistent with the 20:1 ratio of acetyl group:AIP-I in the initial reaction mixture (see above). Also, the specific activity of acetic anhydride [^{3}H] was divided in half, 32 mCi/mmol, to reflect the incorporation of a single acetyl group in AIP-I. Based on a counter efficiency of 63%, the cpm/fmol of incorporated [^{3}H] was calculated to be 0.04755 cpm/fmol. Based on this value and the known cpm/μL of the *Ac-AIP-I solution, the concentration of the peptide was calculated

as 10.22 μM in 2 mL, or 10.2 μg. The theoretical yield should be 100 μM in 2 mL, or 100 μg, thus leading to an overall yield for radioactive labeling and recovery of 10%. This is dramatically lower than the 90% overall yield achieved in large-scale non-radioactive labeling experiments. The precipitation encountered during the reaction could easily explain the decreased yield. In addition, this was the first and only time that the reaction was performed with radioactivity, so it is very likely that yields can be optimized in the future. In addition, the use of radioactive HPLC equipment and radioactive mass spectrometry would vastly improve the quality of the procedure.

Lastly, *Ac-AIP-I was tested for *agr* activation of group I cells, which yielded an EC_{50} of 8 nM (95% CI, 4-14 nM), a value slightly lower than that seen with AIP-I and ~10-fold lower than that with cold Ac-AIP-I, with an EC_{50} of 98 nM (95% CI, 56-173 nM). It seems unusual that the overall yield of the labeling reaction is 10%, while the biological activity of *Ac-AIP-I is 10-fold higher than that observed for the chemically identical (non-radioactive) Ac-AIP-I. However, the calculations have been checked repeatedly, and a source for a possible 10-fold error cannot be identified.

Radioactive Filter Binding to demonstrate AIP-I binding in induced RN8559 cells

250 μL of RN8559 cells (±methicillin) and 250 μL sodium phosphate buffer (pH 5.7) were incubated with 10 μL tritiated AIP-I (final concentration = 200 nM) for five minutes at 37°C. Samples were filtered with a vacuum apparatus using 0.1 micron Millipore filters. Filters were washed 3x with phosphate buffer, pH 5.7, and then sucked dry (the filtration was slow on the order of minutes). The filters were placed in 4 mL ReadySafe scintillation fluid (Beckman Coulter) in 7 mL vials and were counted in a ß-

counter after sitting overnight for effective dispersion, with a 2 minute count per vial to narrow the confidence interval. Similar experiments to this one incorporating varied times of incubation were performed twice more with RN8559, RN9222, and RN6911 cells, using either filter binding or radioactive cell pellet counting (*vide infra* and see Results).

Radioactive cell pellet counting from competition experiments

100 µL of RN8559 or RN6911 cells (3000 kU) were added to an eppendorf tube with 380 µL 0.05 M phosphate buffer, pH 5.7, and 20 µL of a 10.22 µM stock solution of tritiated AIP-I (all done in at least duplicate, and quadruplicate for RN6911). The cells were incubated for 5 minutes at 37°C with shaking, followed by spin-down, saving of supernatants, and a 1x wash of the intact pellet with 1 mL 0.05 M phosphate buffer, pH 5.7. The cell pellet was resuspended in 450 µL of the same phosphate buffer, along with addition of either 50 µL of 25% propylene glycol in 0.05 M phosphate buffer, pH 5.7, or cold (non-radioactive) peptides in the same buffer at final concentrations of 25 µM for AIP-1 and 10 µM for AIP-II. Cells were incubated for 10 minutes at 37°C with shaking, followed by spin-down, saving of supernatants, no washing, and transfer of the pellets into 7 mL scintillation vials, already containing 4 mL ReadySafe fluid, for radioactive counting. The vials were vortexed thoroughly to disperse the pellets from the clipped eppendorf tube tips, and were left standing several hours to overnight prior to radioactive counting. 400 µL of the supernatant was also counted, which is 4/5 of the total supernatant, thus confirming depletion of tritiated AIP-I in those tubes where cell binding

occurred. Similar experiments to this one with varied incubation times were performed several times.

MALDI-ion trap Mass spectrometry.

The MALDI-quadrupole ion trap was constructed by members of the Chait laboratory from a Thermo Finnigan LCQ Deca XP (San Jose, CA) as described for the earlier LCQ version (Krutchinsky et al., 2001). Short ion injection times (typically 0.3 to 5.0 msec) were used for single stage MS experiments in order to prevent overfilling effects. MS/MS and MS^3 experiments were performed at longer injection cycles (200-400 msec) using empirically optimized instrument specific parameters (isolation width: 2.0 Da, normalized collision energy: 35% for AIPs, activation Q: 0.240, activation time: 300 msec). Acquisition times for HMS-MS studies varied from 30 sec to 1 min in order to achieve acceptable signal/noise ratios.

Sample preparation for MS.

Approximately 0.5 mL of Staphylococcal culture supernatant were lyophilized and resuspended in 100 µl 1% TFA/water to which 5 µl of a suspension of hydrophobic Poros 20 R2 beads (PerSeptive Biosystems, Framingham, MA) in 10-fold bed volume 2% formic acid were added to bind the AIPs. Using a 1 mL disposable syringe and a self-made adapter piece (cut from a P200 pipette tip) a portion or the entire sample was squirted through a ZipTip microcolumn (Millipore) that also served as a frit for the Poros material. The column bound material was washed with 20 µL 0.1% TFA before eluting it directly onto the MALDI CD-plate using 2.5 µL of a half saturated solution of 2,5-

dihydroxy benzoic acid (DHB) in 60% methanol / 0.1% trifluoroacetic acid (TFA). Synthetic peptides were simply spotted onto the MALDI CD-plate in 1 μL volumes of 1 nM solutions (or a dilution series) to which 1 μL of matrix solution were added subsequently.

Agr induction by the Lactone *S. intermedius* AIP

This experiment was performed by Yvonne Benito. The stationary-phase filtered bacterial supernatant from an overnight 25 mL culture of S.intermedius strain RN9423 (CCM5739) was lyophilized. BHI broth was also lyophilized to use as a control. From 50 mL of a 1 hour-growing culture, 25 ml were poured in a flask containing the lyophilized supernatant and 25 ml in another flask containing the lyophilized BHI. Timepoints were then taken at 0, 30, 60, and 90 minutes, with 1 mL aliquots taken at each timepoint and cell densities measured. The 1 ml cultures were spun down and the pellets resususpended with dilution or concentration to obtain equal cell densities of 0.5 measured at 540 nm. Equal volumes of cells were then frozen in preparation for Northern blotting. Whole-cell lysates and Nothern blotting were performed as described (*vide supra*). Paranthetically, the procedure of using lyophilized supernatants results in a final concentration of AIPs approximately equal to native conditions, rather than a diluted concentration as would result with addition of supernatants at $1/10^{th}$ volume.

MBP-AgrC fusion constructs

Bacterial strains (*E. coli,* TB1) containing the MBP-$AgrC_{(Ser\text{-}173)}$ and MBP-$AgrC_{(Ser\text{-}199)}$ plasmid constructs, encoding the MBP-3^{rd} loop-TM helix-AgrC HK and

MBP-AgrC HK proteins, respectively, were obtained from G. Lina (Lina et al., 1998). Both plasmid constructs were verified by restriction digest mapping, and the DNA was sequenced for MBP-$AgrC_{(Ser\text{-}173)}$. It is noteworthy that both plasmids were derived from the vector, pMal-p2, rather than pMal-c2, thus directing expression of fusion proteins to the periplasm instead of the cytoplasm of *E. coli.* Bacterial cultures of these two strains were grown at 37°C with shaking and induced with IPTG for two hours at a concentration of 0.5 mM. In accordance with the previous paper (Lina et al., 1998), the proteins were not recovered by osmotic shock of the cells, but rather the cells were lysed by French press or sonication, and the proteins purified from clarified supernatants by affinity chromatography on amylose columns according to the manufacturer's instructions (New England Biolabs). Overall, the yield of protein from lysed cells was ~1 mg/L and >30 mg/L of the MBP-3rd loop-TM helix-AgrC HK and MBP-AgrC HK proteins, respectively. The relatively low yield of MBP-3rd loop-TM helix-AgrC HK resulted from poor expression in comparison to MBP-AgrC HK in whole cell lysates (very little material was detected in the pellet or the supernatant). Attempts to purify the MBP-AgrC HK protein by osmotic shock resulted in a >90% decrease in yield, perhaps due to poor outer cell membrane lysis or due to cytoplasmic expression of protein en route to the periplasm (data not shown).

Two other MBP-fusion protein plasmids were constructed, using the pMAL-c2 cytoplasmic expression vector from NEB. The first of these encodes a protein (named 4A-2) similar to MBP-3rd loop-TM helix-AgrC HK, but with a few extra residues at the junction between MBP and AgrC. The second construct (named 3A-2) encodes the same

version of MBP-AgrC HK, but with an extra Factor Xa site between the MBP and the AgrC HK domain, along with cytoplasmic expression instead of periplasmic expression.

The junction sites of all MBP constructs are illustrated below, with the portions from AgrC-I underlined, a series of N's from MBP included for orientation, an asterisks on *MBP to indicate a signal sequence and periplasmic expression, and the Factor Xa sites (IEGR) highlighted in bold:

4A-2: MBP...NNNNNNNNLG**IEGR**ISEF**IEGR**SQINSDEAKVIRQYS....cont...

MBP-3rd loop-TM helix-AgrC HK:

*MBP...NNNNNNNNLG**IEGR**ISEFSDEAKVIRQYS....cont...

3A-2: MBP...NNNNNNNNLG**IEGR**ISEF**IEGR**SQFLLKEMKYKRNQE...cont...

MBP-AgrC HK: *MBP...NNNNNNNNLG**IEGR**SQFLLKEMKYKRNQEE...cont..

The following non-PAGE-purified primers (Invitrogen) were used for the construction of 4A-2 and 3A-2, with the restriction sites underlined:

4A-2: EcoRI-FXA - 3TMK forward: 5'-CGCCGCGAATTCATCGAAGGTCG

TTCACAAATAAACTCGGATGAAGCTAAAGTAATAAGG-3'

3A-2: EcoRI-FXA - kinase forward: 5'-CGCCGCGAATTCATCGAAGG

TCGTTCTCAATTTCTCCTTAAAGAGATGAAATATAAACGTAATC-3'

Reverse primer used for both constructs:

PstI -kinase reverse primer:

5'-AAAAGACTGCAGTCAACTTTTTGAATAAAAGAAACCATTTTCG-3'

The plasmids were constructed using standard methods (and see below for His-tagged AgrC constructs), and both plasmid constructs were confirmed by DNA sequencing.

The 3A-2 and 4A-2 proteins were expressed and purified as described above, with yields, respectively, of 30 mg/L and 2 mg/L (as determined by comparison to BSA standards run on the same gel). The expression of 4A-2 was low, similar to that seen with the MBP-3rd loop-TM helix-AgrC HK protein, thus suggesting that inclusion of a normally transmembrane helix in these MBP fusion proteins decreases protein expression.

The molecular weights of these proteins are: 3A-2: 69303 Da; 4A-2, 72963 Da; MBP-3rd loop-TM helix-AgrC HK, 74614 Da; and MBP-AgrC HK, 71397 Da. The molecular weight of the added signal sequence in *MBP is 2566 Da, thus accounting in part for the large difference in mass between 3A-2 and MBP-AgrC HK. After purification, all proteins were run on SDS-PAGE gels using molecular weight markers, which confirmed their approximates masses (relative to each other).

Attempts to develop His-tagged AgrC constructs

A cloning strategy was devised to express His-tagged version of AgrC in *E. coli,* for subsequent purification and *in vitro* characterization. Two proteins were envisioned, along the lines of the MBP-AgrC HK and MBP-3rd loop-TM helix-AgrC HK proteins, with the substitution of MBP by a His-tag. These beginning amino acid sequences of these proteins are listed below, where the beginning portion of AgrC-I is underlined and the incorporated FactorXa site highlighted in bold:

His-AgrC HK protein: HHHHHHSSGLVPRGSHM**IEGR**<u>SQFLLKEMKYKRN...cont..</u>

His-3rd loop-TM helix-AgrC HK protein:

HHHHHHSSGLVPRGSHM**IEGR**<u>SQINSDEAKVIR...cont...</u>

The non-PAGE-purified primers (Invitrogen) for this cloning, with the restriction sites underlined, were:

His-AgrC HK protein: NdeI -FXA- kinase forward,

5'-GGGAATTCCATATGATCGAAGGTCGTTCTCAATTTCTCCTTAAAGAGA TGAAATATAAACGTAATC-3'

His-3rd loop-TM helix-AgrC HK protein: NdeI -FXA- 3TMK forward,

5'-GGGAATTCCATATGATCGAAGGTCGTTCACAAATAAACTCGGATGAA GCTAAAGTAATAAGG-3'

The common reverse primer for both constructs was:

BamHI -kinase reverse primer,

5'-CGCCGCGGATCCTCAACTTTTTGAATAAAAGAAACCATTTTCG-3'

The PCR products, using the plasmid pRN7062 as template were restriction-digested with BamHI/NdeI, followed by DpnI digestion to remove plasmid template, and then QiaQuik PCR purification (Qiagen). These digested products were then ligated to the similarly digested and Calf-Intestinal Alkaline Phosphatase (CIP)-treated His-vector, pET15b (Novagen). Unfortunately, after DH5α transformation and plating, no colonies were recovered , indicating that some step of the cloning had failed. The lack of PAGE purification of the primers could have resulted in a primer error, or else the double-digestion with NdeI and BamHI of the PCR product or cloning plasmid may not have gone to completion. In any case, the poor behavior of the AgrC HK domain on its own after cleavage from MBP in the MBP-fusion proteins (see Results) may make the expression of His-tagged AgrC HK domains (with or without transmembrane helices) difficult.

Histidine Kinase Activity Assays

Low NaCl concentration (≤ 25mM) was found to be critical for high HK activity. After purification of MBP-fusion proteins according to the manufacturer's instructions (NEB), the proteins were dialyzed into 20 mM Tris pH7.2, 200 mM NaCl, 5 mM $MgCl_2$, and 0.2 mM DTT, mainly to remove EDTA, to replace ß-Mercaptoethanol with DTT and to add the necessary magnesium cofactor for the enzyme. For the kinase assays, the protein was diluted into phosphorylation buffer, consisting of 20 mM Tris pH7.5, 5 mM $MgCl_2$, 5 mM $MnCl_2$, and 50 mM KCl, to which was added radioactive ATP analogs, cold ATP or buffer. The manganese was included because control experiments utilizing manganese instead of magnesium showed a slight increase in kinase activity with manganese. The dilution of protein by phosphorylation buffer was critical, as 1:2 dilutions resulted in poor activity, while 1:8 dilutions resulted in high activity, leading to the conclusion that low NaCl concentration was critical for high kinase activity, a result found for at least one other HK domain (Wright et al., 1993). The ATPγ^{32}P and ATPγ^{35}S were ordered from NEN, cat #s BLU502A, 250 µCi in 25 µL, and 502H Eztides, 3000 Ci/mmol (sp. Activity), respectively. For most experiments, timepoints were taken at 10, 30, 60 and 90 minutes, with quenching with 6xSDS running buffer, including EDTA. The samples were then loaded and run on SDS-PAGE gels. One gel was dried and subjected to autoradiography. Usually, a parallel gel was Coomassie-stained to verify equal protein loading, as it is well-known that 3-phosphohistidine does not survive the acidic staining procedure. However, athough never fully verified, it was noted on SDS-PAGE analysis

on at least one occasion that a slight band shift upward occurred with MBP-AgrC HK proteins that had been phosphorylated by ATP addition.

Expressing truncated AgrC *in vivo*

The same shuttle vector, pRN7035, was used as for the original group I, II, and IV reporter strains. This vector carries a P3:*blaZ* reporter, an *ori* from pT181 (for replication in *S.aureus*), the *ermC* gene from pE194 (for selection in *S.aureus*), and an ampicillin/ColE1 *ori* fragment from pUC19 (for replication and selection in *E.coli*). PCR fragments, containing truncated forms of *agrC*, full-length *agrA*, and downstream termination signals, amplified from the genomic DNA of *agr* group I, were cloned into the PstI/SphI sites of the pUC polylinker of pRN7035 (that had been adapted for more efficient double-digestion). The following PAGE-purified primers (Integrated DNA Technologies, Inc.) were used in the PCR reactions, with the restriction sites underlined, the *agrC*-derived portions in bold, and the ribsome-binding site (derived from the tetracycline promoter) italicized:

AgrC HK only, forward primer:

5'-GTAAATCTGCAG*TAGAGAGTGTGATAGTAG***ATGCTCCTTAAAGAG**-3'

AgrC-3TM-HK, forward primer:

5'-GTAAATCTGCAG*TAGAGAGTGTGATAGTAG***ATGTCACAAATAAAC**-3'

AgrC-TM3TM-HK, forward primer:

5'-GTAAATCTGCAG*TAGAGAGTGTGATAGTAG***ATGATTAGCACACCA**-3'

The common reverse primer used in these reactions was Orf7 Reverse AgrCA:

5'-GGTGAAGCATGCAGTTTGCCAACATTACAAGAGGTTGAACAAGCA

TTTTAA-3' located in a downstream open-reading frame, Orf7, from the *agr* operon.

Restriction digest mapping and DNA sequencing of the cloning junctions was used to verify the plasmid constructs. Plasmid DNA isolated from single colonies of the *E. coli* DH5α derivative was introduced into the restriction-defective *S. aureus* strain, RN4220, by the protoplast method (Novick, 1991). Plasmids were then moved into the Group I *agr*+ cell line, RN6734, or the *agr*-null cell line, RN6911, by phage transduction (Novick, 1991). Plasmid minipreps of independent clones of *S. aureus* cells verified the presence of the correct molecular weight plasmids, which were further confirmed by restriction digest mapping. The truncated AgrC proteins start with the following amino acid sequences:

AgrC-HK protein: MLLKEMKYKRNQEEIET....cont....

AgrC-3TM-HK protein: MSQINSDEAKVIRQYSFIF....cont....

AgrC-TM3TM-HK: MISTPYLILNKGFLIVISTILLLTFSLF....cont....

Each construct also produces AgrA.

The portions from AgrC in the above constructs consist of the kinase alone, the 3rd extracellular loop-6th TM helix-kinase or the 5th TM helix-3rd extracellular loop-6th TM helix-kinase.

At least two independent plasmid clones from each construct isolated originally in *E. coli* were tested in *S. aureus* for HK activity or a dominant-negative effect, using the nitrocefin method and the δ-toxin HPLC assay (see Results). To test for HK activity, these plasmids were introduced into the *agr*-null strain, RN6911, and the ß-lactamase activity was compared to RN9222, which contains full-length AgrC/AgrA, in the presence or absence of AIP-I at 1 μM. The basal activity of these strains was no different

than that seen previously with the control strain, RN9033, which contains the shuttle vector alone, with no insert. These strains were NOT inducible by AIP-I as compared to RN9222, consistent with the requirement of the sensor domain of AgrC for inducible activation. To test for a dominant-negative effect, the 3 independently derived AgrC HK plasmids were introduced into the *agr*+ strain, RN6734, and their effect on native *agr* activation monitored during cell growth by the nitrocefin method and the δ-toxin HPLC assay. For the nitrocefin method, aliquots were taken during cell growth at different timepoints and analyzed. The control with the pRN9033 plasmid value was performed with triplicate cultures of the same clone, with a single nitrocefin analysis per culture. The ß-lactamase values at the 4 hour timepoint were taken from 3 independently derived clones of AgrC HK in culture, which were each measured by nitrocefin analysis in triplicate and the means of the triplicate nitrocefin analyses combined to generate an overall mean ± SEM for each clone. For the δ-toxin assay, RP-HPLC was used to quantify δ-toxin levels in the supernatant of a single culture of p9033 and in the 3 independently cloned AgrC-HK cultures (single HPLC injection per culture only). This experiment was conducted twice, so the means for pRN9033, 6A, 6B, and 6C from the two assays were independently derived and then combined to generate the overall mean for each clone ± SEM.

Anti-AgrC Antibody Development and Testing

The peptide, C-Ahx-INSDEAKVIRQY, was synthesized (by B. Ayers) on PAM resin using standard Boc-based peptide synthesis methods (*vide supra*). The peptide was purified and subsequently conjugated to maleimide-activated KLH according to the

manufacturer's instructions (Pierce). This material (15 mg) was sent to Charles Rivers Inc. for rabbit polyclonal antibody production. Two rabbits were pre-immune bled and then immunized each with 1 mg of the KLH-peptide, including complete Freund's adjuvant (CFA). The rabbits were boosted (each time with 0.5 mg) and test-bled 4 times at ~ 3 week intervals, followed by a terminal bleed ~ one month after the final boost. The decision to terminally bleed the rabbits came after dot blotting demonstrated reactivity of the test-bleed sera (but not the pre-immune bleed sera) (1:500 dilution) with the C-Ahx-INSDEAKVIRQY peptide down to a dotted dilution amount of 2.88 pmol (but not with 0.288 pmol). Dot blots were performed with 0.2 micron size nitrocellulose membrane (Pierce) to increase the chance of peptide retention on the membrane, with the peptide solutions (5 μL) dotted onto dry membranes, followed by incubation at 37°C to accelerate drying of the dotted mixtures. The sera also recognized dot-blotted KLH-conjugated peptide.

Western blotting with protoplast lysates from *agr*+(RN6390) and *agr*-null (RN6911) early-stationary phase cultures did not reveal any strong band for AgrC, ~50 kDa, in the *agr*+ lysate. In sharp contrast, a very strong doublet signal was detected in *agr*-null lysates at ~46 and 50 kDa. It is well-known that protein A expression is dramatically up-regulatated in *agr*-null strains in stationary phase cultures, due to its lack of down-regulation by the *agr* pathway. Furthermore, it is also well-documented that protein A contains an epitope that is strongly bound by a consensus binding site on the constant fragment (Fc) of immunoglobulin G (IgG) (Hoffman et al., 1996). Therefore, it is not surprising that protein A gave a strong signal in Western blotting. However, the unfortunate co-migration of protein A with AgrC made it very difficult to determine with

any precision whether a faint band was present in the *agr*+ lysate that was not present in the *agr*-null lysate. Furthermore, the sera reacted with many other proteins from the lysate, as evidenced by multiple bands on Western blot, thus indicating that affinity-purification might be helpful.

Affinity purification was carried out using SulfoLink Gel (Pierce) according to the manufacturer's instructions, starting with 14 mL of sera from rabbit #1 and yielding a 2 mL solution of antibody at 0.84 mg/mL. This affinity-purified and concentrated sample recognized 0.288 pmol of the epitope on dot blots at a 1:500 dilution, which confirmed good recovery and concentration of the antibody.

The bacterial strains tested by Western blotting of whole cell lysates or membrane preparations (with and without AgrC and induced or not, with AIP-I or methicillin, depending on the strain) were: RN6390 (*agr*+), RN6911 (*agr*-null, RN9222 *agr*+), RN9033 (*agr*-null), RN7736 (*agr*+ protein A-null), RN9397 (*agr*-null protein A-null), RN8976 (*agr*-null protein A-null), and *S. aureus* strains containing various AgrC truncated proteins (*vide supra* and Results). In addition, various MBP-AgrC fusion proteins purified from *E. coli* were tested as well (see Results).

Appendix 1 –

^{1}H chemical shift assignments for AIPs and analogs derived thereof.

AIP-II chemical shifts in 90% H_2O/10% D_2O, pH 4.0, 298 K

residue	NH	Hα	Hβ	Hγ	others
Gly					
Val	8.41	4.10	2.01	0.86	
Asn	8.53	4.64	2.78, 2.68		-NH_2 7.53, 6.84
Ala	8.3	4.24	1.30		
Cys	8.36	4.49	3.37, 2.99		
Ser	8.53	4.38	3.82		
Ser	8.29	4.24	3.90		
Leu	7.96	4.04	1.17	1.03	0.74, 0.66
Phe	8.43	4.88	3.34, 2.78		Ar. 7.29, 7.19

AIP-II V2A chemical shifts in 90% H_2O/10% D_2O, pH 4.0, 298 K

residue	NH	Hα	Hβ	Hγ	others
Gly					
Val	8.54	4.29	1.31		
Asn	8.46	4.60	2.79, 2.69		-NH_2 7.53, 6.86
Ala	8.27	4.23	1.30		
Cys	8.36	4.48	3.36, 2.99		
Ser	8.54	4.48	3.81		
Ser	8.29	4.25	3.90		
Leu	7.95	4.04	1.17	1.03	0.72, 0.66
Phe	8.43	4.88	3.45, 2.79		Ar. 7.29, 7.19

AIP-II N3A chemical shifts in 90% H_2O/10% D_2O, pH 4.0, 298 K

residue	NH	Hα	Hβ	Hγ	others
Gly					
Val	8.35	4.04	1.95	0.81	
Ala	8.38	4.19	1.26		
Ala	8.25	4.14	1.22		
Cys	8.34	4.42	3.30, 2.90		
Ser	8.53	4.32	3.75		
Ser	8.29	4.18	3.85		
Leu	7.91	3.97	1.19, 1.09	0.96	0.66, 0.60
Phe	8.39	4.83	3.40, 2.72		Ar. 7.24, 7.13

AIP-II S6A chemical shifts in 90% H_2O/10% D_2O, pH 4.0, 298 K

residue	NH	Hα	Hβ	Hγ	others
Gly					
Val	8.41	4.10	2.01	0.85	
Asn	8.54	4.67	2.78, 2.68		-NH_2 7.53, 6.84
Ala	8.29	4.23	1.28		
Cys	8.33	4.42	3.30, 2.90		
Ala	8.52	4.26	1.35		
Ser	8.31	4.23	3.87		
Leu	7.96	4.03	1.19	1.01	0.72, 0.66
Phe	8.47	4.89	3.46, 2.78		Ar. 7.29, 7.20

AIP-II S7A chemical shifts in 90% H_2O/10% D_2O, pH 4.0, 298 K

residue	NH	Hα	Hβ	Hγ	others
Gly					
Val	8.41	4.11	2.03	0.89	
Asn	8.53	4.68	2.79, 2.70		-NH_2 7.53, 6.85
Ala	8.29	4.25	1.31		
Cys	8.36	4.51	3.38, 2.95		
Ser	8.48	4.39	3.78		
Ala	8.46	4.13	1.42		
Leu	7.75	4.09	1.27	1.09	0.74, 0.68
Phe	8.32	4.90	3.48, 2.85		Ar. 7.30, 7.22

AIP-II L8A chemical shifts in 90% H_2O/10% D_2O, pH 4.0, 298 K

residue	NH	Hα	Hβ	Hγ	others
Gly					
Val	8.41	4.09	2.01	0.86	
Asn	8.52	4.63	2.77, 2.67		-NH_2 7.53, 6.84
Ala	8.28	4.23	1.29		
Cys	8.35	4.49	3.37, 2.97		
Ser	8.51	4.42	3.38		
Ser	8.44	4.24	3.92		
Ala	8.14	4.05	0.94		
Phe	8.39	4.85	3.44, 2.79		Ar. 7.29, 7.20

AIP-II F9A chemical shifts in 90% H_2O/10% D_2O, pH 4.0, 298 K

residue	NH	Hα	Hβ	Hγ	others
Gly					
Val	8.41	4.12	2.02	0.88	
Asn	8.52	4.65	2.79, 2.69		-NH_2 7.52, 6.85
Ala	8.28	4.24	1.30		
Cys	8.35	4.45	3.34, 2.96		
Ser	8.51	4.43	3.80		
Ser	8.44	4.23	3.94		
Leu	8.14	4.32	1.73	1.62	0.86, 0.82
Ala	8.39	4.63	1.35		

AIP-II lactam chemical shifts in 90% H_2O/10% D_2O, pH 4.0, 298 K

residue	NH	Hα	Hβ	Hγ	others
Gly					
Val	8.41	4.12	2.04	0.89	
Asn	8.56	4.67	2.81, 2.70		-NH_2 7.54, 7.06
Ala	8.29	4.28	1.33		
Dapa	8.22	4.40	3.79, 3.29		-NH 7.65
Ser	8.46	4.46	3.92		
Ser	8.78	4.02	3.86		
Leu	7.94	3.99	1.23	1.09	0.70, 0.66
Phe	7.75	4.64	3.40, 2.93		Ar 7.31, 7.14

AIP-II linear thioester chemical shifts in 90% H_2O/10% D_2O, pH 4.0, 298 K

residue	NH	Hα	Hβ	Hγ	others
Gly					
Val	8.42	4.09	2.00	0.86	
Asn	8.52	4.65	2.77, 2.68		-NH_2 7.26, 6.85
Ala	8.30	4.21	1.31		
Ala	8.23	4.25	1.33		
Ser	8.17	4.37	3.76		
Ser	8.10	4.36	3.81		
Leu	8.00	4.22	1.44	1.33	0.79, 0.73
Phe	8.38	4.72	3.24, 2.85		Ar 7.28, 6.94

AIP-II in DMSO-d_6, 298 K

residue	NH	Hα	Hβ	Hγ	others
Gly		3.63			
Val	8.44	4.34	1.96	0.89, 0.82	
Asn	8.36	4.56	2.59, 2.40		-NH_2 7.41, 6.94
Ala	7.99	4.26	1.19		
Cys	8.36	4.37	3.18, 2.94		
Ser	8.07	4.23	3.65, 3.52		-OH 5.04
Ser	7.64	4.27	3.61		-OH 5.14
Leu	8.12	3.93	1.40	1.22	0.73
Phe	8.69	4.56	3.32, 2.85		Ar. 7.25, 7.21

AIP-II lactam chemical shifts in DMSO-d_6, 298 K

residue	NH	Hα	Hβ	Hγ	others
Gly		3.65			
Val	8.44	4.35	1.98	0.87	
Asn	8.36	4.57	2.60, 2.41		-NH_2 7.39, 6.94
Ala	7.92	4.30	1.20		
Dapa	8.04	4.38	3.71, 2.89		-NH 7.64
Ser	8.01	4.36	3.85		-OH 5.39
Ser	8.72	3.84	3.65		-OH 5.35
Leu	7.67	3.95	1.25	1.06	0.73, 0.72
Phe	7.44	4.39	3.23, 3.03		Ar 7.26, 7.20

AIP-II linear C-terminal free acid in DMSO-d_6, 298 K

residue	NH	Hα	Hβ	Hγ	others
Gly		3.64			
Val	8.46	4.35	1.99	0.86	
Asn	8.37	4.58	2.61, 2.41		-NH_2 7.42, 6.95
Ala	7.99	4.23	1.22		
Cys	8.15	4.41	2.78		
Ser	7.98	4.33	3.61		-OH 5.12
Ser	7.93	4.32	3.62		
Leu	7.89	4.29	1.60, 1.40	0.84	0.84
Phe	8.03	4.37	3.04, 2.92		Ar 7.26, 7.21

trAIP-II in DMSO-d_6, 298 K

residue	NH	Hα	Hβ	Hγ	others
acetyl	1.86				
Cys	8.46	4.40	3.15, 2.87		
Ser	8.12	4.23	3.66, 3.54		-OH 5.06
Ser	7.61	4.27	3.59		-OH 5.17
Leu	8.14	3.93	1.43	1.23	0.73
Phe	8.69	4.56	3.33, 2.85		Ar. 7.26, 7.21

trAIP-II lactam in DMSO-d_6, 298 K

residue	NH	Hα	Hβ	Hγ	others
acetyl	1.83				
Dapa	8.10	4.38	3.63, 2.86		
Ser	8.03	4.32	3.77		
Ser	8.67	3.85	3.63		
Leu	7.71	3.95	1.26, 1.09	1.38	0.75
Phe	7.48	4.37	3.22, 3.01		Ar. 7.14, 7.31

AIP-I in DMSO-d_6, 298 K

residue	NH	Hα	Hβ	Hγ	others
Tyr		4.03	3.03, 2.80		Ar. 7.07, 6.70 -OH 9.31
Ser	8.73	4.56	3.69, 3.60		-OH 5.21
Thr	7.94	4.25	4.06	1.04	-OH 4.92
Cys	8.22	4.39	3.19, 2.91		
Asp	8.21	4.42	2.48, 2.38		
Phe	7.84	4.49	2.98		Ar. 7.30, 7.21
Ile	8.32	3.73	1.93	0.89	0.85
Met	8.98	4.28	1.94	2.43	2.19

AIP-I linear C-terminal free acid in DMSO-d_6, 298 K

residue	NH	Hα	Hβ	Hγ	others
Tyr		3.97	3.01, 2.76		Ar. 7.06, 6.69 -OH 9.30
Ser	8.71	4.56	3.65, 3.65		
Thr	7.97	4.29	4.10	1.06	
Cys	8.26	4.51	2.63, 2.41		
Asp	7.93	4.44	2.69		
Phe	7.79	4.54	2.98, 2.80		Ar. 7.21, 7.18
Ile	7.96	4.18	1.72	1.46	0.85
Met	8.23	4.32	1.87	2.47	1.99

AIP-I D5N in DMSO-d_6, 298 K

residue	NH	Hα	Hβ	Hγ	others
Tyr		4.00	3.04, 2.79		Ar. 7.07, 6.70 -OH 9.31
Ser	8.71	4.56	3.64		-OH 5.21
Thr	7.91	4.25	4.07	1.04	-OH 4.92
Cys	8.23	4.37	3.18, 2.90		
Asn	8.11	4.40	2.39, 2.28		$-NH_2$ 7.39, 6.90
Phe	7.86	4.48	2.97		Ar. 7.30, 7.21
Ile	8.34	3.76	1.92	1.10	0.75
Met	9.00	4.27	1.93	2.49	2.19

AIP-IV in DMSO-d_6, 298 K

residue	NH	Hα	Hβ	Hγ	others
Tyr		3.98	3.04, 2.78		Ar. 7.07, 6.70 -OH 9.31
Ser	8.70	4.56	3.64		-OH 5.27
Thr	7.93	4.21	4.09	1.00	-OH 4.86
Cys	8.21	4.27	3.16, 2.87		
Tyr	7.99	4.20	2.59		Ar. 6.80, 6.60 -OH 9.16
Phe	8.00	4.47	2.95		Ar. 7.30, 7.22
Ile	8.22	3.76	1.93	1.14	0.75
Met	9.07	4.23	1.92	2.48	2.19

AIP-IV Y5F in DMSO-d_6, 298 K

residue	NH	Hα	Hβ	Hγ	others
Tyr		4.03	3.05, 2.80		Ar. 7.08, 6.70 -OH 9.33
Ser	8.74	4.55	3.70, 3.56		-OH 5.27
Thr	7.94	4.18	4.09	0.97	-OH 4.85
Cys	8.18	4.26	3.15, 2.87		
Phe	8.08	4.25	2.68		Ar. 7.21, 7.03
Phe	8.05	4.50	2.97		Ar. 7.31, 7.22
Ile	8.23	3.78	1.93	1.15	0.76
Met	9.07	4.24	1.93	2.49	2.18

AIP-I D5A in DMSO-d_6, 298 K

residue	NH	Hα	Hβ	Hγ	others
Tyr		4.04	3.02, 2.80		Ar. 7.07, 6.69 -OH 9.33
Ser	8.72	4.56	3.63		-OH 5.22
Thr	7.95	4.26	4.04	1.06	-OH 4.93
Cys	8.22	4.26	3.16, 2.89		
Ala	8.03	4.25	1.03		
Phe	7.80	4.50	2.95		Ar. 7.27, 7.19
Ile	8.28	3.77	1.93	1.15	0.76
Met	9.06	4.26	1.93	2.48	2.17

AIP-I M8I in DMSO-d_6, 298 K

residue	NH	Hα	Hβ	Hγ	others
Tyr		4.02	3.04, 2.79		Ar. 7.08, 6.70 -OH 9.32
Ser	8.74	4.55	3.70, 3.59		-OH 5.20
Thr	7.95	4.26	4.04	1.03	-OH 4.86
Cys	8.20	4.35	3.17, 2.90		
Asp	8.30	4.44	2.52, 2.42		
Phe	7.70	4.54	2.98		Ar. 7.28, 7.20
Ile	8.48	3.58	1.97	1.02	0.72
Ile	8.91	4.21	1.65	1.04	0.88

AIP-I linear C-terminal free acid in DMSO-d_6, 298 K

residue	NH	Hα	Hβ	Hγ	others
Tyr		3.97	3.01, 2.76		Ar. 7.06, 6.69 -OH 9.30
Ser	8.71	4.56	3.65		
Thr	7.97	4.29	4.10	1.06	
Cys	8.26	4.51	2.63, 2.41		
Asp	7.93	4.44	2.69		
Phe	7.79	4.54	2.98, 2.80		Ar. 7.21, 7.18
Ile	7.96	4.18	1.72	1.46	0.85
Met	8.23	4.32	1.87	2.47	1.99

Acetyl-AIP-I in DMSO-d_6, 298 K

residue	NH	Hα	Hβ	Hγ	others
acetyl	1.74				
Tyr	8.01	4.48	2.92, 2.62		Ar. 7.05, 6.63 -OH 9.13
Ser	8.15	4.39	3.62		-OH 5.11
Thr	7.70	4.21	4.03	1.01	-OH 4.84
Cys	8.22	4.36	3.18, 2.91		
Asp	8.18	4.39	2.45, 2.37		
Phe	7.85	4.48	2.97		Ar. 7.27, 7.19
Ile	8.32	3.74	1.91	1.10	0.76
Met	8.99	4.26	1.93	2.45	2.18

trAIP-I in DMSO-d_6, 298 K

residue	NH	Hα	Hβ	Hγ	others
acetyl	1.83				
Cys	8.44	4.28	3.13, 2.83		
Asp	8.14	4.34	2.46, 2.30		
Phe	7.90	4.48	2.97		Ar. 7.26, 7.19
Ile	8.33	3.82	1.90	1.17	0.76
Met	9.07	4.29	1.95	2.48	2.17

trAIP-IV in DMSO-d_6, 298 K

residue	NH	Hα	Hβ	Hγ	others
acetyl	1.76				
Cys	8.41	4.23	3.05, 2.84		
Tyr	7.80	4.08	2.46		Ar. 6.84, 6.59 -OH 9.20
Phe	8.07	4.53	2.95		Ar. 7.29, 7.22
Ile	8.06	3.85	1.90	1.20	0.78
Met	9.17	4.14	1.94	2.47	2.19

trAIP-I D2A in DMSO-d_6, 298 K

residue	NH	Hα	Hβ	Hγ	others
acetyl	1.85				
Cys	8.47	4.25	3.14, 2.84		
Ala	8.11	4.03	1.04		
Phe	7.75	4.52	2.95		Ar. 7.27, 7.20
Ile	8.32	3.73	1.97	1.14	0.76
Met	9.06	4.25	1.94	2.48	2.18

AIP-II/I in DMSO-d_6, 298 K

residue	NH	Hα	Hβ	Hγ	others
Gly		3.61			
Val	8.44	4.31	1.96	0.86	
Asn	8.36	4.55	2.58, 2.40		$-NH_2$ 7.39, 6.92
Ala	7.92	4.24	1.15		
Cys	8.42	4.30	3.15, 2.93		
Asp	8.09	4.41	2.39, 2.34		
Phe	7.88	4.49	2.97		Ar. 7.25, 7.20
Ile	8.28	3.78	1.91	1.14	0.77
Met	9.04	4.25	1.94	2.42	2.19

AIP-I/II in DMSO-d_6, 298 K

residue	NH	Hα	Hβ	Hγ	others
Tyr		4.04	3.03, 2.80		Ar. 7.07, 6.70 -OH 9.31
Ser	8.73	4.56	3.69, 3.60		-OH 5.24
Thr	7.97	4.26	4.08	1.05	-OH 4.93
Cys	8.20	4.42	3.19, 2.91		
Ser	8.12	4.22	3.66, 3.51		-OH 5.03
Ser	7.63	4.27	3.60		-OH 5.14
Leu	8.12	3.94	1.39	1.22	0.72
Phe	8.69	4.55	3.32, 2.86		Ar. 7.26, 7.22

AIP-III heptapeptide in DMSO-d_6, 298 K

residue	NH	Hα	Hβ	Hγ	others
Ile		3.61	1.82	1.15	0.92
Asn	8.60	4.58	2.47		-NH_2 7.30, 6.93
Cys	8.31	4.34	3.14, 2.79		
Asp	8.17	4.47	2.43		
Phe	7.93	4.40	2.98		Ar. 7.26, 7.21
Leu	8.34	3.97	1.62, 1.46	1.17	0.77
Leu	8.78	4.23	1.67		0.87

AIP-III octapeptide in DMSO-d_6, 298 K

residue	NH	Hα	Hβ	Hγ	others
Tyr		4.02	2.76		Ar. 7.03, 6.72 -OH 9.30
Ile	8.55	4.29	1.75	0.89	
Asn	8.40	4.56	2.39		-NH_2 7.30, 6.89
Cys	8.04	4.33	3.16, 2.74		
Asp	8.23	4.48	2.45, 2.41		
Phe	7.93	4.37	2.98		Ar. 7.22, 7.08
Leu	8.36	3.96	1.63, 1.45	1.24	0.79
Leu	8.74	4.22	1.67		0.88

AIP-III nonapeptide in DMSO-d_6, 298 K

residue	NH	Hα	Hβ	Hγ	others
Ala		3.75	1.32		
Tyr	8.49	4.56	2.94, 2.68		Ar. 7.08, 6.65 -OH 9.18
Ile	8.01	4.21	1.74, 1.45	1.08, 0.83	
Asn	8.28	4.53	2.51, 2.39		-NH_2 7.28, 6.88
Cys	8.01	4.33	3.16, 2.75		
Asp	8.24	4.48	2.51, 2.39		
Phe	7.93	4.40	2.98		Ar. 7.28, 7.19
Leu	8.37	3.97	1.61, 1.43	1.18	0.76
Leu	8.73	4.26	1.67		0.88

References

Abdelnour, A., Arvidson, S., Bremell, T., Ryden, C., and Tarkowski, A. (1993). The accessory gene regulator (agr) controls *Staphylococcus aureus* virulence in a murine arthritis model. Infect Immun *61*, 3879-85.

al-Obeidi, F., Hruby, V. J., and Sawyer, T. K. (1998). Peptide and peptidomimetic libraries. Molecular diversity and drug design. Mol Biotechnol *9*, 205-23.

Ansaldi, M., Marolt, D., Stebe, T., Mandic-Mulec, I., and Dubnau, D. (2002). Specific activation of the Bacillus quorum-sensing systems by isoprenylated pheromone variants. Mol Microbiol *44*, 1561-73.

Arunlakshana, O. S., H.O. (1959). Some quantitative uses of drug antagonists. *Brit. J. Pharmacol.* ***14***, 48-57.

Axelsson, L., and Holck, A. (1995). The genes involved in production of and immunity to sakacin A, a bacteriocin from Lactobacillus sake Lb706. J Bacteriol *177*, 2125-37.

Barnett, D. A., Ding, L., Ells, B., Purves, R. W., and Guevremont, R. (2002). Tandem mass spectra of tryptic peptides at signal-to-background ratios approaching unity using electrospray ionization high-field asymmetric waveform ion mobility spectrometry/hybrid quadrupole time-of-flight mass spectrometry. Rapid Commun Mass Spectrom *16*, 676-80.

Bax, A., Byrd, RA, Aszalos, A.J. (1984). J. Am. Chem. Soc. *106*, 7632-7633.

Bondebjerg, J., Xiang, Z., Bauzo, R. M., Haskell-Luevano, C., and Meldal, M. (2002). A solid-phase approach to mouse melanocortin receptor agonists derived from a novel thioether cyclized peptidomimetic scaffold. J Am Chem Soc *124*, 11046-55.

Booth, M. C., Atkuri, R. V., Nanda, S. K., Iandolo, J. J., and Gilmore, M. S. (1995). Accessory gene regulator controls Staphylococcus aureus virulence in endophthalmitis. Invest Ophthalmol Vis Sci *36*, 1828-36.

Camarero, J. A., Cotton, G. J., Adeva, A., and Muir, T. W. (1998). Chemical ligation of unprotected peptides directly from a solid support. J Pept Res *51*, 303-16.

Cheung, A. L., Eberhardt, K. J., Chung, E., Yeaman, M. R., Sullam, P. M., Ramos, M., and Bayer, A. S. (1994). Diminished virulence of a sar-/agr- mutant of Staphylococcus aureus in the rabbit model of endocarditis. J Clin Invest *94*, 1815-22.

Christopoulos, A., Coles, P., Lay, L., Lew, M. J., and Angus, J. A. (2001). Pharmacological analysis of cannabinoid receptor activity in the rat vas deferens. Br J Pharmacol *132*, 1281-91.

Christopoulos, A., Parsons, A. M., and El-Fakahany, E. E. (1999). Pharmacological analysis of the novel mode of interaction between xanomeline and the M1 muscarinic acetylcholine receptor. J Pharmacol Exp Ther *289*, 1220-8.

Dawson, P. E., Muir, T. W., Clark-Lewis, I., and Kent, S. B. (1994). Synthesis of proteins by native chemical ligation. Science *266*, 776-9.

Demirev, P. A., Ramirez, J., and Fenselau, C. (2001). Tandem mass spectrometry of intact proteins for characterization of biomarkers from Bacillus cereus T spores. Anal Chem *73*, 5725-31.

Dufour, P., Jarraud, S., Vandenesch, F., Greenland, T., Novick, R. P., Bes, M., Etienne, J., and Lina, G. (2002). High genetic variability of the agr locus in Staphylococcus species. J Bacteriol *184*, 1180-6.

Dutta, R., and Inouye, M. (2000). GHKL, an emergent ATPase/kinase superfamily. Trends Biochem Sci *25*, 24-8.

Dutta, R., Qin, L., and Inouye, M. (1999). Histidine kinases: diversity of domain organization. Mol Microbiol *34*, 633-40.

Ehrmann, M., Boyd, D., and Beckwith, J. (1990). Genetic analysis of membrane protein topology by a sandwich gene fusion approach. Proc Natl Acad Sci U S A *87*, 7574-8.

Falck, J. R. L., Jing-Yu; Cho, Su-Dong; Yu, Jurong. (1999). Alkyl thioether synthesis via imidazole mediated Mitsunobu condensation. Tetrahedron Letters *40*, 2903-2906.

Falke, J. J., and Hazelbauer, G. L. (2001). Transmembrane signaling in bacterial chemoreceptors. Trends Biochem Sci *26*, 257-65.

Fenselau, C., and Demirev, P. A. (2001). Characterization of intact microorganisms by MALDI mass spectrometry. Mass Spectrom Rev *20*, 157-71.

Fisher, S. L., Jiang, W., Wanner, B. L., and Walsh, C. T. (1995). Cross-talk between the histidine protein kinase VanS and the response regulator PhoB. Characterization and identification of a VanS domain that inhibits activation of PhoB. J Biol Chem *270*, 23143-9.

Freeman, J. A., Lilley, B. N., and Bassler, B. L. (2000). A genetic analysis of the functions of LuxN: a two-component hybrid sensor kinase that regulates quorum sensing in Vibrio harveyi. Mol Microbiol *35*, 139-49.

Fuqua, C., and Greenberg, E. P. (2002). Signalling: Listening in on bacteria: acyl-homoserine lactone signalling. Nat Rev Mol Cell Biol *3*, 685-95.

Fuqua, C., Parsek, M. R., and Greenberg, E. P. (2001). Regulation of gene expression by cell-to-cell communication: acyl- homoserine lactone quorum sensing. Annu Rev Genet *35*, 439-68.

Gilbert, H. F. (1994). Protein chaperones and protein folding. Curr Opin Biotechnol *5*, 534-9.

Gillaspy, A. F., Hickmon, S. G., Skinner, R. A., Thomas, J. R., Nelson, C. L., and Smeltzer, M. S. (1995). Role of the accessory gene regulator (agr) in pathogenesis of staphylococcal osteomyelitis. Infect Immun *63*, 3373-80.

Giraudo, A. T., Rampone, H., Calzolari, A., and Nagel, R. (1996). Phenotypic characterization and virulence of a sae- agr- mutant of *Staphylococcus aureus*. Can J Microbiol *42*, 120-3.

Goodman, M., and McGahren, W. J. (1967). Mechanistic studies of peptide oxazolone racemization. Tetrahedron *23*, 2031-50.

Groisman, E. A. (2001). The pleiotropic two-component regulatory system PhoP-PhoQ. J Bacteriol *183*, 1835-42.

Havarstein, L. S., Gaustad, P., Nes, I. F., and Morrison, D. A. (1996). Identification of the streptococcal competence-pheromone receptor. Mol Microbiol *21*, 863-9.

Hayashi, T., and Sasagawa, T. (1993). A method for identifying the carboxy terminal amino acid of a protein. Anal Biochem *209*, 163-8.

Hidaka, Y., Park, H., and Inouye, M. (1997). Demonstration of dimer formation of the cytoplasmic domain of a transmembrane osmosensor protein, EnvZ, of Escherichia coli using Ni- histidine tag affinity chromatography. FEBS Lett *400*, 238-42.

Higuchi, R., Krummel, B., and Saiki, R. K. (1988). A general method of in vitro preparation and specific mutagenesis of DNA fragments: study of protein and DNA interactions. Nucleic Acids Res *16*, 7351-67.

Hoch, J. A. (2000). Two-component and phosphorelay signal transduction. Current Opinion in Microbiology *3*, 165-70.

Hoffman, W. L., Ruggles, A. O., and Tabarya, D. (1996). Chicken anti-protein A prevents *Staphylococcus aureus* protein A from binding to human and rabbit IgG in immunoassays and eliminates most false positive results. J Immunol Methods *198*, 67-77.

Jarraud, S., Lyon, G. J., Figueiredo, A. M., Gerard, L., Vandenesch, F., Etienne, J., Muir, T. W., and Novick, R. P. (2000). Exfoliatin-producing strains define a fourth agr specificity group in *Staphylococcus aureus*. J Bacteriol *182*, 6517-22.

Ji, G., Beavis, R., and Novick, R. P. (1997). Bacterial interference caused by autoinducing peptide variants. Science *276*, 2027-30.

Ji, G., Beavis, R. C., and Novick, R. P. (1995). Cell density control of staphylococcal virulence mediated by an octapeptide pheromone. Proc Natl Acad Sci U S A *92*, 12055-9.

Kenakin, T. (1997). Pharmacologic Analysis of Drug-Receptor Interaction: Lippincott-Raven).

Kessler, H., Griesinger, C., Kerssebaum, R., Wagner, K. (1987). J. Am. Chem. Soc. *109*, 607-609.

Kornblum, J. S., Projan, S. J., Moghazeh, S. L., and Novick, R. P. (1988). A rapid method to quantitate non-labeled RNA species in bacterial cells. Gene *63*, 75-85.

Koshland, D. E., Jr. (1996). The structural basis of negative cooperativity: receptors and enzymes. Curr Opin Struct Biol *6*, 757-61.

Kratchmarova, I., Kalume, D. E., Blagoev, B., Scherer, P. E., Podtelejnikov, A. V., Molina, H., Bickel, P. E., Andersen, J. S., Fernandez, M. M., Bunkenborg, J., Roepstorff, P., Kristiansen, K., Lodish, H. F., Mann, M., and Pandey, A. (2002). A Proteomic Approach for Identification of Secreted Proteins during the Differentiation of 3T3-L1 Preadipocytes to Adipocytes. Mol Cell Proteomics *1*, 213-22.

Krutchinsky, A. N., and Chait, B. T. (2002). On the nature of the chemical noise in MALDI mass spectra. J Am Soc Mass Spectrom *13*, 129-34.

Krutchinsky, A. N., Kalkum, M., and Chait, B. T. (2001). Automatic identification of proteins with a MALDI-quadrupole ion trap mass spectrometer. Anal Chem *73*, 5066-77.

Langone, J. J., Das, C., Bennett, D., and Terman, D. S. (1983). Radioimmunoassays for protein A of Staphylococcus aureus. J Immunol Methods *63*, 145-57.

Lasker, M., Bui, C. D., Besant, P. G., Sugawara, K., Thai, P., Medzihradszky, G., and Turck, C. W. (1999). Protein histidine phosphorylation: increased stability of thiophosphohistidine. Protein Sci *8*, 2177-85.

Lau, G. W., Haataja, S., Lonetto, M., Kensit, S. E., Marra, A., Bryant, A. P., McDevitt, D., Morrison, D. A., and Holden, D. W. (2001). A functional genomic analysis of type 3 Streptococcus pneumoniae virulence. Mol Microbiol *40*, 555-571.

Lesley, J. A., and Waldburger, C. D. (2001). Comparison of the Pseudomonas aeruginosa and E. coli PhoQ sensor domains: Evidence for distinct mechanisms of signal detection. J Biol Chem Papers in Press *12*, 12.

Lew, M. J., and Angus, J. A. (1995). Analysis of competitive agonist-antagonist interactions by nonlinear regression. Trends Pharmacol Sci *16*, 328-37.

Lina, G., Jarraud, S., Ji, G., Greenland, T., Pedraza, A., Etienne, J., Novick, R. P., and Vandenesch, F. (1998). Transmembrane topology and histidine protein kinase activity of AgrC, the agr signal receptor in *Staphylococcus aureus*. Mol Microbiol *28*, 655-62.

Lyon, G. J., Mayville, P., Muir, T. W., and Novick, R. P. (2000). Rational design of a global inhibitor of the virulence response in *Staphylococcus aureus*, based in part on localization of the site of inhibition to the receptor-histidine kinase, AgrC. Proc Natl Acad Sci U S A *97*, 13330-5.

Lyon, G. J., Wright, J. S., Christopoulos, A., Novick, R. P., and Muir, T. W. (2002). Reversible and Specific Extracellular Antagonism of Receptor-Histidine Kinase Signaling. J Biol Chem *277*, 6247-6253.

Lyon, G. J., Wright, J. S., Muir, T. W., and Novick, R. P. (2002). Key Determinants of Receptor Activation in the agr Autoinducing Peptides of *Staphylococcus aureus*. Biochemistry *41*, 10095-10104.

Maniatis, T., E. F. Fritsch, and J. Sambrook. (1982). Molecular cloning: a Laboratory Manual (N.Y.: Cold Spring Harbor Laboratory, Cold Spring Harbor,).

Manoil, C., and Beckwith, J. (1986). A genetic approach to analyzing membrane protein topology. Science *233*, 1403-8.

Marina, A., Mott, C., Auyzenberg, A., Hendrickson, W. A., and Waldburger, C. D. (2001). Structural and mutational analysis of the PhoQ histidine kinase catalytic domain. Insight into the reaction mechanism. J Biol Chem *276*, 41182-90.

Mayville, P., Ji, G., Beavis, R., Yang, H., Goger, M., Novick, R. P., and Muir, T. W. (1999). Structure-activity analysis of synthetic autoinducing thiolactone peptides from Staphylococcus aureus responsible for virulence. Proc Natl Acad Sci U S A *96*, 1218-23.

McDowell, P., Affas, Z., Reynolds, C., Holden, M. T. G., Wood, S. J., Saint, S., Cockayne, A., Hill, P. J., Dodd, C. E. R., Bycroft, B. W., Chan, W. C., and Williams, P. (2001). Structure, activity, and evolution of the group I thiolactone peptide quorum-sensing system of *Staphylococcus aureus*. Molecular Microbiology *41*, 503-512.

Mendal, M. (1992). Tetrahedron Lett *33*, 3077–3080.

Miller, M. B., Skorupski, K., Lenz, D. H., Taylor, R. K., and Bassler, B. L. (2002). Parallel quorum sensing systems converge to regulate virulence in Vibrio cholerae. Cell *110*, 303-14.

Morrison, D. A. (1997). Streptococcal competence for genetic transformation: regulation by peptide pheromones. Microb Drug Resist *3*, 27-37.

Nakayama, J., Cao, Y., Horii, T., Sakuda, S., Akkermans, A. D., de Vos, W. M., and Nagasawa, H. (2001). Gelatinase biosynthesis-activating pheromone: a peptide lactone that mediates a quorum sensing in *Enterococcus faecalis*. Mol Microbiol *41*, 145-154.

Nakayama, J., Cao, Y., Horii, T., Sakuda, S., and Nagasawa, H. (2001). Chemical synthesis and biological activity of the gelatinase biosynthesis-activating pheromone of Enterococcus faecalis and its analogs. Biosci Biotechnol Biochem *65*, 2322-5.

Novick, R. P., Ross, H.F., Figueiredo, A.M.S., Abramochkin, G., Muir, T. (2000). Activation and inhibition of the Staphylococcal AGR system. Science *287*, 391a.

Novick, R. P. (1991). Genetic systems in staphylococci. Methods Enzymol *204*, 587-636.

Novick, R. P., and Muir, T. W. (1999). Virulence gene regulation by peptides in staphylococci and other Gram- positive bacteria. Curr Opin Microbiol *2*, 40-5.

Novick, R. P., Ross, H. F., Projan, S. J., Kornblum, J., Kreiswirth, B., and Moghazeh, S. (1993). Synthesis of staphylococcal virulence factors is controlled by a regulatory RNA molecule. Embo J *12*, 3967-75.

Otto, M., Echner, H., Voelter, W., and Gotz, F. (2001). Pheromone Cross-Inhibition between *Staphylococcus aureus* and *Staphylococcus epidermidis*. Infect Immun *69*, 1957-1960.

Otto, M., and Gotz, F. (2000). Analysis of quorum sensing activity in staphylococci by RP-HPLC of staphylococcal delta-toxin. Biotechniques *28*, 1088, 1090, 1092, 1096.

Otto, M., Sussmuth, R., Jung, G., and Gotz, F. (1998). Structure of the pheromone peptide of the Staphylococcus epidermidis agr system. FEBS Lett *424*, 89-94.

Otto, M., Sussmuth, R., Vuong, C., Jung, G., and Gotz, F. (1999). Inhibition of virulence factor expression in Staphylococcus aureus by the Staphylococcus epidermidis agr pheromone and derivatives. FEBS Lett *450*, 257-62.

Park, H., and Inouye, M. (1997). Mutational analysis of the linker region of EnvZ, an osmosensor in Escherichia coli. J Bacteriol *179*, 4382-90.

Pliska, V. (1999). Partial agonism: mechanisms based on ligand-receptor interactions and on stimulus-response coupling. J Recept Signal Transduct Res *19*, 597-629.

Qin, L., Dutta, R., Kurokawa, H., Ikura, M., and Inouye, M. (2000). A monomeric histidine kinase derived from EnvZ, an *Escherichia coli* osmosensor. Mol Microbiol *36*, 24-32.

Qin, X., Singh, K. V., Weinstock, G. M., and Murray, B. E. (2001). Characterization of fsr, a regulator controlling expression of gelatinase and serine protease in *Enterococcus faecalis* OG1RF. J Bacteriol *183*, 3372-82.

Rew, Y. M., Shelle; Svensson, Camilla; Yaksh, Tony L.; Chung, Nga N.; Schiller, Peter W.; Cassel, Joel A.; DeHaven, Robert N.; Goodman, Murray (2002). Synthesis and Biological Activities of Cyclic Lanthionine Enkephalin Analogues: d-Opioid Receptor Selective Ligands. Journal of Medicinal Chemistry *45*, 3746-3754.

Rizzitello, A. E., Harper, J. R., and Silhavy, T. J. (2001). Genetic evidence for parallel pathways of chaperone activity in the periplasm of *Escherichia coli*. J Bacteriol *183*, 6794-800.

Saenz, H. L., Augsburger, V., Vuong, C., Jack, R. W., Gotz, F., and Otto, M. (2000). Inducible expression and cellular location of AgrB, a protein involved in the maturation of the staphylococcal quorum-sensing pheromone. Arch Microbiol *174*, 452-5.

Sakakibara, H., Taniguchi, M., and Sugiyama, T. (2000). His-Asp phosphorelay signaling: a communication avenue between plants and their environment. Plant Mol Biol *42*, 273-8.

Schauder, S., and Bassler, B. L. (2001). The languages of bacteria. Genes Dev *15*, 1468-80.

Schnölzer, M., Alewood, P., Jones, A., Alewood, D., and Kent, S. B. H. (1992). *Int. J. Pept. Protein Res* ***40***, 180–193.

Steer, D. L., Lew, R. A., Perlmutter, P., Smith, A. I., and Aguilar, M. I. (2002). Beta-amino acids: versatile peptidomimetics. Curr Med Chem *9*, 811-22.

Stock, A. M., Robinson, V. L., and Goudreau, P. N. (2000). Two-component signal transduction. Annu Rev Biochem *69*, 183-215.

Stone, M., and Angus, J. A. (1978). Developments of computer-based estimation of pA2 values and associated analysis. J Pharmacol Exp Ther *207*, 705-18.

Tanaka, T., Saha, S. K., Tomomori, C., Ishima, R., Liu, D., Tong, K. I., Park, H., Dutta, R., Qin, L., Swindells, M. B., Yamazaki, T., Ono, A. M., Kainosho, M., Inouye, M., and Ikura, M. (1998). NMR structure of the histidine kinase domain of the E. coli osmosensor EnvZ. Nature *396*, 88-92.

Tegmark, K., Morfeldt, E., and Arvidson, S. (1998). Regulation of agr-dependent virulence genes in Staphylococcus aureus by RNAIII from coagulase-negative staphylococci. J Bacteriol *180*, 3181-6.

Tomomori, C., Tanaka, T., Dutta, R., Park, H., Saha, S. K., Zhu, Y., Ishima, R., Liu, D., Tong, K. I., Kurokawa, H., Qian, H., Inouye, M., and Ikura, M. (1999). Solution structure of the homodimeric core domain of Escherichia coli histidine kinase EnvZ. Nat Struct Biol *6*, 729-34.

Tortosa, P., and Dubnau, D. (1999). Competence for transformation: a matter of taste. Curr Opin Microbiol *2*, 588-92.

Toyoda-Yamamoto, A., Shimoda, N., and Machida, Y. (2000). Genetic analysis of the signal-sensing region of the histidine protein kinase VirA of Agrobacterium tumefaciens. Mol Gen Genet *263*, 939-47.

Trabi, M., and Craik, D. J. (2002). Circular proteins--no end in sight. Trends Biochem Sci *27*, 132-8.

Unson, C. G., Wu, C-R., Jiang, Y., Yoo, B., Cheung, C., Sakmar, T.P., Merrifield, R.B. (2002). Roles of Specific Extracellular Domains of the Glucagon Receptor in Ligand Binding and Signaling. Biochemistry *41*, 11795-11803.

Vandenabeele-Trambouze, O., Albert, M., Bayle, C., Couderc, F., Commeyras, A., Despois, D., Dobrijevic, M., and Loustalot, M. F. (2000). Chiral determination of amino acids by capillary electrophoresis and laser-induced fluorescence at picomolar concentrations. J Chromatogr A *894*, 259-66.

Vandenesch, F., Kornblum, J., and Novick, R. P. (1991). A temporal signal, independent of agr, is required for hla but not spa transcription in Staphylococcus aureus. J Bacteriol *173*, 6313-20.

Vannini, A., Volpari, C., Gargioli, C., Muraglia, E., Cortese, R., De Francesco, R., Neddermann, P., and Marco, S. D. (2002). The crystal structure of the quorum sensing protein TraR bound to its autoinducer and target DNA. Embo J *21*, 4393-401.

Vuong, C., Gotz, F., and Otto, M. (2000). Construction and characterization of an agr deletion mutant of Staphylococcus epidermidis. Infect Immun *68*, 1048-53.

Wright, G. D., Holman, T. R., and Walsh, C. T. (1993). Purification and characterization of VanR and the cytosolic domain of VanS: a two-component regulatory system required for vancomycin resistance in Enterococcus faecium BM4147. Biochemistry *32*, 5057-63.

Wright, J. S., 3rd, and Kadner, R. J. (2001). The phosphoryl transfer domain of uhpb interacts with the response regulator uhpa. J Bacteriol *183*, 3149-59.

Wright, J. S., Olekhnovich, I. N., Touchie, G., and Kadner, R. J. (2000). The histidine kinase domain of UhpB inhibits UhpA action at the Escherichia coli uhpT promoter. J Bacteriol *182*, 6279-86.

Yu, E. W., and Koshland, D. E., Jr. (2001). Propagating conformational changes over long (and short) distances in proteins. Proc Natl Acad Sci U S A *98*, 9517-20.

Zhang, L., Gray, L., Novick, R. P., and Ji, G. (2002). Transmembrane Topology of AgrB, the Protein Involved in the Post- translational Modification of AgrD in Staphylococcus aureus. J Biol Chem *277*, 34736-34742.

Zhang, L., Jacobsson, K., Strom, K., Lindberg, M., and Frykberg, L. (1999). Staphylococcus aureus expresses a cell surface protein that binds both IgG and beta2-glycoprotein I. Microbiology *145*, 177-83.

Zhang, L., Jacobsson, K., Vasi, J., Lindberg, M., and Frykberg, L. (1998). A second IgG-binding protein in Staphylococcus aureus. Microbiology *144*, 985-91.

Zhang, L., Rosander, A., Jacobsson, K., Lindberg, M., and Frykberg, L. (2000). Expression of staphylococcal protein sbi is induced by human IgG [In Process Citation]. FEMS Immunol Med Microbiol *28*, 211-8.

Zhou, N. E., Mant, C. T., and Hodges, R. S. (1990). Effect of preferred binding domains on peptide retention behavior in reversed-phase chromatography: amphipathic alpha-helices. Pept Res *3*, 8-20.

Zhu, Y., and Inouye, M. (2002). The role of the G2 box, a conserved motif in the histidine kinase superfamily, in modulating the function of EnvZ. Mol Microbiol *45*, 653-63.

Zhu, Y., Qin, L., Yoshida, T., and Inouye, M. (2000). Phosphatase activity of histidine kinase EnvZ without kinase catalytic domain. Proc Natl Acad Sci U S A *97*, 7808-13.

Zhu, Y. F., Curran, I. H., Joris, B., Ghuysen, J. M., and Lampen, J. O. (1990). Identification of BlaR, the signal transducer for beta-lactamase production in Bacillus licheniformis, as a penicillin-binding protein with strong homology to the OXA-2 beta-lactamase (class D) of Salmonella typhimurium. J Bacteriol *172*, 1137-41.

Zou, K., Cheley, S., Givens, R. S., and Bayley, H. (2002). Catalytic subunit of protein kinase A caged at the activating phosphothreonine. J Am Chem Soc *124*, 8220-9.